

SULPHLEX ENGINEERING PROPERTIES



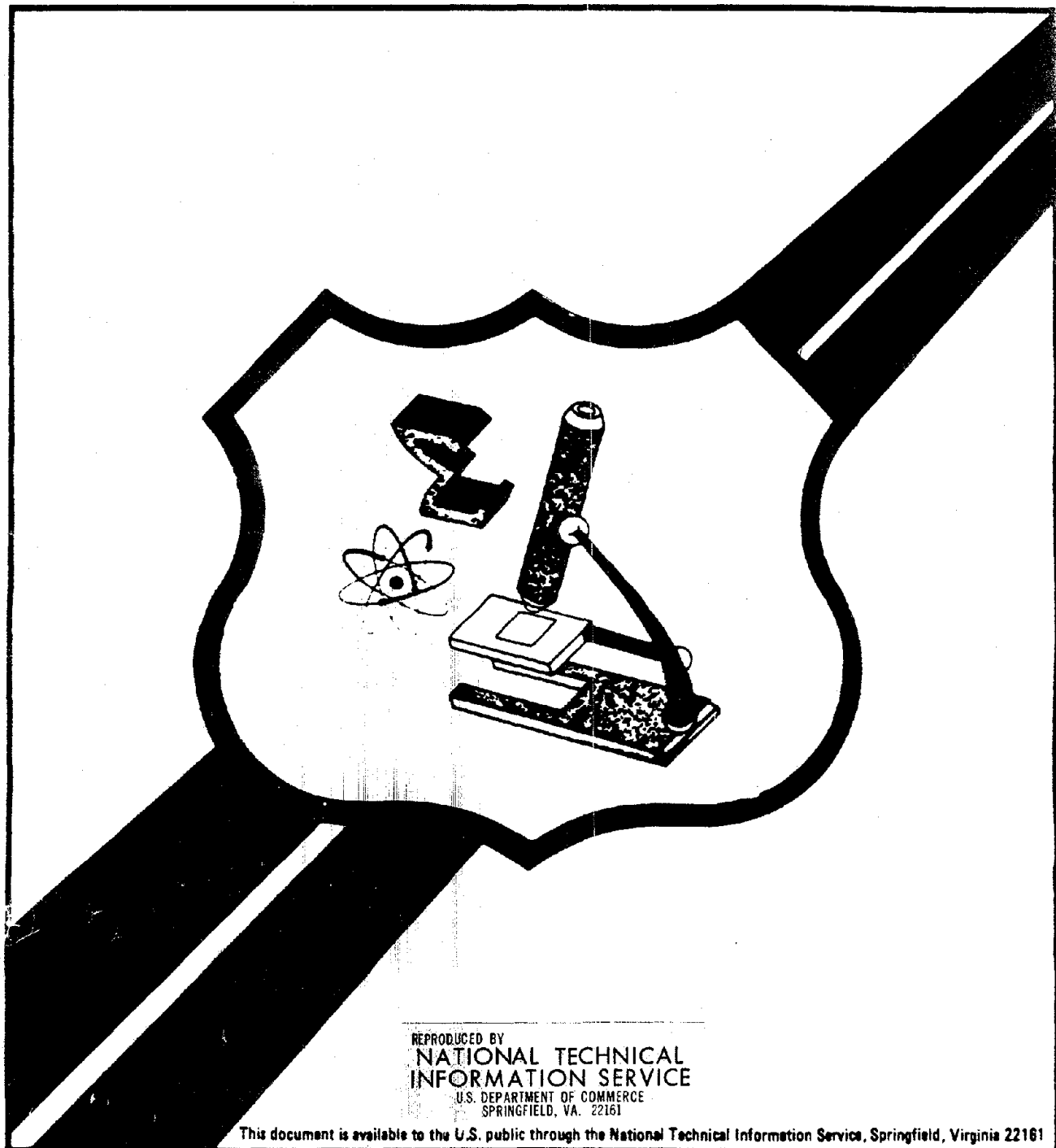
U.S. Department
of Transportation
**Federal Highway
Administration**

Research, Development,
and Technology

Turner-Fairbank Highway
Research Center
6300 Georgetown Pike
McLean, Virginia 22101

Report No.
FHWA/RD-85/032

Final Report
March 1985




REPRODUCED BY
**NATIONAL TECHNICAL
INFORMATION SERVICE**
U.S. DEPARTMENT OF COMMERCE
SPRINGFIELD, VA. 22161

This document is available to the U.S. public through the National Technical Information Service, Springfield, Virginia 22161

FOREWORD

The information in this report should be of interest to research and development personnel concerned with the development and use of materials to replace asphalt in the construction of flexible highway pavements. The report provides extensive information on the engineering capabilities and structural characteristics of Sulphlex binders, a group of materials formed by the reaction of elemental sulfur with several hydrocarbon modifiers, and designed to completely replace asphalt in flexible paving mixtures.

Additional copies are available from the National Technical Information Service (NTIS), U.S. Department of Commerce, 5285 Port Royal Road, Springfield, Virginia 22161.


Richard E. May, Director
Office of Engineering and
Highway Operations
Research and Development

NOTICE

This document is disseminated under the sponsorship of the Department of Transportation in the interest of information exchange. The United States Government assumes no liability for its contents or use thereof.

The contents of this report reflect the views of the authors who are responsible for the facts and the accuracy of the data presented herein. The contents do not necessarily reflect the official policy of the Department of Transportation.

The report does not constitute a standard, specification, or regulation.

The United State Government does not endorse products or manufacturers. Trademarks or manufacturers' names appear herein only because they are considered essential to the object of this document.

1. Report No. FHWA/RD-85/032		2. Government Accession No.		3. Recipient's Catalog No. PB86 186483 /AS	
4. Title and Subtitle Engineering Characterization of Sulphlex Binders				5. Report Date March 1986	
				6. Performing Organization Code	
7. Author(s): Dallas N. Little, Adli H. Al-Balbissi, Chuck Gregory and Barry Richey				8. Performing Organization Report No.	
9. Performing Organization Name and Address Texas Transportation Institute Texas A&M University College Station, Texas 77843				10. Work Unit No. (TRIS) 34D2-013	
				11. Contract or Grant No. DTFH61-80-C-00048	
12. Sponsoring Agency Name and Address Offices of Research, Development, and Technology Federal Highway Administration 6300 Georgetown Pike McLean, Virginia 22101				13. Type of Report and Period Covered Final Report	
				14. Sponsoring Agency Code MTC/0063	
15. Supplementary Notes FHWA Technical Representative: Dr. E. T. Harrigan, (HNR-30)					
16. Abstract <p>A chemically-modified sulfur called SULPHLEX (a trademark of Southwest Research Institute) was studied. This binder consists of 70 percent elemental sulfur and 30 percent of a combination of hydrocarbons which chemically react with molten sulfur. This chemical reaction allows the polymeric, molten sulfur to retain, at least to some extent, certain favorable engineering properties after cooling. The goal of this research was to study not only the engineering characteristics but also the chemical stability and characteristics of this material; the chemical characterization of SULPHLEX is presented in a separate report (FHWA/RD-85/033).</p> <p>This report presents the results of an extensive engineering characterization including: (1) mixture design considerations, (2) flexural fatigue, (3) fracture potential, (4) low temperature fracture properties, (5) deformation potential, (6) creep compliance and stiffness response, (7) aging characteristics and (8) resilient and dynamic moduli properties. In addition a pavement performance prediction of SULPHLEX as a paving material under various climates and traffic conditions was made using a systems pavement analysis approach. This approach consisted of an initial screening of literally thousands of pavement design alternatives by the pavements system Model FPS-BISTRO. This was followed by a detailed analysis of the best alternatives by VESYS IIM, a sophisticated structural pavement subsystem which considers the fatigue, deformation and time dependent/temperature dependent compliance of the materials.</p>					
17. Key Words Sulfur, SULPHLEX, plasticized sulfur, IVEYS, fatigue, FPS-BISTRO, fracture potential, mix design, performance prediction, chemically modified sulfur.			18. Distribution Statement No original distribution by the sponsoring agency. This document is available to the public only through the National Technical Information Service, Springfield, Virginia 22161.		
19. Security Classif. (of this report) Unclassified		20. Security Classif. (of this page) Unclassified		21. No. of Pages 300	22. Price

METRIC CONVERSION FACTORS

APPROXIMATE CONVERSIONS FROM METRIC MEASURES

SYMBOL WHEN YOU KNOW MULTIPLY BY TO FIND SYMBOL

LENGTH

in	inches	2.5	centimeters	cm
ft	feet	30	centimeters	cm
yd	yards	0.9	meters	m
mi	miles	1.6	kilometers	km

AREA

in ²	square inches	6.5	square centimeters	cm ²
ft ²	square feet	0.09	square meters	m ²
yd ²	square yards	0.6	square meters	m ²
mi ²	square miles	2.6	square kilometers	km ²
	acres	0.4	hectares	ha

MASS (weight)

oz	ounces	28	grams	g
lb	pounds	0.45	kilograms	kg
	short tons (2000 lb)	0.9	tonnes	t

VOLUME

tsp	teaspoons	5	milliliters	ml
tbsp	tablespoons	15	milliliters	ml
fl oz	fluid ounces	30	milliliters	ml
c	cups	0.24	liters	l
pt	pints	0.47	liters	l
qt	quarts	0.95	liters	l
gal	gallons	3.8	liters	l
ft ³	cubic feet	0.03	cubic meters	m ³
yd ³	cubic yards	0.76	cubic meters	m ³

TEMPERATURE (exact)

°F	Fahrenheit temperature	5/9 (after subtracting 32)	Celsius temperature	°C
----	------------------------	----------------------------	---------------------	----

APPROXIMATE CONVERSIONS FROM METRIC MEASURES

SYMBOL WHEN YOU KNOW MULTIPLY BY TO FIND SYMBOL

LENGTH

mm	millimeters	0.04	inches	in
cm	centimeters	0.4	inches	in
m	meters	3.3	feet	ft
m	meters	1.1	yards	yd
km	kilometers	0.6	miles	mi

AREA

cm ²	square centimeters	0.16	square inches	in ²
m ²	square meters	1.2	square yards	yd ²
km ²	square kilometers	0.4	square miles	mi ²
ha	hectares (10,000 m ²)	2.5	acres	

MASS (weight)

g	grams	0.035	ounces	oz
kg	kilograms	2.2	pounds	lb
t	tonnes (1000 kg)	1.1	short tons	

VOLUME

ml	milliliters	8.03	fluid ounces	fl oz
l	liters	2.1	pints	pt
l	liters	1.06	quarts	qt
l	liters	0.26	gallons	gal
m ³	cubic meters	36	cubic feet	ft ³
m ³	cubic meters	1.3	cubic yards	yd ³

TEMPERATURE (exact)

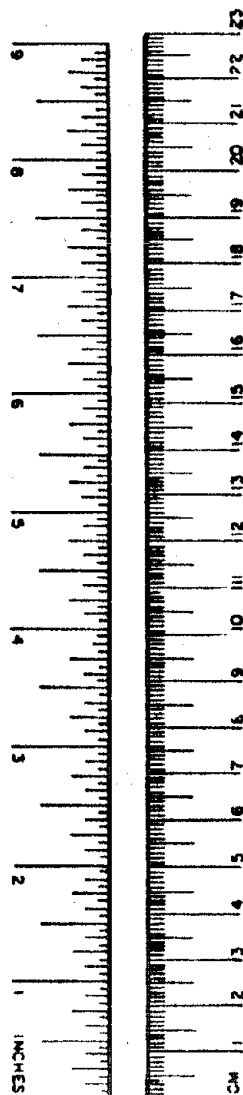
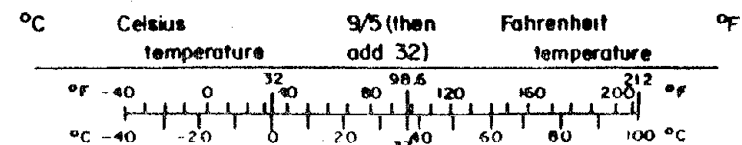


TABLE OF CONTENTS

	Page
CHAPTER I - SUMMARY	1
CHAPTER II - RESEARCH OVERVIEW	7
Purpose and Objectives	7
Report Organization	7
Materials	8
Asphalt Cement	8
SULPHLEX	9
Aggregate Properties	9
Field Specimens	14
Laboratory Testing	19
CHAPTER III - NATURE OF SULPHLEX	22
Background	22
Composition and Chemistry	23
Raw Materials and Formulation	23
Process Variables	23
Variations in Temperature and Time of Reaction	25
Selection of Binders for Analysis	27
Preparation of Binders	28
CHAPTER IV - MIXTURE DESIGN METHODS AND MIXTURE OPTIMIZATION	30
Background	30
Research Approach	32
Sensitivity to Fabrication Variables	32

TABLE OF CONTENTS (continued)

	Page
Selection of Mixture Design Method	37
The Marshall Method	37
A Unique Approach to Mixture Design	44
The Strain Energy Concept	46
The Failure Envelope	46
Mixture Design Procedure	55
Optimum Mixture Design	60
CHAPTER V - STRUCTURAL ENGINEERING PROPERTIES (1):	
FATIGUE CRACKING	62
Selection of Approach	62
Phenomenological Regresssion Approach	62
Fracture Mechanics	63
Relationship Between Phenomenological and Fracture Mechanics Parameters	69
Experimental Design	71
Phenomenological Method	71
Fracture Mechanics Study	71
Results of Phenomenological Study	76
Tensile Strain Versus Load Repetitions	76
Validity of Phenomenological Test Results	79
K_1 and K_2 Parameters at 70°F	79
Temperature Effects on K_1 and K_2	83
Results of Fracture Mechanics Study	87
Rate of Crack Growth	87
Energy Release Rate Relationships	94
J^* Versus dc/dN Relationship	94
Effect of Specimen Thickness	97

TABLE OF CONTENTS (continued)

	Page
Effect of Displacement Rate	100
Effect of Rest Periods	103
Laboratory to Field Shift Factors	107
Background	107
Shift Factor Development	108
Approach	109
Results	112
Selection of Shift Factors	114
CHAPTER VI - STRUCTURAL ENGINEERING PROPERTIES (2):	
FRACTURE STRENGTH	116
Background	116
Research Approach	117
Traditional Approach	118
Fracture Mechanics Based Approach	122
Results of Analysis	124
Traditional Approach	124
Fracture Mechanics Approach	129
CHAPTER VII - STRUCTURAL ENGINEERING PROPERTIES (3):	
DEFORMATION CHARACTERISTICS	133
Viscoelastic Response	133
General	133
Viscoelastic Characterization of SULPHLEX Mixtures	135
Results of Theological Testing	143
VESYS Deformation Parameters	153
General	153
Measuring ALPHA and GNU	157

TABLE OF CONTENTS (continued)

	Page
Results of VESYS Pavement Deformation Testing	159
The Shell Method of Estimating Deformation Potential	169
General	169
S_{mix} Versus S_{bit} Curves	173
Deformation Analysis.	175
CHAPTER VIII - STRUCTURAL ENGINEERING PROPERTIES (4):	
MODULUS PROPERTIES	176
General.	176
Resilient Modulus	178
Creep Stiffness	182
Dynamic Modulus and Flexural Modulus	183
Relaxation Moduli	183
Summary of Modulus Properties	187
CHAPTER IX - MOISTURE DAMAGE AND THERMAL AGING	189
Moisture Damage of SULPHLEX Mixtures	189
Background	189
Basic Mechanisms	189
Testing Approach	191
Results	194
Effects of Aging on SULPHLEX Mixtures	200
Background	200
Research Approach	202
Effect of Aging on Stress Relaxation Modulus	204
Effect on Aging on Stress Energy and Resilient Modulus	204
Materials Subjected to In Situ Aging	207

TABLE OF CONTENTS (continued)

	Page
Results of Stress Relaxation Analysis	207
Results of DSE and Resilient Modulus Analysis.	211
Results of In Situ Aging	216
CHAPTER X - PAVEMENT DESIGN AND STRUCTURAL ANALYSIS.	221
General	221
Approach	223
Pavement System	223
FPS-BISTRO	223
Flexural Fatigue at the Bottom of the Surface Course	229
Permanent Deformation - Mid-depth of Granular Base Course	230
Flexural Fatigue at Bottom of Course	231
Permanent Deformation at the Top of Subgrade	231
Preparation of Input for FPS-BISTRO	232
VESYS Analysis	239
Traffic.	239
System Geometry	243
Environment	243
Material Properties	244
System Properties	246
System Performance Bounds	246
Results	250
VESYS Structural Analysis	250
Results of VESYS Analysis	251

TABLE OF CONTENTS (continued)

	Page
Comparative Analysis with Crushed Limestone Base	256
Thin Pavement Over Hard Subgrade	256
Thin Surface Over Soft Subgrade	256
Thick Surface Over Hard Subgrade	262
Thick Pavement Over Soft Subgrade	262
CHAPTER XI - CONCLUSIONS AND RECOMMENDATIONS	263
REFERENCES	268
APPENDIX A - PREPARATION OF BINDERS	277
APPENDIX B - OVERLAY TESTER	281

LIST OF TABLES

Table		Page
1	Characteristics of Laboratory Standard Asphalt	10
2	SULPHLEX Binder Properties	12
3	Physical Properties of Crushed Limestone	16
4	Physical Properties of Rounded Gravel	17
5	Physical Properties of Crushed Basalt (Traprock)	18
6	A Summary of the Test Procedures Followed in this Study of the Engineering Characterization of SULPHLEX Mixtures	20
7	Sources and Purity of Raw Materials Used in the Preparation of SULPHLEX 233	24
8	Properties of SULPHLEX 233 Made at Various Temperatures and Reaction Times	26
9	Formulation and Processing Conditions for SULPHLEX Binders Analyzed in this Study	29
10	Factorial Analysis of Factors which Affect the Mixture Fabrication Process	34
11	Duncan Multiple Range Summary for the Dependent Variable Resilient Modulus at 32, 77, and 104°F as a Measure for the Effects of Fabrication Variables	36
12	Optimum Binder Contents for All Mixtures Based on Marshall Test Method	43
13	Summary of Optimum Mixture Designs and Mixture Properties at Optimum Design Conditions	61
14	Experimental Design for Controlled Stress Beam Fatigue Tests	72
15	Experiment Design for the Overlay Tests	74
16	Summary of Phenomenological Fatigue Data from Extensively Used and Documented Studies	78
17	Summary of K_1 and K_2 Values from Phenomenological Beam Fatigue Testing	81

LIST OF TABLES (continued)

Table		Page
18	List of Regression Coefficients of the Relationships Between Crack Length and Number of Cycles to Failure (All Tests at 77°F)	89
19	Summary of Results and Test Conditions of Initial Overlay Tests (All Tests at 77°F)	90
20	Summary of ANOVA Results on Number of Load Cycles to Failure, N_f , Caused by Material Type Effects, Table 19 (All Tests at 77°F)	92
21	Summary of Analysis of Variance on the Slope of c-N Relationship, Table 18 (All Tests at 77°F)	92
22	Recapitulative Summary of Number of Cycles to Failure, N_f (All Tests at 77°F)	93
23	Summary of Analysis of Variance of Number of Load Cycles to Failure Considering the Effects of Rest Period and Displacement Magnitude (All Tests at 77°F)	93
24	List of Regression Coefficients of the Relationships Between Energy Normalized for Thickness and Crack Length . .	96
25	Summary of Fabrication Data for Beams Used in J* Versus dc/dN Relationships.	98
26	Summary of Results and Analysis of Relationships Between dc/dN and J* (Paris Relationship)	98
27	Summary of Regression Analysis on Experiments at Different Displacement Rates	102
28	Laboratory to Field Shift Factors Used in This Study for Asphalt Concrete and SULPHLEX	114
29	Summary of Tensile Strength for Indirect Tensile Testing at Low Temperatures (All Mixtures Were Composed of Crushed Limestone Aggregate)	119
30	Summary of J_{IC} Values Versus Temperature	131
31	Partial Factorial Experiment For the Evaluation of Factors Influencing Creep Compliance	144
32	Power Law Representations of Creep Compliance Data for SULPHLEX and Control Mixtures.	149
33	Summary of BETA Values	154
34	Experiment Design for Determination of Permanent Deformation Parameters	160

LIST OF TABLES (continued)

Table		Page
35	VESYS Deformation Parameters for SULPHLEX and Control Mixtures (From Log-Log Plot of Accumulated Permanent Strain Versus Load Application)	161
36	Comparison of VESYS Permanent Deformation Parameters at 70°F for SULPHLEX, Sulfur-Extended Asphalt and Recycled Asphalt	167
37	Summary of Resilient Moduli of SULPHLEX and Control Mixtures	181
38	Summary of Creep Stiffnesses, Dynamic Moduli and Flexural Moduli for all Mixtures	185
39	Relaxation Moduli at 73°F, 0.1 Second Load Duration for SULPHLEX and Control (Asphalt Concrete) Samples. (All Specimens Contain Crushed Limestone Aggregates)	188
40	Effect of Moisture Damage of Unconfined Compressive Strength	195
41	Effects of One Cycle Lottman Conditioning on Mixtures of SULPHLEX and Asphalt Cement (Control) with Crushed Limestone	198
42	Effect of Seven-Day Soak on Mixtures of SULPHLEX and Asphalt Cement (Control) and Crushed Limestone	199
43	Summary of Effects of Aging at 140°F as Reflected by Resilient Modulus and Dissipated Strain Energy	212
44	Changes in Resilient Modulus with Age on Field Cores from Loop 1604, San Antonio, Texas	217
45	Summary of Resilient Modulus Testing of SULPHLEX Specimens Aged In Situ in Four Environments	218
46	Organization of Structural Design and Analysis Study	222
47	List of Variables Considered in Pavement Design Procedure	225
48	Summary of Texas FPS-BISTRO Input Data	233
49	Material Properties Used in Texas FPS-BISTRO Program	238
50	Optimum Design Schemes as Determined by Texas FPS-BISTRO (70°F)	240
51	Optimum Design Schemes as Determined by Texas FPS-BISTRO (51°F)	241

1
2
3
4
5
6
7
8
9
10
11
12
13
14
15
16
17
18
19
20
21
22
23
24
25
26
27
28
29
30
31
32
33
34
35
36
37
38
39
40
41
42
43
44
45
46
47
48
49
50
51
52
53
54
55
56
57
58
59
60
61
62
63
64
65
66
67
68
69
70
71
72
73
74
75
76
77
78
79
80
81
82
83
84
85
86
87
88
89
90
91
92
93
94
95
96
97
98
99
100

LIST OF TABLES (continued)

Table		Page
52	Optimum Design Schemes as Determined by Texas FPS-BISTRO (40°F)	242
53	Creep Properties Used in VESYS IIM Analysis	245
54	Phenomenological Fatigue Constants Used in VESYS IIM Analysis	247
55	Summary of VESYS IIM Results Using Optimum FPS-BISTRO Pavement Thicknesses. (Interstate Highway Traffic) . . .	252
56	Summary of VESYS IIM Results Using Optimum FPS-BISTRO Pavement Thickness (State Highway Traffic)	253
57	Effects of Load Duration on Performance of Full-Depth Pavements from FPS-BISTRO (100°F)	255
58	Summary of VESYS IIM Analysis (6-Inch Crushed Limestone Base)	257

LIST OF FIGURES

Figure		Page
1	A Summary of Important Material Responses for SULPHLEX at Low, Intermediate, and High Temperature	3
2	Viscosity - Temperature Relationship for Laboratory Standard Asphalt (AC-10)	11
3	Gradation Curves for Aggregates Used in Mixtures of SULPHLEX	15
4	Structures of SULPHLEX Raw Materials	24
5	Marshall Stability Versus Binder Content for Mixtures Tested	38
6	Marshall Flow Versus Binder Content for Mixtures Tested	39
7	Percent Air Voids Versus Binder Content for Mixtures Tested	40
8	Percent Voids in Mineral Aggregate, VMA, for Mixtures Tested	41
9	The Effect of Binder Content on Strain Energy or Toughness	47
10	Effect of Temperature on Strain Energy or Toughness	47
11	Illustration of the Ultimate Stress-Strain Behavior of an Ideal Elastomer	48
12	Failure Envelope for a Mixture of Crushed Limestone and SULPHLEX Binder CR1	48
13	The Effect of Binder Content on the Failure Envelope (CR1 Binder and Crushed Limestone)	50
14	The Effect of Aggregate Type on Failure Envelope (CR1 Binder).	50
15	Hypothetical "Window of Acceptability" for Failure Envelope	51
16	Hypothetical Boundary Curves for Thermally Induced Stresses	51

LIST OF FIGURES (continued)

Figure		Page
17	Thermally Induced Stresses Computed by the Computer Program Developed by Chang et al. (28)	53
18	Thermal Stress Boundary Curves Developed for SULPHLEX Binder CR1 and Crushed Limestone	53
19	Schematic Representation of the Shift of the Failure Envelope with an Increase in Binder Content	54
20	Mixture Stiffness Versus Binder Stiffness for SULPHLEX Binder CR1 and Crushed Limestone (Based on the Shell Method (29))	54
21	Permanent Deformation Versus Binder Content Calculated by Means of Shell Method	56
22	Permanent Deformation Boundary Curves for SULPHLEX Binder CR1 and Crushed Limestone Aggregate	57
23	Load-Displacement Response in Overlay Tester Recorded on X-Y Plotter	57
24	Mixture Design Failure Envelopes Plotted Against Boundary Curves for Thermal Cracking and Permanent Deformation	59
25	Mixture Design Resilient Modulus - Temperature Curves Plotted Against Constant Fatigue Contours	59
26a	State of Stress at Tip of Mode I (Tensile) Crack	65
26b	Stress State as Represented by the Stress Intensity Factor, a Function of Crack Length (a or c) and Stress (σ).	65
27	Schematic of Overlay Tester	68
28	Load - Displacement Response in Overlay Tester Recorded on X-Y Plotter	70
29	General Controlled Stress Phenomenological Fatigue Test Results for Ten Different Mixtures	77
30	Relationship between K_1 and K_2 Based on Results Summarized by Kennedy and Rauhut (57)	80
31	Phenomenological Fatigue Results for All Beams Tested (Each Mixture was Composed of Binder and Crushed Limestone)	82

LIST OF FIGURES (continued)

Figure		Page
32	Comparison of Phenomenological Data from Simply Supported Beams and Those Supported by Elastic Foundations	84
33	Effect of Temperature on Fatigue Curves of AC-10 and SULPHLEX CR5 Mixtures	85
34	The Effect of Temperature on the Phenomenological Fatigue Parameter K_1 (after Rauhut et al. (57))	86
35a	Crack Length Versus Number of Load Applications for 0.02-Inch Opening Displacement (Each Curve is the Average of Four Tests)	88
35b	Crack Length Versus Number of Load Applications for 0.04-Inch Opening Displacement (Each Curve is the Average of Four Tests)	88
36	Relationship Between Energy Required to Drive Crack per Unit Thickness of Specimen and Crack Length (Each Curve is Result of Four Tests)	95
37a	J^* Versus dc/dN Relationships for SULPHLEX and Asphalt Concrete Mixtures at 65°F	99
37b	Effect of Temperature on J^* Versus dc/dN Relationship	99
38	Relationship Between Crack Growth Rate and Energy Release Rate for Three Displacement Rates	101
39	Effects of Rest Period Duration on Energy Required for Crack Propagation (Specimens were CR5 and Crushed Limestone).	104
40	Relationships Between (1) Number of Cycles to Failure and Number of Rest Periods and (2) Sum of Added Energy and Number of Rest Periods	106
41	Illustration of the Hypothesized Laboratory to Field Shift Process	110
42	Shift Factors Calculated for Effects of (1) Residual Stresses and Relaxation of the Materials and (2) Healing Effect of Material	113
43	Illustration of Laboratory to Field Shifts for Laboratory Standard Asphalt Concrete (Control Mix)	115
44	Thermally Induced Stresses Computed from COLD Computer Program	121

LIST OF FIGURES (continued)

Figure		Page
45	Thermally Induced Stresses Computed from the Computer Model Developed by Chang et al. (28)	123
46	Photograph of the Bend Fracture Specimen in the MTS System with KRAK Gage Mounted	125
47	Typical Load-Displacement Plot from Bend Fracture Test	126
48	Thermal Stress Fracture Analysis Using Traditional Approach (All Mixtures were Fabricated with Crushed Limestone Aggregate)	127
49	Thermal Stress Fracture Analysis Using Traditional Approach (All Mixtures were Fabricated with River Gravel Aggregate)	130
50	Change in Critical J Integral with Temperature	132
51	Graphical Procedure for Predicting the Recovery Strain of a Linear Viscoelastic Material	136
52	Creep and Recovery Test for a SULPHLEX CR1 - Crushed Limestone Mix	137
53	Comparison of Compliance Curves and the Effects of Load Conditioning	139
54	Stiffness Curves for All Mixtures Fabricated with Crushed Limestone	146
55	Stiffness Curves for All Mixtures Fabricated with Basaltic Aggregates	146
56	Stiffness Curves for All Mixtures Fabricated with Gravel Aggregate	147
57	Stiffness Curves for Mixtures Fabricated with AC-10 and CR5 and Crushed Limestone Before and Following 1 Cycle Lottman Aggregate	147
58	Time-Temperature Shift Factor for Mixtures with Crushed Limestone Aggregate	151
59	Time-Temperature Shift Factor for Mixtures with Basalt Aggregate	151
60	Time-Temperature Shift Factor for Mixtures with River Gravel Aggregate	152

LIST OF FIGURES (continued)

Figure		Page
61	Typical Ranges of ALPHA and GNU Permanent Deformation Parameters. (The various lines represent data on asphalt concrete developed by Rauhut (57), and the area between the extreme lines represents a region of "typical" ALPHA and GNU values)	158
62	VESYS Permanent Deformation Plots for SULPHLEX and Asphalt Concrete Mixtures with Crushed Limestone Aggregate (40°F).	162
63	VESYS Permanent Deformation Plots for SULPHLEX and Asphalt Concrete Mixtures with Crushed Limestone Aggregate (70°F)	162
64	Permanent Deformation Plots for SULPHLEX and Asphalt Concrete Mixtures with Crushed Limestone Aggregate (100°F)	163
65	VESYS Permanent Deformation Plots for SULPHLEX and Asphalt Concrete Mixtures with Basaltic Aggregate (40°F).	163
66	VESYS Permanent Deformation Plots for SULPHLEX and Asphalt Concrete Mixtures with Basaltic Aggregate (70°F)	164
67	VESYS Permanent Deformation Plots for SULPHLEX and Asphalt Concrete Mixtures with Basaltic Aggregate (100°F)	164
68	Permanent Deformation Characteristics of CR1 - Crushed Limestone Mixtures	165
69	Permanent Deformation Characteristics of CR1 - River Gravel Mixtures	165
70	Plot of S_{binder} Versus S_{mix} for Mixtures of CR1 or AC-10 with Crushed Limestone Aggregate	174
71	Simplified Illustration of Components of Stiffness: Elastic, Viscoelastic and Viscous	177
72	Load Pulse of the Resilient Modulus Device	179
73	Resilient Moduli Versus Temperature for SULPHLEX and Asphalt Concrete Fabricated with Crushed Limestone	180
74	Creep Stiffness Versus Temperature for all Mixtures	184
75	Dynamic Moduli Versus Temperature for all Mixtures	186

LIST OF FIGURES (continued)

Figure		Page
76	Sequence of Testing for Moisture Effects	192
77	Evaluation of Changes in Material Response with Aging	203
78	Hysteresis Loop and the Dissipated Strain Energy Concept	206
79	Effects of Aging at 140°F on the Compressive Stress Relaxation Modulus Versus Duration of Loading for AC-10 - Crushed Limestone Mixtures	208
80	Effects of Aging at 140°F on the Compressive Stress Relaxation Modulus Versus Duration of Loading for CR1 - Crushed Limestone Mixtures	208
81	Effects of Aging at 140°F on the Compressive Stress Relaxation Modulus Versus Duration of Loading for CR2 - Crushed Limestone Mixtures	209
82	Effects of Aging at 140°F on the Compressive Stress Relaxation Modulus Versus Duration Loading for CR3 - Crushed Limestone Mixtures	209
83	Effects of Aging at 140°F on the Compressive Stress Relaxation Modulus Versus Duration of Loading of CR5 - Crushed Limestone Mixtures	210
84	Change in Dissipated Strain Energy with Aging at 140°F for all Mixtures	214
85	Change in Resilient Modulus with Aging at 140°F for all Mixtures	215
86	Schematic of Pavement Design Procedure	224
87	Pavement Section Analyzed by FPS-BISTRO	226
88	Load Geometry in Surface Curvature Index Calculations	228
89	Cracking Index Versus Time (VESYS IIM Analysis).	258
90	Rut Depth Versus Time (VESYS IIM Analysis)	259
91	Slope Variance Versus Time (VESYS IIM Analysis)	260
92	Serviceability Index Versus Time (VESYS IIM Analysis)	261
93	Schematic of Kettle Used to Prepare Pilot Quantities of SULPHLEX 233 at Different Temperatures	278

LIST OF FIGURES (continued)

Figure		Page
94	Schematic of 25-Gallon SULPHLEX Pilot Plant	280

CHAPTER I

SUMMARY

This report is one of three reports which presents the findings of a comprehensive study of the chemical and engineering characterization of plasticized sulfur binders. The major objective of this report is to establish the engineering behavior of a family of plasticized sulfur binders, known as SULPHLEX¹, in mixtures with aggregates. A second report describes the chemical characterization of SULPHLEX, and a third report describes a mixture design procedure developed specifically for SULPHLEX.

Five SULPHLEX binders which are similar to asphalt cement in terms of their ability to be mixed with aggregates, their workability, and their predicted mixture properties were produced. Four binders were produced at CAL-RESIN, Vallejo, California, under the direction and supervision of Matrecon, Inc. of Oakland, California. These binders designated CR1, CR2, CR3, and CR5 are variations of the SULPHLEX-233 formulation developed by Southwest Research Institute in 1978. The only difference among the binders (except for CR1) was the temperature of reaction which varied from 302 to 338°F. Binder CR1 was produced with a slight variation in the sulfur and dipentene content. Thus, binder CR1 possesses a slightly lower sulfur content and a slightly higher dipentene content than the other CR series binders.

The fifth binder, 233A, was produced at Texas A&M University at a reaction temperature of 302°F. The formulation of 233A was different from the CR series binders in that a terpene called Solvenol No. 2 replaced an equal amount of the plasticizer dipentene used in the CR series.

The first step in the SULPHLEX mixture characterization was to establish an acceptable mixture design procedure. It was established through a factorial study of mixture fabrication variables that

1. SULPHLEX is a registered trade name of Southwest Research Institute.

SULPHLEX can be fabricated identically to asphalt concrete in the laboratory. However, the behavior of SULPHLEX mixtures was quite different. SULPHLEX exhibited much higher stabilities (Marshall and Hveem) than asphalt concrete even at lower binder contents. In addition, an unmistakable trend of high Marshall flows was exhibited for SULPHLEX even though concomitant stabilities were much greater than for asphalt concrete.

The significantly different mixture behavior resulted in the search for a new approach (different from Marshall or Hveem which are based on historical asphalt concrete performance) to SULPHLEX mixture design. The approach selected employs strain energy density and a stress-strain failure envelope developed over a range of test temperatures and durations of loading. The mode of testing is the indirect tensile test. In recent years this test has been used in research and in in-depth studies of asphalt concrete and is available or at least easily accessible to State and Federal agencies.

The engineering characterization of SULPHLEX mixtures was based on mixtures designed in accordance with the failure envelope - strain energy density concept. The engineering characterization included analyses of the following properties:

1. Resilient modulus.
2. Creep compliance.
3. Relaxation modulus.
4. Stiffness modulus.
5. Low temperature fracture.
6. Flexural fatigue.
7. Fracture potential.
8. Deformation potential.

The results of these analyses are discussed in great detail in this report. The most important findings may be discussed by reference to Figure 1.

Figure 1 is a general synopsis of the nominal or average behavior of typical SULPHLEX binders (CR1, CR2, CR3, CR5, and 233A). These binders exhibit excellent properties at midrange temperatures but are questionable in terms of their performance at the temperature extremes.

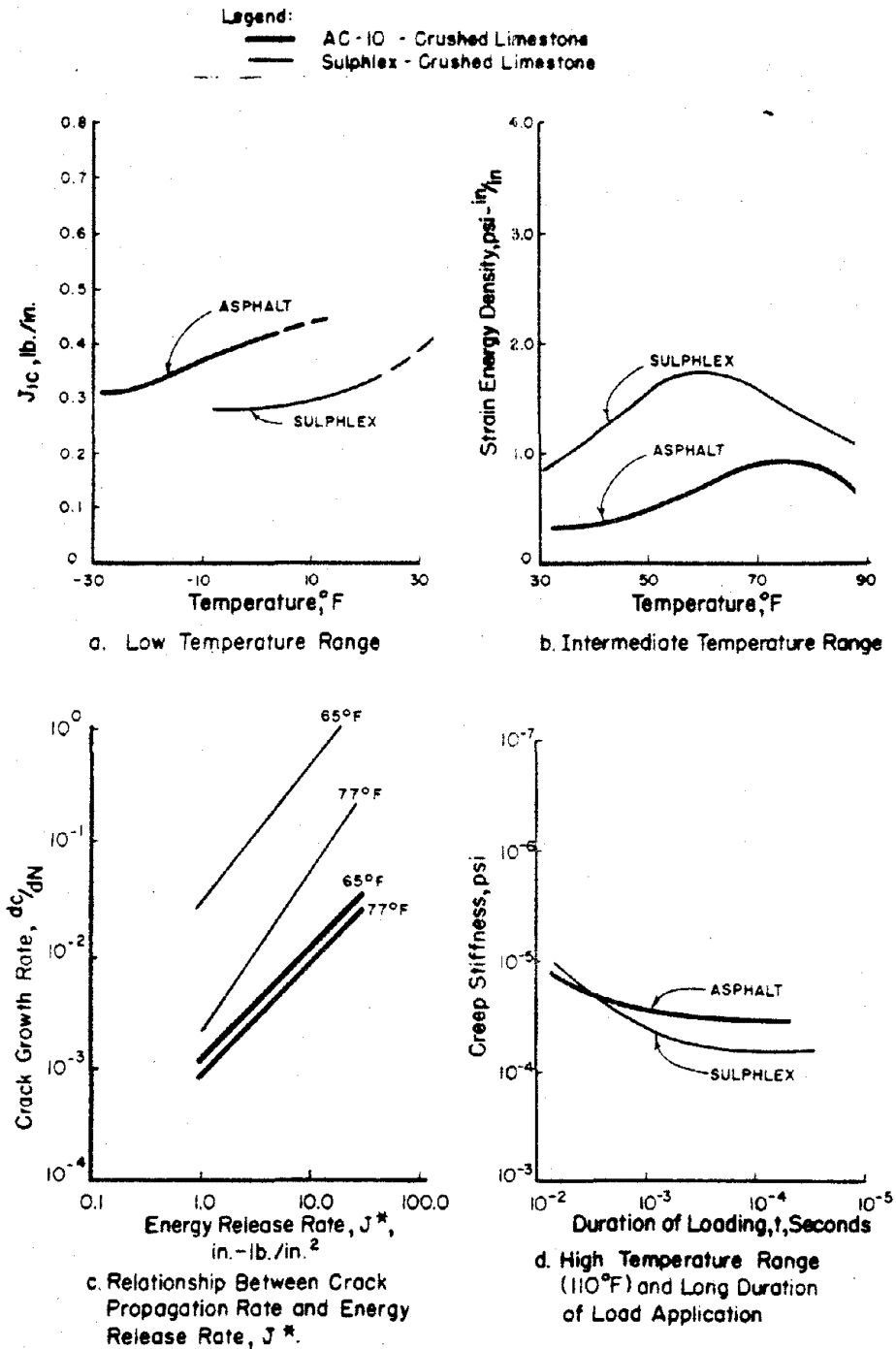


Figure 1. A Summary of Important Material Responses for SULPHLEX at Low, Intermediate, and High Temperatures.

Figure 1a is a plot of J_{IC} , the critical elastic-plastic fracture energy, or energy required to cause crack growth, versus temperature. It is evident that the asphalt concrete mixture has superior fracture properties at low temperatures, between about 30°F and -30°F. (The dashed portion of the curves represent hypothesized trends). The primary reason for the superior behavior for asphalt concrete in this region is the glass transition temperature, T_g , which is approximately -15 to -20°F for asphalt concrete and only about 20°F for SULPHLEX. Obviously, the more viscous and plastic behavior above T_g results in greater fracture toughness.

In Figure 1b strain energy density (SED) derived from the indirect tensile test is plotted versus temperature (30°F to 90°F). Clearly the SED curve for the SULPHLEX; which represents the approximate average response of binders CR1, CR2, CR3, and CR5; illustrates superior toughness than for the control asphalt concrete. However, Figure 1c illustrates the rate of crack propagation at the midrange temperatures of 65 and 77°F. Clearly asphalt concrete has a greater fracture toughness, J^* , and is less sensitive to relatively small temperature variations within the midrange of temperatures.

In Figure 1d, the creep stiffness is plotted at 104°F for various durations of load application. SULPHLEX is substantially stiffer than asphalt concrete at shorter load durations and for lower temperatures. However, at long durations of loading, i.e., 10^4 seconds, the stiffness exhibits a somewhat linear viscous response much like that of a linear amorphous polymer.

SULPHLEX possesses favorable stiffness, compliance, and resilient modulus properties within the intermediate temperature regions. These properties indicate its superior ability to resist permanent deformation due to cyclic loading, and to favorably distribute vertical stresses and protect vulnerable subgrades. However, observation of experimental field sections has revealed susceptibility to low temperature cracking. No evidence of permanent deformation due to repeated loading has been observed in field trials or in the

laboratory. However, the curious increase in compliance at very long load duration deserves consideration of deformation potential during long term loading, i.e., parking lots.

SULPHLEX has demonstrated susceptibility to moisture damage especially at high air void content. This characteristic eliminates the option of producing SULPHLEX mixtures at low binder contents (high voids) even though acceptable stabilities (Marshall) may be achieved at these binder contents. Low air void contents similar to those used for asphalt concrete are recommended. Moisture effects were substantially reduced by pretreating the aggregate with hydrated lime or by the addition of tall oil to the mixtures.

The final chapter of this report presents the optimum pavement designs developed for specific climatic regions of the United States. Selection of optimal designs was based on a systems approach which considers not only structural responses but also costs, construction operations, required rehabilitation schemes, and user utility.

The VESYS IIM Structural Subsystem was used to validate the selection of designs based on the systems approach.

The results of the structural evaluation show that SULPHLEX may perform comparably, and in some cases, superior to asphalt concrete in relatively thick pavement layers when a controlled stress mode of flexure exists. However, in thin pavements with a very high modular ratio between the very stiff SULPHLEX surface and relatively soft base (controlled strain mode of flexure), rapid flexural fatigue cracking is a major concern.

As long as SULPHLEX is used in well-designed, relatively thick, pavement layers free from excessive moisture damage potential, it is expected to perform at least as well as the asphalt concrete control mixture.

SULPHLEX pavement and asphalt concrete pavements which are designed to perform comparably from a structural standpoint under identical conditions of loading and in the same environment and

climate differ vastly in first cost and total life cost. Based on current material costs, SULPHLEX cannot compete with asphalt concrete from a systems design approach.

CHAPTER II RESEARCH OVERVIEW

Purpose and Objectives

The purpose of this research is to evaluate SULPHLEX as a third binder material, distinct from asphalt and portland cement. It was realized from the outset that adaptations of asphalt and/or portland cement technology to the study of SULPHLEX would be appropriate in many cases. However, it was also realized that in many instances the development of fresh research approaches would be necessary.

This report is one of three final reports which present the findings of this research effort. This report deals specifically with the engineering properties of SULPHLEX mixtures and the optimization of pavement designs containing SULPHLEX layers.

A second and separate report discusses in depth the chemical characterization of SULPHLEX binders. A third report, also separately presented, presents in detail the mixture design procedure developed specifically for SULPHLEX. This procedure is based on the failure envelope concept discussed briefly in Chapter III.

Report Organization

This report is divided into ten chapters. The first chapter is an executive summary of the pertinent findings. This chapter, Chapter II, presents the objectives and organization of the overall study as well as those of this report. Chapter II also describes the test procedures and materials used throughout the study.

Chapter III deals with the nature of SULPHLEX as a unique binder. For a more detailed discussion of the chemistry and composition of SULPHLEX, the reader is referred to a companion report entitled "Chemical Characterization of SULPHLEX Binders," Reference 1.

Chapter IV summarizes the mixture design procedure developed for SULPHLEX and presents mixture properties of optimum SULPHLEX mixtures based on the new design procedure. A detailed discussion of the

mixture design procedure may be found in "A Mixture Design Procedure for SULPHLEX Based on the Failure Envelope Concept," Reference 2.

Chapters V through VIII contain the essence of this report, the structural engineering properties of SULPHLEX. In these chapters special attention is given to fatigue and fracture as well as deformation characteristics.

The effects of moisture on the engineering properties of SULPHLEX mixtures and the effects of thermal aging on SULPHLEX mixtures and the concomitant effects on engineering behavior are discussed in Chapter IX.

Chapter X draws from the information presented in the first nine chapters and a computerized systems pavement design model called FPS-BISTRO to select a prioritized list of acceptable pavement designs for various typical climatic and traffic conditions within the United States. Certain selected designs are then evaluated by the VESYS II M structural subsystem. The performances of pavements containing a SULPHLEX layer or layers are compared with pavements containing asphalt concrete layers.

Chapter XI presents the conclusions and recommendations based on this research.

Materials

SULPHLEX binders were mixed with three aggregate types in this study. The SULPHLEX mixture properties were compared to those of asphalt concrete made from the same aggregates. This section of the report explains the important physical properties of the binders and aggregates used to fabricate the mixtures discussed throughout the remainder of this report.

Asphalt Cement

The asphalt selected was the laboratory standard which is a viscosity graded AC-10 petroleum asphalt cement produced by the American Petrofina Company. Standard tests were performed on the

original (prior to mixing) asphalt to determine the basic physical and chemical characteristics. Most of these tests are described by either the American Society for Testing and Materials (3) or the American Association of State Highway and Transportation Officials (4) or both. The test for relative viscosity is described by the Texas State Department of Highways and Public Transportation (5).

Two non-standard tests entitled Actinic Light Hardening Test (6) and Thermal Neutron Activation (7) were conducted to determine the asphalt hardening effects of chemically active (ultraviolet) light and the vanadium content of the asphalt, respectively. Hardening effects were determined by comparing the asphalt viscosity at 77°F before and after exposure to actinic light. Hardening Index was computed by dividing viscosity of exposed asphalt by its initial viscosity. The types of tests performed and the results are presented in Table 1. Viscosity as a function of temperature is graphically displayed on a standard chart (ASTM D 2493) in Figure 2.

SULPHLEX

Five SULPHLEX binders were evaluated during this study. The processing of these binders is discussed in Chapter III. Four of the binders carry the CR designation which identifies them as being produced by CAL-RESIN of Vallejo, California, under the direction of Matrecon, Inc. These binders are CR1, CR2, CR3, and CR5.

The fifth binder was produced at the research annex of Texas A&M University. This binder is identified as 233A.

Table 2 presents pertinent physical properties of the five SULPHLEX binders.

Aggregate Properties

Three types of aggregates were used in this study. A very hard crushed limestone was obtained from White's Mines at a quarry near Brownwood, Texas. This limestone aggregate was the primary aggregate used during the study. Secondary mixture studies were performed using a river gravel and a basalt or traprock.

Table 1. Characteristics of Laboratory Standard Asphalt.

Characteristic Measured	Test Designation	Test Results
Viscosity, 77°F	TEX-527-C	5.8×10^5 poise
Viscosity, 140°F	ASTM D 2171	1570 poise
Viscosity, 275°F	AASHTO T202	3.76 poise
Penetration, 77°F	ASTM D 5	118 dmm
Penetration, 39.2°F	AASHTO T49	26 dmm
Softening Point, Ring and Ball	ASTM D 36	107°F
	AASHTO T53	
Penetration Index	Shell Method	+ 0.25
	Pfeiffer-VanDoornal	- 1.4
Specific Gravity, 77°F	ASTM D 70	1.020
	AASHTO T228	
Ductility, 77°F	ASTM D 113	150+ cm
	AASHTO T44	
Flash Point and Fire Point	ASTM D 92	615°F
	AASHTO T48	695°F
Spot Test	AASHTO T102	Negative
Thin Film Oven Test	ASTM D 1754	68 dmm 150+ cm
Penetration of Residue, 77°F	AASHTO T179	
Ductility of Residue, 77°F		
Hardening Index	Actinic Light Hardening Test	1.9
Vanadium Content	Thermal Neutron Activation Analysis	3.5 ± 0.3 ppm
Solubility in Trichloroethylene	ASTM D 2042	99.9%
	AASHTO T44	

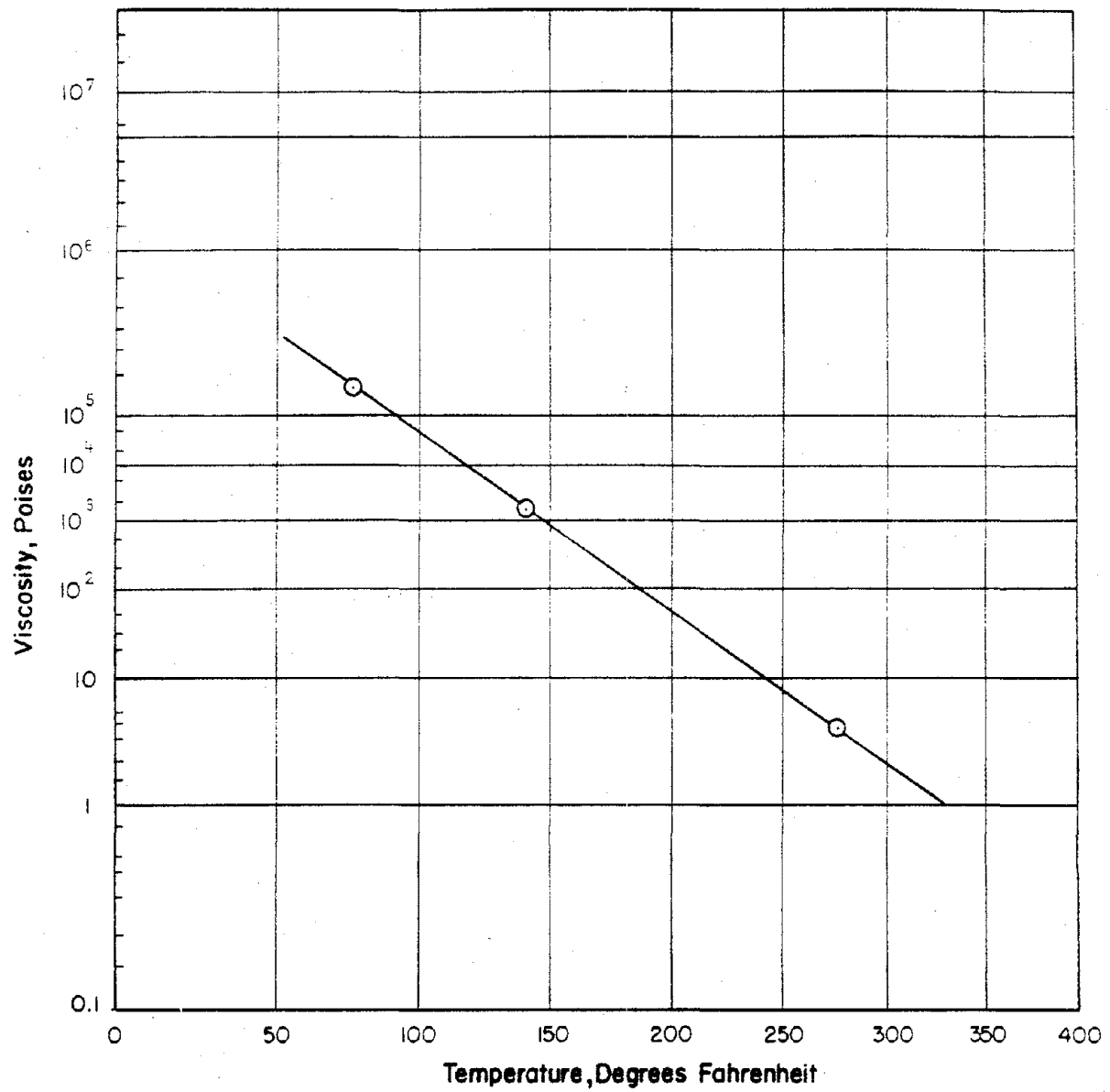


Figure 2. Viscosity - Temperature Relationship for Laboratory Standard Asphalt (AC-10).

Table 2. SULPHLEX Binder Properties.

Test	Binder	Designation	Test Result
Specific Gravity	CR1	AASHTO T288	1.568
	CR2		1.536
	CR3		1.550
	CR5		1.540
	233A		1.537
Penetration @ 77°F	CR1	AASHTO T49	32
	CR2		158
	CR3		29
	CR5		78
	233A		110
Absolute Viscosity @ 140°F, Poises	CR1	AASHTO T202	10,900
	CR2		891
	CR3		12,071
	CR5		2,650
	233A		910
Kinematic Viscosity @ 275°F, cSt	CR1	AASHTO T201	761
	CR2		213
	CR3		581
	CR5		254
	233A		250
Solubility in Chloroform, %	CR1	AASHTO T44	61
	CR2		79
	CR3		76
	CR5		80
	233A		--

Table 2. SULPHLEX Binder Properties (continued).

Test	Binder	Designation	Test Result
Rolling Thin Film Oven Test: % Wt. Loss	CR1	AASHTO T179	2.3
	CR2		3.8
	CR3		--
	CR5		--
	233A		3.92
Thin Film Oven Test: Penetration 77°F	CR1	AASHTO T179	9
	CR2		20
	CR3		--
	CR5		--
	233A		24
Absolute Viscosity 140°F, Poises	CR1		6.65
	CR2		5.76
	CR3		
	CR5		
	233A		
Kinematic Viscosity 275°F, cSt	CR1		1,030
	CR2		890
	CR3		--
	CR5		--
	233A		780

The river gravel is a rounded, silicious gravel obtained from a Gifford-Hill plant near the Brazos River at College Station, Texas.

The basalt is a very dense, very hard aggregate obtained from White's Mines near Knippa, Texas.

Standard sieves (ASTM E 11) were used to separate the aggregates into fractions sized from 3/4 inch to minus No. 200 mesh. Prior to mixing with asphalt, the various aggregate sizes were recombined according to the ASTM D 1663-5A grading specification. The project gradation design for each aggregate type as well as the upper and lower limits of the specification are shown in Figure 3. Standard tests were conducted to determine various physical properties of the aggregates such as specific gravity, absorption capacity, abrasion resistance, and unit weight. One additional test (8) was conducted to estimate the optimum asphalt content. The types of tests and results are presented in Table 3 for the crushed limestone, Table 4 for the rounded gravel, and Table 5 for the basalt.

The gradations selected and presented in Figure 3 represent the gradations which yielded the best composite mixture properties.

Field Specimens

Within this report comparisons are made between the performance of laboratory molded SULPHLEX mixtures composed of SULPHLEX binders fabricated at CAL-RESIN and mixtures actually used in SULPHLEX demonstration projects.

Materials from two demonstration projects were studied: Loop 1604 in San Antonio, Texas, and US Highway 70 near Safford, Arizona. The SULPHLEX binder for both projects was manufactured by Chemical Enterprises, Inc. at their Odessa, Texas, plant. Field cores were taken from Loop 1604 in San Antonio at 0, 0.25, 2, 6, 12, and 24 months after construction. These cores were shipped to Texas A&M for testing and analysis.

Virgin SULPHLEX and limestone aggregate from US Highway 70 Stafford, Arizona, were received at Texas A&M, and specimens were fabricated from these materials in the laboratory. These specimens

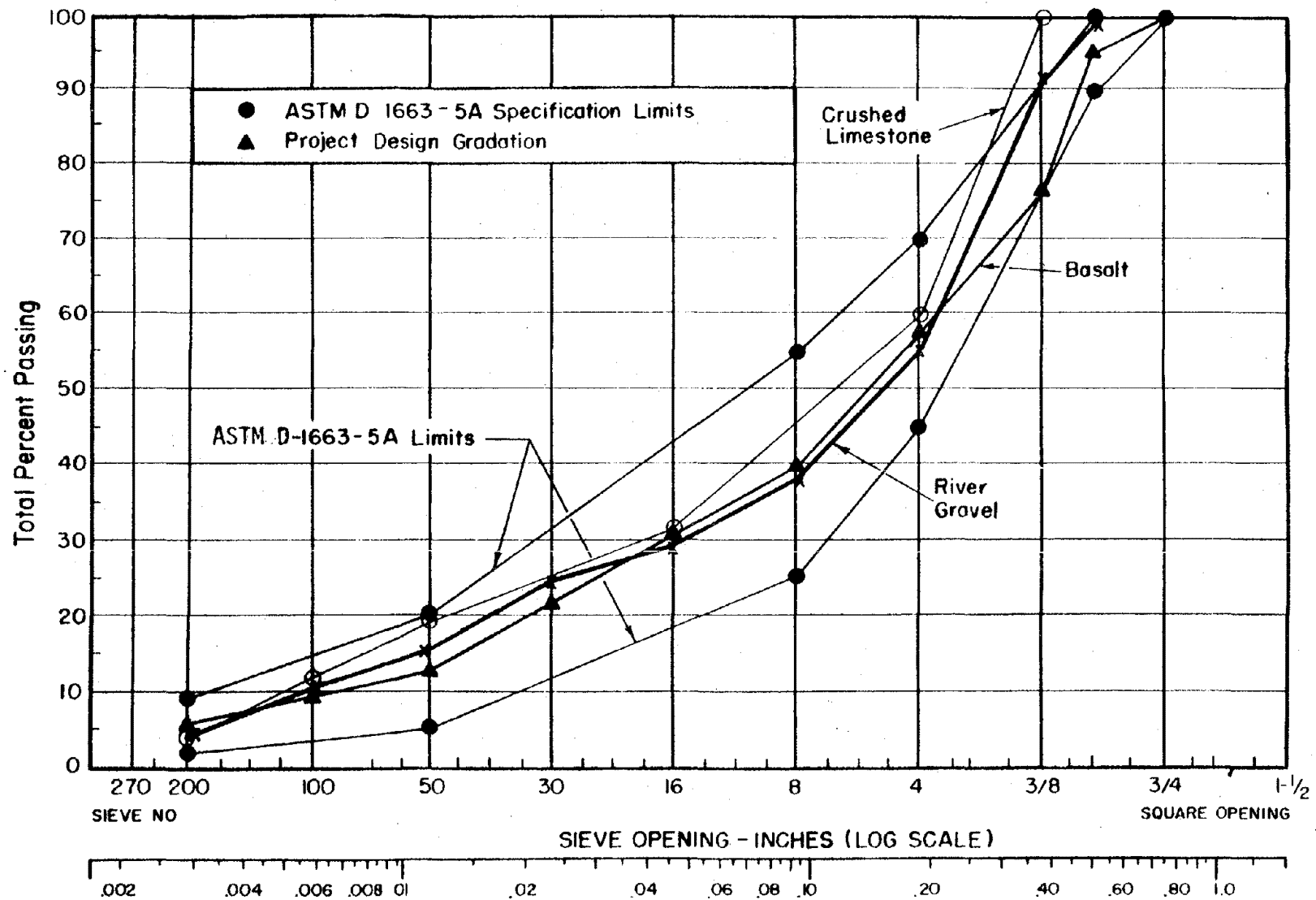


Figure 3. Gradation Curves for Aggregates Used in Mixtures of SULPHLEX.

Table 3. Physical Properties of Crushed Limestone.

Physical Property	Test Designation	Aggregate	Test Results
Bulk Specific Gravity	ASTM C 127 AASHTO T85	Coarse Material*	2.663
Bulk Specific Gravity (SSD)			2.678
Apparent Specific Gravity			2.700
Absorption, percent			0.7
Bulk Specific Gravity	ASTM C 128 AASHTO T84	Fine Material**	2.537
Bulk Specific Gravity (SSD)			2.597
Apparent Specific Gravity			2.702
Absorption, percent			2.2
Bulk Specific Gravity	ASTM C 127 & C 128 AASHTO T84 & T85	Project Design Gradation	2.589
Apparent Specific Gravity			2.701
Absorption, percent			1.56
Abrasion Resistance, percent loss	ASTM C 131 AASHTO T96	Grading C	23
Dry Rodded Unit Weight, pcf	ASTM C 29 AASHTO T19	Project Design Gradation	122
Surface Capacity, percent by wt. dry aggregate	Centrifuge Kerosene Equivalent	Fine Material**	4.1
Surface Capacity, percent by wt. dry aggregate	Oil Equivalent	-3/8 inch to + No. 4	2.3
Estimated Optimum Asphalt Content, percent by wt. dry aggregate	C.K.E. and Oil Equivalent	Project Design Gradation	5.5

* Material retained on No. 4 sieve from Project Design Gradation.

** Material passing No. 4 sieve from Project Design Gradation.

Table 4. Physical Properties of Rounded Gravel.

Physical Property	Test Designation	Aggregate Grading	Test Results
Bulk Specific Gravity			2.621
Bulk Specific Gravity (SSD)	ASTM C 127	Coarse Material*	2.640
Apparent Specific Gravity	AASHTO T85		2.672
Absorption, percent			0.7
Bulk Specific Gravity			2.551
Bulk Specific Gravity (SSD)	ASTM C 218	Fine Material**	2.597
Apparent Specific Gravity	AASHTO T84		2.675
Absorption, percent			1.8
Bulk Specific Gravity			2.580
Apparent Specific Gravity	ASTM C 127 & C 128	Project Design Gradation	2.671
Absorption, percent	AASHTO T84 & T85		1.3
Abrasion Resistance, percent loss	ASTM C 131 AASHTO T96	Grading C	19
Dry Rodded Unit Weight, pcf	ASTM C 29 AASHTO T19	Project Design Gradation	129
Surface Capacity, percent by wt. dry aggregate	Centrifuge Kerosene Equivalent	Fine Material**	3.0
Surface Capacity, percent oil retained by wt. agg.	Oil Equivalent	-3/8 inch to + No. 4	1.8
Estimated Optimum Asphalt Content, percent by wt. dry aggregate	C.K.E. and Oil Equivalent	Project Design Gradation	4.7

* Material retained on No. 4 sieve from Project Design Gradation.

** Material passing No. 4 sieve from Project Design Gradation.

Table 5. Physical Properties of Crushed Basalt (Traprock).

Physical Property	Test Designation	Aggregate Grading	Test Results
Bulk Specific Gravity	ASTM C 127 AASHTO T85	Coarse Material*	2.960
Bulk Specific Gravity (SSD)			2.980
Apparent Specific Gravity			3.010
Absorption, percent			0.7
Bulk Specific Gravity	ASTM C 218 AASHTO T84	Fine Material**	2.911
Bulk Specific Gravity (SSD)			2.939
Apparent Specific Gravity			2.998
Absorption, percent			1.1
Bulk Specific Gravity	ASTM C 127 & C 128 AASHTO T84 & T85	Project Design Gradation	2.925
Apparent Specific Gravity			2.950
Absorption, percent			0.9
Abrasion Resistance, percent loss	ASTM C 131 AASHTO T96	Grading C	16
Compacted Unit Weight, pcf	ASTM C 29 AASHTO T19	Project Design Gradation	145
Surface Capacity, percent by wt. dry aggregate	Centrifuge Kerosene Equivalent	Fine Material **	4.0
Surface Capacity, percent oil retained by wt. agg.	Oil Equivalent	-3/8 inch to + No.4	2.1
Estimated Optimum Asphalt Content, percent by wt. dry aggregate	C.K.E. and Oil Equivalent	Project Design Gradation	5.4

* Material retained on No. 4 sieve from Project Design Gradation.

** Material passing No. 4 sieve from Project Design Gradation.

were fabricated to represent, as closely as possible, the material placed in the field. Of course, every attempt was made to achieve binder contents and realistic air void contents when compared to the field mixture.

Laboratory Testing

Laboratory testing of all mixtures was performed in accordance with standardized procedures.

Table 6 presents the references to the test procedures used in this study. Where applicable either ASTM, AASHTO, or FHWA publications are referenced.

Table 6. A Summary of the Test Procedures Followed in this Study of the Engineering Characterization of SULPHLEX Mixtures.

<u>Test Category</u>	<u>Test Name</u>	<u>Test Properties or Material Properties of Significance</u>	<u>Test Procedures Used</u>
Mixture Design	Marshall Stability	Marshall Stability	ASTM D 1559
		Marshall Flow	ASTM D 1559
	Bulk Density	Bulk Density	ASTM D 2726
	Specific Gravity	Maximum Gravity	ASTM D 2041
	Void Content	Air Voids	Asphalt Institute, Ref. 9.
		VMA	Asphalt Institute, Ref. 9.
Modulus	Diametral Resilient Modulus	Resilient Modulus	Ref. 10, pp. 66-69
	Flexural Fatigue	Flexural Modulus	Ref. 11, pp. 82-86 VESYS Users Manual, Ref. 12.
	Indirect Tensile	Initial Tangent Modulus	Ref. 13, pp. 29-42 and pp. 68-70 Ref. 14.
Deformation	Creep	Creep Compliance	VESYS Users Manual, Ref. 12.
	Permanent Deformation	α , μ , S , I and ϵ_r	VESYS Users Manual, Ref. 12.
	Shell Method	Deformation	Shell Pavement Design Manual, Ref. 15.
Strength	Unconfined Compressive Strength	Compressive	AASHTO T-165, T-167
	Indirect Tensile Test	Ultimate Tensile Strength and Ultimate Tensile Strain	Ref. 13.
	Beam Fatigue	N_f , K_1 , K_2 and Repeated Strain	Ref. 11, pp. 82-86 and VESYS Users Manual
	Fracture Mechanics Based Testing	J^* , dc/dN , A , and n	Ref. 12.

Table 6. A Summary of the Test Procedures Followed in this Study of the Engineering Characterization of SULPHLEX Mixtures (continued).

<u>Test Category</u>	<u>Test Name</u>	<u>Test Properties of Material Properties of Significance</u>	<u>Test Procedures Used</u>
Moisture Effects	Lottman Procedure	Strength Loss Due to Moisture	Ref. 16 and Ref. 17
	Vacuum Saturation and Soak	Strength Loss Due to Moisture	Ref. 17

CHAPTER III

NATURE OF SULPHLEX

Background

In June of 1980 Southwest Research Institute reported the development of three formulations of plasticized sulfur binders called SULPHLEX. These three binders were selected from the testing of approximately 450 different formulations of elemental sulfur and plasticizers. SULPHLEX is a trade name for a family of pavement binders composed of chemically modified sulfur. The results of the Southwest Research Institute Investigation are contained in reference 18.

It was initially recognized that if sulfur were to be used as a pavement binder, it would have to exhibit more plastic characteristics. The term plasticized sulfur is often used to describe the modification of sulfur to achieve the characteristics of flexibility, workability, and extensibility.

It has long been known that when elemental sulfur is heated to above its transition temperature and rapidly quenched it exhibits a plastic character. However, the material quickly hardens with the formation of orthorhombic S_8 sulfur crystals. Evidence exists that above 320°F molten sulfur consists of a mixture of S_8 rings and S_x chains where the value of x can be very large. Exactly how the plasticization occurs at this point is uncertain and speculative. In any case the mechanism of plastic sulfur is brought about by a physical change that does not lend itself to practical application in the preparation of binders for paving.

What must be done to retain the desirable behavior of the plasticized sulfur is to convert the sulfur to a plastic by a chemical reaction, a mechanical change, or a combination of these. Prior to the research performed for the Federal Highway Administration by Southwest Research, efforts at plasticization had dealt with a single additive. The SULPHLEX mixtures are based on the reaction of multiple additives with elemental sulfur. Once reacted, all of the SULPHLEX formulations resemble asphalt in terms of their handling characteristics.

This research effort will investigate the 233 binder, which was reported to possess properties similar to asphalt concrete both during the construction process and in the pavement layer.

Composition and Chemistry

SULPHLEX 233 is a manufactured product. Specifically, molten, elemental sulfur is reacted in a vessel at 300°F with a blend of plasticizers or chemical modifiers: dicyclopentadiene (DCPD), vinyl toluene, and dipentene. The formulation for the 233 binder is 70 percent by weight of elemental sulfur, 12 percent DCPD, 10 percent dipentene, and 8 percent vinyl toluene.

Raw Materials and Formulation

At the beginning of this project it was agreed that work should be started with the SULPHLEX 233 formulation and preparation procedure, and that the raw materials used in the preparation of laboratory and pilot plant batches should be as pure as possible from commercial sources.

The chemical structures of the reactants of SULPHLEX 233 are shown in Figure 4. Two of the reactants, DCPD and dipentene, are diolefins which have two double bonds for potential reaction with sulfur. Vinyl toluene has one double bond. The specific materials that were selected for use in this project are listed in Table 7. All of these ingredients, except the dipentene, are of relatively high purity. The specific dipentene used in this work has the highest purity of the dipentenenes that are commercially available.

Process Variables

The SULPHLEX production process requires considerable study of the variables that are involved in order that specifications can be set and reproducible products can be made. In the case of SULPHLEX 233, four raw materials are involved which can interact with each other in a variety of ways, depending on the reaction conditions. The

Table 7. Sources and Purity of Raw Materials Used in The Preparation of SULPHLEX 233.

Reactant	Trade Name	Purity, %	Source
Sulfur	Anchor Velvet Flowers of Sulfur Sublimed sulfur N.F.	99.8	Stauffer Chemical
Dicyclopentadiene	Dicyclopentadiene	97	Exxon Chemical
Dipentene	ACINTENE ^R DP	68	Arizona Chemical
Vinyl toluene	Vinyl toluene	<u>ca.</u> 100	Dow Chemical

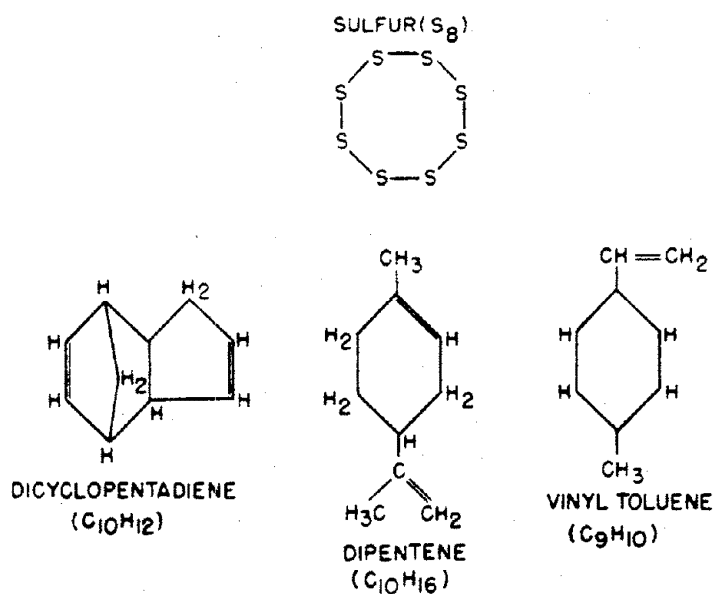


Figure 4. Structures of SULPHLEX Raw Materials.

variations in properties among different lots of SULPHLEX 233 are very apparent (18; 19). Without changing the basic formulations there are a number of variables involved, such as (19):

1. Temperature.
2. Time.
3. Pressure.
4. Stirring.
5. Reactor size.
6. Order of addition of raw materials.
7. Slight deviations in the ratios of the reactants in the charge.

A systematic study of these variables is reported in a companion report (1). The results pertinent to this study and to the selection of binders studied will be discussed briefly in the following paragraphs.

Variations in Temperature and Time of Reaction

The effects of temperature and time of preparation on the penetration, specific gravity, and viscosity of the SULPHLEX are shown in Table 8.

At 284⁰F and 302⁰F it is generally true that the longer the reaction time, the lower the penetration and the higher the specific gravity and viscosity. The data for the 338⁰F preparations became increasingly more scattered with the increases in the batch size. It appears that since the reaction is faster at 338⁰F, there is less change between 2.5 hours and 6.5 hours than at the lower temperature.

In general, the well-reacted samples made at low temperatures have lower penetration and higher viscosities than those made at higher temperatures.

The initial scale syntheses of SULPHLEX 233 at 338⁰F indicated that a total reaction time of 6.5 hours was probably more than adequate for complete reaction of the sulfur and olefins. However, to

Table 8. Properties of SULPHLEX 233 Made at Various Temperatures and Reaction Times.

Run Number	Total Reaction Time, Hours	Penetration at 77°F	Specific Gravity	Viscosity at 275°F	
				Centistokes	Centipoises
Prepared at 284°F					
M-9-1	2.5	>248	1.529	84	129
M-9-4	4.5	96	1.538	179	276
M-9-2	6.5	54	1.544	337	521
M-9-3	12.5	19	1.548	817	1,270
Prepared at 302°F					
M-2	0.5	(a)	1.516	33.8	51
M-3	2.5	52	1.541	357	550
M-6-1	6.5	28	1.548	604	935
M-6-5 ^b	6.5	28	1.540	518	829
M-CR-1 ^c	6.5	34	1.568	671	1,050
Prepared at 338°F					
M-4	0.5	(a)	1.530	81	124
M-5	2.5	93	1.540	280	432
M-7	6.5	92	1.544	297	459
M-7-5 ^b	6.5	109	1.544	265	410
M-CR-2 ^c	6.5	165	1.536	213	323

^aToo soft to measure.

^bLarge laboratory runs (approximately one-gallon).

^cTwelve-gallon batches run at Cal-Resins.

confirm this a sample was aged at 338°F under nitrogen and monitored for a change in viscosity as a measure of continued reaction. Essentially no change occurred after 24 hours. However, if the sample is held at 338°F for 96 hours there is a sharp rise in viscosity which is probably due to polymerization of the product.

The effects of preparation temperature on the properties of SULPHLEX are discussed in Reference 1. From that part of the study it was found that the molecular weight determinations showed that SULPHLEX made at lower temperatures has more high weight fractions and less free sulfur than that made at 338°F. The studies of plasticization stability showed that the rate of crystallization of sulfur is greatest in samples prepared at 338°F. SULPHLEX made at 284°F is higher in viscosity and less prone to crystallization than SULPHLEX 233 made at higher temperatures (1).

SULPHLEX 233 prepared at 338°F is a very different product from SULPHLEX 233 prepared at 284°F or 302°F (all products with a 6.5 hour reaction time). The product prepared at 338°F is more thermally stable as it changes less upon further heating. However, the product is initially low in viscosity (as compared to products produced at lower temperatures), but much of the free sulfur soon crystallizes resulting in a hard product that remains unchanged on further standing. From the hardness of the crystallized material, the 338°F product would seem to produce a paving material more like portland cement than asphalt concrete (1).

The SULPHLEX 233 made at lower temperatures, 284 or 302°F, is more like asphalt. Initially it is more viscous than the 338°F product, but on storage at room temperature it remains a viscous, one-phase product much longer. This indicates that the free sulfur crystallizes out more slowly. The product made at the lower temperatures is not as thermally stable in the sense that on further heating the properties change and approach those of the 338°F product.

Selection of Binders for Analysis

Five SULPHLEX binders were included in the mixture testing and characterization program. Four of the five binders were fabricated by

Cal-Resin of Vallejo, California, under the supervision of Matrecon, Inc. The fifth binder was produced at Texas A&M University. This binder, SULPHLEX 233A, is similar to the SULPHLEX binders which were ultimately used in the SULPHLEX pavement construction projects throughout the United States.

The formulations and processing conditions of all five binders are shown in Table 9.

Preparation of Binders

Binder preparation is briefly discussed in Appendix B.

Table 9. Formulation and Processing Conditions for SULPHLEX Binders Analyzed in this Study.

Binder Identification	Formulation	Reaction Temperature, °F	Reaction Time, Hours	Penetration at 77°F, (1 day old), dmm	Viscosity at 275°F, (1 day old), poises
CR1	68% Sulfur 12% DCPD ** 12% DP *** 8% Vinyl Toluene SULPHLEX Catalyst (1% of mix)	302	6.5	35	10.2
CR2	70% Sulfur 12% DCPD 10% DP 8% Vinyl Toluene SULPHLEX Catalyst (1% of mix)	338	6.5	165	4.0
CR3	70% Sulfur 12% DCPD 10% DP 8% Vinyl Toluene SULPHLEX Catalyst (1% of mix)	302	6.5	22	5.8
CR5	70% Sulfur 12% DCPD 10% DP 8% Vinyl Toluene SULPHLEX Catalyst (1% of mix)	320	6.5	78	2.5
233A	68% Sulfur 12% DCPD 10% Solvenol 10% Vinyls Toluene SULPHLEX Catalyst (1% of mix)	300-350	4.5	40	11.0

* Expressed as percent by weight. **DCPD = Dicyclopentadiene ***DP = Dipentene

CHAPTER IV

MIXTURE DESIGN METHODS AND MIXTURE OPTIMIZATION

Background

A pressing need in the development of SULPHLEX as a binder material for paving mixtures is the definition of desirable SULPHLEX mixture properties and development of a mixture design method which will assure that, within acceptable levels of risk, these desirable properties will be achieved.

Monismith (2) has defined six desirable mix properties which are essential for an asphalt paving mixture for a specific application. These properties are: (1) stability, (2) durability, (3) flexibility, (4) skid resistance, (5) perviousness, and (6) workability.

Stability is defined as the resistance of the mixture to deformation under load and can be considered as the load or stress to cause a certain amount of deformation or strain, this deformation or strain depending upon expected field conditions.

Durability of a paving mixture is defined as its resistance to weathering and the abrasive action of traffic. Included under the effects of weathering are (1) changes in the characteristics of the asphalt and (2) changes in the mixture due to the action of water.

Flexibility is defined as either (1) the ability of the mixture to conform to long-term variation in base and subgrade elevations or (2) the ability of the paving mixture to bend repeatedly without fracture.

Skid resistance is the ability of an asphalt paving mixture to provide a surface, under all environmental conditions, that will embody sufficient friction to allow a vehicle to stop within a reasonable distance. High skid resistance in asphalt paving mixtures is generally promoted by the same factors which promote high stability, i.e., proper asphalt contents and aggregates with rough, wear-resistant surfaces.

Permeability or perviousness of an asphalt mixture is concerned with the ease with which air, as well as water, may pass into or through the mixture. Of course, both the nature and the quantity of voids affect the permeability.

Workability is that characteristic of a paving mixture that results in a smooth-finished surface texture when placed and compacted.

Certainly, SULPHLEX mixtures, like asphalt mixtures, must provide acceptable levels of the properties just mentioned. However, the question of acceptance criteria is what becomes critical. Asphalt concrete and SULPHLEX mixtures, as will be shown in this report, are quite different in certain aspects of their engineering responses. In other words, the acceptance criteria for asphalt concrete should not be applied indiscriminately to SULPHLEX mixtures.

The basic philosophy of asphalt mix design was summarized by Monismith (20) as follows: "As much asphalt as possible should be incorporated with a given aggregate to insure a durable, water-resistant mixture that will be flexible, but not so much asphalt that the stability of the mix will be reduced below some minimum desirable value consistent with loading and environment." Once again the same basic statement should reasonably apply to mix designs that utilize SULPHLEX as the binder. The question is, what are the criteria which may be applied to laboratory mix design, which define acceptable stability, flexibility, and durability.

A prime example of how the different nature of SULPHLEX and asphalt may affect mixture design is the way SULPHLEX ages due to environmental effects. Asphalt is very sensitive to aging due to oxidation. The oxidative process obviously occurs most rapidly when the asphalt is accessible to air. Concomitant with this may be the degradation of the asphalt by water which may result in stripping of the asphalt cement from the aggregate surface and removal by leaching action. To reduce the potential for this degenerative action, densely graded asphalt mixture designs usually require air voids ranging from three to five percent. Since SULPHLEX ages quite differently than asphalt and its hardening is apparently not accelerated by the accessibility of air, the air void target requirement of three to five percent may be questionable.

Research Approach

The approach to the development of a mixture design procedure for SULPHLEX and for the optimization of SULPHLEX mixtures was to (1) evaluate the validity of the traditional approaches to mixture design when these approaches were used in designing SULPHLEX mixtures and (2) search for a design procedure founded on fundamentally sound theory and based on mixture properties.

However, before either principle objective could be realized, it was necessary to carefully evaluate the effects of variation in laboratory mixture fabrication factors on SULPHLEX. To achieve this objective, a factorial experiment was designed.

Sensitivity to Fabrication Variables

Of perhaps as much importance as the engineering properties of SULPHLEX mixtures is the suitability of SULPHLEX as a binder to be used in a batch or drum dryer plant operation to produce paving mixtures that can be placed and compacted by conventional equipment.

If variations in the laboratory mixture fabrication process affect SULPHLEX mixtures more than similar variations affect a common mixture property in asphalt concrete, then the sensitivity should be accounted for in the fabrication process. For example, laboratory mix design equipment and compaction processes attempt to duplicate field densities after about two to three summers of traffic. This may not be true for SULPHLEX mixtures.

A factorial experiment was designed which considers the following mixture fabrication factors and interactions of factors:

1. Method of compaction
 - a. Impact type (Marshall hammer)
 - b. Kneading type compaction (as used in many Hveem procedures)
2. Level of compaction energy
 - a. High level of energy
 - b. Low level of energy

3. Mixing temperatures
 - a. High temperature (295°F)
 - b. Low temperature (265°F)
4. Binder type
 - a. SULPHLEX: CR1 and CR2
 - b. Asphalt cement: AC-10.

The factorial format of these factors and interactions is illustrated in Table 10. The philosophy behind the approach was that if the SULPHLEX mixtures exhibited more sensitivity to any of the independent variables (factors) than the asphalt concrete mixtures, then special consideration should be given to that variable in the development of the mixture design procedure. On the other hand, if sensitivities to these variables were similar between the asphalt concrete and SULPHLEX mixtures, then the sample fabrication methods used for asphalt concrete could be confidently extended to SULPHLEX.

The selection of the independent variables in Table 10 was based on experience. These factors are considered the most critical in the fabrication process. For example, the different physical and chemical nature of SULPHLEX (as compared to asphalt cement) may cause the effects of kneading compaction to be more critical than for asphalt concrete, and certainly the level of compactive effort and temperatures of mixing may be critically important for the same reason.

The mixing temperatures selected for the sensitivity analysis were based on the viscosity-temperature relationships for the binders (AC-10, CR1 and CR2). These temperatures represent the maximum practical limits. All mixture compaction was performed within the range of 260 to 270°F.

Several dependent variables were used to evaluate the effects of the independent variables on mixture properties. These were: (1) resilient modulus at 32, 77, and 104°F, (2) Marshall stability, (3) Marshall flow, (4) Hveem Stability, (5) air void content and (6) moisture susceptibility.

The computer system for data analysis "Statistical Analysis Systems" (SAS) was used to store, catalog, and analyze data from the factorial experiment. The statistical procedure General Linear Models

Table 10. Factorial Analysis of Factors which Affect the Mixture Fabrication Process.

Mixing Temperature, °F	Level of Compaction	Compaction Method	Binder Type*	CR1		CR2		AC-10	
				Impact	Kneading	Impact	Kneading	Impact	Kneading
265	low			3**	3	3	3	3	3
	high			3	3	3	3	3	3
295	low			3	3	3	3	3	3
	high			3	3	3	3	3	3
265	low			3	3	3	3	3	3
	high			3	3	3	3	3	3
295	low			3	3	3	3	3	3
	high			3	3	3	3	3	3

* Each binder was mixed with crushed limestone aggregates in this sensitivity analysis.

** Number of replicate specimens tested for each condition.

(GLM), a form of analysis of variance, was used to analyze the data. In each case the effect of the independent variables and interactions of variables on the dependent variables were evaluated for the following cases:

1. Independent variable effects between AC-10 and CR1.
2. Independent variable effects between AC-10 and CR2.
3. Independent variable effects between CR1 and CR2.
4. Independent variable effects within each binder.

Obviously, this study resulted in an enormous volume of data to be digested and analyzed. A summary of the results of the analysis of variance of the factorial study is presented in the following paragraphs. A level of significance of 0.05 was used to identify statistically significant effects.

The dependent variables of resilient moduli at 32, 77, and 104°F were the most sensitive indicators of the effects of variations in the levels of the independent variables considered. Table 11 summarizes the results of the Duncan Multiple Range test based on resilient modulus as the measure of sensitivity. Duncan Multiple Range test is an analysis of variance technique which groups means which are not significantly different ($\alpha = 0.05$) and separates them from means which are statistically different.

When analyses similar to those summarized in Table 11 for the other independent variables were cumulatively digested, it was apparent that the asphalt concrete mixtures were more sensitive to the fabrication variables than were the SULPHLEX mixtures. The only exception was the dependent variable M_R at 104°F which revealed more sensitivity of the SULPHLEX binders than for the asphalt binder to the type of mixing. However, even though the differences reflected here were significant, they were not large differences.

The following conclusions were drawn from the sensitivity to fabrication variables analysis:

1. Asphalt concrete mixtures are generally at least as sensitive to the fabrication variables as are SULPHLEX mixtures.
2. A mixing temperature of between 285 to 290°F is recommended for SULPHLEX. Lower temperatures may result in substantially lower stiffnesses at the higher test temperatures of 77 and 104°F.

Table 11. Duncan Multiple Range Summary for the Dependent Variable Resilient Modulus at 32, 77 and 104°F as a Measure for the Effects of Fabrication Variables.

Binder	Dependent Variable	Independent Variable	Is Difference Significant at $\alpha = 0.05$?
AC	M_R @ 32°F	Compaction Method	yes
		Compaction Effort	yes
		Mixing Temperature	no
CR1	M_R @ 32°F	Compaction Method	yes
		Compaction Effort	no
		Mixing Temperature	no
CR2	M_R @ 32°F	Compaction Method	no
		Compaction Effort	no
		Mixing Temperature	no
AC-10	M_R @ 77°F	Compaction Method	no
		Compaction Effort	no
		Mixing Temperature	yes
CR1	M_R @ 77°F	Compaction Method	no
		Compaction Effort	no
		Mixing Temperature	yes
CR2	M_R @ 77°F	Compaction Method	no
		Compaction Effort	yes
		Mixing Temperature	yes
AC-10	M_R @ 104°F	Compaction Method	no
		Compaction Effort	no
		Mixing Temperature	no
CR1	M_R @ 104°F	Compaction Method	yes
		Compaction Effort	no
		Mixing Temperature	yes
CR2	M_R @ 104°F	Compaction Method	yes
		Compaction Effort	yes
		Mixing Temperature	yes

3. Based on resilient modulus at 104°F, SULPHLEX is more sensitive to the method of compaction than is asphalt concrete. Kneading-type compaction produces significantly stiffer mixtures at a testing temperature of 104°F.
4. Asphalt concrete and SULPHLEX demonstrated similar sensitivity to the other fabrication factors.

Based on the sensitivity analysis it was decided that both SULPHLEX and asphalt concrete mixtures would be prepared in accordance with the following guidelines:

Compaction method : Kneading type or gyratory
Compaction energy : Standard
Mixing temperature : 285 to 290°F

Selection of Mixture Design Method

The Marshall Method

The Marshall and Hveem methods of laboratory mixture design were considered for design of SULPHLEX mixtures. The Hveem method was not pursued extensively as the sensitivity analysis to mixture fabrication variables revealed Hveem stability to be much less sensitive to the independent variables studied than was Marshall stability.

The approach to the analysis of the acceptability of the Marshall test method was to evaluate Marshall test data over a range of binder contents for SULPHLEX binders CR1 and CR2 and for the control mixture, asphalt concrete. In the analysis, asphalt cement percentages ranged from four to eight percent by weight of mixture and SULPHLEX binder contents ranged from four to twelve percent by weight of mixture.

Based on Figures 5 through 8 several observations may be made:

1. Marshall stabilities of SULPHLEX mixtures are higher than those of the corresponding asphalt concrete mixtures. These differences may be quite substantial.
2. Asphalt concrete mixtures have a more well-defined peak at optimum binder content, while SULPHLEX seems to be less

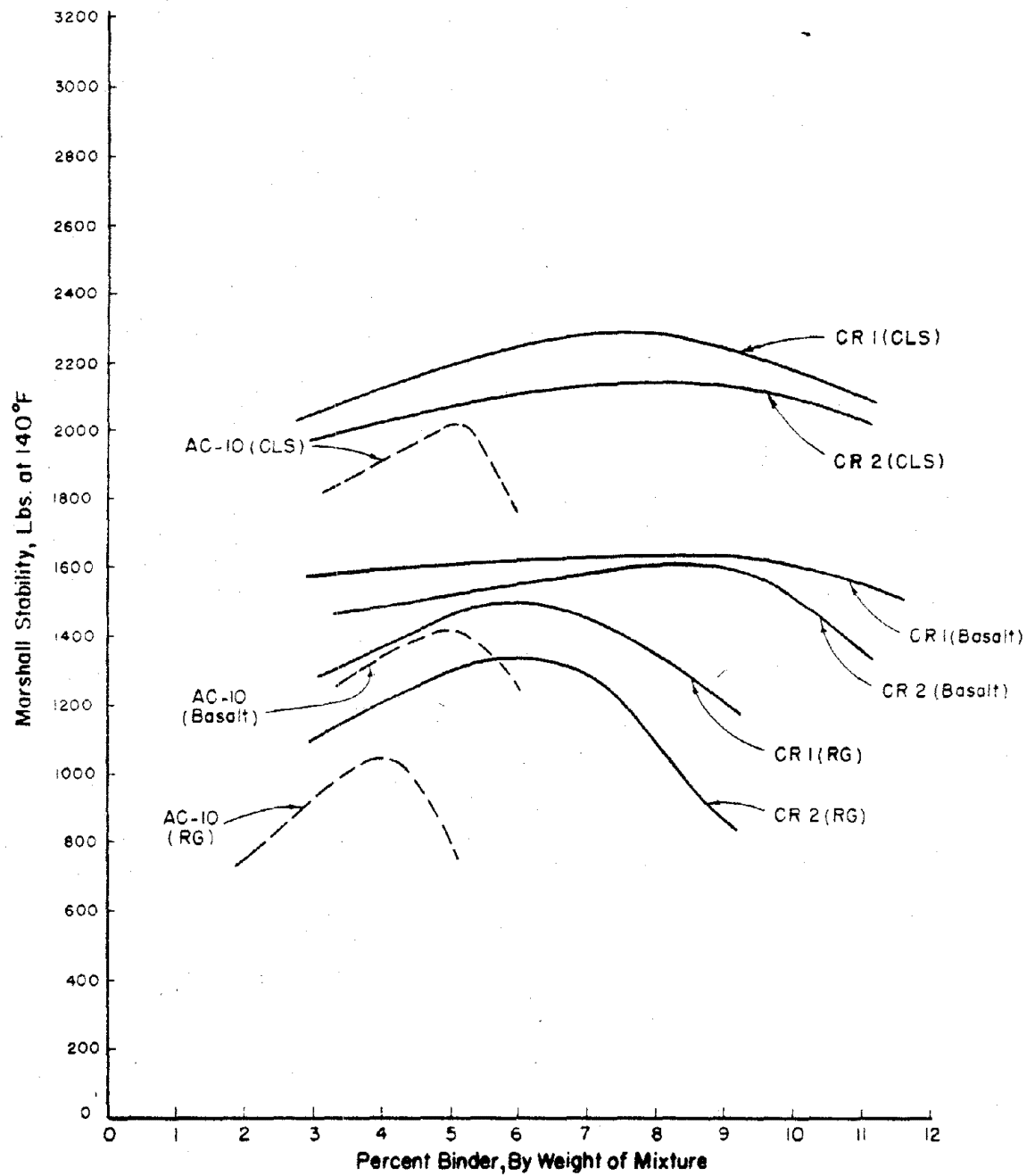


Figure 5. Marshall Stability Versus Binder Content for Mixtures Tested.

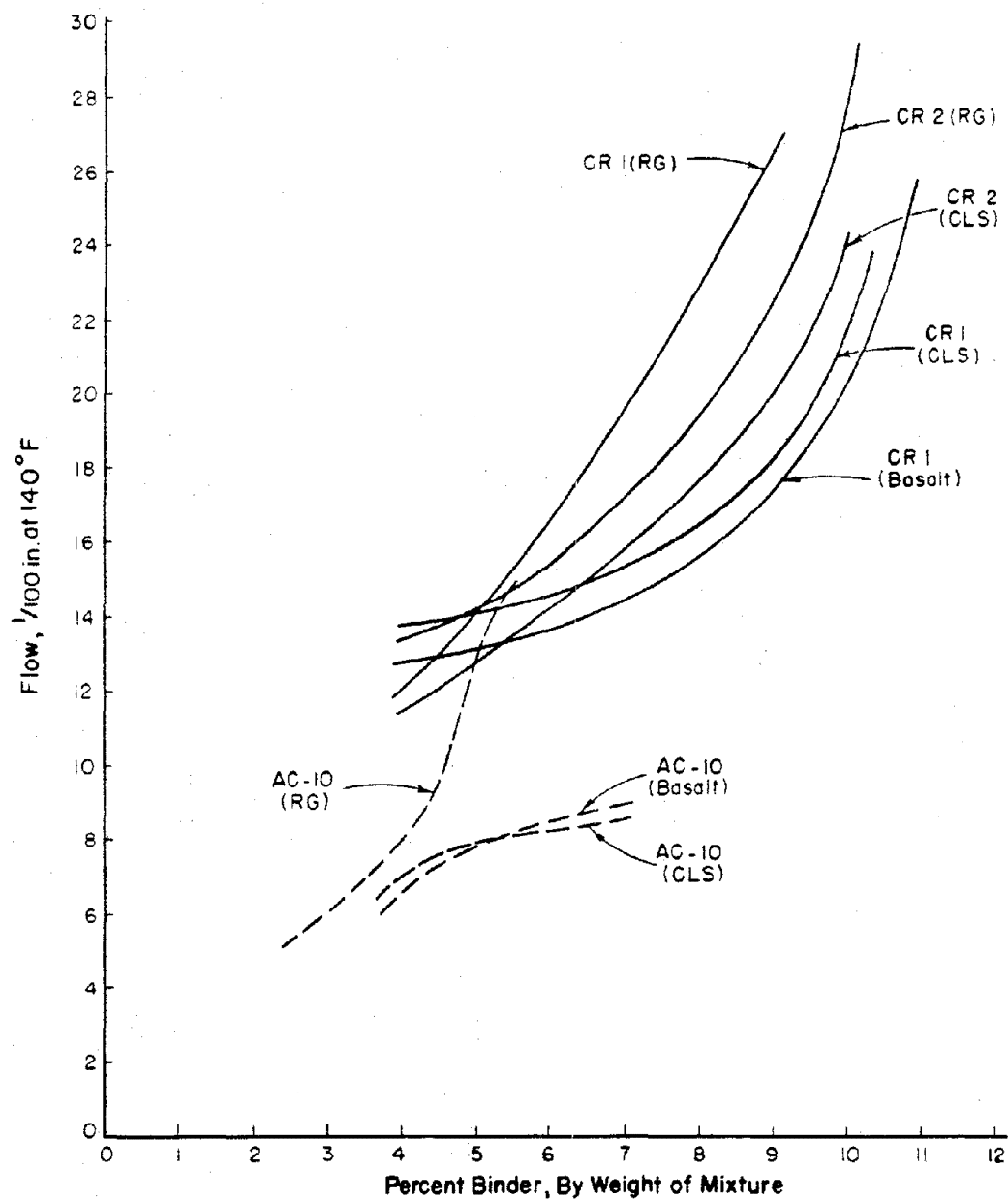


Figure 6. Marshall Flow Versus Binder Content for Mixtures Tested.

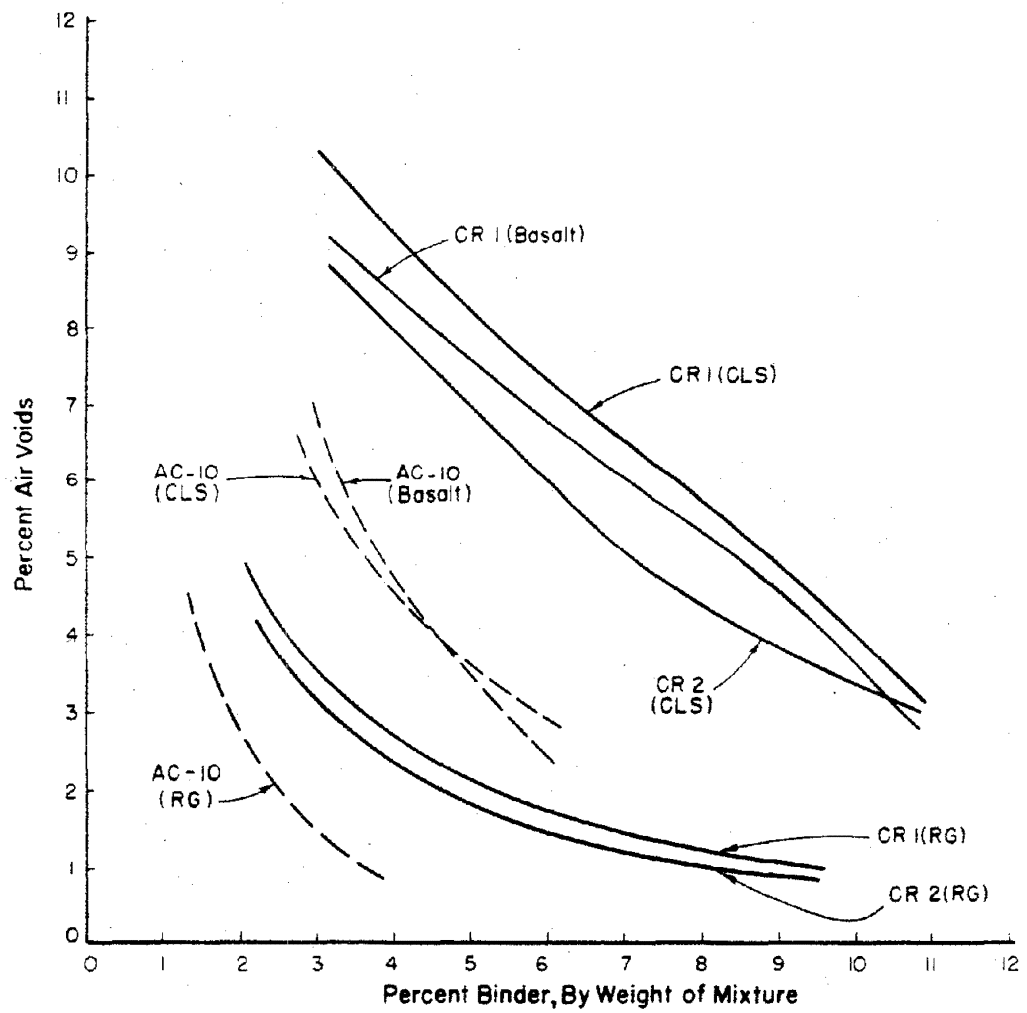


Figure 7. Percent Air Voids Versus Binder Content for Mixtures Tested.

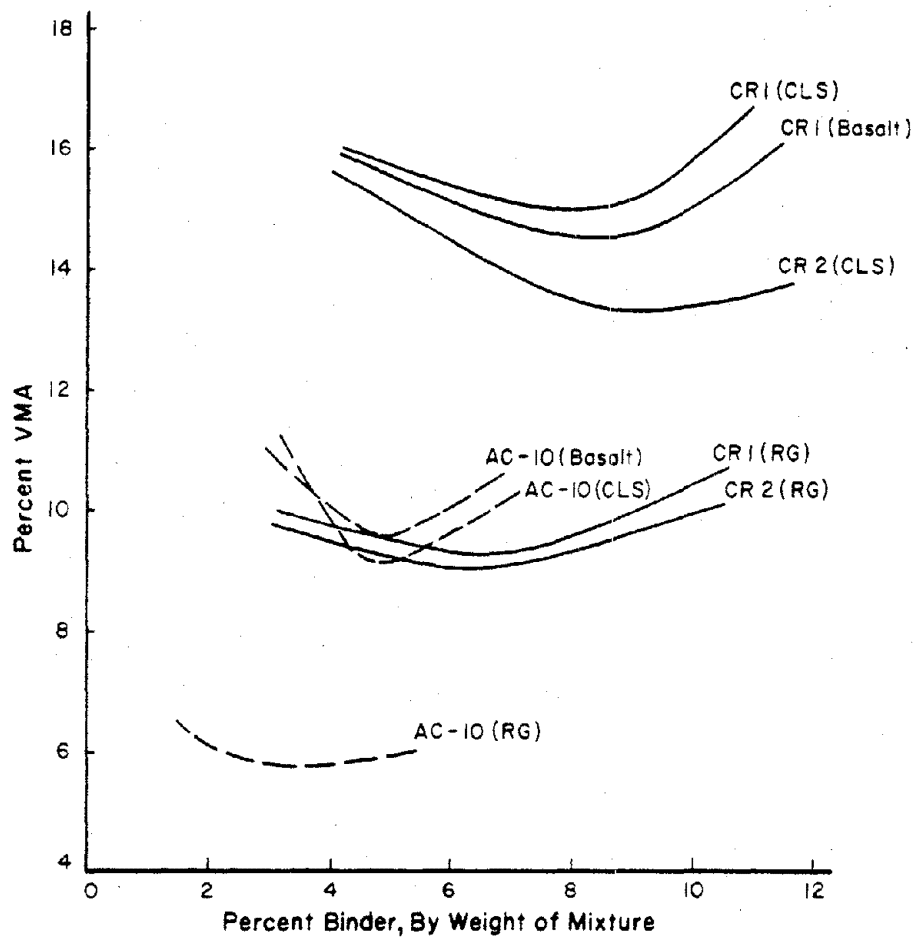


Figure 8. Percent Voids in Mineral Aggregate, VMA, for Mixtures Tested.

sensitive to the binder content. This is true especially for the limestone and basalt aggregates which are not as dense as the river gravel aggregate.

3. The level of stability for SULPHLEX is quite satisfactory for each mixture indicating a strong, stable mixture in each case.
4. In the region of peak Marshall stability, flows for SULPHLEX mixtures are generally beyond the boundaries established for conventional asphalt concrete mixtures by the Asphalt Institute (9), i.e., 8 to 16 for heavy traffic. The flows for the various SULPHLEX systems selected from Figure 6 are as follows:

<u>SULPHLEX Mixtures</u>	<u>Binder Content at Peak Stability, %</u>	<u>Corresponding Flow, 1/100 in</u>
CR1 (CLS)	8	18
CR2 (CLS)	8	17
CR1 (RG)	6	17
CR2 (RG)	6	15
CR1 (Basalt)	9	18

These flow values are approximately twice those for the corresponding asphalt mixture at equal binder contents by volume. (Since the specific gravity of SULPHLEX is approximately 1.54, the weight percentage of SULPHLEX which provides an equal volume percentage when compared to asphalt cement can be obtained by multiplying the optimum asphalt cement weight percents by 1.54, Figures 5 to 8).

On the basis of the Marshall curves in Figures 5 through 8, the respective optimum binder contents are as shown in Table 12.

SULPHLEX mixtures can be tailored to meet criteria established for asphalt concrete. However, the applicability of these criteria are questionable. For example, SULPHLEX when replacing asphalt cement in a selected mixture at approximately equal portions by volume can provide highly satisfactory stability as well as satisfactory air void

Table 12. Optimum Binder Contents for All Mixtures Based on Marshall Test Method.

Mixture Identification	Weight percent at Maximum Density	Weight percent at Maximum Stability	Weight percent at 4% Air Voids	Optimum percent by Weight	Optimum percent by Volume
AC-10 (CLS)	5.0	5.0	4.7	4.9	11.1
AC-10 (RG)	3.5	4.0	2.0	3.5	8.4
AC-10 (Basalt)	5.1	5.3	4.6	5.0	11.2
CR1 (CLS)	8.3	7.9	9.5	8.5	12.4
CR1 (RG)	5.9	5.9	2.1	5.5	8.3
CR1 (Basalt)	8.9	9.1	9.6	9.2	13.2
CR2 (CLS)	8.7	8.5	8.9	8.7	12.6
CR2 (RG)	5.8	6.0	2.1	5.8	9.1
CR2 (Basalt)	8.9	8.7	8.9	8.8	12.7
CR3 (CLS)	8.7	8.4	8.7	8.6	12.5
CR3 (RG)	5.6	6.0	2.1	5.5	8.2
CR3 (Basalt)	8.7	8.6	8.7	9.0	13.1
CR5 (CLS)	8.6	8.4	8.9	8.7	12.7
CR5 (RG)	5.7	6.1	2.2	5.6	8.2
CR5 (Basalt)	8.7	8.7	8.8	9.0	13.2

content and VMA content. However, the concomitant flows are excessive when compared to those developed with the asphalt cement or compared to Marshall mixture designs criteria. Therefore, how to account for the high flow values is a difficult question. Should different criteria be used for SULPHLEX than for asphalt concrete?

Lentz and Harrigan (21) state that Marshall criteria were empirically developed based on the performance of asphalt concrete pavements. It may not be desirable or necessary to use the same criteria for selection of SULPHLEX content in a mixture.

Lentz and Harrigan (21) also add another point worthy of thoughtful consideration. While it is necessary to keep the air void content low for asphalt concrete in order to prevent excessive hardening of the asphalt cement with a resultant loss in durability, the hardening of SULPHLEX appears to be independent of its exposure to air or water. Therefore, since it will harden irrespective of its exposure to air or water and may have already done so by the completion of the mixing process, it may be inappropriate to apply the maximum air void criterion of the Marshall mix design method.

It is impossible to either endorse or reject the Marshall design procedure for SULPHLEX when a decision must be made during a very short period of time without field performance verification. However, it certainly is possible to make educated engineering judgements based on the knowledge of SULPHLEX acquired during this study. Because SULPHLEX is quite different from asphalt in terms of its aging or hardening characteristics and because it possesses certain unique rheological characteristics (i.e., higher glass transition temperature than asphalt, linear amorphous polymeric response at long durations of loading, high Marshall stability yet high Marshall flows at 140°F, etc.), a modified or even a unique mixture design method is needed for SULPHLEX.

A Unique Approach to Mixture Design

Despite some of the differences between SULPHLEX and asphalt discussed previously, they share some very important similarities.

The most notable is that identical laboratory specimen fabrication techniques can be used to produce mixtures of acceptable quality. Of course, this extends into the field where equipment traditionally used in the hot mix industry has been effectively used to produce SULPHLEX for experimental projects (22). This similarity in the temperature response of SULPHLEX and asphalt in the viscosity range required for acceptable workability is perhaps the most important single similarity between the two binders both in terms of construction considerations and laboratory testing.

Since conventional laboratory asphalt concrete fabrication techniques may be extended to SULPHLEX, the goals of the development of a mixture design procedure were to:

1. Select a test procedure which has been well-researched and which is well known to and accepted by asphalt technologists.
2. Select a test which measures a material property, not a test property, which can be used to evaluate the mixture against rationally developed acceptance criteria.
3. Select a relatively simple, easy to perform test which is available or at least readily accessible to State highway departments and/or government agencies.

The indirect tension test (IDT) was chosen for SULPHLEX mixture design. The IDT is quick and easy to perform and yields two material properties: the tensile strength and tensile strain at failure. The test has been well-researched (13, 14, 23, 24, 25, and 26). The test involves loading a cylindrical sample, such as a Marshall sample, with a compressive load along the vertical diametral plane. A relatively uniform tensile stress is generated along the vertical diametral plane, and failure occurs in tension.

The indirect tension test as used at Texas A&M in this study is explained in references 2, 24, 25, and 26. Reference 2 is a companion report which explains the SULPHLEX mixture design procedure based on the IDT in detail. The following paragraphs summarize the mixture design procedures.

The Strain Energy Concept

One method of analyzing the indirect test results is by applying the strain energy or toughness concept. Strain energy is the amount of work required to bring a unit volume of a sample to failure. It is measured in lb-in/in^3 and is the area under the tensile stress-strain curve.

As the binder content for a given aggregate is increased, the toughness reaches a peak value as shown in Figure 9. The binder content producing this maximum strain energy was found to be very close to the optimum binder content determined by Marshall analysis. Strain energy has proven to be a very good first estimate of the optimum or design binder content. Although the peak strain energy occurs at the same binder content regardless of the temperature or loading rate used in testing, the peak is more well-defined at conditions of 77°F and 2.0 inches per minute loading rate.

Figure 9 also shows that differences in aggregate angularity and type are reflected by strain energy. It was found, as expected, that an increased loading rate generally increased the value of strain energy. Strain energy reaches a peak value as temperature is varied, as shown in Figure 10. SULPHLEX and asphalt mixes reach a peak strain energy in the temperature range between 50 and 80°F . However, the strain energy at low and high temperatures (less than 32°F or greater than 100°F) is a much better indicator of pavement performance, as these are the temperatures at which an actual pavement is much more susceptible to pavement distress.

The Failure Envelope

The indirect tension results may also be analyzed through the use of failure envelope. Smith (27) presented the failure envelope, shown in Figure 11, to describe the behavior of an ideal elastomer. If stress-strain curves are obtained at different combinations of temperature and strain rate, the failure points are connected to form a failure envelope. As temperature is decreased or the strain rate is

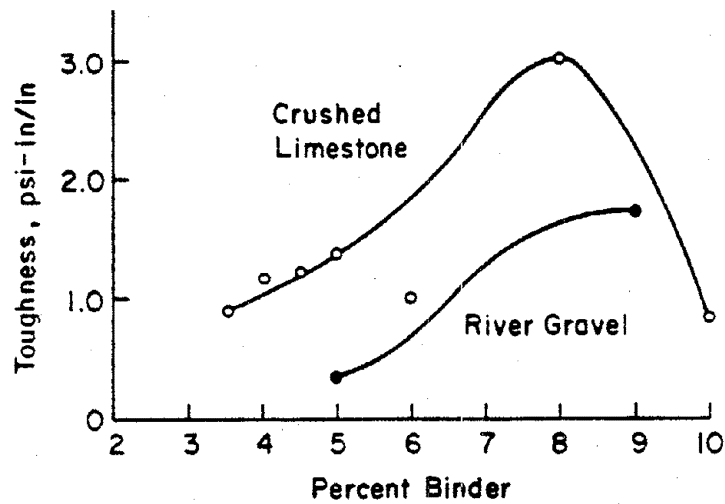


Figure 9. The Effect of Binder Content on Strain Energy or Toughness.

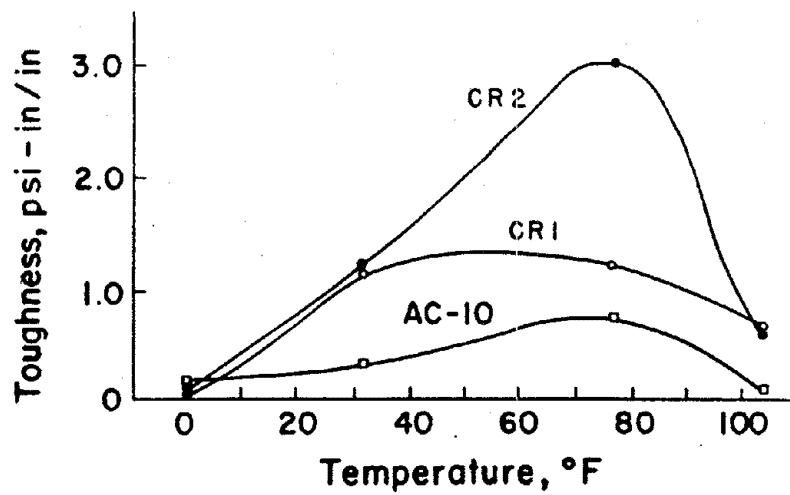


Figure 10. Effect of Temperature on Strain Energy or Toughness.

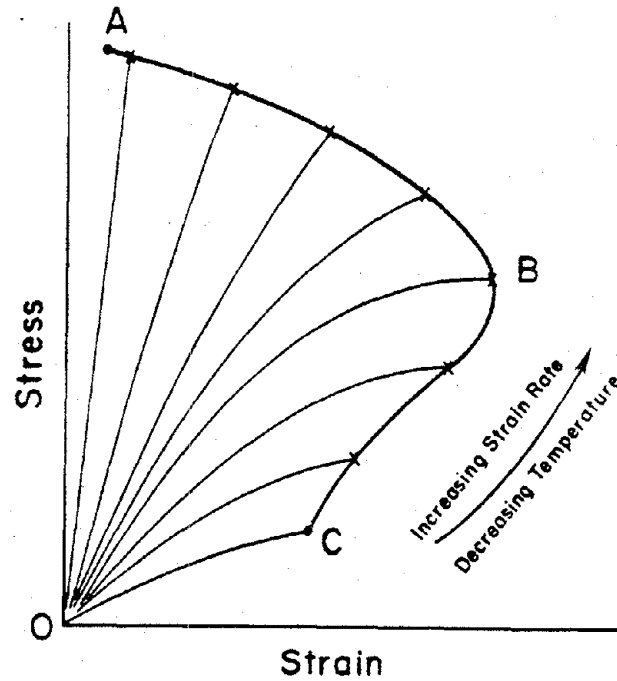


Figure 11. Illustration of the Ultimate Stress-Strain Behavior of an Ideal Elastomer.

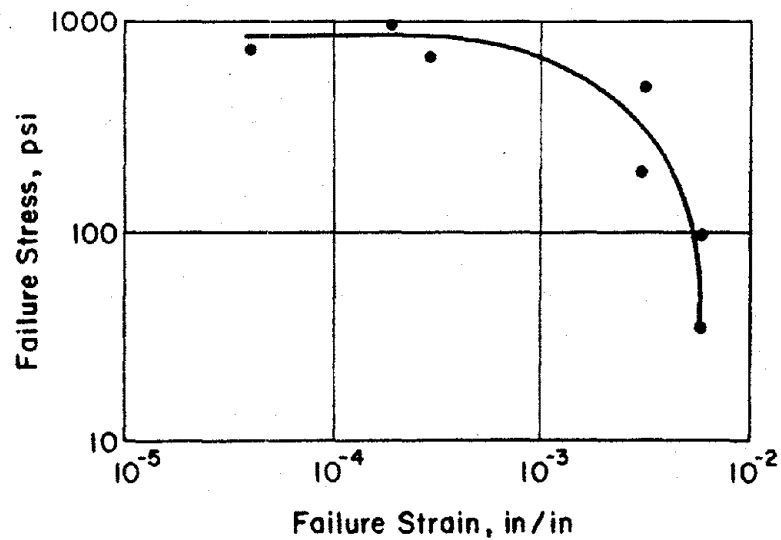


Figure 12. Failure Envelope for a Mixture of Crushed Limestone and SULPHLEX Binder CR1.

increased, the failure point moves counterclockwise around the envelope. Point A on the failure envelope in Figure 11 represents elastic behavior. Moving towards point B, the viscous components become more dominant, and the total strain to failure increases. From B to C the rate of bond rupture, or the damage factor, increases faster than the strain rate, and the failure occurs. Smith states that this behavior must occur if a material is linearly viscoelastic and that the failure envelope is independent of the type of test employed. Thus the failure envelope is a basic way to characterize the ultimate tensile properties of a paving material.

Both SULPHLEX and asphalt concrete have been shown to be approximately linearly viscoelastic materials (2, 12). Indirect tensile results from this study were used to create failure envelopes for SULPHLEX CR1, CR2, CR3, CR5, and AC-10 mixtures. Figure 12 gives an example of a failure envelope for a CR1 crushed limestone mix containing eight percent binder. It was found that for all mixtures tested, an increase in the binder content shifted the failure envelope upward and to the right. An example of this behavior is shown in Figure 13. Similarly, a change in the aggregate being used will cause the failure envelope to shift, as in Figure 14.

The relative position of the failure envelope on the stress-strain plot is an indication of the type of material tested. A failure envelope positioned far to the left on the stress-strain plot represents a material which may fail at low strains. This type of material would be susceptible to fatigue or thermal cracking. A failure envelope to the far right on the stress-strain plot would indicate a low stiffness material which exhibits a large failure strain. Such a mixture would be susceptible to excessive permanent deformation or rutting. A set of boundary curves can be superimposed on this stress-strain plot to indicate areas in which the mixture might be too brittle or too ductile. The curves will form a window, shown in Figure 15, into which the failure envelope of a satisfactory paving mix will fall. Such boundary curves were developed for SULPHLEX binders based on thermal cracking and permanent deformation modes of distress.

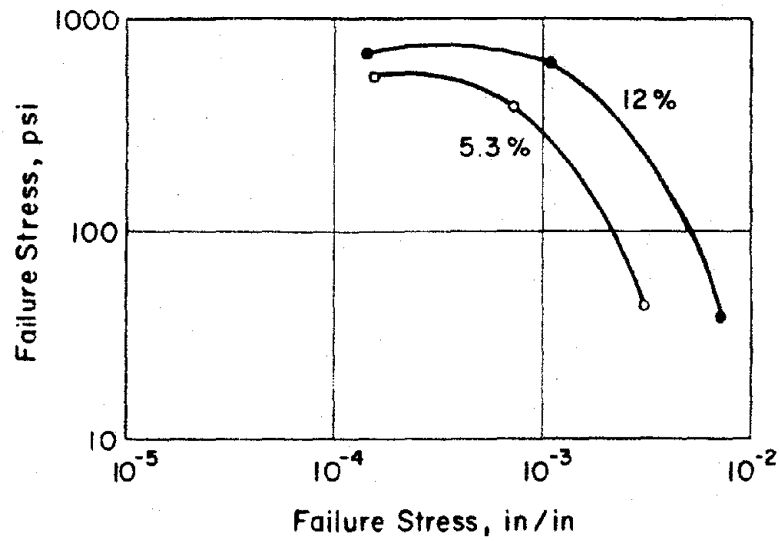


Figure 13. The Effect of Binder Content on the Failure Envelope (CR1 Binder and Crushed Limestone).

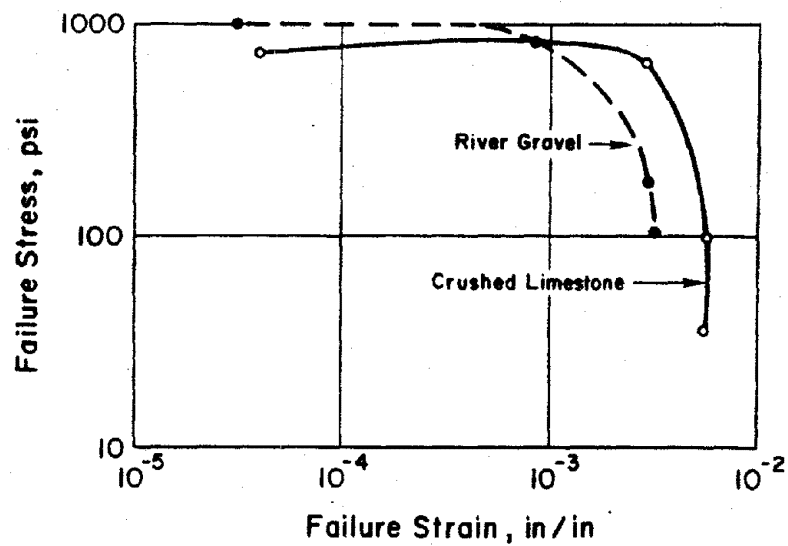


Figure 14. The Effect of Aggregate Type on Failure Envelope (CR1 Binder).

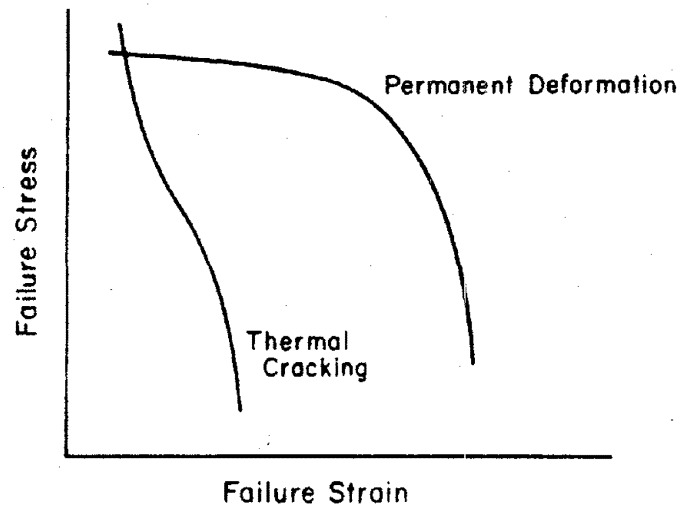


Figure 15. Hypothetical "Window of Acceptability" for Failure Envelope.

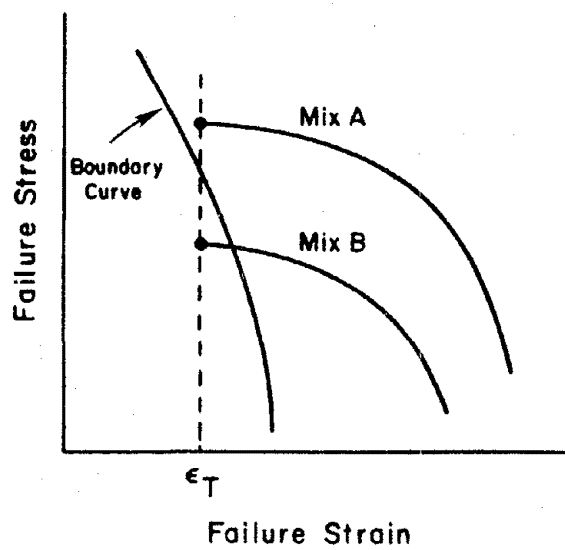


Figure 16. Hypothetical Boundary Curves for Thermally Induced Stresses.

The boundary curve for thermal cracking was based on the calculated thermally induced tensile stress for a pavement. It was noted that at low temperatures the failure strain is independent of the binder content. The failure strain is used as the basis for predicting thermal cracking. The boundary curve shown in Figure 16 represents the thermally induced stress expected at different temperatures plotted against the failure strain occurring at the corresponding temperature. For a low temperature, T , and a corresponding failure strain level, ϵ_T , a failure envelope plotting above the boundary curve at ϵ_T , mix A, would represent a mixture with sufficient tensile strength to resist thermal cracking. The thermally induced stress would exceed the tensile strength of a mixture with a failure envelope below the boundary curve, mix B, and thermal cracking would occur. The expected thermally induced stress was calculated using a viscoelastic solution contained in a computer program developed by Chang et al. (28). Plots of thermally induced stress versus temperature were developed for different cooling rates, as shown in Figure 17. By plotting the expected thermally induced stress against the failure strain at the corresponding temperature or rate of loading, boundary curves were developed as shown in Figure 18.

The permanent deformation boundary curves were based on rut depths predicted by the Shell method (29, 30). As the binder content is increased, the lower portion of the failure envelope moves progressively to the right, as shown schematically in Figure 19. For a specific climate, pavement thickness and number of load applications, each binder content represents a rut depth. The failure envelope corresponding to the binder content yielding a limiting, or critical, rut depth becomes the boundary curve. A failure envelope plotting to the right of the boundary curve indicates an excessive binder content and excessive permanent deformation. A failure envelope plotting to the left of the boundary curve indicates no rutting problems.

Rut depths were calculated for several combinations of pavement thickness, climate, number of load applications, and binder content for each type of binder using the Shell method. The Shell method is based

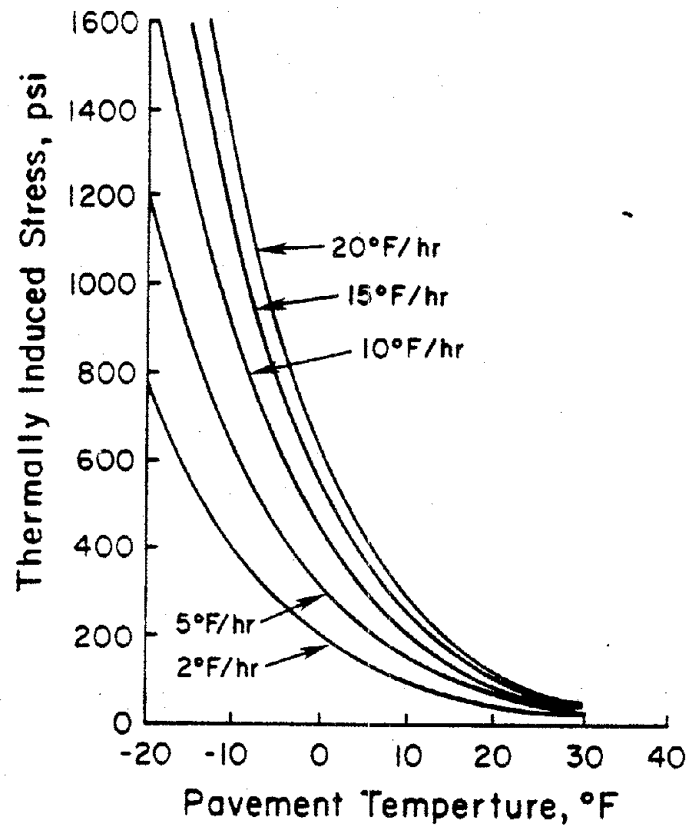


Figure 17. Thermally Induced Stresses Computed by the Computer Program Developed by Chang et al. (28)

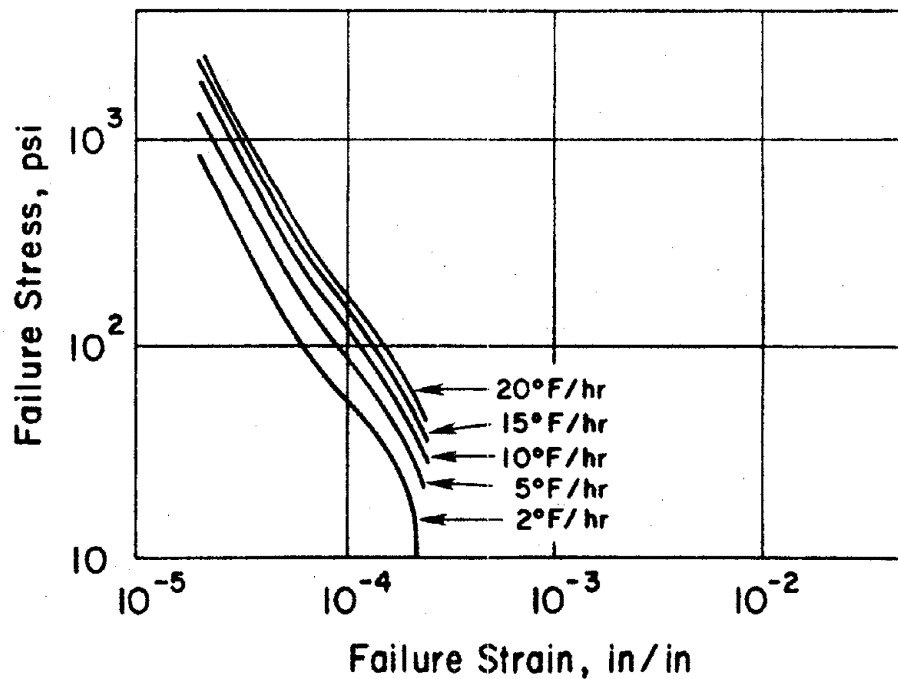


Figure 18. Thermal Stress Boundary Curves Developed for SULPHLEX Binder CRI and Crushed Limestone.

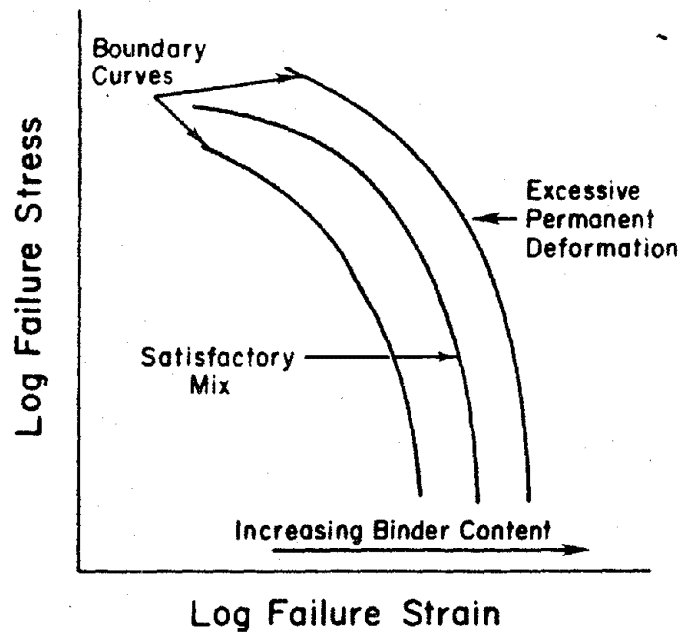


Figure 19. Schematic Representation of the Shift of the Failure Envelope with an Increase in Binder Content.

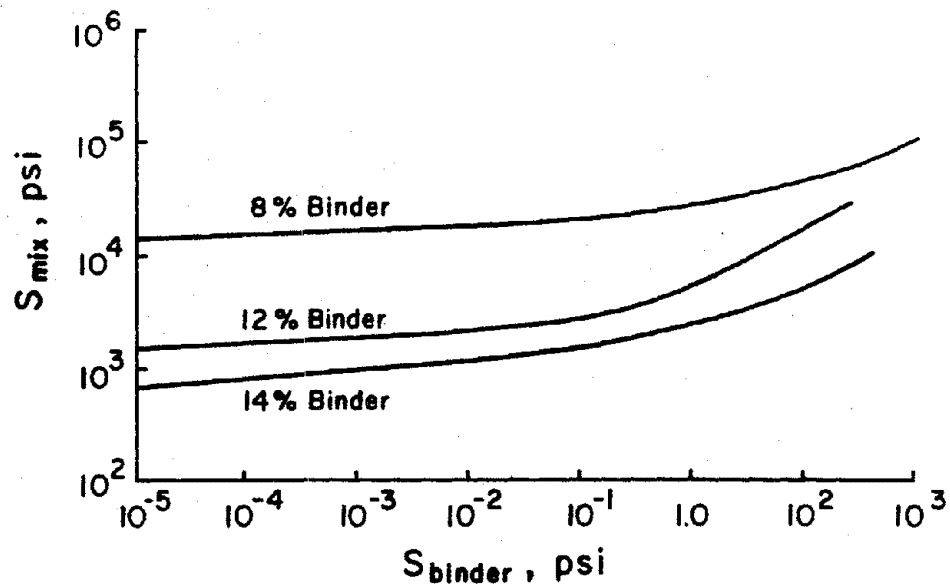


Figure 20. Mixture Stiffness Versus Binder Stiffness for SULPHLEX Binder CR1 and Crushed Limestone (Based on the Shell Method (29)).

on a plot of mixture stiffness as a function of binder stiffness. Such a diagram was developed for each binder; an example is given in Figure 20. The calculated rut depth for each combination of conditions was plotted versus binder content, as in Figure 21. A limiting rut depth of 0.25 inches was set. The failure envelope of the binder content which yields the limiting rut depth becomes the boundary curve for each set of conditions. An example of the permanent deformation boundary curves is given in Figure 22.

A quick method for estimating the fatigue life of SULPHLEX mixtures using the resilient modulus was developed. Constant stress beam fatigue tests were performed on mixtures made with each binder. From the test results an empirical relation of the form

$$N_f = K_1 (1/\epsilon)^{K_2}$$

was derived. The term N_f is the number of load applications to failure, ϵ is the bending strain and K_1 and K_2 are equation constants. The fatigue life was calculated for many combinations of resilient modulus and temperature. The constants K_1 and K_2 were varied with temperature according to the guidelines discussed later in Chapter V. Knowing the elastic modulus (resilient modulus), the critical tensile strain in a pavement layer, ϵ , was calculated using a two-layer elastic solution given by Santucci (31). A laboratory to field shift factor of 13 was applied. Fatigue design charts were developed by plotting contours of constant fatigue life on a resilient modulus versus temperature diagram, as in Figure 23. Fatigue life can be estimated from this chart by plotting the resilient modulus of a mix at the effective yearly pavement temperature.

Mixture Design Procedure

The following procedure is suggested for determining the optimum SULPHLEX binder content.

1. Test a group of samples in indirect tension over a range of binder contents varying in one percent increments (two specimens at each binder content). Plot strain energy as a

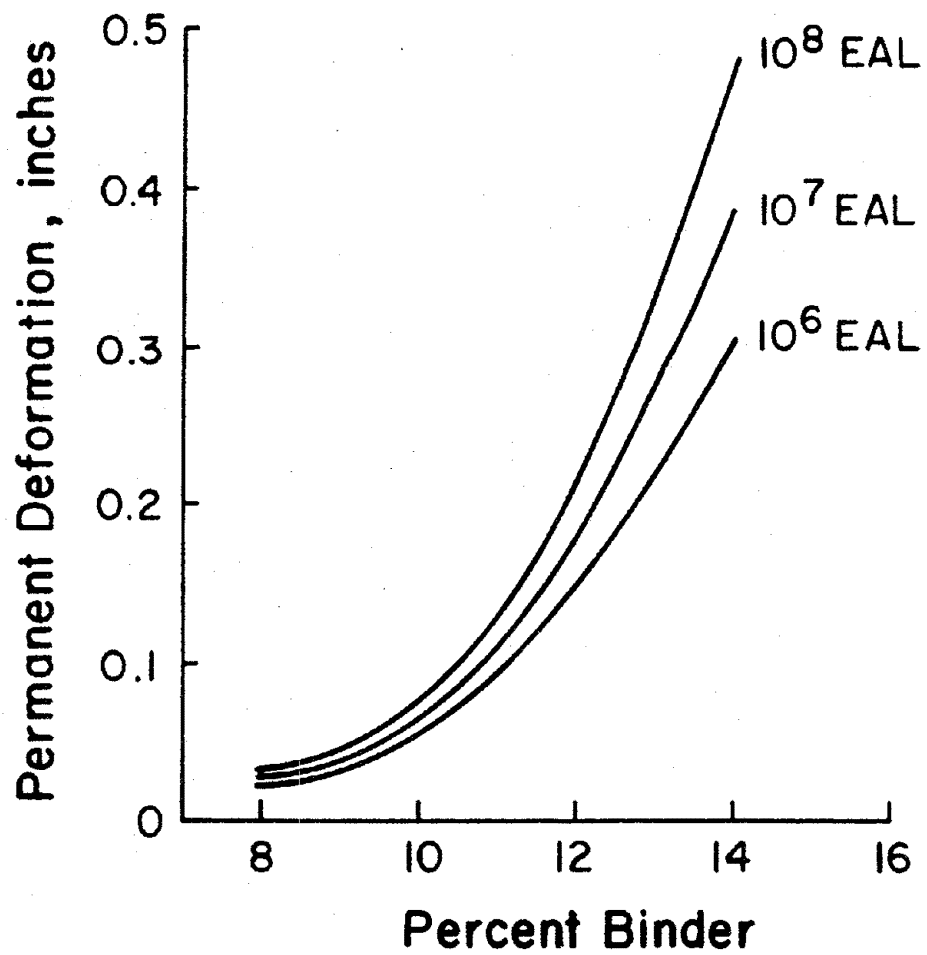


Figure 21. Permanent Deformation Versus Binder Content Calculated by Means of Shell Method (29).

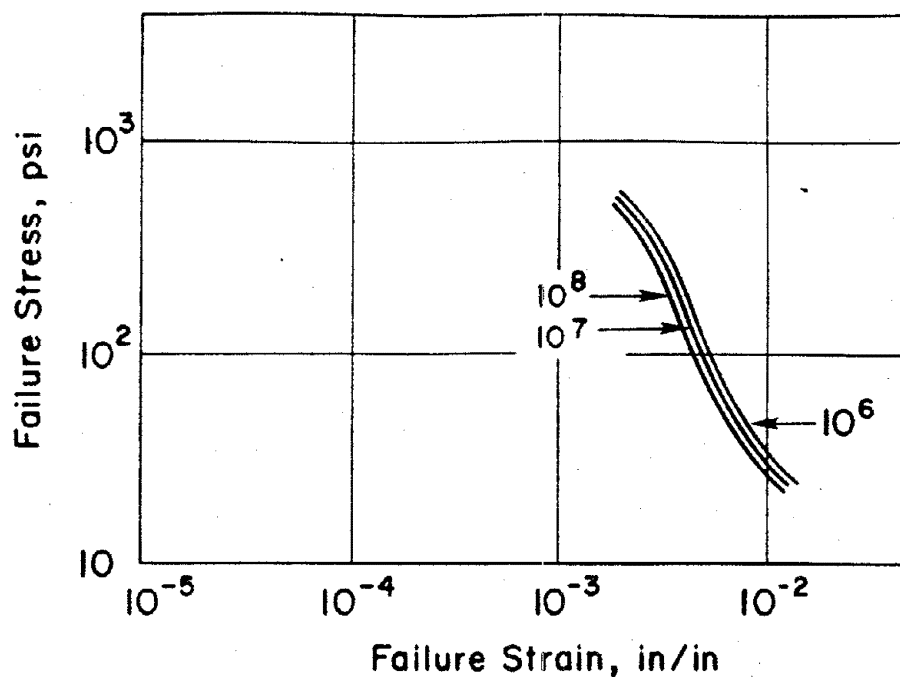


Figure 22. Permanent Deformation Boundary Curves for SULPHLEX Binder CR1 and Crushed Limestone Aggregate.

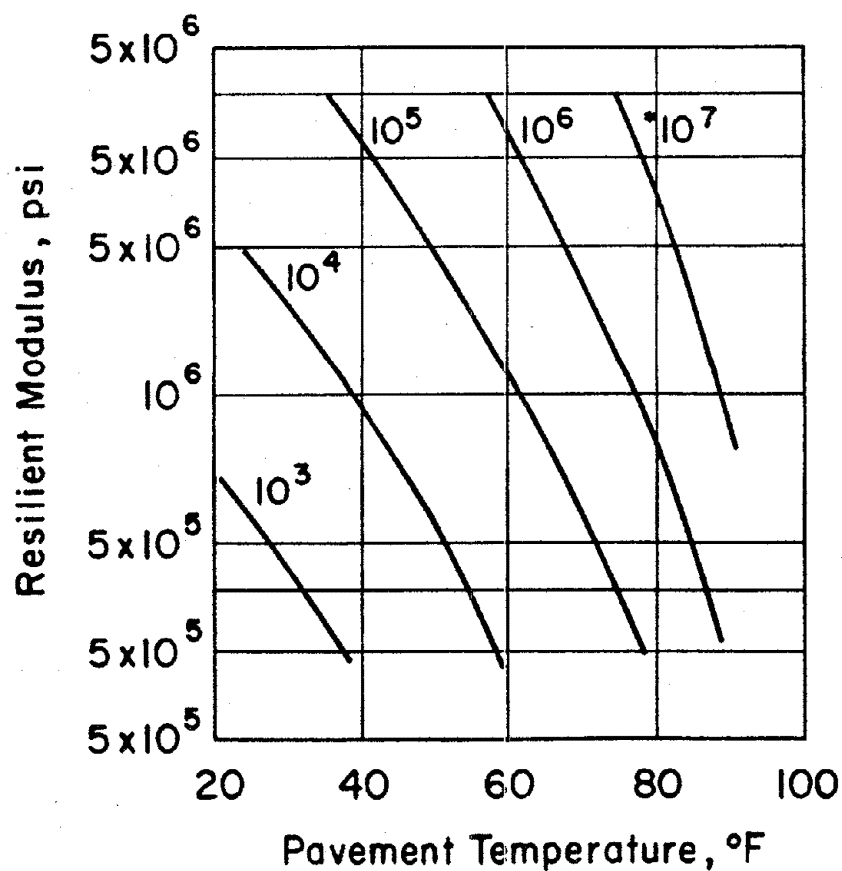


Figure 23. Load-Displacement Response in Overlay Tester Recorded on X-Y Plotter.

function of binder content. A small range of binder contents at the maximum strain energy is selected for further analysis using the failure envelope concept.

2. Failure envelopes for the small range of binder content found in step (1) are developed by testing at several temperatures including the lowest and highest temperature expected in service. The design charts are based on a loading rate of 0.02 inches per minute (two specimens at each temperature are suggested).
3. A boundary curve for thermal cracking is selected for the type of binder and the winter cooling rate. A permanent deformation boundary curve is selected considering climate, type of binder, pavement thickness and number of load applications. A large number of design charts are given in reference 26.
4. The failure envelopes are plotted on a graph with the boundary curves. The failure envelope best fitting within the window of acceptability formed by the boundary curves represents the design binder content.
5. This binder content is checked for fatigue resistance by performing resilient modulus tests at the yearly effective pavement temperature. If the fatigue life is not adequate, the design binder content may be adjusted.
6. A moisture-conditioning procedure, such as the Immersion-Compression Test (AASHTO T165, T167) or the Lottman procedure (16), should be used to check for water susceptibility.

An example is included for clarification. For a dense-graded crushed limestone and CR1 mixture, the strain energy versus binder content plot indicated that the maximum toughness occurred at about 8-percent binder. Failure envelopes for binder contents of 7, 8, and 9 percent were plotted with the boundary curves. Figure 24 shows that the 7-percent binder content mixture would have potential thermal cracking problems. The fatigue chart and the results of the resilient modulus tests in Figure 25 show that the 9 percent content mixture would have

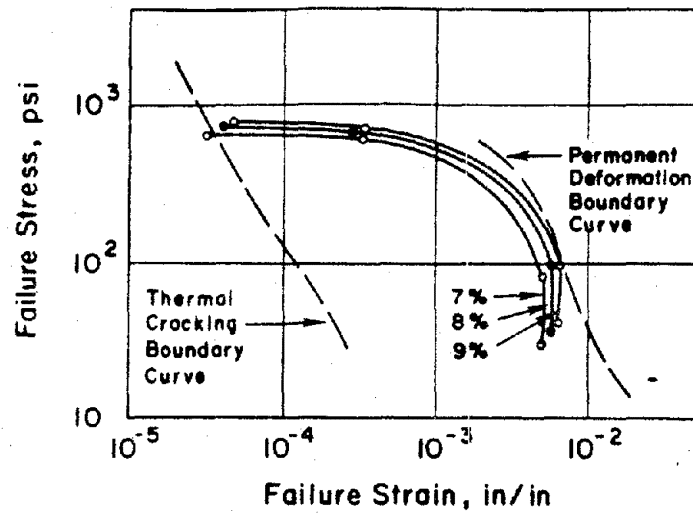


Figure 24. Mixture Design Failure Envelopes Plotted Against Boundary Curves for Thermal Cracking and Permanent Deformation.

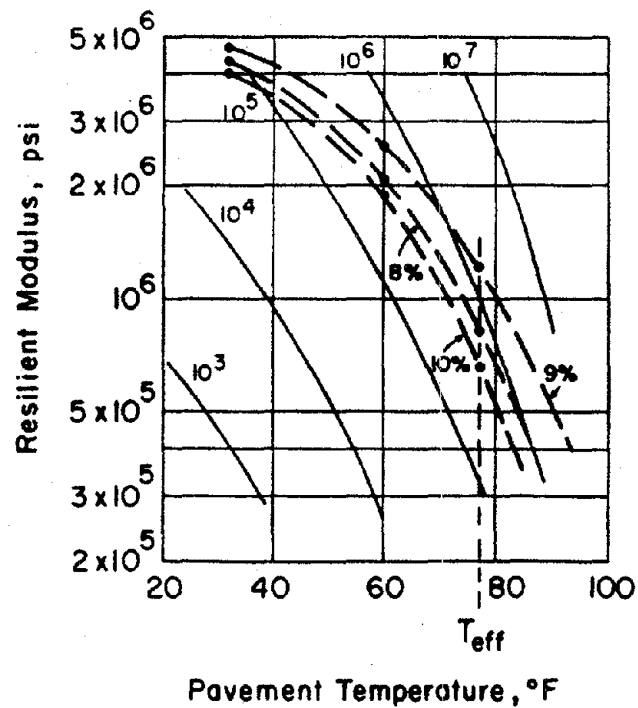


Figure 25. Mixture Design Resilient Modulus - Temperature Curves Plotted Against Constant Fatigue Contours.

the maximum fatigue life. However, permanent deformation performance for the predicted traffic is marginal with 9-percent binder content. A design binder content of 8.5 percent is recommended.

Optimum Mixture Design

The optimum mixture designs and typical mixture properties for SULPHLEX mixtures and asphalt concrete mixtures based on the failure envelope concept are summarized in Table 13.

It is recommended that the mixture design selected on the basis of failure envelope concept should then be tested for compressive strength (AASHTO T167) following one Lottman conditioning cycle (17) where the specimen reaches at least 75 percent saturation during the vacuum saturation phase. It is suggested that following Lottman conditioning the samples should have a compressive strength of at least 70 percent of the original strength and at least 250 psi.

Table 13. Summary of Optimum Mixture Designs and Mixture Properties at Optimum Design Conditions.

Mixture	Optimum Percent Binder by Total Weight of Mixture	Marshall Stability, lbs.	Marshall Flow, 1/100 in.	Percent Air Voids	Percent VMA	Retained Compressive Strength from Compression Test (77°F) Following 1 Cycle Lottman Condition- ing, psi (Average of 2 Specimens).
AC-10 and Crushed Limestone	5.0	2000	10	3.6	14.0	400 (85)*
AC-10 and River Gravel	3.5	1020	7	1.0	11.0	---
AC-10 and Basalt	5.0	1390	8	3.6	15.8	---
CR1 and Crushed Limestone	8.5	2360	18	5.2	14.5	510 (70)
CR1 and River Gravel	5.0	1490	16	2.2	11.5	---
CR1 and Basalt	9.0	1650	17	4.5	16.0	---
CR2 and Crushed Limestone	8.5	2180	19	5.1	14.8	270 (40)
CR2 and River Gravel	5.0	1320	16	2.0	11.8	---
CR2 and Basalt	8.5	1500	18	4.9	16.2	---
CR3 and Crushed Limestone	9.0	1600	18	5.5	14.8	640 (75)
CR5 and Crushed Limestone	8.5	1550	17	5.6	15.0	300 (40)

* Percent Strength Loss.

CHAPTER V
STRUCTURAL ENGINEERING PROPERTIES (1): FATIGUE CRACKING

Selection of Approach

Two methods of fatigue testing and analysis were selected: the phenomenological regression approach and the fracture mechanics approach. The primary reasons for selecting these two methods were the background experience at Texas A&M, the repository of data and literature on experimental techniques and the confidence in these methods established in the literature.

Phenomenological Regression Approach

The phenomenological regression approach is the most common method used in fatigue testing or analysis of highway materials. The very familiar relationship used to represent the fatigue response is of the form:

$$N_f = K_1 (1/\epsilon_t)^{K_2} \quad (1)$$

where N_f is the number of repetitions or application to failure, ϵ_t is the repeatedly induced tensile strain, and K_1 and K_2 are regression constants. These parameters are influenced by several variables including type and rate of load, type of test, mixture properties (air voids, stiffness, asphalt content, aggregate gradation, etc.), and temperature (32). Hence, K_1 and K_2 are not material properties.

The specific procedure for beam fatigue testing detailed in the VESYS IIM User's Manual (12) were followed in this research.

The beam fatigue tests may be performed either in a controlled strain mode or a controlled stress mode. The proper test mode depends upon what type of pavement is being simulated. Epps and Monismith (32) reported that a controlled stress mode of loading is encountered in thick, stiff pavements typically 6 inches thick or thicker. Controlled strain loading is, on the other hand, typically encountered in thin pavement sections (2 inches thick or thinner). Since the

results of controlled stress and controlled strain laboratory testing are quite different in terms of the K_1 and K_2 derived from regression analysis, it is imperative that the mode selected actually represent the in situ condition.

Generally, the phenomenological approach has provided a reasonably simple approach which has been almost universally adopted. However, it bears the limitation that it cannot account for both crack initiation and propagation. Such distinctions may be very important in estimating fatigue life of a new material expected to be used for a wide range of applications. It seems reasonable that a stiff but brittle material may perform well in a controlled stress laboratory test, but may fail rapidly due to immediate crack propagation if the material is used in situ for controlled strain applications.

Fracture Mechanics

A mechanistic approach proposed by several researchers (33, 34, 35, 36, 37, and 38) considers fatigue as a process of cumulative damage and utilizes fracture mechanics to investigate this property. In this approach, fatigue life, under a given stress state, is defined as the period of time during which damage increases according to a crack propagation law from an initial state to a critical or final level. The method accounts for the changes in state of stress due to cracking, geometric, and boundary conditions, material characteristics and variability. The fatigue life can be obtained from both controlled stress and controlled strain tests. The method is independent of the mode of testing.

In order to describe the fatigue process and to predict the fatigue life of any system, it is essential to establish the laws governing the crack growth from the initial stage to the final stage. The process of crack growth in materials like SULPHLEX or asphalt can basically be described as blunting and sharpening of the crack tip during cyclic loading and can be explained in terms of the energy balance at the crack tip. During the loading stage, the plastic zone at the crack tip becomes larger and, hence, the crack tip becomes blunt. During unloading the crack tip sharpens as a result of the substantial reduction in the size of the plastic zone ahead of the

crack tip. The unloading stage can also leave some permanent deformation that will result in reduction of the amount of available strain energy for the next cycle. This will increase the amount of total deformation that the material can take during the next loading stage.

A variety of crack propagation laws have been proposed in the literature (39-44), among which the Paris equation is most significant for this research:

$$dc/dN = A(\Delta K_I)^n \quad (2)$$

where dc/dN is the change in crack length per cycle, N , and A and n are material constants. The term, ΔK , is the change in stress intensity factor. This factor provides a single parameter characterization of the state of stress at the crack tip including the effects of specimen geometry and configuration, boundary condition, and load. The normal stresses and shear stress at a point a distance r from the crack front which make an angle θ with the crack plane are related to the mode I stress intensity factor by:

$$\sigma_y = \frac{K_I}{2\pi r} \cos \frac{\theta}{2} \left(1 + \sin \frac{\theta}{2} \sin \frac{3\theta}{2}\right)$$

$$\sigma_x = \frac{K_I}{2\pi r} \cos \frac{\theta}{2} \left(1 - \sin \frac{\theta}{2} \sin \frac{3\theta}{2}\right)$$

$$\tau_{xy} = \frac{K_I}{2\pi r} \left(\sin \frac{\theta}{2} \cos \frac{\theta}{2} \cos \frac{3\theta}{2}\right)$$

Figure 26 illustrates these stresses and the mode I crack surface displacement. The above relations were derived by Irwin (40). They describe the stress in the vicinity of crack tips subjected to mode I deformation. The stress intensity factor K_I also provides a means of estimating the size of the plastic region around the crack tip.

Utilizing the Paris law, failure life, N_f , could be expressed as:

$$N_f = \frac{c_f}{c_0} \int \left(\frac{1}{A \Delta K_I^n} \right) dc$$

where c_f is the crack size at failure, and c_0 is the initial crack or flaw size.

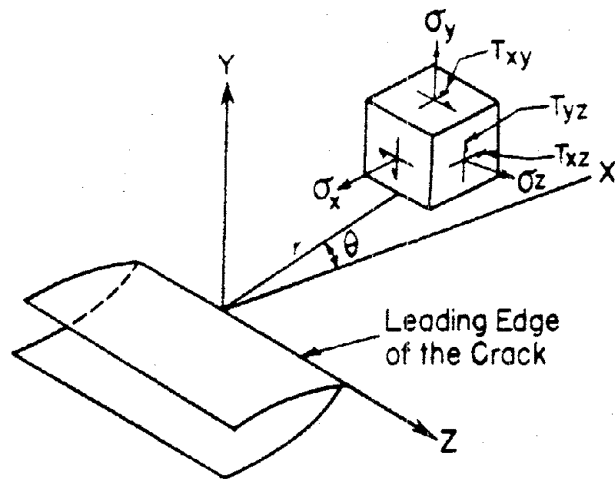


Figure 26a. State of Stress at Tip of Mode I (Tensile) Crack.

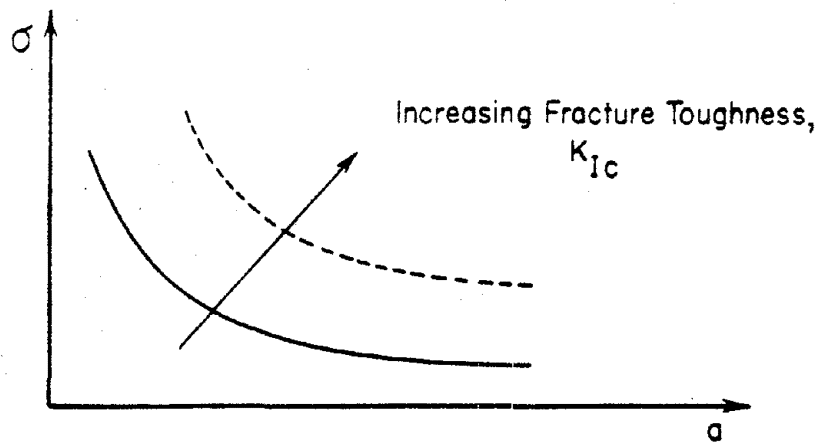


Figure 26b. Stress State as Represented by the Stress Intensity Factor, a Function of Crack Length (a or c) and Stress (σ).

The advantages of the mechanistic method are: (1) that the critical stress intensity factor, K_{IC} , is a material property, independent of mode of loading and specimen geometry; and (2) failure is defined realistically be either rapid brittle crack propagation at the critical crack size or by stable crack growth through the entire specimen depth. The disadvantages are: (1) the inherent computational complexity in obtaining K_I for all but the simplest geometries and (2) the inherent assumptions of linear elasticity and an infinitely sharp crack tip at all times. The first disadvantage may be overcome by testing specimens of simplified geometry for which K_I computations have been accomplished. The second disadvantage is prohibitive for virtually every condition with the possible exception of testing at very low temperatures (below T_g).

The fracture energy under plane strain conditions where elastic-plastic conditions exist may be determined by the J integral. The path-independent J integral proposed by Rice (45) characterizes the stress-strain field at the tip of a crack by an integration path taken sufficiently far from the crack tip to be substituted for a path close to the crack-tip region. Thus, even though considerable yielding occurs in the vicinity of the crack tip, if the region away from the crack tip can be analyzed, behavior of the crack-tip region can be inferred.

The energy line integral, J, is defined for the two-dimensional case for either elastic or elastic-plastic behavior as follows:

$$J = \int_{\Gamma^*} (w dy - T \frac{\partial u}{\partial x} ds)$$

where w is strain energy density, Γ is a closed contour followed counterclockwise in surrounding an area in a stressed solid, T is the tension vector perpendicular to Γ , dy is the incremental distance in the y direction, u is the displacement in the x direction and ds is an element of Γ . For a closed curve, Γ^* , Rice (45) has shown that

$$J = \int_{\Gamma^*} (w dy - T \frac{\partial u}{\partial x} ds) = 0$$

From a more physical viewpoint, J may be interpreted as the potential energy difference between two identically loaded bodies

having incrementally different crack sizes or

$$J = \frac{1}{B} \frac{du}{da}$$

where u is the potential energy and B is thickness. In other words, J is a generalized relation for the energy release due to crack propagation, which may be valid if there is appreciable crack tip plasticity.

The usefulness of the J integral lies in the fact that the conditions of specimen size and thickness need not be as stringent as in the case of G_{IC} or K_{IC} . The requirements for limited plasticity can be dropped when using the J integral. In principle this allows determination of J_{IC} from a small specimen; and, thus, G_{IC} or K_{IC} for actual pavement geometries may be predicted from small laboratory specimens.

The J integral was used in this research to analyze results of the overlay test device. The rationale was that the amount of energy released by a specific material per unit area of crack extension will be the same regardless of the size of the specimen. Thus the J integral provides a method of computation of energy release rate from small specimens that may have some plastic deformation. These energy release rates may be compared to those calculated from three-dimensional field conditions where the plastic zone is very small compared to the confining area which results in an elastic response. This procedure is being developed more extensively at Texas A&M University under contract DTFH-61-81-C-00080 for the Federal Highway Administration.

The overlay test, developed at Texas A&M (46), was selected for the great majority of testing in the fracture mechanics based study. The fabrication procedure for the beam specimens used in this test is identical to that used in beam fatigue testing. This relatively large specimen size allows the use of typical mixture aggregate gradations. The overlay tester was calibrated to apply a maximum ram displacement of 0.04 or 0.02 inches in a manner illustrated schematically in Figure 27. The oscillating horizontal movement was designed to simulate the opening and closing of pavement cracks produced by thermal contraction and expansion of pavement materials.

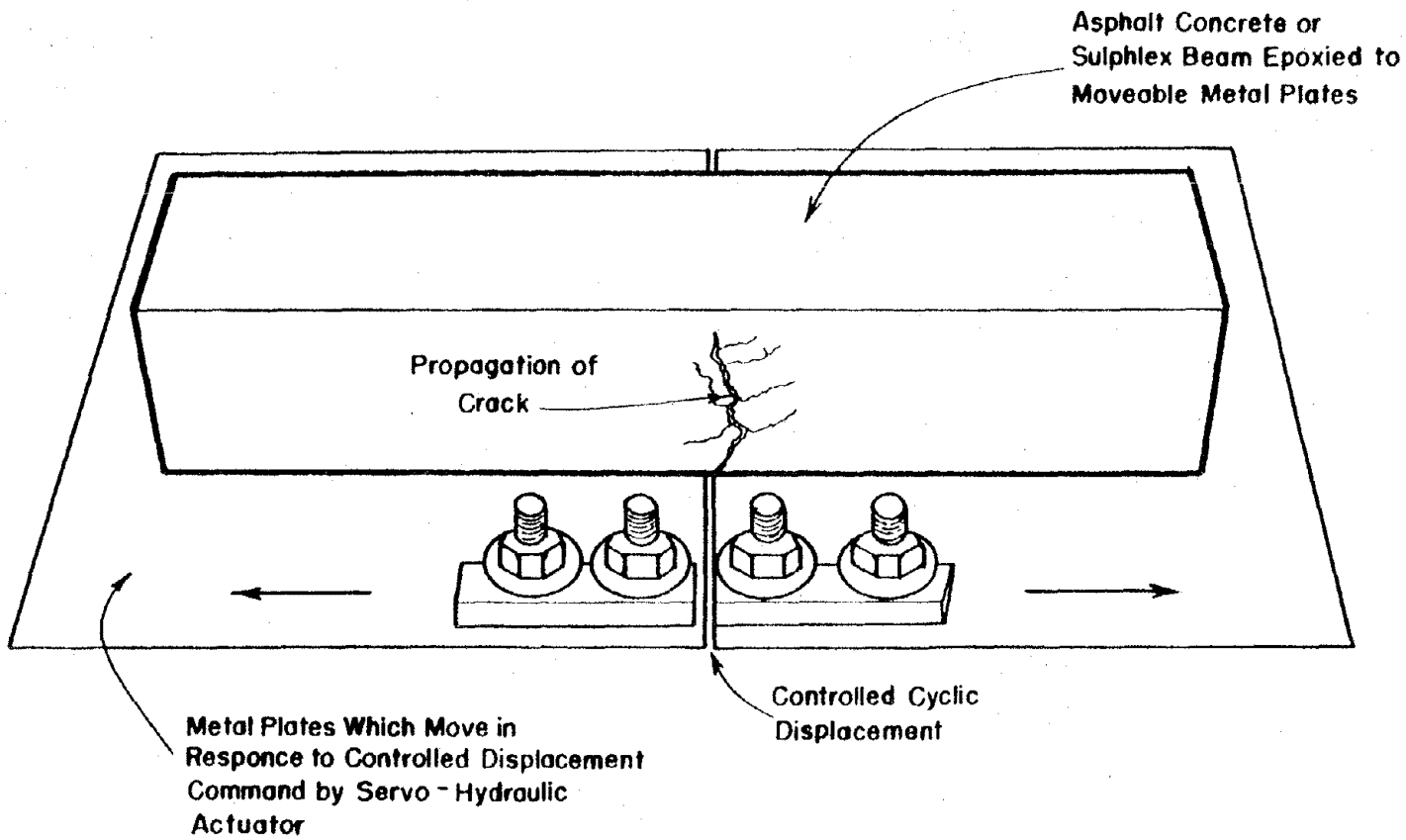


Figure 27. Schematic of Overlay Tester.

A loading rate of one cycle per ten seconds was used throughout most of the test program. The load and displacement values were monitored and recorded on an X-Y plotter as illustrated in Figure 28. The change in crack length with each loading cycle was visually measured.

The cyclic loading and unloading which occurs in the overlay test suggests that the J integral cannot be used. This is because the path independence of the J integral has been shown only using deformation theory of plasticity which does not allow for unloading (47, 48, and 49).

For this analysis the definition of the J integral has been modified by including the effects of unloading as:

$$J^* = \frac{1}{B} \frac{\partial u^*}{\partial a}$$

where u^* reflects the energy released by the material and includes the effects of unloading. The J^* integral is analagous to the J integral. The J^* integral should be suitable in a comparative analysis of energy release rates among various SULPHLEX binders and asphalt.

Relationship Between Phenomenological and Fracture Mechanics Parameters

A general form of the stress intensity factor for elastic conditions in an infinitely large cracked plate would be:

$$K_I = K_{IC} = a\sigma\sqrt{c} \quad (3)$$

where a is a function of specimen and crack geometry and is a constant, σ is stress and c is flaw size or crack length.

The Paris equation (equation 2) may be rearranged by separation of variables and integrated for $N = 1$ to $N = \text{failure } (N_f)$ to yield:

$$N_f = 1 + \int_{c_0}^{c_f} \frac{dc}{AK_I^n}$$

where c_f is the crack length at "failure." Now by substituting equation 3 for K_I , equation 4 is obtained

$$N_f = 1 + \frac{1}{Aa^n \sigma^n c^{n/2}} \int_{c_0}^{c_f} dc \quad (4)$$

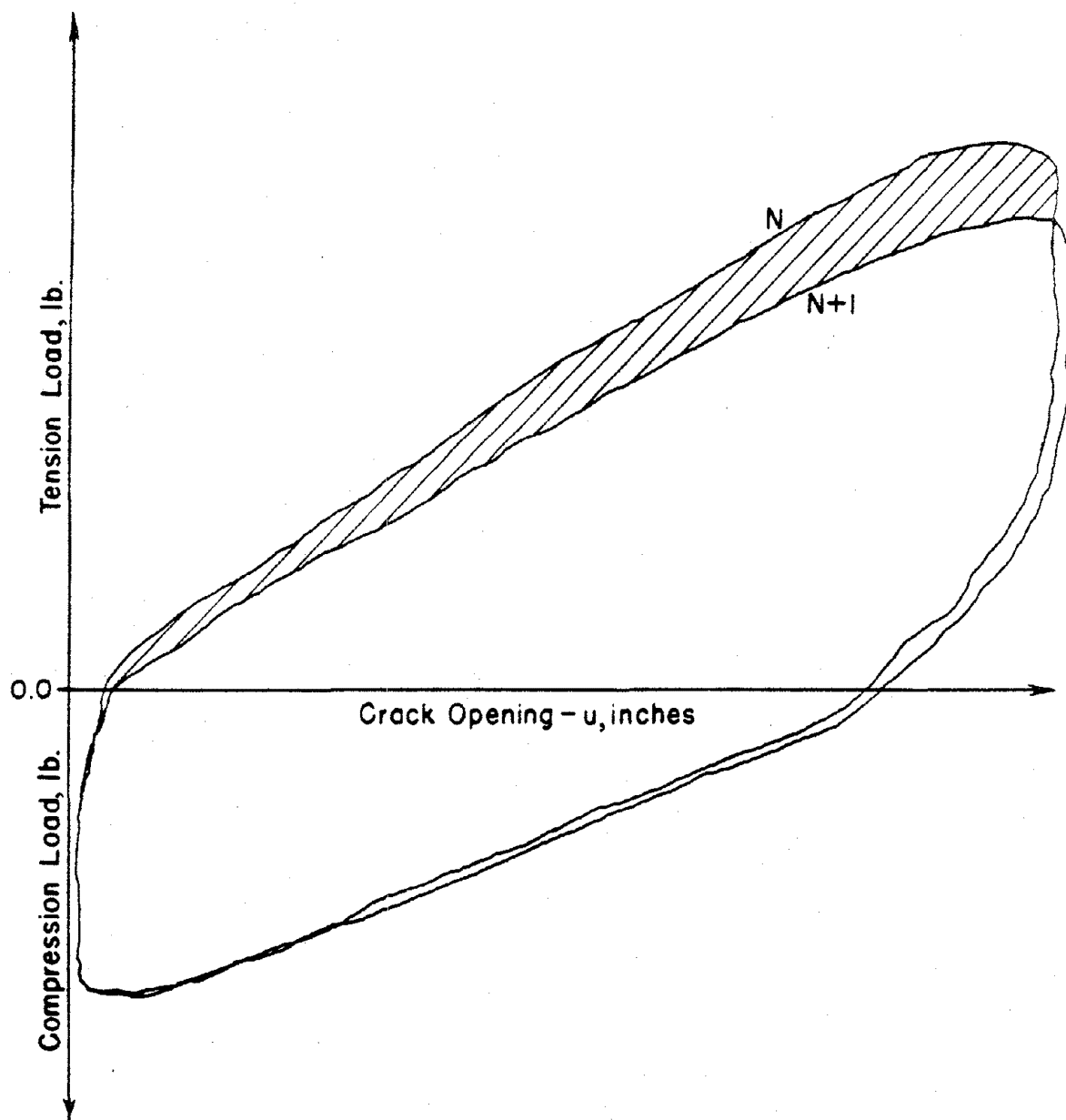


Figure 28. Load - Displacement Response in Overlay Tester Recorded on X-Y Plotter.

which may be simplified to yield

$$N_f = \frac{(c_f - c_o)^{c-n/2}}{Aa^n c^n}$$

or since $E = \sigma/\epsilon$

$$N_f = \frac{(c_f - c)^{c-n/2}}{Aa^n E^n \epsilon^n}$$

From the basic phenomenological regression equation for flexural fatigue results (equation 1), it is easy to see that

$$K_2 \sim n \quad \text{and} \quad K_1 \sim \frac{(c_f - c)^{c-n/2}}{Aa^n E^n}$$

Thus, the fatigue parameters K_1 and K_2 can be shown to be related to the basic principles of fracture mechanics and the Paris equation.

Experimental Design

Phenomenological Method

Two complete factorial experiments were performed to examine the effects of binder type, stress level, and temperature on fatigue life. The experiment design is shown in Table 14.

The first set of tests, Table 14a, examined the effects of binder type and stress level. In the second experiment, Table 14b, the effect of temperature was evaluated on only one binder. Binder CR5 was selected for the study of temperature effects following the results of the first set of tests, Table 14a, and after partially evaluating results of fracture mechanics based testing. Binder CR5 proved to have the overall most acceptable fatigue life of the SULPHLEX binders studied.

Fracture Mechanics Study

Epps and Monismith (32) have clearly proven that mixture variables as well as test variables affect the fatigue test results. Obviously,

Table 14. Experimental Design for Controlled-Stress Beam Fatigue Tests.

(a)

Binder Type	Stress Level, psi			
	100	150	200	250
CR1	n = 3	3	3	3
CR2	3	3	3	3
CR3	3	3	3	3
CR5	3	3	3	3
AC10	3	3	3	3

All tests @ 68°F.

(b)

Temperature	Stress Level, psi			
	100	150	200	250
40°F	3	3	3	3
68°F	3	3	3	3
104°F	3	3	3	3

Testing in part b was exclusively on CR5 and AC-10 mixtures with crushed limestone aggregate.

a factorial experiment to account for all possible variable effects is far beyond the scope of this study.

The primary purpose of the fracture mechanics based fatigue study was to compare the properties of asphalt concrete with the plasticized sulfur binders evaluated and to, if possible, differentiate among the binders as to their fatigue resistance potential. Secondly, to ensure that the fracture parameters computed were actually material properties, the factors of specimen thickness and displacement magnitudes and rate were evaluated. Finally, the polymeric nature of SULPHLEX suggests the potential to heal fractures under certain conditions. Thus, the influence of rest periods was evaluated.

Practical research limitations prevented a complete factorial or even a fractional factorial experiment. Instead, a series of experimental designs were implemented to examine the main effects or trends caused by each factor considered. Naturally, this procedure will not allow the possibility of investigating all factor interactions. However, the nature of the factors investigated permits the assumption that interactions are insignificant.

Table 15 presents the implemented series of experiments. Only two plasticized binders were tested (CR3 and CR5). These represent two very different materials. The initial tests, Table 15a, examined the effects of displacement magnitude, binder type, and rest periods.

The influence of rest period duration was examined, Table 15b. Three different durations were evaluated: 1 hour, 4 hours, and 24 hours. The influence of displacement magnitude was also incorporated into this experiment, Table 15b. Displacements of 0.02 and 0.04 inches were evaluated.

Thickness effects were investigated for binder CR3 only, Table 15c. Specimen thicknesses of 1, 2 and 3 inches were examined. The width in the direction perpendicular to the crack was held constant. The purpose of these tests was to examine the effect of geometry on material behavior and on plastic zone size ahead of the crack tip. In order to maintain plane strain conditions, which represents the critical condition for a brittle fracture, the specimen thickness must be sufficiently large.

Table 15. Experiment Design for the Overlay Tests.

(a)

Binder Type	With Rest Periods		No Rest Periods	
	Displacement Magnitude			
	0.02 in.	0.04 in.	0.02 in.	0.04 in.
CR3	n = 2	2	2	2
CR5	2	2	2	2
AC-10	3	3	2	2

Specimen thickness 3 in.

(b)

Binder Type	Rest Period Duration					
	1 hr.		4 hrs.		24 hrs.	
	Displacement Magnitude					
	0.02 in.	0.04 in.	0.02 in.	0.04 in.	0.02 in.	0.04 in.
CR3	n = 1	1	---	1	1	---
CR5	1	1	1	---	---	1

Specimen thickness 3 in.

(c)

Binder Type	Thickness		
	1 in.	2 in.	3 in.
CR3	n = 1	1	1

No rest periods
0.04 in. Displacement.

Table 15. Experiment Design for the Overlay Tests (continued).

(d)

Binder Type	Number of Rest Periods						
	1-10	11-20	21-30	31-40	41-50	51-60	No Rest
CR5	n = 1	1	1	1	1	1	1
AC-10	1	1	1	1	1	1	1

0.04 in. displacement
specimen thickness 3 in.

(e)

Binder Type	Displacement Rate (cycle/min.)			
	3	6	12	30
CR5	n = 1	1	1	1

No rest Periods
0.04 in. displacement
specimen thickness 3 in.

Frequency of rest periods was examined for both CR5 and AC-10, Table 15d. Binder CR5 was selected as it showed greatest potential for more ductile behavior and healing potential in preliminary testing. AC-10 was used for comparison purposes not only in the rest period experiment but also as a control for the binder type influence study. All tests, Table 15d, were performed at 0.04 inches displacement per loading cycle in order to examine the healing process under the most adverse conditions.

The effect of displacement rate was evaluated, Table 15e. Rates of 3, 6, 12, and 38 cycles per minute were evaluated on CR5 plasticized sulfur binder.

Results of Phenomenological Study

Tensile Strain Versus Load Repetitions

Figure 29 illustrates the phenomenological fatigue relationship based on the results of controlled stress tests and with data presented in terms of number of load repetitions versus tensile strain induced per load repetition.

Curves 1 through 5 in Figure 29 represent laboratory beam fatigue data from asphalt concrete mixtures which are considered typical of high quality, densely graded asphalt concrete. Table 16 summarizes the K_1 and K_2 parameters as well as the description of each mix. Curves 6 and 7 represent beam fatigue data for beams supported on elastic foundations for asphalt concrete and SULPHLEX, respectively.

Several trends are apparent from Figure 29. First, the fatigue response of laboratory beams which are supported on elastic foundations during testing are superior to beams which are simply supported at each end (compare curves 4 and 6 to curves 1, 2, and 3). Second, the SULPHLEX beam specimens (CR5) tested at Texas A&M possess fatigue properties which are generally comparable to those of tests for asphalt concrete beams tested in the same manner (compare the CR5 results to the AC-10 results at Texas A&M and to curves 1, 2, 3, and 5). Finally, it should be noted that when compared directly to an

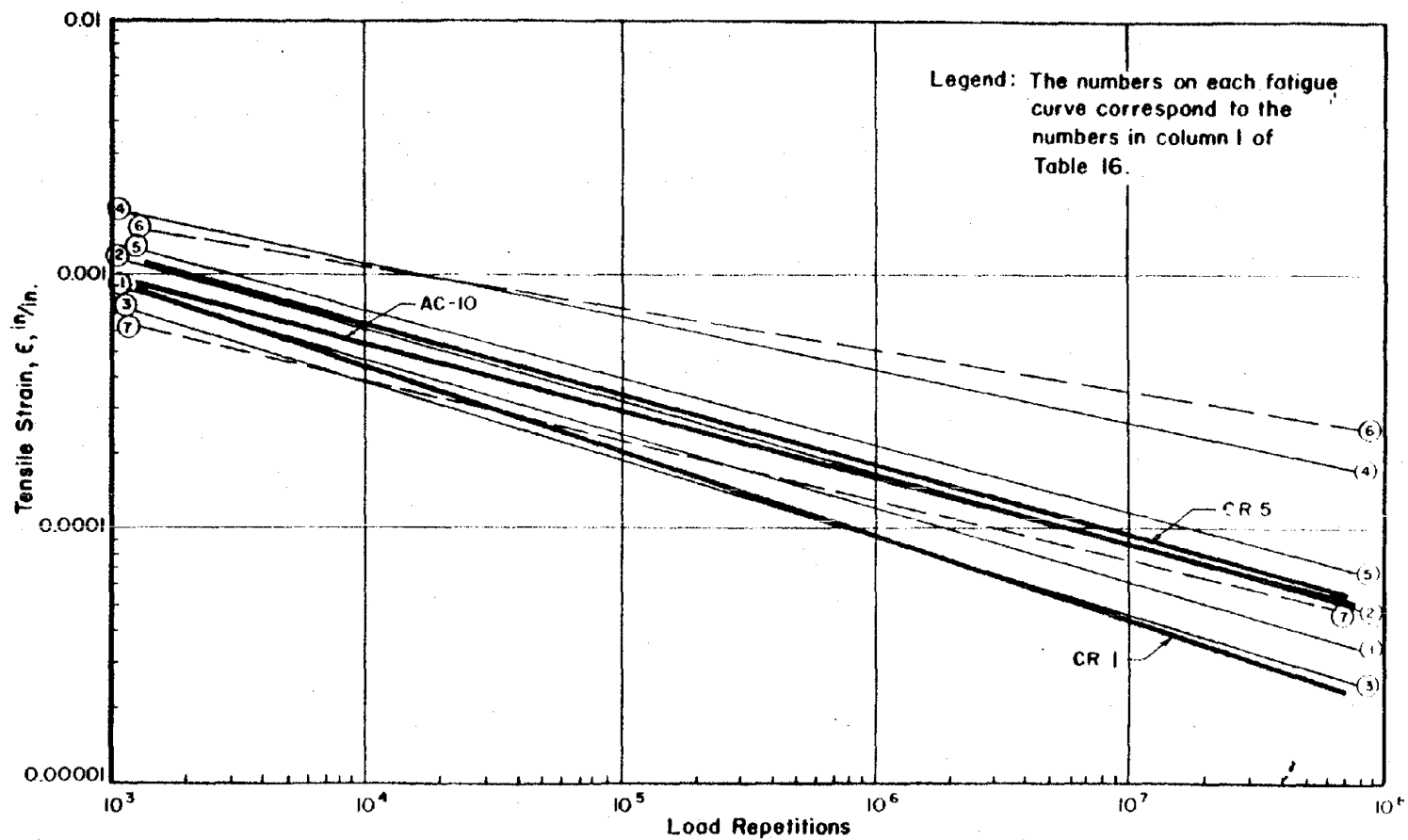


Figure 29. General Controlled Stress Phenomenological Fatigue Test Results for Ten Different Mixtures.

Table 16. Summary of Phenomenological Fatigue Data from Extensively Used and Documented Studies.

Fatigue Relationship Number on Plot	Reference Number	Authors	Type of Data	Fatigue Coefficient K_1	Fatigue Exponent K_2
1	32	Monismith and Epps	Laboratory Beam Tests of Univ. of California Mix 8	6.11×10^{-8}	3.38
2	50	Monismith	Laboratory Beam Tests on Dense Graded Mix by California Procedure	2.0×10^{-7}	3.38
3	51	Monismith	Laboratory Beam Tests on AASHTO Road Test Materials, NCHRP Project 1-10	5.33×10^{-8}	3.29
4	52	Barksdale	Laboratory Beam Tests with Elastic Support (Black Base Mix with 5% AC-40)	1.74×10^{-11}	4.99
5	53	Chevron Asphalt Research Company Richmond, CA	Laboratory Beam Tests on Emulsified Asphalt Mixes with 5% Air Voids, 11% Asphalt Volume and Dynamic Modulus	1.85×10^{-5}	3.04
6	54	Sherwood and Kenis	Laboratory Beam Tests on Elastic Foundations (75°F) for Asphalt Concrete Using AC-20	3.75×10^{-4}	5.92
7	54	Sherwood and Kenis	Laboratory Beam Tests on Elastic Foundations (75°F) for SULPHLEX (4% by weight) Specimens	4.75×10^{-4}	4.22

asphalt concrete control for specific test conditions, SULPHLEX CR1 and SULPHLEX 233 (investigated by Sherwood and Kenis (54)) are inferior to asphalt concrete (compare CR1 to AC-10 and curve 7 to curve 6). The various SULPHLEX binders will be more fully evaluated in the following paragraphs.

Validity of Phenomenological Test Results

Sizeable data variation is inherent in phenomenological fatigue testing. Thus, verification of a good test or an accurate test is difficult. However, a relationship between K_1 and K_2 was established by Rauhut (55) and extended by Pickett et al. (56). This relationship is presented in Figure 30 together with the locus of K_1 and K_2 from the beam fatigue results for SULPHLEX testing at Texas A&M. These results are summarized in Table 17. Note that in all cases the locus of K_1 and K_2 plots is very close to the regression curves established from previous analyses. This indicates that these values are reasonable. If the plot of the locus of values is too far below the regression lines, then the data are suspect.

K_1 and K_2 Parameters at 70°F

From Table 17 and Figure 31 it is clear that CR5 beams (fabricated of CR5 and crushed limestone) behaved much more like the AC-10 beams than did any of the other SULPHLEX beams. Beams fabricated using binder CR3 also appear to have performed well in the controlled stress mode of testing. However, a close evaluation of the data shows a great deal of scatter at the higher stress levels; and, due to the very high stiffness of the specimens, the induced strain per load repetition was relatively low. Thus, the CR3 data may be deceptive to the extent that it is a function of the type of test performed. Beam specimens composed of mixtures utilizing binders CR1 and CR2 possess noticeably poorer flexural fatigue properties than do either mixtures employing either CR3 or CR5. In fact, the comparisons among CR1, CR2, and AC-10 in this study yield similar results when compared with the

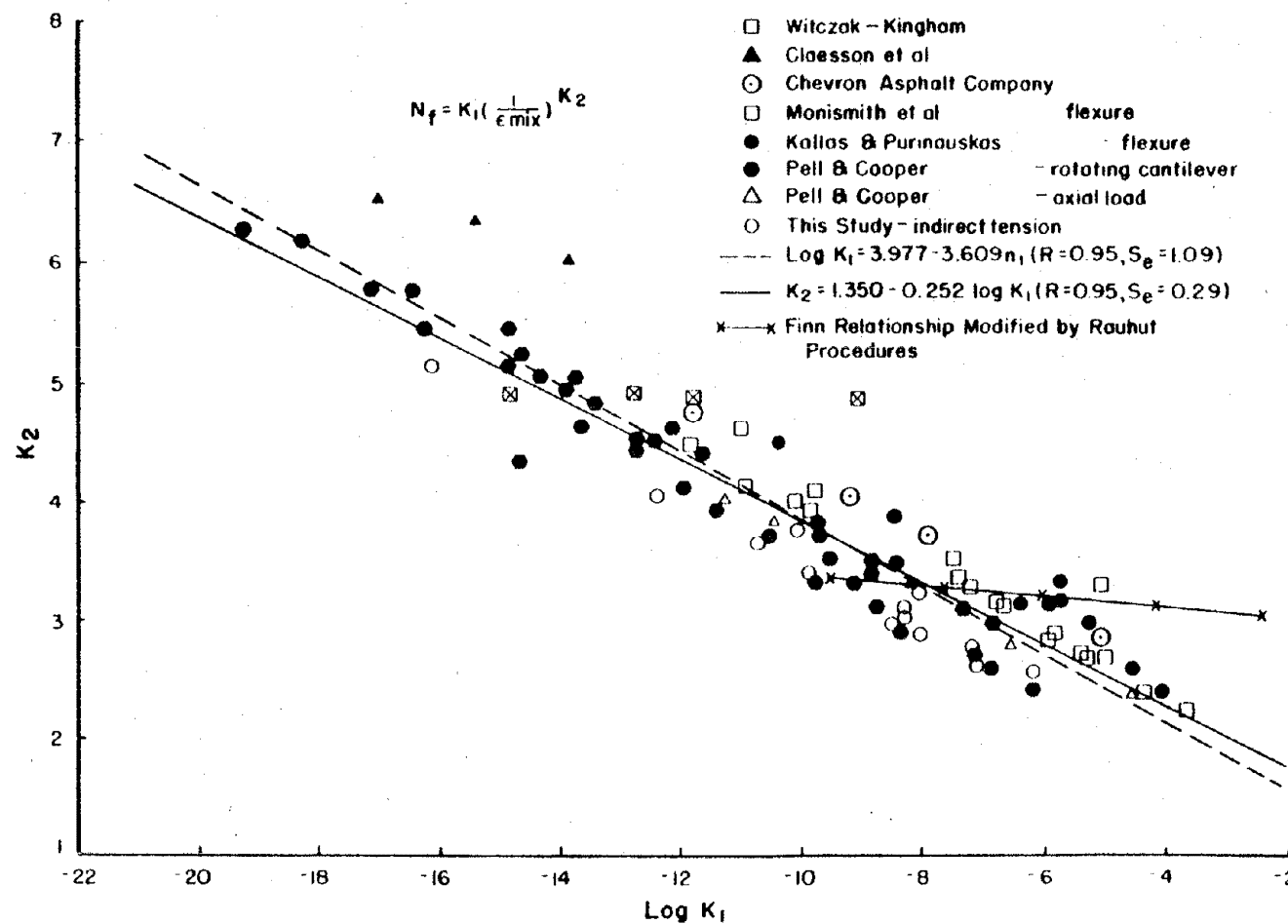


Figure 30. Relationship between K_1 and K_2 Based on Results Summarized by Kennedy and Rauhut (57).

Table 17. Summary of K_1 and K_2 Values from Phenomenological Beam Fatigue Testing.

Material	K_1	K_2	R Square of Regression Line	Test Temperature, °F
AC-10 Mixture	7.26×10^{-11}	3.90	0.80	40
AC-10 Mixture	8.00×10^{-9}	3.74	0.72	70
AC-10 Mixture	5.60×10^{-7}	3.60	0.82	100
CR1 Mixture	2.30×10^{-6}	2.88	0.80	70
CR2 Mixture	3.49×10^{-5}	2.53	0.50	70
CR3 Mixture	1.73×10^{-6}	4.43	0.69	70
CR5 Mixture	1.74×10^{-7}	3.39	0.72	70
CR5 Mixture	2.12×10^{-9}	3.50	0.68	40
CR5 Mixture	1.25×10^{-5}	3.29	0.75	100

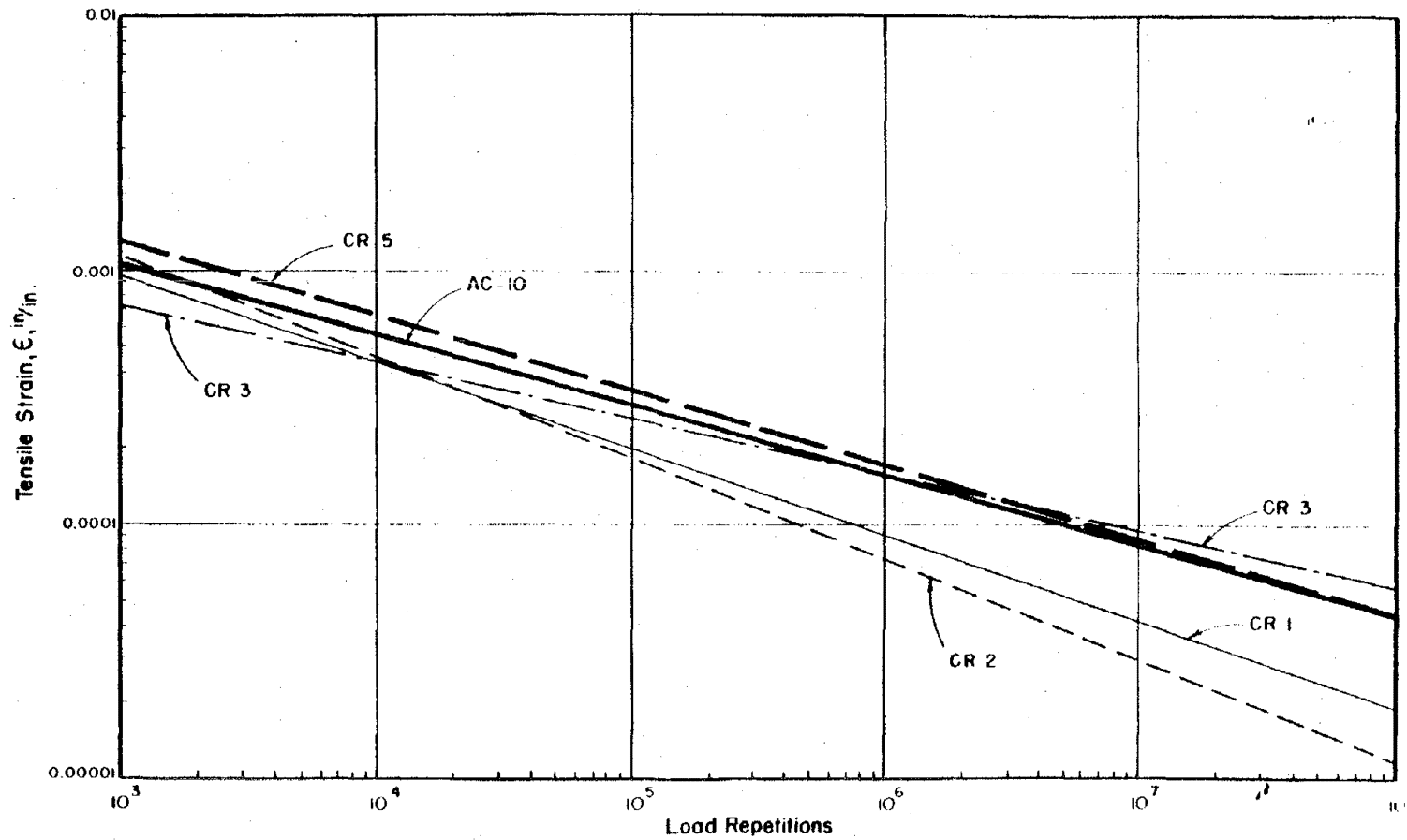


Figure 31. Phenomenological Fatigue Results for All Beams Tested (Each Mixture was Composed of Binder and Crushed Limestone).

AC-20 beams and the SULPHLEX 233 in the Sherwood and Kennis (54) study, Figure 32.

The data from this study and the Sherwood and Kenis study cannot be directly compared because of the different modes of testing involved, i.e., simply supported beams versus beams on elastic foundations. However, the trend shown in Figure 32 comparing within study results should be valid.

Temperature Effects on K_1 and K_2

The effects of temperature variation on fatigue parameters K_1 and K_2 were evaluated for beams fabricated from CR5 SULPHLEX binder. The results are presented in Table 17 and Figure 33. Also shown in Figure 33 and Table 17 are the K_1 and K_2 changes that occur in the control mixture composed of AC-10 and crushed limestone. As would be expected the temperature variations have a pronounced effect on the fatigue response. The temperature effects on the SULPHLEX are quite similar to those on the control mix. In both cases the effect on K_1 of temperature variation is quite pronounced while the effects on K_2 are actually quite small.

Based on a substantive literature review, Kennedy and Rauhut (57) suggest that K_1 for asphalt concrete should be modified for the effects of temperature according to the following relationship:

$$\log K_1(T_1) / K_1(T_2) = 0.00058 (T_1^2 - T_2^2) \quad (5)$$

Figure 34 shows the relationship Rauhut selected in the VESYS II Sensitivity Analysis (58). This plot is the basis for equation 5. The results of the AC-10 and CR5 data are superimposed on this plot. Clearly, the effect of temperature variation on K_1 and K_2 is quite similar for both SULPHLEX and asphalt.

The phenomenological fatigue test results for CR5 mixtures indicate that fatigue performance between 48°F and 100°F is similar to asphalt concrete. In addition, the effects of temperature variation on fatigue parameters K_1 and K_2 within this temperature range are similar for asphalt and SULPHLEX CR5. This similarity in performance

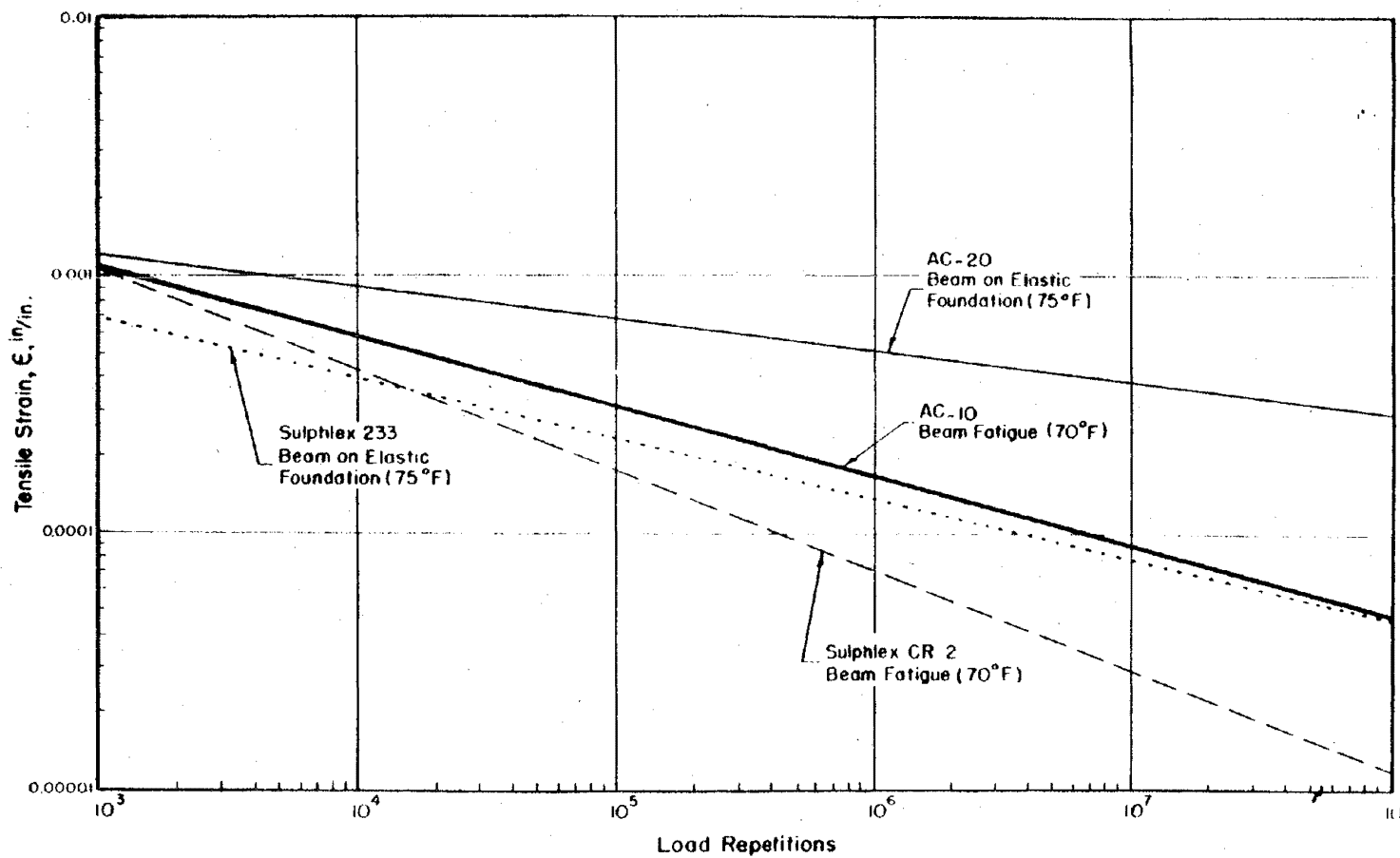


Figure 32. Comparison of Phenomenological Data from Simply Supported Beams and Those Supported by Elastic Foundations.

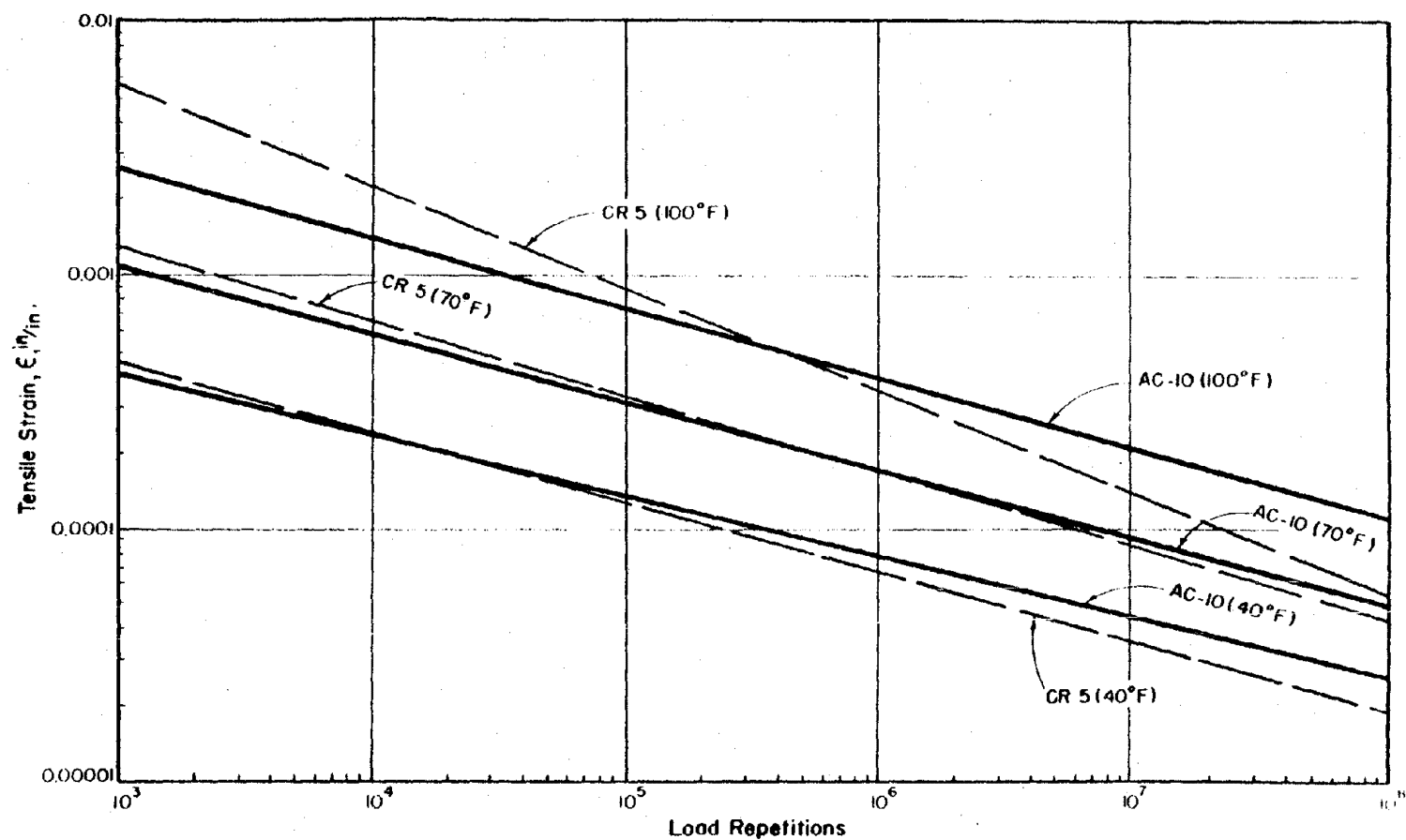


Figure 33. Effect of Temperature on Fatigue Curves of AC-10 and SULPHLEX CR5 Mixtures.

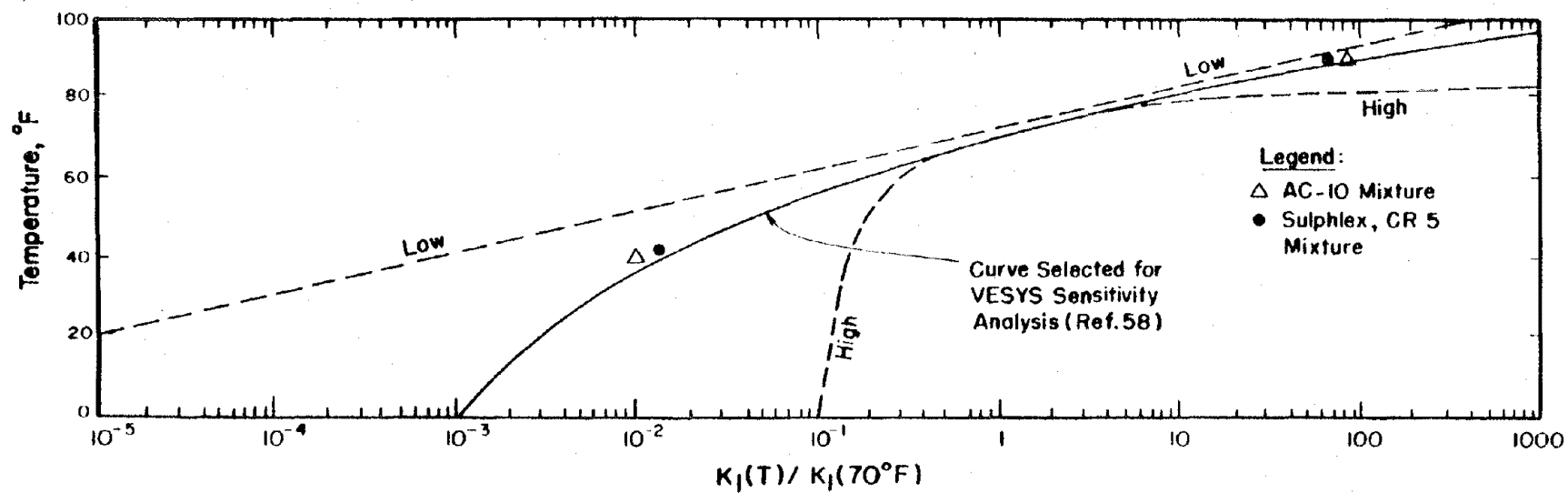


Figure 34. The Effect of Temperature on the Phenomenological Fatigue Parameter K_I (after Rauhut et al. (57)).

between CR5 SULPHLEX and asphalt concrete will be partially substantiated in the results of the fracture mechanics study.

Results of Fracture Mechanics Study

Rate of Crack Growth

Figure 35 is an illustration of the relationship between crack length and cycles of loading. All data presented in Figure 35 and in Tables 18 and 19 are for fatigue tests performed at 77°F.

The mathematical form which best defines the relationship between crack length and number of cycles is:

$$c = aN^b$$

where c is crack length, N is number of cycles and a and b are regression constants. Table 18 summarizes the regression constants which were derived to define the crack length versus number of cycles relationship for the specimens tested. The high R square values indicate a very good fit of the model and show that it explains most of the data variation. Table 19 summarizes the variation in test conditions and number of cycles recorded until failure occurred for each test condition.

Generally, the following characteristics were observed from the analysis of rate of crack growth:

1. Crack growth generally decreases as N increases. The decrease is very drastic in the first inch of the specimen thickness and levels to a fairly constant value after about 100 cycles.
2. Slopes, b , are generally greater for displacements of 0.04 inches than for displacements of 0.02 inches, indicating a faster rate of crack growth for the larger displacements, Table 19.
3. Slopes, b , are higher for CR3 specimens than for CR5 specimens or AC-10 specimens indicating the more brittle nature of CR3,

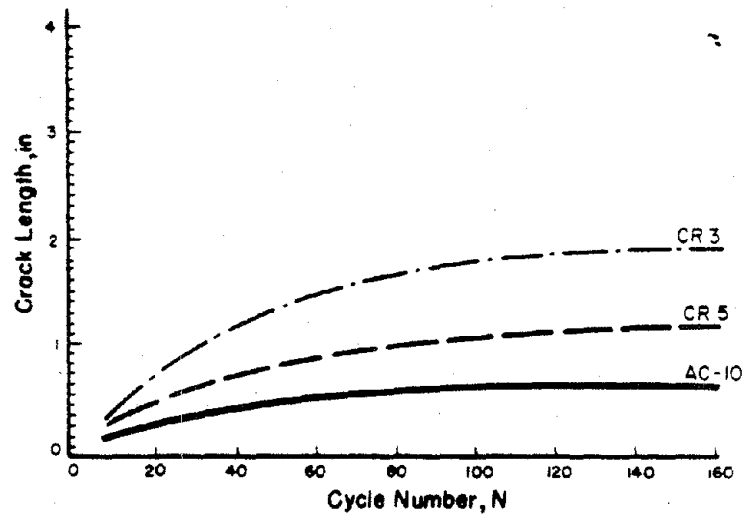


Figure 35(a). Crack Length Versus Number of Load Applications for 0.02-Inch Opening Displacement. (Each Curve is the Average of Four Tests.)

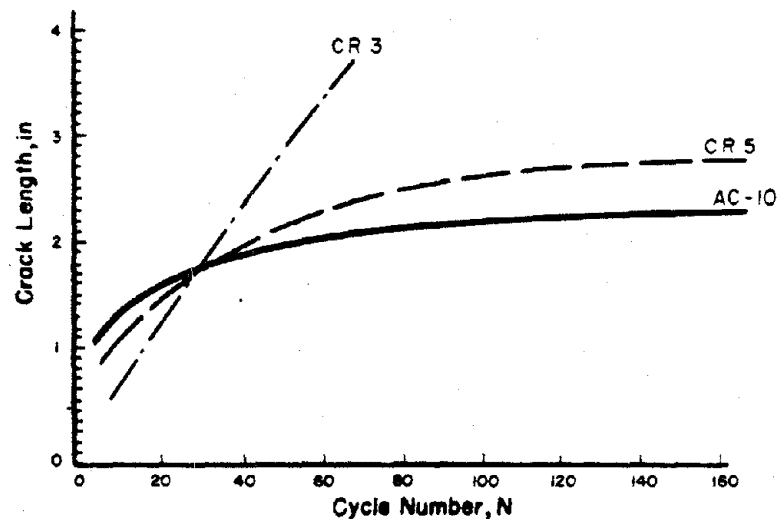


Figure 35(b). Crack Length Versus Number of Load Applications for 0.04-Inch Opening Displacement. (Each Curve is the Average of Four Tests.)

Table 18. List of Regression Coefficients of the Relationships Between Crack Length and Number of Cycles to Failure. (All Tests at 77°F.)

Binder Type and Specimen No.	Intercept (a)	Slope (b)	R ²
CR3 - 19	0.032	1.230	0.945
20	0.043	0.844	0.975
21	0.009	1.233	0.923
22	0.178	0.585	0.868
23	0.013	0.832	0.959
24	0.245	0.365	0.930
25	0.332	0.302	0.962
26	0.097	0.473	0.973
CR5 - 27	0.163	0.302	0.904
28	0.235	0.422	0.944
29	0.475	0.373	0.980
30	0.286	0.290	0.862
31	0.286	0.431	0.963
32	0.142	0.392	0.967
33	0.271	0.315	0.960
34	0.621	0.223	0.983
AC10 - 2	0.623	0.266	0.984
7	0.273	0.197	0.841

Table 19. Summary of Results and Test Conditions of Initial Overlay Tests. (All Tests at 77°F.)

Binder Type and Specimen No.	Air Voids, %	Displacement, in.	Rest Period	Cycles to Failure, N_f
CR3 - 19	5.58	0.04	1 hr. @ #10*	43
20	6.42	0.04	4 hr. @ #7	130
21	6.12	0.04	None	133
22	6.58	0.04	None	124
23	6.55	0.02	None	600
24	6.58	0.02	None	816
25	5.91	0.02	24 hr. @ #7	619
26	6.88	0.02	1 hr. @ #50	691
CR5 - 27	5.75	0.02	1 hr. @ #6	3588
28	5.65	0.04	1 hr. @ #52	281
29	5.71	0.04	None	211
30	4.74	0.02	None	2224
31	6.19	0.04	24 hr. @ #7	224
32	5.20	0.02	4 hr. @ #7	1639
33	5.85	0.02	None	1000
34	6.67	0.04	None	328
AC10 - 2	4.77	0.04	None	265
7	5.17	0.02	None	2266

* Number of cycle at which rest period is made.

Table 18. This is substantiated by the shorter lives of CR3 specimens when compared with CR5 and/or AC-10 specimens, Table 19...

4. The rate of crack growth in CR5 specimens and AC-10 specimens is similar while the rate of crack growth in CR3 specimens is quite dissimilar to either AC-10 or CR5 specimens, Table 19.
5. Variations among observations obtained under identical conditions are small.

Table 20 presents the results of analysis of variance (ANOVA) on the number of load cycles to failure caused by material effects only. (Table 19 data). Although the variables represent regression coefficients and are not actual observations, ANOVA is still appropriate as long as the parameters investigated are normally distributed, independent, and have equal variance. The first two conditions are satisfied. The small standard errors associated with the parameter estimates permit the assumption of equal variances.

Table 21 presents the ANOVA results on the slope of the C-N relationships, including Duncan Multiple Range (DMR) tests, caused by material effects, rest periods and displacement magnitudes. Duncan Multiple Range is a statistical procedure used to compare the mean values of groups with different numbers of observations. The group means are tested for statistically significant differences at a specified level of accuracy. The ANOVA results confirm the similarity between AC-10 and CR5 and their difference from CR3. The ANOVA also indicate the significant effect of displacement magnitude on the c-N relationship and the lack of significance of the single rest period on the c-N relationship.

Table 22 is a recapitalation of the number of load cycles to failure data illustrating the effects of material type, rest periods and displacements magnitude. Table 23 presents the ANOVA (Duncan Multiple Range) results for the effects of rest period, displacement magnitude.

Table 20. Summary of ANOVA Results on Number of Load Cycles to Failure, N_f , Caused by Material Type Effects, Table 19 (All Test at 77°F.)

Test Type	F Value	F Critical	Significant Difference @ $\alpha = 0.1$
Effect of Material AC-10 vs CR3	3.37	3.14	Significant
Effect of Material AC-10 vs CR5	0.13	3.14	Not Significant
Effect of Material CR3 vs CR5	6.04	3.14	Significant
Effect of Material AC-10 vs all CR	4.59	3.14	Significant

Table 21. Summary of Analysis of Variance on the Slope of c-N Relationship, Table 18 (All Test at 77°F.)

Type of Test	F Value	F Critical	Significant Difference @ $\alpha = 0.1$
Effect of Material AC10 vs CR3	6.37	3.14	Significant
Effect of Material AC10 vs CR5	0.27	3.14	Not Significant
Effect of Material CR3 vs CR5	11.07	3.14	Significant
Effect of Single Rest Period	0.04	3.14	Not Significant
Effect of Displacement Magnitude	4.63	3.14	Significant
Differences in Duncan Means of CR3 vs AC10 & CR5	-----	----	Significant
Differences in Duncan Means of AC10 vs CR5	-----	----	Not Significant
Difference in Duncan Means Between Single Period and No Rest	-----	----	Not Significant

Table 22. Recapitulative Summary of Number of Cycles to Failure,
 N_F (All Tests at 77°F.)

Binder Type		1 Rest Period		No Rest	
		0.02in.	0.04in.	0.02in.	0.04in.
CR3	Test 1	619	43	600	133
	Test 2	691	130	816	124
CR5	Test 1	3588	281	2224	211
	Test 2	1639	224	1000	328
AC10	Test 1	---	---	2266	265

Table 23. Summary of Analysis of Variance of Number of Load Cycles to
 Failure Considering the Effects of Rest Period and Displacement
 Magnitude (All Tests at 77°F.)

Type of Test	F Value	F Critical	Significant Difference @ = 0.1
Effect of single rest period	0.48	3.14	Not Significant
Effect of displacement magnitude	18.30	3.14	Highly Significant
Differences in Duncan means between rest and no rest	---	---	Not Significant
Differences in Duncan means between 0.02 in. and 0.04 in. displacements	---	---	Significant

Energy Release Rate Relationships

Figure 36 represents a typical relationship between dissipated energy per unit thickness and crack length. This relationship is once again best defined by a loglinear relationship of the form

$$U/B = a'c^{b'}$$

where U is energy, B is specimen thickness and a' and b' are regression constants. Table 24 summarizes the results of these relationships. The high R square values prove this relationship is acceptable in explaining the variation in the data. From these data the following conclusions are drawn:

1. The energy released per unit thickness and the energy release rate, J^* , follow a similar pattern of change for each specimen tested as the crack grows through the specimen. The released energy decreases in a pattern similar to the decrease of rate of crack growth.
2. No significant differences in energy release patterns exist between specimens with no rest and those with one rest period.
3. The energy per unit thickness of the specimens is substantially greater for a given crack length for CR3 and CR5 mixtures than for AC-10 mixture.

J^* Versus dc/dN Relationship

The primary relationship derived from this study is that between the rate of crack growth, dc/dN , and the modified J integral, J^* . The parameter J^* is a measure of material "toughness." As would be expected, the loglinear form defines the relationship well:

$$dc/dN = A(J^*)^n$$

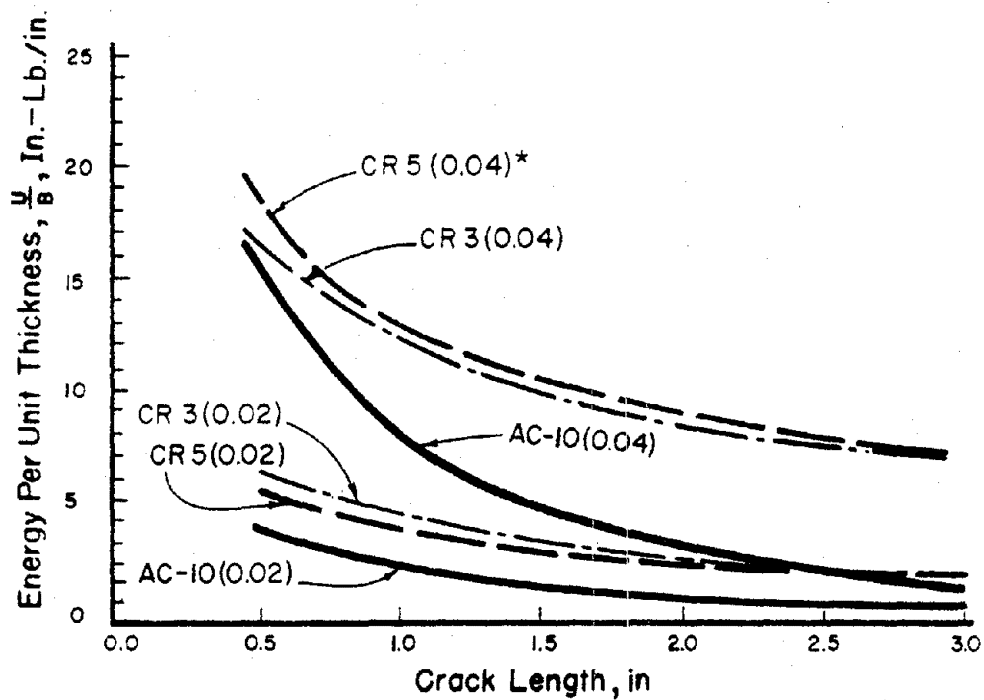


Figure 36. Relationship Between Energy Required to Drive Crack per Unit Thickness of Specimen and Crack Length. (Each Curve is Result of Four Tests.)

* Indicates Level of Displacement in Inches.

Table 24. List of Regression Coefficients of the Relationships Between Energy Normalized for Thickness and Crack Length.

Binder Type and Specimen No.	Intercept (a')	Slope (b')	R ²
CR3 - 19	14.300	-0.624	0.295
20	10.158	-0.466	0.883
21	10.857	-0.377	0.860
22	11.603	-0.693	0.800
23	3.617	-0.428	0.854
24	3.800	-0.675	0.924
25	4.782	-0.929	0.933
26	3.824	-0.592	0.955
CR5 - 27	3.318	-0.574	0.941
28	10.251	-0.499	0.800
29	14.378	-0.519	0.946
30	3.907	-0.663	0.859
31	11.899	-0.607	0.876
32	3.275	-0.555	0.887
33	3.787	-0.587	0.889
34	14.807	-0.732	0.958
AC10 - 2	7.789	-1.127	0.892
7	1.967	-0.833	0.806

Table 25 presents the fabrication data for the specimens from which the J^* versus dc/dN relationships were developed. Table 26 presents the regression constants A and n for each test.

Figure 37 illustrates the results of the crack growth rate versus energy release rate relationship. In reviewing Figure 37 one must remember that the test is a controlled displacement test, and crack growth rate is initially large but moderates rapidly as the crack grows and thus the J^* value decreases.

From Figure 37 several conclusions were drawn:

1. At 68°F, Figure 37a, the asphalt concrete mixtures are statistically significantly less brittle than the comparable SULPHLEX mixtures (CR3 or CR5).
2. Although the CR3 mixtures in Figure 37a appear to be more brittle than CR5 mixtures, the differences are not statistically significant.
3. The temperature effects on the fatigue relationships are substantially greater for the SULPHLEX binders than for the asphalt concrete binders. A temperature variance of 19°F (77°F to 58°F) for asphalt concrete produces a relatively small, though certainly detectable, variance in fatigue properties. However, a variance of only 12°F (77°F to 65°F) produces a substantial variance in SULPHLEX (CR5) fatigue properties. This sensitivity to controlled strain or controlled displacement fatigue is apparent for SULPHLEX mixture.
4. Although CR5 mixtures may be comparable to asphalt concrete in terms of fracture propagation properties at 77°F (Figure 35 and 36 and Tables 18 through 24) asphalt concrete is clearly superior at lower temperatures, as little as 12°F lower.

Effect of Specimen Thickness

Specimen thickness greatly affects the state of stress at the crack tip. In a test specimen, in order to maintain plane strain conditions, which is the critical condition for a brittle fracture, specimen thickness must be sufficiently large. In thin specimens, where the plastic zone is not small compared to the thickness, plane

Table 25. Summary of Fabrication Data for Beams Used in J^* Versus dc/dN Relationships.

Specimen Identification	Binder Type and Mixture Description	Air Void Content, %	Magnitude of Cyclic Opening Displacement, Inches	Temperature of Test, °F
CR3 - 1	CR3 and Crushed	5.2	0.02	65
2	Limestone	6.0	0.02	65
CR5 - 1	CR5 and Crushed	6.0	0.02	65
2	Limestone	5.2	0.02	65
3		5.0	0.02	77
AC10 - 1	AC-10 and	5.0	0.02	58
2	Crushed Limestone	5.2	0.02	65
3		5.8	0.02	65
4		6.0	0.02	77
5		5.7	0.02	77

Table 26. Summary of Results and Analysis of Relationships Between dc/dN and J^* (Paris Relationship).

Specimen Identification	Intercept A	Slope (n)	R^2 of $\frac{dc}{dn} = A(J^*)^n$ Relationship
CR3 - 1	4.30×10^{-2}	1.10	0.95
2	4.00×10^{-2}	1.30	0.92
CR5 - 1	4.15×10^{-2}	0.90	0.91
2	1.20×10^{-2}	1.66	0.92
3	2.00×10^{-3}	1.50	0.90
AC10 - 1	2.04×10^{-3}	0.99	0.90
2	1.87×10^{-3}	1.20	0.94
3	1.72×10^{-3}	1.11	0.99
4	1.090×10^{-3}	1.20	0.94
5	1.013×10^{-3}	1.24	0.96

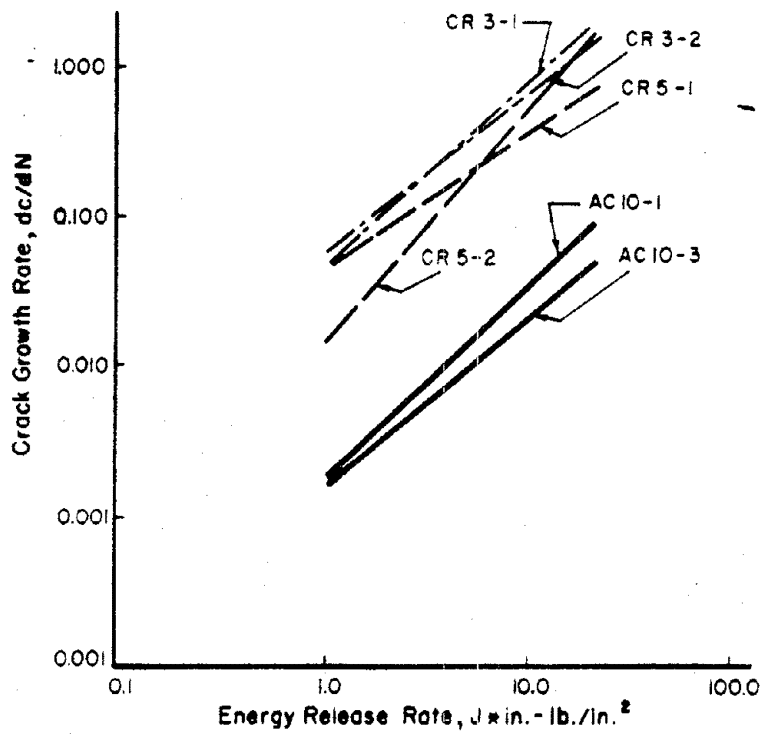


Figure 37(a). J^* Versus dc/dN Relationships for SULPHLEX and Asphalt Concrete Mixtures at 65°F.

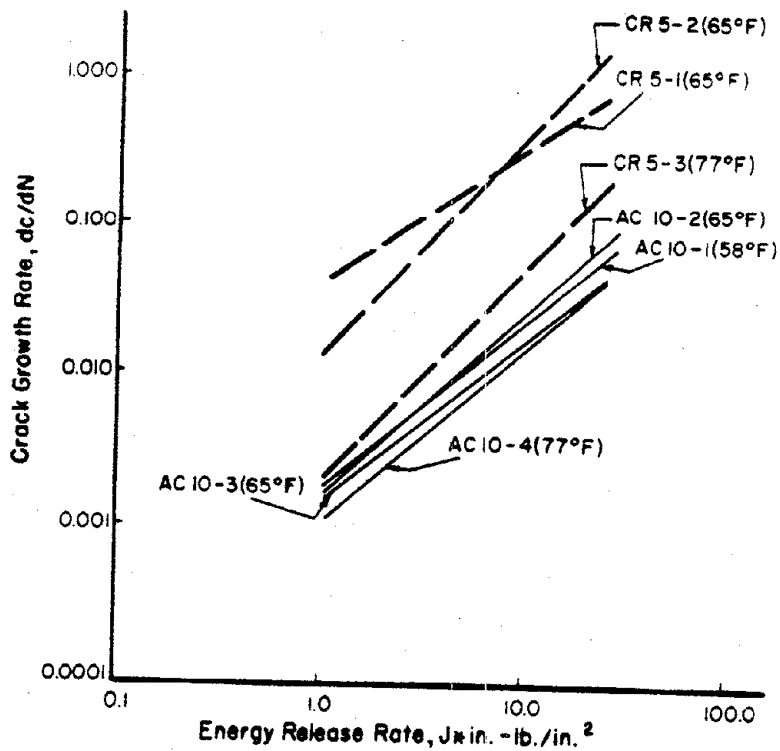


Figure 37(b). Effect of Temperature on J^* Versus dc/dN Relationship.

stress develops. In this case a higher stress intensity factor is required to cause crack propagation.

One-inch by three-inch, two-inch by three-inch and three-inch by three-inch specimens were tested to evaluate the effects of thickness on crack propagation. The one-inch thick specimens were too thin and failed immediately. However, the two-inch thick specimens showed a crack growth pattern similar to the three-inch specimens. The regression coefficients for the J^* versus dc/dN relationship and the magnitude of the J^* values for the two-inch specimens were comparable to those of the three-inch specimens. This emphasizes the validity of the approach and indicates that material properties (A and n) do not change with variation in specimen geometry. This also verifies that the amount of energy released per unit area of crack extension is a material property.

Effect of Displacement Rate

Crack resistance is a function of the plastic behavior of the material at the crack tip. This behavior is strain rate dependent, i.e., the yield stress increases and the fracture strain decreases at higher strain rates. At the tip of a crack moving at high velocity the strain rates are very high, and it must be expected that the material behavior is more brittle at the higher crack speed. Bucknall (59) has demonstrated that rapid decrease in critical strain energy release rate at high crack speeds is attributed to the increase in yield stress, thus decreasing the size of the plastic zone at the crack tip.

In this study the influence of displacement rate, which directly affects crack speed, was examined. Experiments were performed at rates of 3, 12, and 30 cycles per minute (and at 0.04-inch displacement magnitude). These experiments are summarized in Figure 38 and Table 27.

Test results show increasing fracture life with decreasing displacement rates, Table 27. The damage done per cycle is indeed greater at the faster displacement rates. The total dissipated energy per cycle is lower for these faster displacement rates.

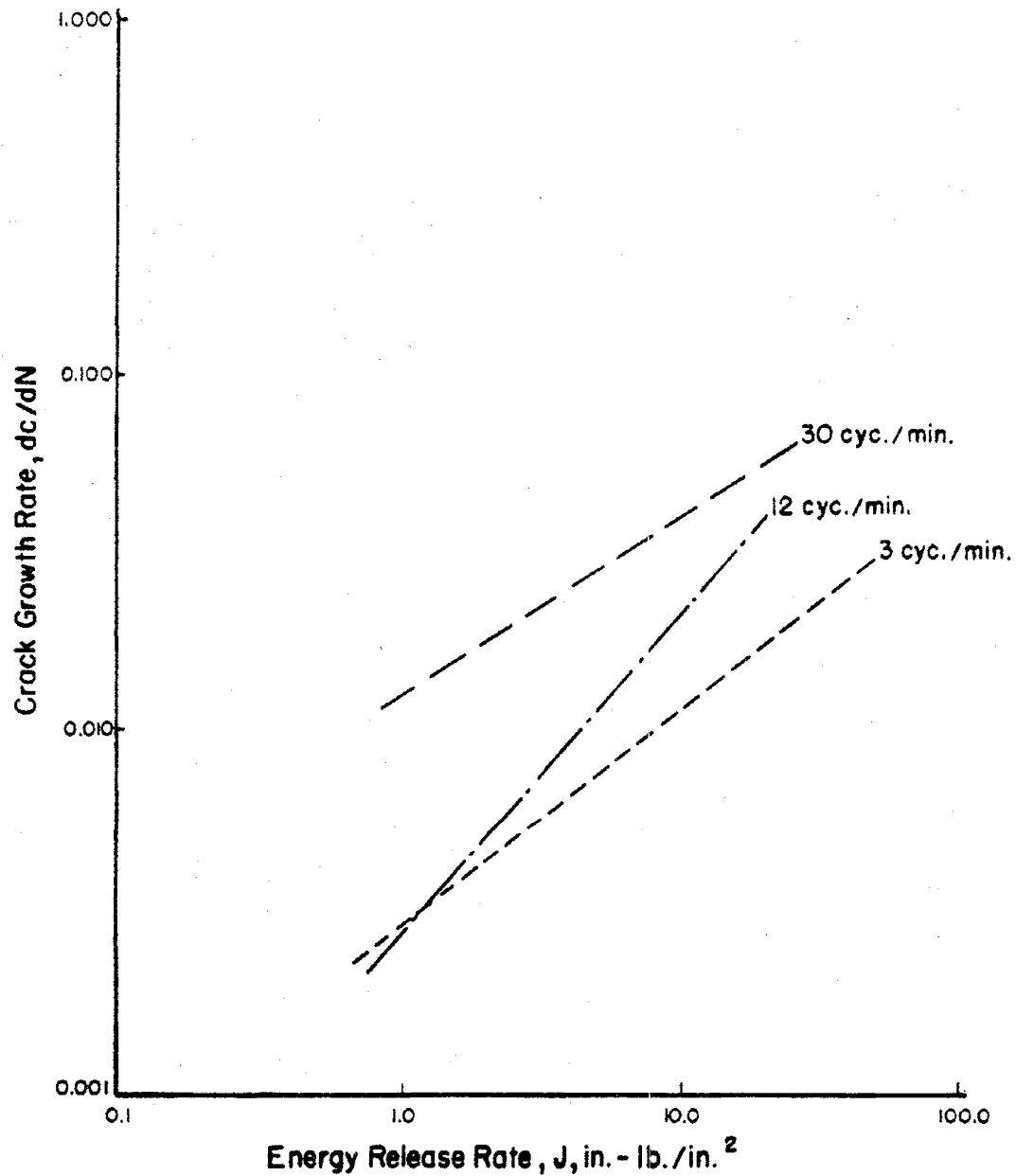


Figure 38. Relationship Between Crack Growth Rate and Energy Release Rate for Three Displacement Rates.

Table 27. Summary of Regression Analysis on Experiments at Different Displacement Rates.

(a) Crack length versus cycle number relationships.

Displacement Rate (cycle/min)	Intercept	Slope	R^2	N_f
3	0.111	0.494	0.905	564
12	0.259	0.384	0.916	261
30	0.182	0.558	0.983	126

(b) Energy/thickness versus crack length relationship.

Displacement Rate (cycle/min)	Intercept	Slope	R^2
3	6.390	-0.512	0.738
12	7.972	-0.617	0.924
30	9.166	-0.513	0.694

(c) dC/dN versus J^* relationship.

Displacement Rate (cycle/min)	Intercept	Slope	R^2
3	0.003	0.613	0.911
12	0.003	0.910	0.928
30	0.012	0.514	0.956

These test results are best summarized by Figure 38 where for a given energy release rate the dc/dN increases with increase in displacement rate.

Effect of Rest Periods

Recently it has been shown through research based on fracture mechanics (60, 61, 61, and 63) that a certain degree of healing can be expected to take place in polymeric materials. The basic mechanism of this healing process has not been adequately explained, but its existence has been empirically demonstrated (63, 64, and 65). The practical effects of healing, due to extended rest periods between loads, will be manifested in extended fatigue life. This will be discussed in the section entitled "Fatigue Shift Factor."

Indeed an assessment and quantification of the degree to which a material, which is polymeric in nature, has a propensity to heal is of critical importance in terms of the ultimate ability to characterize the fatigue properties of the material and to predict performance.

Preliminary testing, Table 23, showed that a single rest period had no significant effect on fracture characteristics. A more complete study of the rest period effects on AC-10 specimens and CR5 specimens was conducted. The rest period duration and frequency was considered in the expanded analysis. The indicator of material recovery following the rest period was the increase in energy required to open the crack to the selected constant displacement level. This energy increase was assessed by the area within the load-displacement plot.

The effects of rest period duration at 77°F for AC-10 and CR5 specimens are shown in Figure 39. The duration of each rest period for a specific test specimen was randomly selected as was the stage of rest period application so that the interaction of rest period duration and stage of testing (stage of crack propagation) was not an influencing factor. As would be expected, a great deal of data scatter is apparent. However, it is clear that within a period of from 15 to 40 minutes, a considerable portion of the recovery for the CR5 specimen takes place, and longer rest periods of one or two days

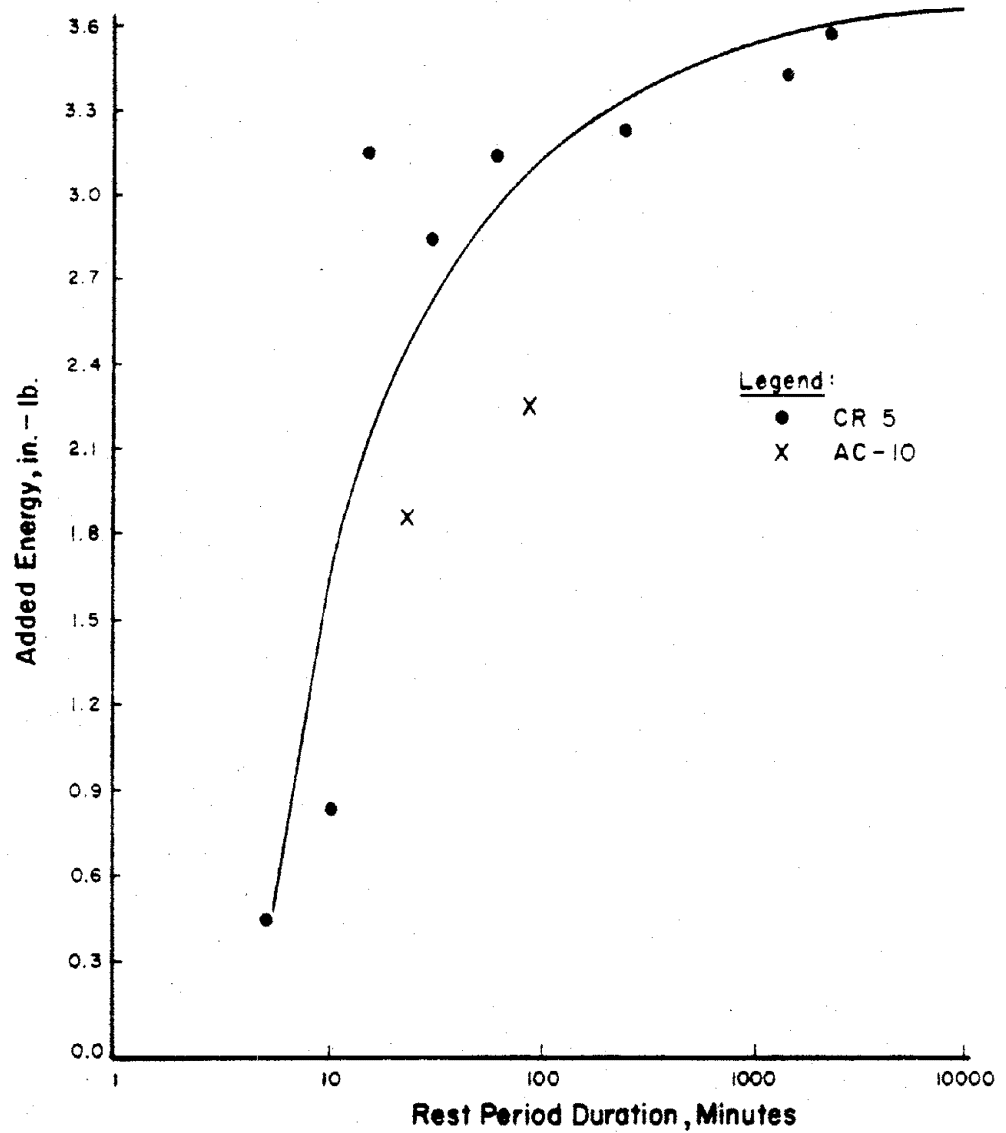


Figure 39. Effects of Rest Period Duration on Energy Required for Crack Propagation (Specimens were CR5 and Crushed Limestone).

do not substantially increase the recovery. For practical purposes 15 minute rest periods were used throughout the remainder of the study.

The model which best defines the increase in energy for crack propagation caused by rest periods is of the form

$$\Delta u = e^h \log t$$

where Δu is the added energy, t is duration of the rest period and h is a constant ($h = 0.45$ based on the test data).

Although a full analysis of changes in crack propagation energy due to rest duration for AC-10 specimens was not undertaken, the magnitudes of energy increase for 15 and 100 minute rest periods are shown in Figure 39. This indicates similarity between AC-10 and CR5 in terms of healing or recovery potential.

The effects of number or frequency of rest periods was examined. The result was an increase in fatigue life by a factor of from two to five when rest periods were introduced for CR5 specimens. The beneficial effects of rest periods are plotted in Figure 40 and are expressed in the following ways:

1. A linear regression between the number of rest periods and number of cycles to failure and
2. A linear regression between the added energy for crack propagation due to the introduction of rest periods and the number of rest periods.

As illustrated by Figure 40, the introduction of rest periods increases the number of cycles of applied load (constant deformation) necessary to propagate a crack in both CR5 and AC-10 specimens. In fact, the CR5 specimens responded even more sensitively to the application of rest periods than did AC-10 specimens. Thus, it is apparent that rest periods affect fatigue performance life and must be considered in the development of field fatigue criteria.

It must be emphasized that all the fracture mechanics testing was performed at 77°F. Certainly the effects of temperature on the fracture properties of SULPHLEX are highly significant. These will be discussed under the section "Low Temperature Cracking."

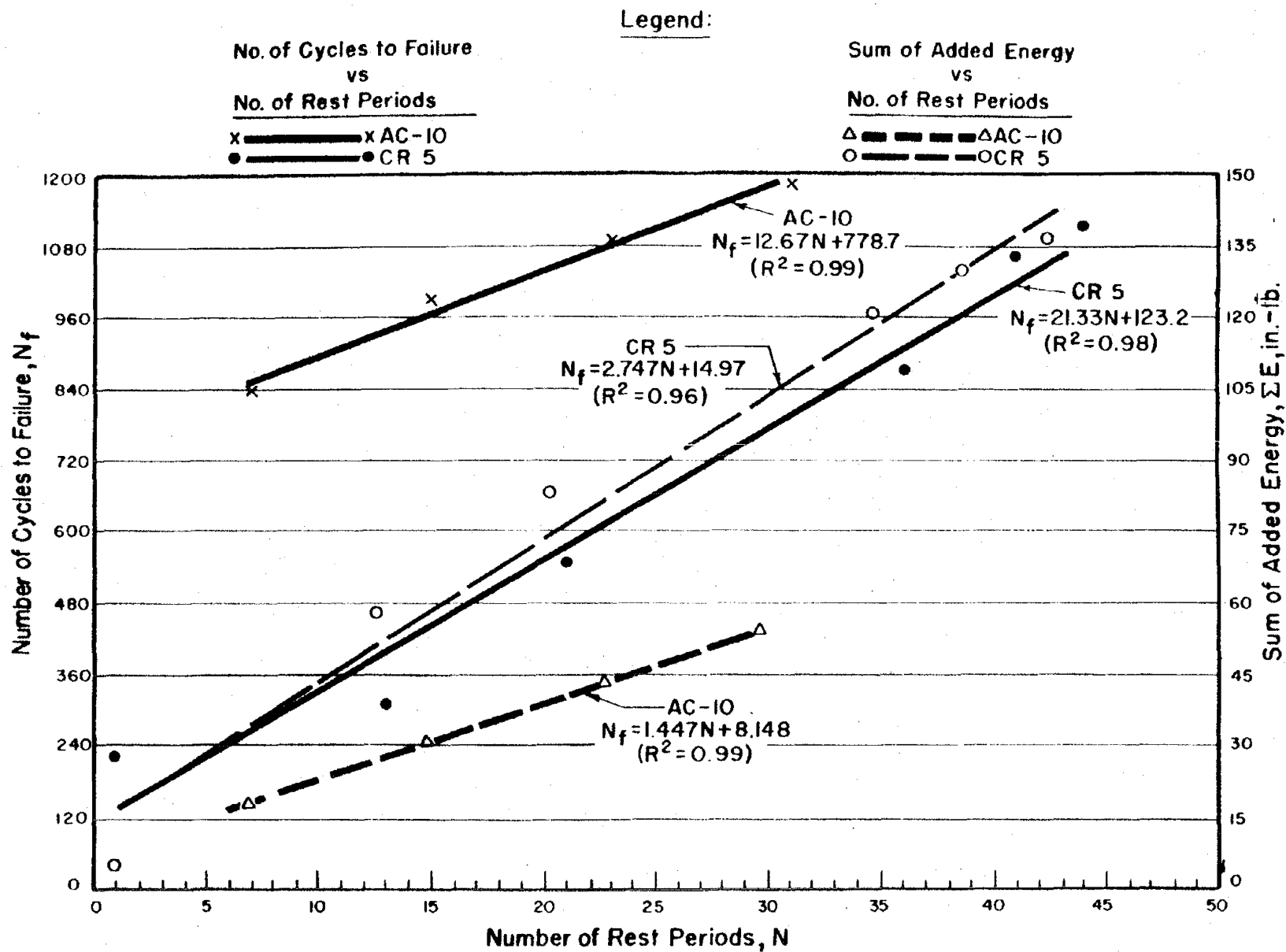


Figure 40. Relationships Between (1) Number of Cycles to Failure and Number of Rest Periods and (2) Sum of Added Energy and Number of Rest Periods.

Laboratory to Field Shift Factors

Background

Without question laboratory phenomenological fatigue curves, which are required as performance criteria for both the FPS-BISTRO and VESYS structural pavement subsystems used in this study for optimization of structural pavement design, underpredict field behavior. The laboratory phenomenological fatigue relationship does not account for a number of important factors such as healing of the pavement between stress applications, residual stresses, rest periods between application, and variability of the position of the load wheel.

The data available dealing with fatigue shift factors ranges widely. For example, Van Dijk (66) suggested a horizontal shift factor of 3. That is

$$N_{\text{field}} = 3N_{\text{lab}}$$

Finn et al. (67) used actual AASHTO Road Test data and fatigue data on laboratory fabricated beams of asphalt concrete, which were made from exactly the same materials as those used in the Road Test, to develop a horizontal shift factor of 13. Santucci (68) suggested a shift factor which accounted for the percent air voids and asphalt contained in the mixture. His shift factors range from 0.02 to 32. Pickett et al. (56) recommended a shift factor of the form

$$N_{\text{field}} = G \times N_{\text{lab}}$$

where

$$G = 0.516 \times 10^{0.0147T} \text{ and}$$

T = temperature ($^{\circ}\text{F}$)

for sulfur extended asphalt mixes. Their assumption was that the shift factor should get larger as the temperature increased to account for the greater probability of healing at higher temperatures. These shift factors ranged between 3 and 42.

Pickett et al. (56) selected a different shift factor for asphalt concrete which accounted for the effects of temperature as well as a suggested intersection point between laboratory and field data between 10^7 and 10^8 repetition (69 and 70). These shift factors varied between 0.56 and 19.

Results of wheel cracking tests made by Shell Laboratorium (71) show that fatigue cracking of bituminous pavements occurs in several sequential stages. These stages are the progressive developments of fatigue crack which eventually result in pavement failure. It is believed that the fatigue lives measured in the laboratory (beam fatigue) more accurately describe the number of cycles necessary for initial crack formation. The more important action in terms of pavement life occurs as a result of crack propagation and widening of the initial cracks. Of course, healing rest periods and residual stresses could easily, although in a complex way, affect the resultant pavement fatigue life in the field. Fracture mechanics techniques and the overlay tester were used to evaluate the effects of rest periods on the laboratory to field fatigue shift factor.

Shift Factor Development

Lytton and Yandell (72) have verified that substantial residual compressive strains exist in surface pavement layers resulting from previous wheel load applications. This residual strain may reduce the critical tensile strain induced by a wheel load by as much as 20 percent. The occurrence of residual stresses coupled with the relaxation capabilities of a pavement material may have substantial effect on the prediction of a shift factor.

Perhaps the most dramatic effect on the proposed laboratory to field shift factor is that of healing. Healing of fractures has been conclusively shown to occur in the extensive research of Wool et al. (60, 61, and 62).

The study discussed herein deals with the healing potential during rest periods and its role in the laboratory to field shift factor. Of course, without field results no true shift factor can be developed. However, a sound theoretical model will be submitted which accounts

for the effects of residual stresses and healing. The material healing characteristics of both asphalt concrete and SULPHLEX were evaluated using this model. Then, a comparative analysis of the role of the shift factor in pavement design was made between asphalt concrete and SULPHLEX.

The primary purpose of this effort was to evaluate the healing and relaxation potential of SULPHLEX with that of asphalt concrete using the proposed shift factor model as a basis. It has been shown that the shift from laboratory to field results has an enormous effect on predicted performance; therefore, any fatigue analysis would be incomplete without consideration of these overpowering effects.

Approach

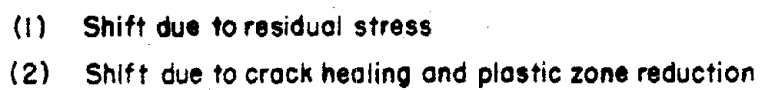
Lytton (73) has proposed a laboratory to field shift factor which accounts for the effects of residual stresses and healing, Figure 41. During a rest period two recovery processes may take place. In one process (labeled 1) the material relaxes and loses some of its residual compressive strain. This is a deleterious process. The material is, in effect, losing, through relaxation, some of the prestressing developed by the previous wheel load.

In the second process (labeled 2), the material is allowed to heal from its distressed state. During this period, the plastic zone size ahead of the crack tip is reduced, and the existing crack may even be closed upon removal of the applied load due to compression resulting from bond forces within the material. The intersection of laboratory and field fatigue curves at approximately 10^7 load repetitions is based on the efforts of several researchers (69).

Binder CR5 was the only binder evaluated in this study. it was selected as it had proven to be the binder most similar to asphalt concrete.

It was postulated that the shift factor consisted of two components:

$$SF = (SF_R) \times (SF_H)$$



110

where SF_R is the shift factor due to residual stresses, and SF_H is the shift factor due to healing and plastic zone size reduction.

A typical relaxation curve was used to model SF_R . The curve has the general form

$$E(t)/E_0 = t^{-n}$$

where $E(t)$ and E_0 are elastic moduli at times t and zero, respectively, and n is the slope of the relaxation curve.

The relationship between strain at a given time, $\epsilon(t)$, to the initial strain ϵ_0 can be represented as follows:

$$\epsilon(t) = 1 - (1 - \epsilon_0)t^{-n'}$$

Here ϵ_0 is the approximate initial strain (approximately 80 percent of the induced strain due to residual stresses). A clear resemblance exists between the relaxation in elastic modulus with time and the recovery of strain with time. Thus the parameter n can be realistically assumed to equal n' .

Then the effects of relaxation are incorporated with the effects of residual stress to yield a shift factor

$$SF_R = \left[\frac{1}{1 - (1 - P_0)t^{-n}} \right]^{K_2}$$

where K_2 is the slope of the laboratory $(N_f - \epsilon)$ fatigue relationship.

The development of the shift factor related to healing is based on the rest period analysis discussed previously. The rest period analysis produced a relationship between added energy and the logarithm of rest duration of the form

$$\Delta u = e^h \log t$$

The rest period study also revealed that as the total energy added to the system by rest periods increases, so does the fatigue life

$$N_f = a + m(\Delta u)$$

or

$$N_f = a + m(e^h \log t) \quad (6)$$

Based on equation 6, the following relationship was derived from the rest period analysis of CR5 specimens

$$\frac{N_f}{N_0} = 1 + (5.685 \times 10^{-3} e^{1.965 \log t}) n_r$$

This empirical relationship states that the ratio of the fracture propagation life with rest periods, N_f , to the fracture propagation life without rest periods, N_0 , is described by equation 6 and is a function of the duration of the rest period, t , and the number periods, n_r .

Combining the two shift factors reveals the final form

$$SF = \left[\frac{1}{1 - (1 - \epsilon_0) t^{-n}} \right]^{k_2} [1 + 5.685 \times 10^{-3} e^{1.965 \log t \cdot n_r}] \quad (7)$$

Results

By entering the proper values of n (from stress relaxation data), t and n_r for CR5 specimens, a shift factor may be computed. Two components of the SF equation may be obtained from Figure 42.

Although equation 7 and Figure 42 do not provide an exact shift factor, they do indicate that:

1. The magnitude of the SF may be quite comparable to that of asphalt concrete.
2. The healing effect is very pronounced at the 73°F test temperature and is by far the major component of the shift factor.

Limited rest period testing on AC-10 specimens and CR3 specimens at room temperature reveal that:

1. Although the fracture propagation life, N_f , is superior for AC-10 specimens compared to CR5 specimens, healing properties at 73°F are similar.
2. CR3 specimens show inferior healing potential when compared to CR5 or AC-10 specimens.

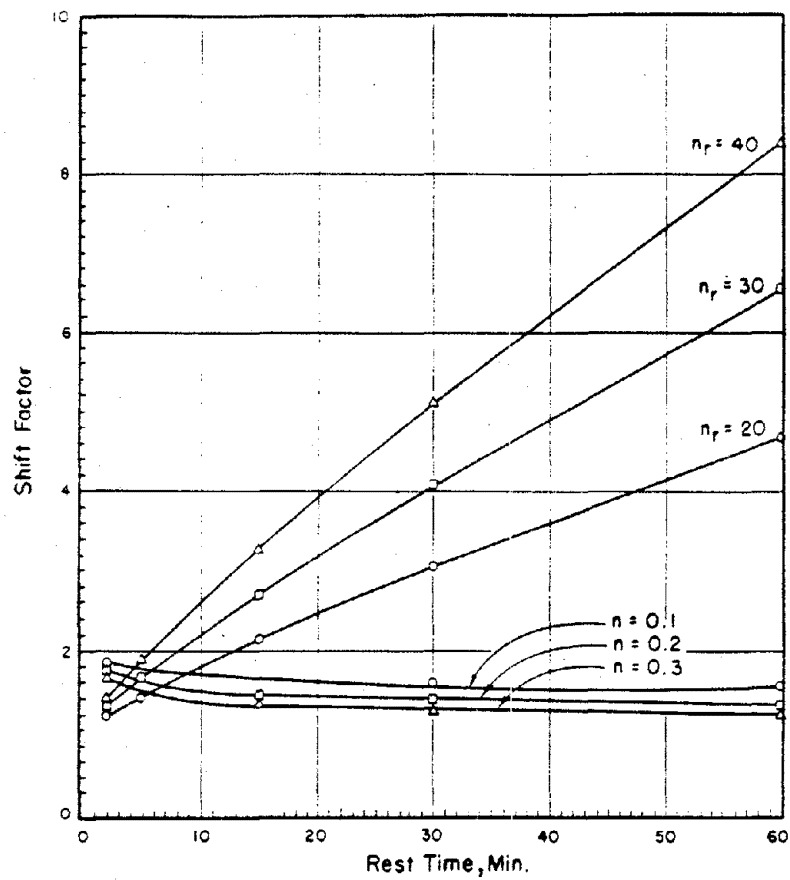


Figure 42. Shift Factors Calculated for Effects of (1) Residual Stresses and Relaxation of the Materials and (2) Healing Effect of Material.

Selection of Shift Factors

For use in VESYS IIM and FPS-BISTRO analysis it was necessary to shift the phenomenological fatigue curves to represent field conditions. The shift factors suggested by Pickett et al. (56), Table 28, were selected for both asphalt concrete and SULPHLEX for the following reasons:

1. Utilization of identical shift factors for asphalt and SULPHLEX is considered an acceptable approach until field verification indicates that different factors should be used,
2. The rest period analysis points out a similar healing response for SULPHLEX CR5 and AC-10 specimens and
3. Shifting AC-10 laboratory beam fatigue data by means of the Pickett factors yields a realistic failure criterion, very comparable to Finn et al. data (67), Figure 43.

Table 28. Laboratory to Field Shift Factors Used in this Study for Asphalt Concrete and SULPHLEX.

N _{lab}	Shift Factors		
	T = 36°F	T = 68°F	T = 110°F
10 ²	18.8	12.9	7.9
10 ³	10.5	7.7	5.3
10 ⁴	5.8	4.6	3.5
10 ⁵	3.2	2.8	2.3
10 ⁶	1.8	1.7	1.5
10 ⁷	1.0	1.0	1.0
10 ⁸	0.56	0.60	0.66

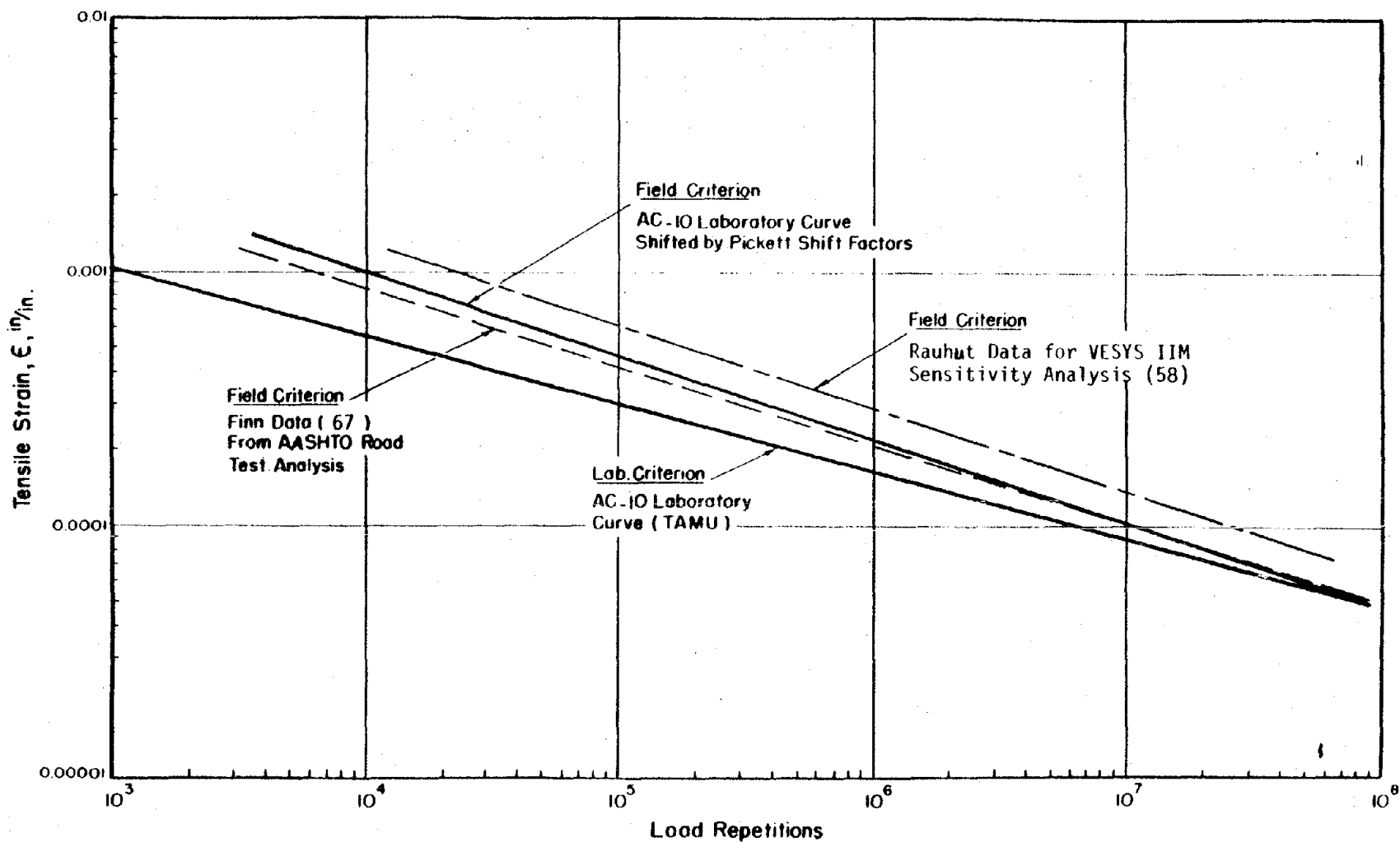


Figure 43. Illustration of Laboratory to Field Shifts for Laboratory Standard Asphalt Concrete (Control Mix).

CHAPTER VI

STRUCTURAL ENGINEERING PROPERTIES (2): FRACTURE STRENGTH

Background

The available data suggest that fracture strength of asphalt concrete under low temperatures and/or rapid loading rates is at its highest level, but fracture occurs at small strains. In fact Finn (74) defined the limiting strain for asphalt concrete at relatively low temperatures to be approximately 1.0×10^{-3} in./in. This is about one order of magnitude greater than allowable strain levels in fatigue loading.

The critical condition for fracture in asphalt concrete occurs at low temperatures and/or rapid loading rates. It is here that the asphalt behaves in a most brittle manner.

McLeod (75) has used the bitumen stiffness as a fundamental indicator of the asphalt cement characteristics; limits are placed on the bitumen stiffness at a given low temperature to eliminate transverse cracking. McLeod concluded that cracking will not occur if mix stiffness is less than 1×10^6 psi at 20,000 seconds loading time for the minimum anticipated temperature. Saal (76) used virtually the same approach as McLeod. Saal calculated that the limiting stiffness for asphalt concrete was approximately 715,000 psi for a loading time of 10^4 seconds and a change in temperature from 32°F to 14°F .

Monismith et al. (77), using the principles of linear viscoelasticity and creep compliance data, computed by numerical methods the stresses at the surface of an asphalt concrete slab subjected to a range of temperature distributions. They showed that in the north central U.S. and in Canada surface stresses in excess of 3,300 psi could be induced. This far exceeds the fracture strength of any asphalt concrete.

The postulated mechanism for cracking is traditionally based on the concept of induced thermal stresses, which exceed the tensile strength

$$\sigma(\dot{T}) = \alpha \int_{T_0}^{T_f} S(\Delta T) \cdot (\Delta T)$$

where $\sigma(\dot{T})$ = accumulated thermal stress for a particular cooling rate \dot{T}

α = average thermal contraction coefficient over the temperature drop, $T_0 - T_f$

T_0, T_f = initial and final temperature

$S(\Delta T)$ = stiffness at the midpoint of discrete temperature intervals ΔT over the range of T_0 and T_f , using a loading time corresponding to the time interval for the T change

Of course, if the predicted thermal stress as a function of temperature exceeds the tensile strength of the mix at that temperature, fracture occurs.

The above relationship clearly illustrates the fact that very stiff mixtures are susceptible to low temperature fracture even if they possess high fracture strength because of the high stresses induced during cooling. SULPHLEX is a very stiff material. Therefore, it was quite logical to be concerned about its potential for low-temperature cracking.

In order to evaluate the potential for low-temperature cracking in SULPHLEX, it was necessary to establish:

1. Fracture strength at various temperatures.
2. Coefficient of thermal contraction.
3. Stiffness at various temperatures.
4. Limiting strain levels at which fracture is likely to occur.

The following paragraphs discuss the research approach.

Research Approach

Two approaches were used to evaluate the low-temperature fracture potential of SULPHLEX binders: (1) the traditional fracture strength versus induced-stress approach, as outlined previously, and (2) a fracture mechanics-based approach employing the J-integral.

Traditional Approach

The traditional approach employs the indirect tensile test (IDT) apparatus to measure ultimate tensile stress and ultimate tensile strain at failure over a range of temperatures and loading rates. The IDT is explained in Reference 13.

Indirect tensile tests were performed at a low loading rate, as specified by Anderson et al. (78), 0.02 inches per minute, on mixes of AC-10 and SULPHLEX at various temperatures. The failure stresses and strains of these mixes are summarized in Table 29.

Results from IDT testing were compared to the stresses induced within the pavement layers by temperature changes. These stresses were predicted by the computer program COLD (79) and by Chang's model of thermal stresses in a restrained viscoelastic slab (28).

The computer program COLD was developed by Finn et al. (79), as an aid in calculating thermally induced stresses for a given set of climatological data. COLD utilizes a pseudoelastic beam analysis for the estimation of the thermal stress, $\sigma_x(t)$

$$\sigma_x(t) = \int_{t_0}^t S(\Delta t, T) \cdot \alpha_0(T) \cdot dt(t)$$

where $S(\Delta t, T)$ is the time and temperature-dependent stiffness modulus, and $\alpha_0(T)$ is the average coefficient of thermal expansion. A constant time of loading of 7200 seconds is assumed, and stiffness is only a function of temperature. Using the trapezoidal rule to evaluate the integral, the thermal stress at a temperature T_f is

$$(\sigma_x)_f = (\sigma_x)_i + \frac{\alpha}{2} (S_f + S_i)(T_f - T_i)$$

Through comparison with field data, the loading rate of 7200 seconds used for determining stiffness values has been shown to correspond to a cooling rate of 5°F per hour.

A more exact solution for thermal stresses in a restrained slab based on viscoelasticity is given by Chang (28). This approach has as its basis the hereditary integral. The one-dimensional constitutive equation is

$$\sigma = \int_0^t E(t - \tau) \frac{d\sigma}{d\tau} d\tau$$

Table 29. Summary of Tensile Strength for Indirect Tensile Testing at Low Temperatures
(All Mixtures Were Composed of Crushed Limestone Aggregate).

Binder	Stroke Rate, in/min.	Test Temperature, °F	Failure Strees, psi			Failure Strain, in. in.	
			Mean	Std. Dev.	n*	Mean	n*
CR1	0.02	32	620	100	10	0.00056	10
		0	750	150	10	0.00005	10
		-10	760	170	10	---	10
CR2	0.02	32	700	120	10	0.00020	10
		0	740	160	10	0.00060	10
		-10	700	170	10	---	10
CR3	0.02	32	600	100	6	0.00010	6
		0	770	117	6	0.00007	6
		-10	720	200	6	---	6
CR5	0.02	32	550	100	6	0.00080	6
		0	610	110	6	0.00007	6
		-10	650	90	6	---	6
233	0.02	32	600	90	6	0.00010	6
		0	650	75	6	0.00001	6
		-10	640	100	6	---	6
AC-10	0.02	32	150	50	10	0.0040	10
		0	350	70	10	0.0003	10
		-10	410	75	10	---	10

*n = Number of Samples

where σ is the stress, and $E(t)$ is the relaxation modulus. The uniaxial stress, σ , due to an axial strain, ϵ , and temperature change, $T = T - T_0$, is

$$\sigma = E_e (\epsilon - \alpha \Delta T) + a_f \int_0^t \Delta E (\xi - \xi') \frac{d(\epsilon - \alpha \Delta T)}{d\tau} d\tau$$

where α is the coefficient of thermal expansion

E_e is the equilibrium modulus (0 for asphalt)

$\Delta E (\xi)$ is the transient component of the relaxation modulus

a_f is a temperature dependent coefficient which is unity for thermorheologically simple materials

If a constant thermal expansion coefficient, α , and a constant rate of cooling is assumed, the equation reduces to

$$\sigma = (\epsilon - \alpha \Delta T) E_{eff} = \epsilon_T E_{eff}$$

where ϵ_T is the strain due to the stress

ξ and ξ' are integrated forms of reduced time

E_{eff} , the effective modulus, is equal to

$$E_e + \frac{1}{t} \int_0^t \Delta E (\xi - \xi') dt'$$

Chang has developed a computer code for evaluating the thermal stress based on a constant rate of cooling. A comparison with experimental data given in Reference 28 shows this computer code is capable of predicting tensile stresses much more accurately than other methods.

Thermally induced stresses were calculated with the aid of the computer program COLD. The linear coefficient of thermal expansion was determined by taking comparator measurements on an eight inch tall cylinder of SULPHLEX as the cylinder was cooled from 68°F to -20°F. The average coefficient of thermal expansion was 1.2×10^{-5} in/in/°F for SULPHLEX. This compares with values ranging from 1.2 to 1.5×10^{-5} in/in/°F for asphalt concrete (74). The stiffness of the materials was determined from uniaxial creep tests. Figure 44 gives an example of the calculated thermal stresses for CR1. The program COLD predicted stresses for reliability levels of 50, 75, 98, and 99 percent. A reliability level of 90 percent indicates that only

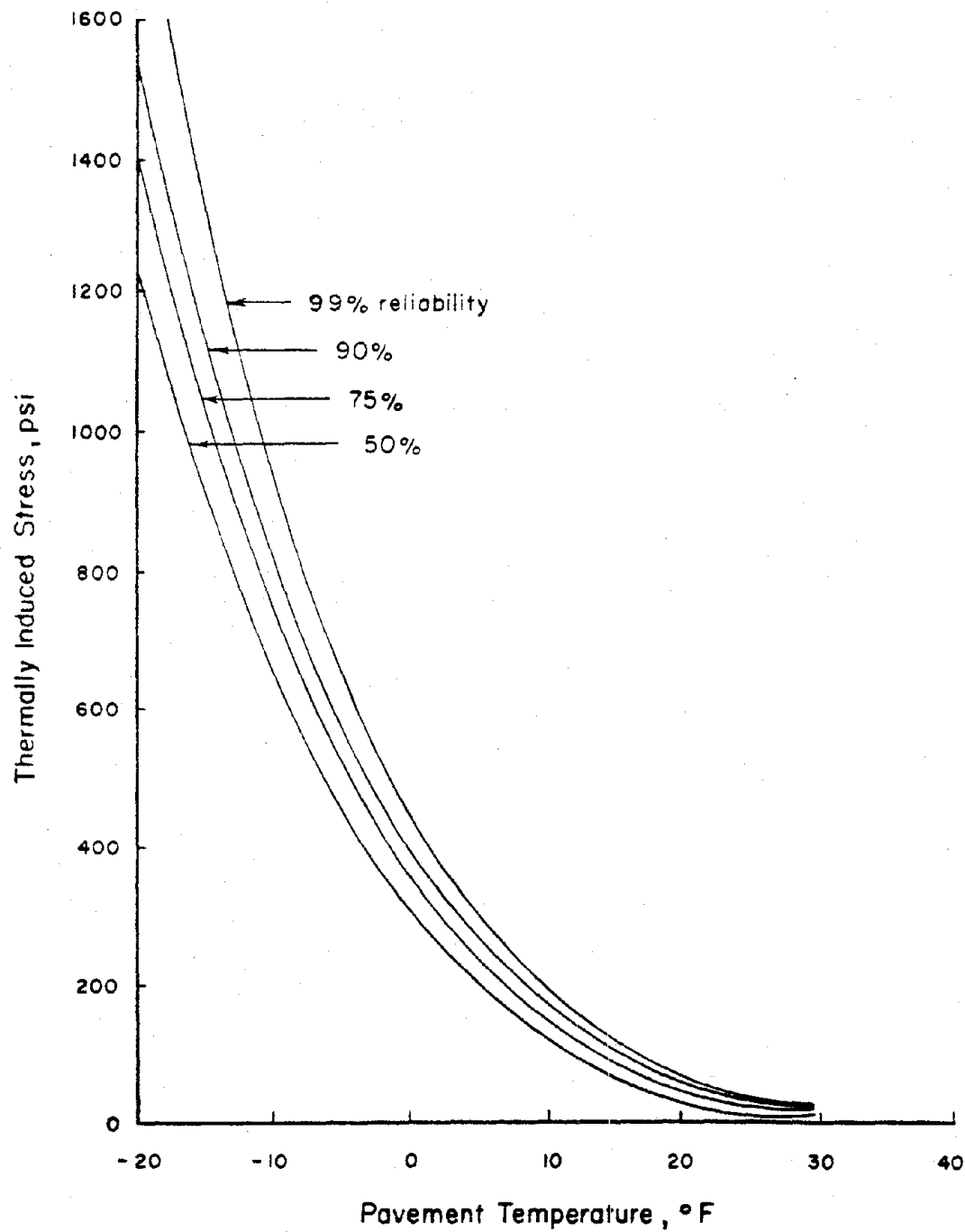


Figure 44. Thermally Induced Stresses Computed from COLD Computer Program.

10 percent of a group of pavements will exceed the estimated thermal stress.

The computer code developed by Chang was used to determine the thermally induced stresses with a greater degree of accuracy. Figure 45 gives the result of a typical analysis for SULPHLEX CR1. Thermal stresses were calculated for cooling rates of 2, 5, 10, 15, and 20°F per hour. It can be seen that much higher stresses are generated at the faster rates of cooling. The magnitude of the thermally induced stresses is also a reflection of the relative stiffness of the mix. All SULPHLEX mixtures have a higher stiffness modulus than AC-10 and accordingly SULPHLEX mixes are capable of generating higher thermal stresses.

An examination of the stresses calculated by COLD and Chang's computer code reveals no great difference. At a cooling rate of 5°F per hour, the 50 percent reliability (median) thermal stresses from COLD are very nearly the same as those calculated by Chang's program for a cooling rate of 5°F/hr. However, COLD does not offer the flexibility in varying the cooling rate and viscoelastic properties of the binder that Chang's program allows.

Fracture Mechanics Based Approach

The traditional approach is sound provided that the laboratory-measured fracture strengths accurately describe what occurs in the field. Unfortunately, the indirect tensile test has limitations. Rigid assumptions are made which describe the method of load application and the behavior of the material during load application (linearly elastic) (80). These assumptions are to at least some degree, violated during every test. Therefore, the test provides at best an estimate of fracture strength.

The J-integral, a measurement of fracture toughness in an elastic-plastic material, was used as an alternate approach to the low-temperature fracture problem. The fundamental J-integral is discussed in chapter V.

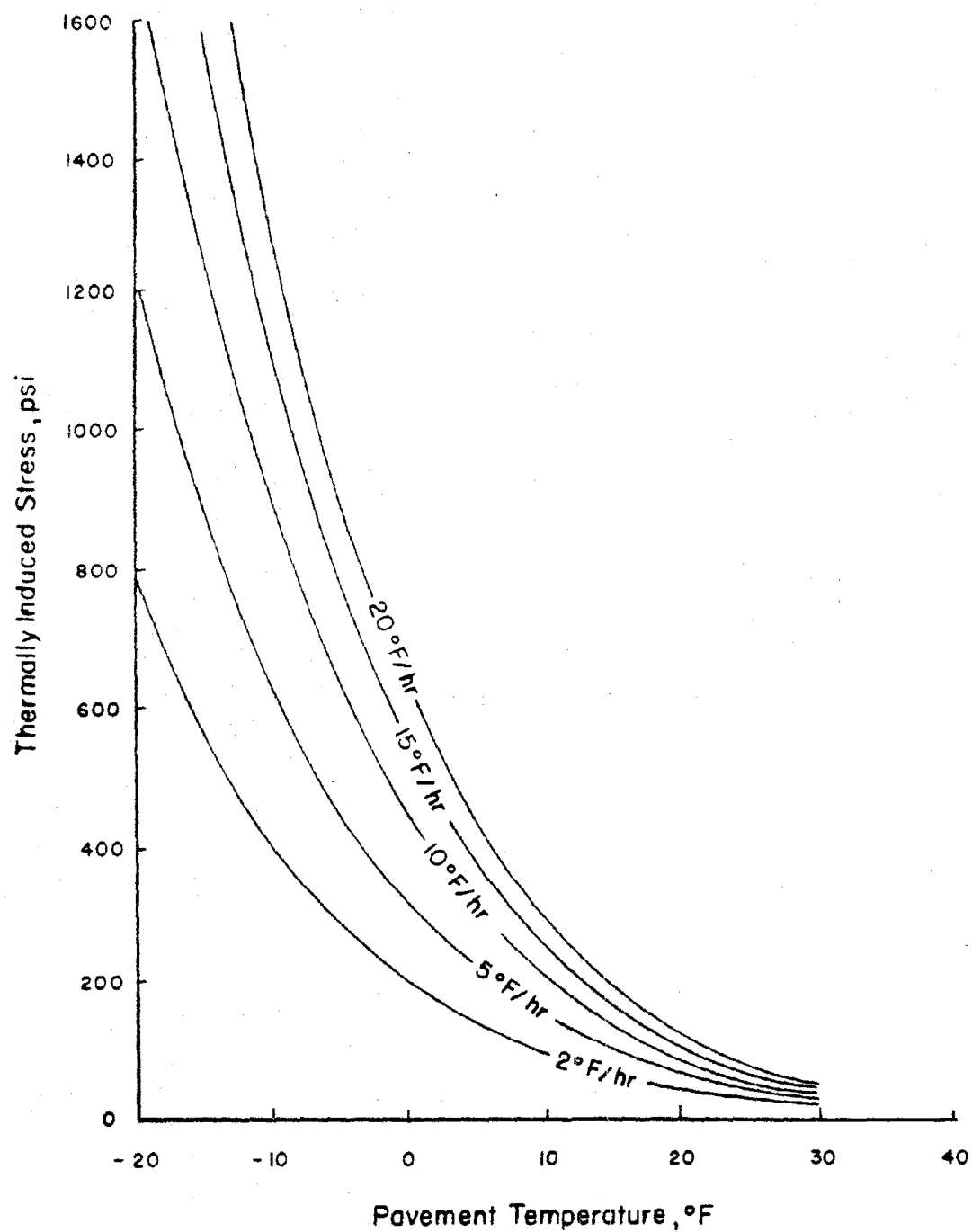


Figure 45. Thermally Induced Stresses Computed from the Computer Model Developed by Chang et al. (28).

The critical value of J-integral, termed J_{IC} , may be found by the method established in ASTM E 813 (81). The critical J_{IC} is the energy required to drive a sharp tipped crack or the energy released as the sharp crack tip propagates.

Bend specimens (82) of the type shown in Figure 46 were used in this work. As the specimens were loaded monotonically at the mid point, a linear variable transformer (LVDT) recorded the crack opening displacement. A load displacement plot was recorded, Figure 47. The area within the plot of load versus displacement was recorded and used in the calculation of the J-integral with crack growth. The crack length progression may be followed by several techniques. The most common way is to relate the crack length to the change in compliance of the beam. The compliance is the slope of the load-reload lines, Figure 47. A less common but more accurate way to measure crack growth is by a "KRAK gage" (83) which is bonded to the specimen, Figure 46. The crack progresses and tears the metal foil gage, changing the electrical resistance monitored across the gage, and resulting in a very accurate measure of crack growth. The "KRAK gage" was used in this research.

It is not practical to use the bend specimen to compute J_{IC} values at temperatures much above T_g . This is because the material begins to behave plastically and viscously to the point where the propagation of a sharp tipped crack in this bend specimen geometry is not possible because the area of the plastic zone ahead of the crack tip is too large relative to specimen geometry. However, at temperatures near or below T_g , the test works very well.

The parameters J_{IC} were computed for AC-10, CR1, CR2, CR3, CR5, and 233 over a range of temperatures. These values are tabulated in Table 30.

Results of Analysis

Traditional Approach

Figure 48 graphically presents the results of the traditional analysis. In Figure 48, 50, and 99 percent reliability curves for

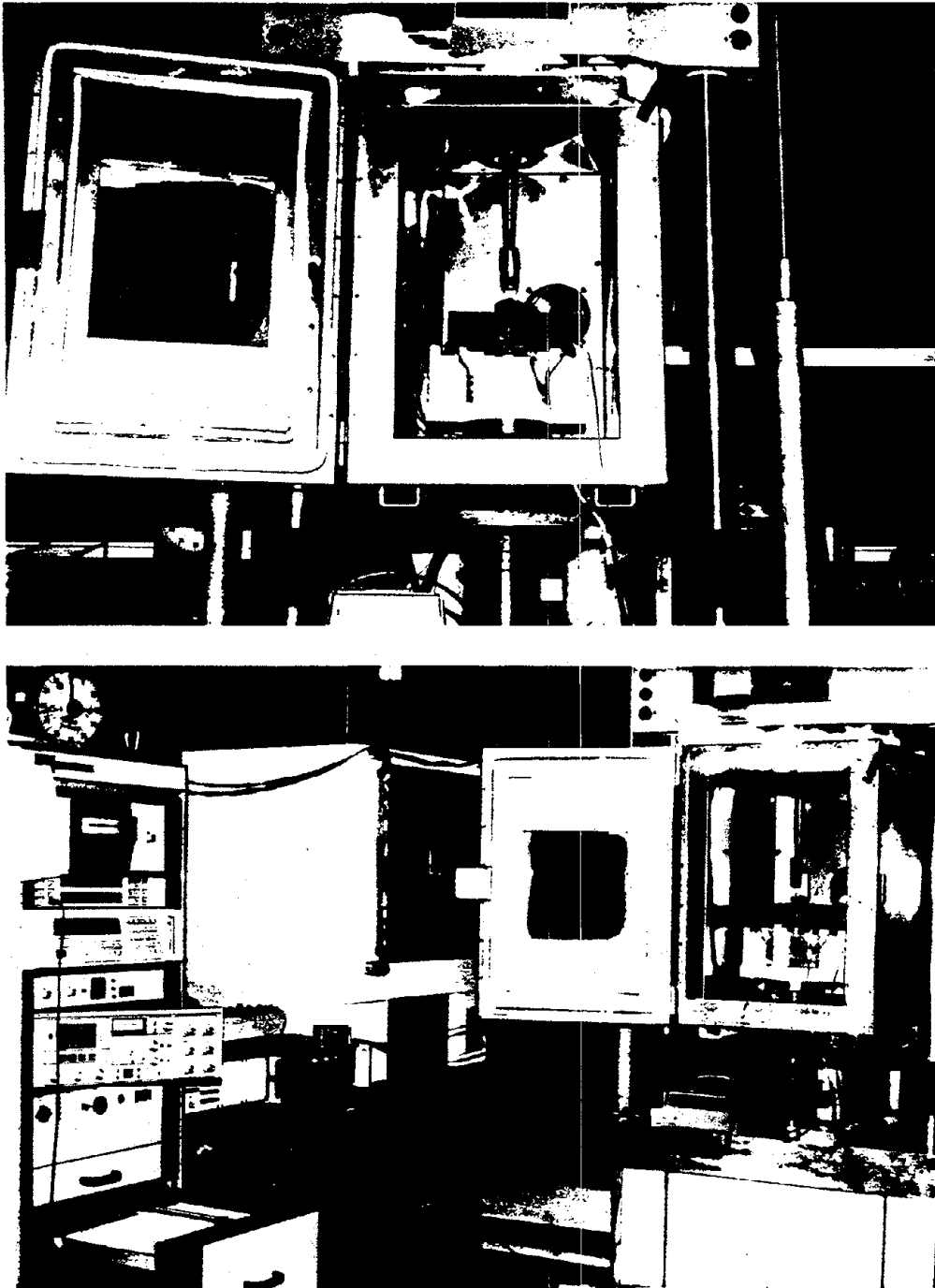


Figure 46. Photograph of the Bend Fracture Specimen in the MTS System with KRAK Gage Mounted.

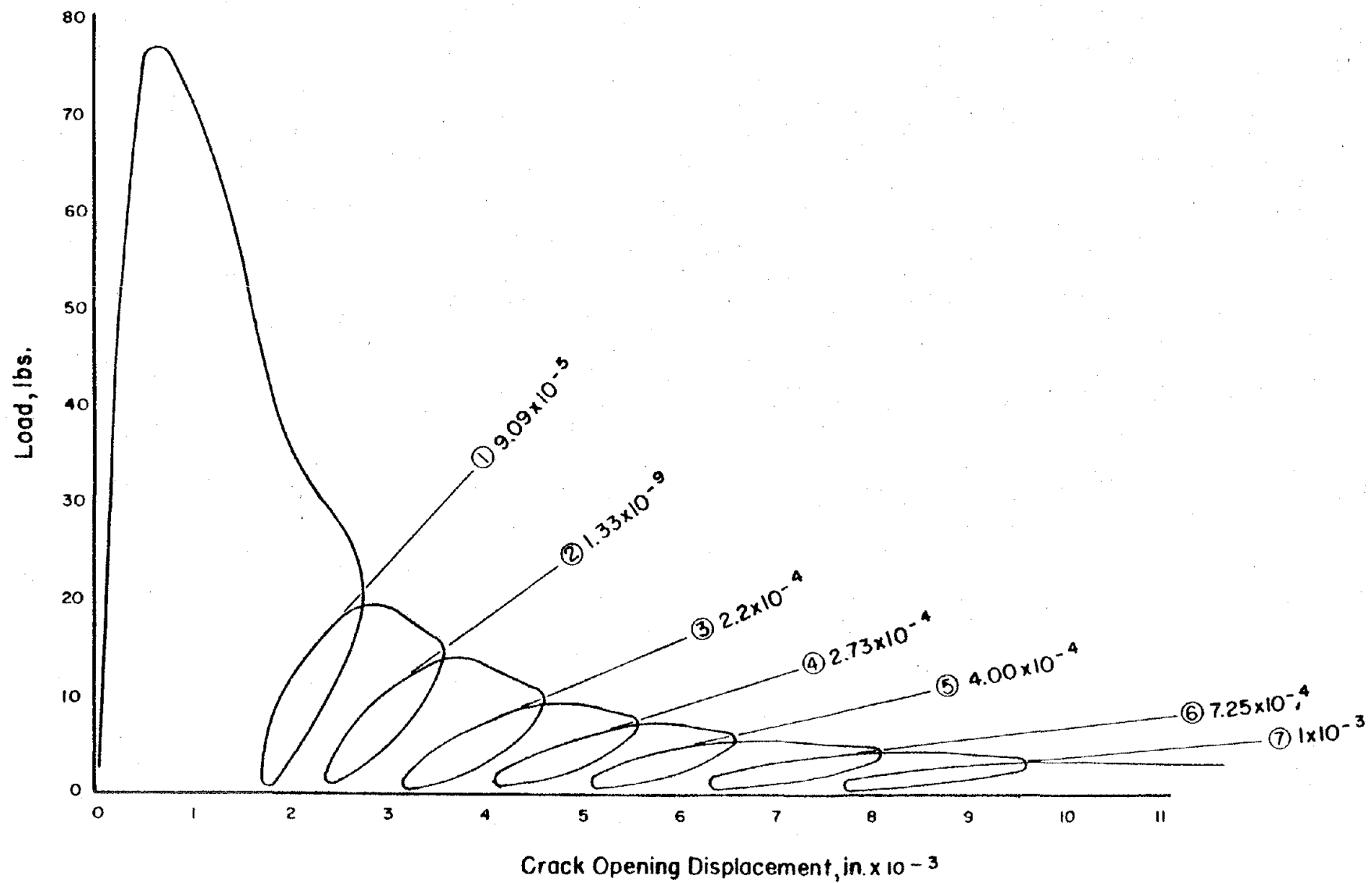


Figure 47. Typical Load-Displacement Plot from Bend Fracture Test.

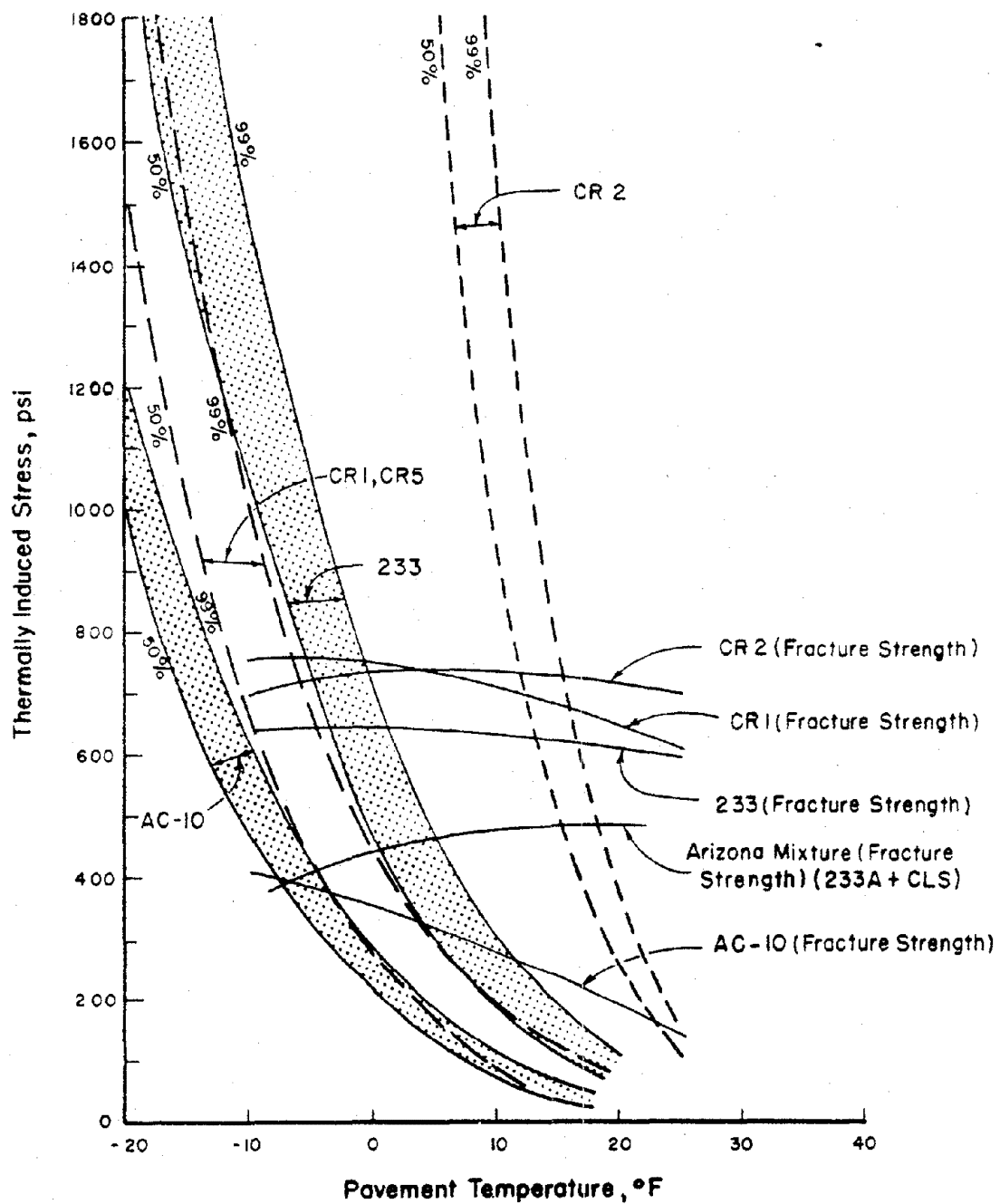


Figure 48. Thermal Stress Fracture Analysis Using Traditional Approach (All Mixtures were Fabricated with Crushed Limestone Aggregate).

thermally induced stresses for a cooling rate of 5°F per hour are plotted for the binders AC-10, CR1, CR2, CR5, and 233. The area between the two reliability curves represents the band within which the reliability level would be chosen for design purposes. The solid lines labeled fracture strength for each binder represent the ultimate indirect tensile strength for a selected binder as a function of test temperature.

The intersection of the thermally induced stress line and the fracture strength versus temperature line indicates that the thermally induced stress equals the fracture strength of the paving material, and fracture is initiated. For a 99 percent reliability level fracture is predicted to occur at the following pavement temperatures:

AC-10,	-4°F
CR1,	-6°F
CR2,	16°F
CR5,	-4°F
233,	2°F

Thus, only the CR2 binder is dramatically different from the AC-10 control binder according to the analysis. Binders CR1 and CR5 actually respond as well as AC-10.

The analysis represented in Figure 48 was performed only with the crushed limestone aggregate. The master stiffness curves for all mixtures tested, Figures 54 through 56, pages 146 through 147, illustrates how much the mixture stiffness can indeed change for a different aggregate. From Figure 56 it is clear that the low temperature stiffnesses for CR1 and CR2 are quite near the stiffness of the CR2 - crushed limestone aggregate mixtures, in fact, a bit stiffer. Thus CR1 and CR2 - river gravel mixtures have the potential for low-temperature cracking.

It is difficult to explain exactly why the CR1 and CR2 river gravel mixtures are stiffer at low temperatures than the CR1 crushed limestone mixture. Perhaps the difference is related to some unintentional variation in binder storage or mixing, although every

effort was made to prevent such a discrepancy. Perhaps the mineralogy and gradation of the aggregates are the keys to the variation. Whatever the reason, a wide variation in mixture stiffnesses at low temperatures for SULPHLEX binders has been established. Mixtures which possess stiffnesses at the upper limit of this range will doubtless experience severe low-temperature fracture problems. Figure 49 illustrates the fracture potential for CR1 and CR2 binders used in river gravel mixtures. Fracture is predicted to occur at 12 to 16 degrees higher for the SULPHLEX binders than for AC-10.

Fracture Mechanics Approach

Differential scanning calorimetry (DSC) analyses performed under this contract identify the glass transition temperature of all SULPHLEX binders tested in this study (CR1, CR2, CR3, CR5, and 233) as being substantially above that of asphalt concrete, Table 30 (approximately 40°F above). This fact can also be predicted simply by observing the creep compliance, stiffness, or resilient modulus data from SULPHLEX and asphalt concrete mixtures presented in this report.

Figure 50 presents the J_{IC} values for AC-10 and SULPHLEX CR5 and CR1 plotted versus temperature up to the T_g . No tests were made above T_g , but it is hypothesized that fracture toughness will increase dramatically above T_g as shown by the dashed lines. It may be predicted that J_{IC} should be relatively constant below T_g instead of increasing with increasing temperature as shown in Figure 50. However, this occurrence is not surprising considering the rate dependency of T_g on heating or cooling which may be affected by variation in testing techniques among specimens.

Of greatest practical importance is the fact that at any specific low temperature (say below freezing, 32°F), the J_{IC} or fracture toughness is substantially greater for the AC-10 mixtures tested than for the SULPHLEX mixtures tested.

The fact that SULPHLEX responds to the glass transition at a much higher temperature than asphalt suggests that low temperature cracking is inevitable in cold climates or climates subject to rapid

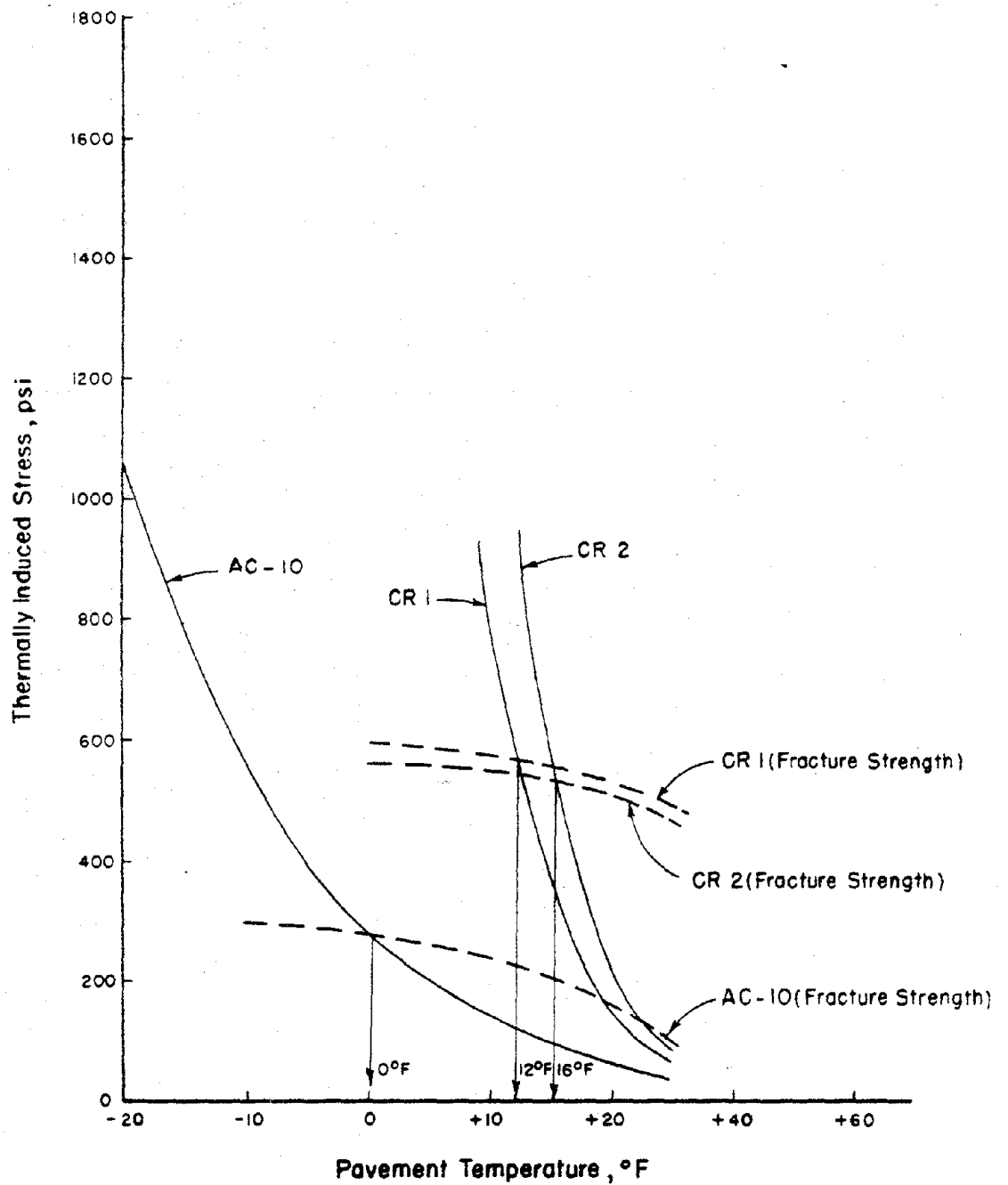


Figure 49. Thermal Stress Fracture Analysis Using Traditional Approach (All Mixtures were Fabricated with River Gravel Aggregate).

temperature drops. It has been previously shown, Figure 1, that strain energy densities of asphalt concrete and SULPHLEX will become at least comparable within the nominal temperature range which normally affects pavements. Thus, one would expect SULPHLEX to behave much more favorably when compared with asphalt concrete in flexural fatigue at 68°F than in resistance to fracture at low temperatures. This conclusion is borne out by the results presented here.

Table 30. Summary of J_{IC} Values Versus Temperature.

Binder	T_g , °F*	Test Temperature, °F	J_{IC} , (lb/in)
AC-10	-20	-30	0.25
		-15	0.40
CR5	+20	-15	0.28
		+ 5	0.38
		+20	0.45
CR2	+20	0	0.31
		+ 5	0.35
CR3	+20	0	0.27
233	+23	0	0.29

* T_g values are based in differential scanning calorimetry.

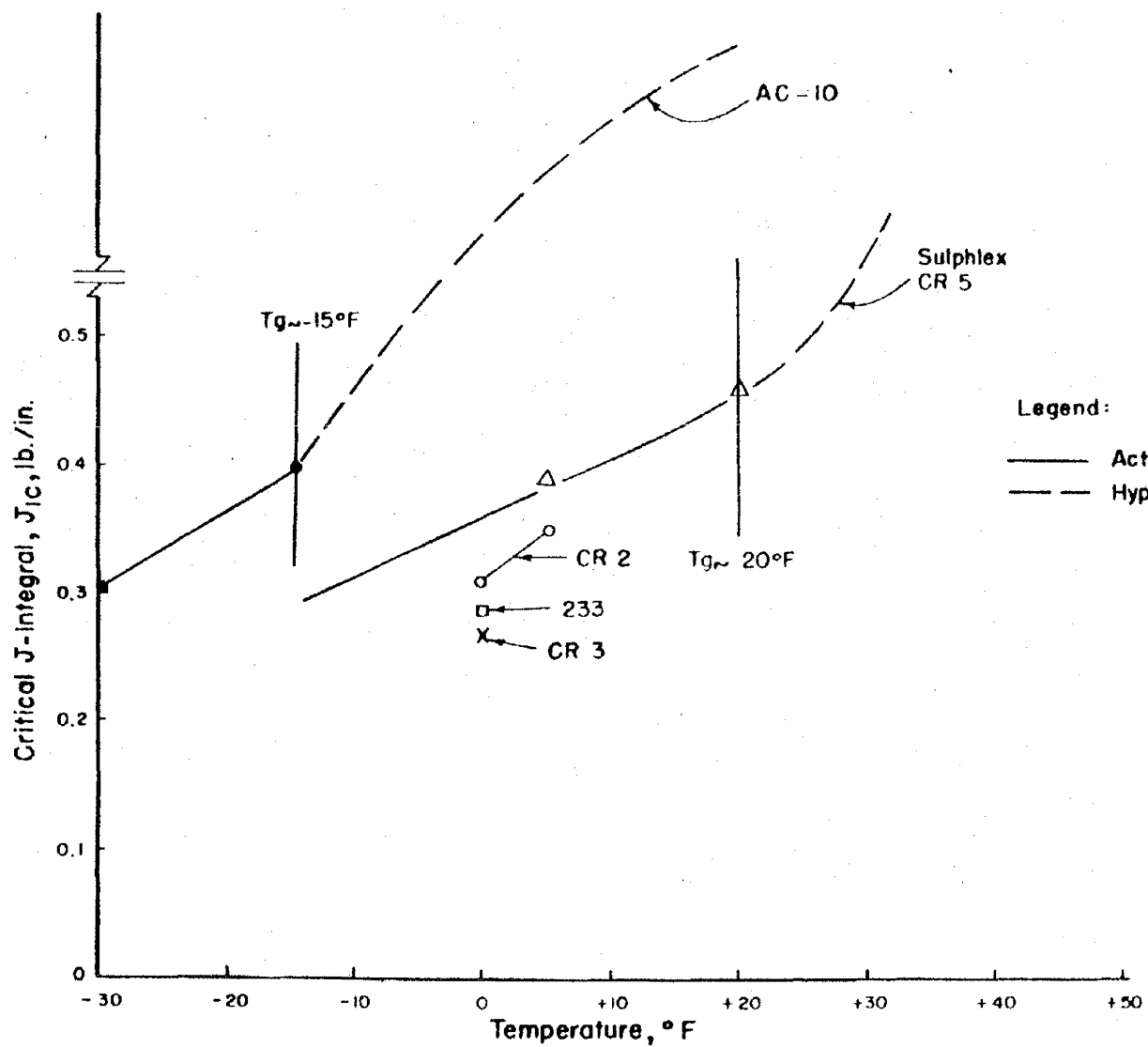


Figure 50. Change in Critical J Integral with Temperature.

CHAPTER VII

STRUCTURAL ENGINEERING PROPERTIES (3): DEFORMATION CHARACTERISTICS

Viscoelastic Response

General

Secor and Monismith (84) have shown that a satisfactory measure of stiffness, accurate to at least the level required by engineers, can be obtained by considering asphalt concrete to be a linear viscoelastic material and one which is thermorheologically simple. Papazian (85) and Pagen (86) used sinusoidal loading and creep testing to substantiate these results. Pagen (86) demonstrated the applicability of the time-temperature superposition principle to asphalt mixture behavior.

Although asphalt concrete may be viewed as linearly viscoelastic for engineering purposes or to a first approximation linearly viscoelastic and thermorheologically simple, one must remember the limitations of these assumptions and the ranges within which they may be applied. For example, Deacon (87) has shown that stiffness modulus at a particular time of loading is dependent on the stress level at which it is measured. Thus, one must insure that the stresses used to define the viscoelastic response are not too great, so that nonlinear effects will be minimized.

Pagen and Ku (88) have demonstrated the effects of mixture variables on the creep behavior of asphalt concrete. In this investigation the effects of asphalt type (temperature susceptibility characteristics), aggregate gradation, and aggregate type were studied. Aggregate gradation appeared to have more influence than aggregate type (all mixes at the same asphalt content), particularly at longer times of loading. The asphalt temperature susceptibility had a pronounced influence only at longer times of loading.

Krokosky et al. (89) have shown that asphalt concrete exhibits nonlinear and nonviscoelastic behavior in compression, the degree of which is dependent on the magnitude of deformation, particularly that

associated with the aggregate. The deviation from linear behavior was shown to be least in stress relaxation, more so in creep and largest in constant rate of strain.

Brodangan (90) has extended the description of complexity of the viscoelastic response of asphalt concrete as it is reflected in the time-temperature superposition principle and shift factor, a_T . His data indicate that the influence of temperature on mixture behavior is related to the asphalt but that it is not simply determined in all instances by a relationship based on the viscosity of the asphalt.

Pagen and Ku (88) have demonstrated that if the response is measured after a number of load applications (mechanical conditioning), the behavior of the material tends to be more reproducible, and linear viscoelastic theory may be more appropriately used to define behavior.

The techniques used to measure rheological responses in this study were developed after careful consideration of the points discussed above. The procedures for performing creep testing and stress relaxation testing were those established in the VESYS IIM User's Manual (12). These procedures insure that all testing is on conditioned specimens and that stresses do not exceed the linear viscoelastic range of the material.

It is assumed that if the proper test procedures are followed, such as those in reference 12, asphalt concrete will behave in a linear viscoelastic manner, at least for engineering purposes.

SULPHLEX was tested for linear viscoelastic behavior. In a linear viscoelastic material, the stress is directly proportional to the strain, and the ratio of stress to strain depends only on time. Therefore, if linearly viscoelastic, a SULPHLEX mix should comply with the following criteria: (1) the creep compliance is independent of the stress level, and (2) the principle of superposition applies. To test the first requirement, creep compliance (constant stress) tests were performed at different stress levels. The results proved compliance was independent of the stress level. For the second requirement a creep and recovery test was used. In this test a

constant stress, σ_0 , was applied up to time t_1 and then removed; strain ϵ_t , was measured during both creep and recovery periods. The temperature was held constant during the test. Strain in the recovery period was then compared with that predicted by the equation

$$\epsilon_t = D_t \sigma = D_t \sigma_0 - D(t - t_1) \sigma_1$$

$$\epsilon_t = D_t - D(t - t_1) \sigma_0$$

if $\sigma_1 = \sigma_0$. D_t is the creep compliance for a load of duration t . The recovery strain can be predicted from the creep strain by the graphical procedure shown in Figure 51. The recovery strain at any time, t , is equal to the creep strain that would have existed had the stress remained on the material, $D_t \sigma_0$, minus the creep strain due to a stress applied at t_1 , $D(t - t_1) \sigma_0$. If the predicted recovery strain equals the actual recovery strain, the material is linearly viscoelastic. The result of this test performed on SULPHLEX, CR1, and crushed limestone mixture, is shown in Figure 52. For engineering purposes, a SULPHLEX mix may be considered as a linear viscoelastic material.

In this research effort both asphalt concrete, the control mixture, and SULPHLEX were treated as thermorheologically simple, linear viscoelastic materials. This assumption was carried over to the pavement design and structural pavement optimization study.

Viscoelastic Characterization of SULPHLEX Mixtures

The most commonly used method to characterize the viscoelastic response of highway materials is creep compliance. Compliance tests are typically performed at a constant stress level, and strains are measured with time. The compliance is then the strain, $\epsilon(t)$, divided by the constant stress, σ_0 . Creep compliance is usually plotted versus corresponding load duration in time and has the units psi^{-1} .

All creep testing in this study was performed in strict accordance with Federal Highway Administration's VESYS IIM Users Manual (12). The techniques of specimen preparation and test performance will not

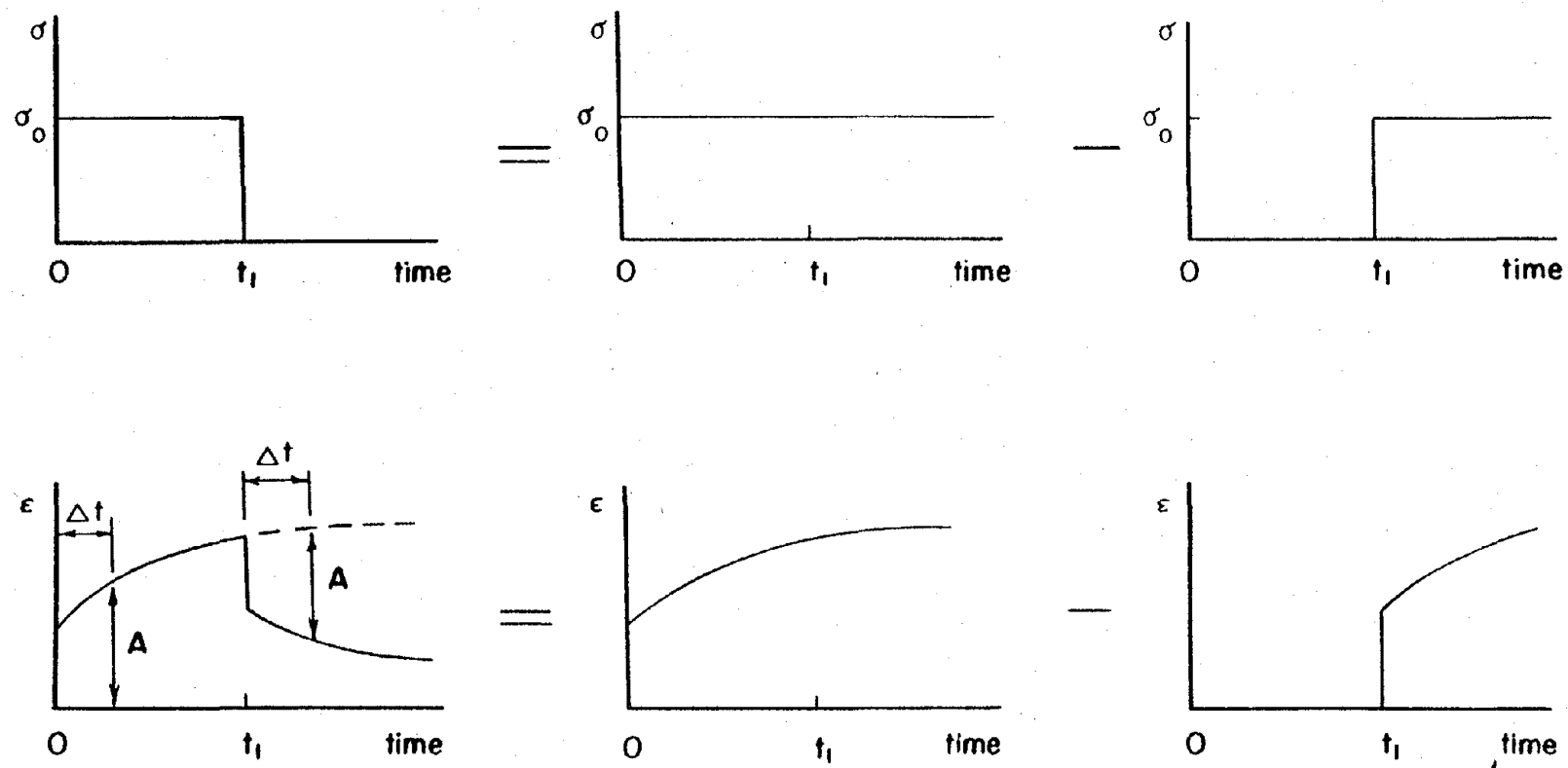


Figure 51. Graphical Procedure for Predicting the Recovery Strain of a Linear Viscoelastic Material.

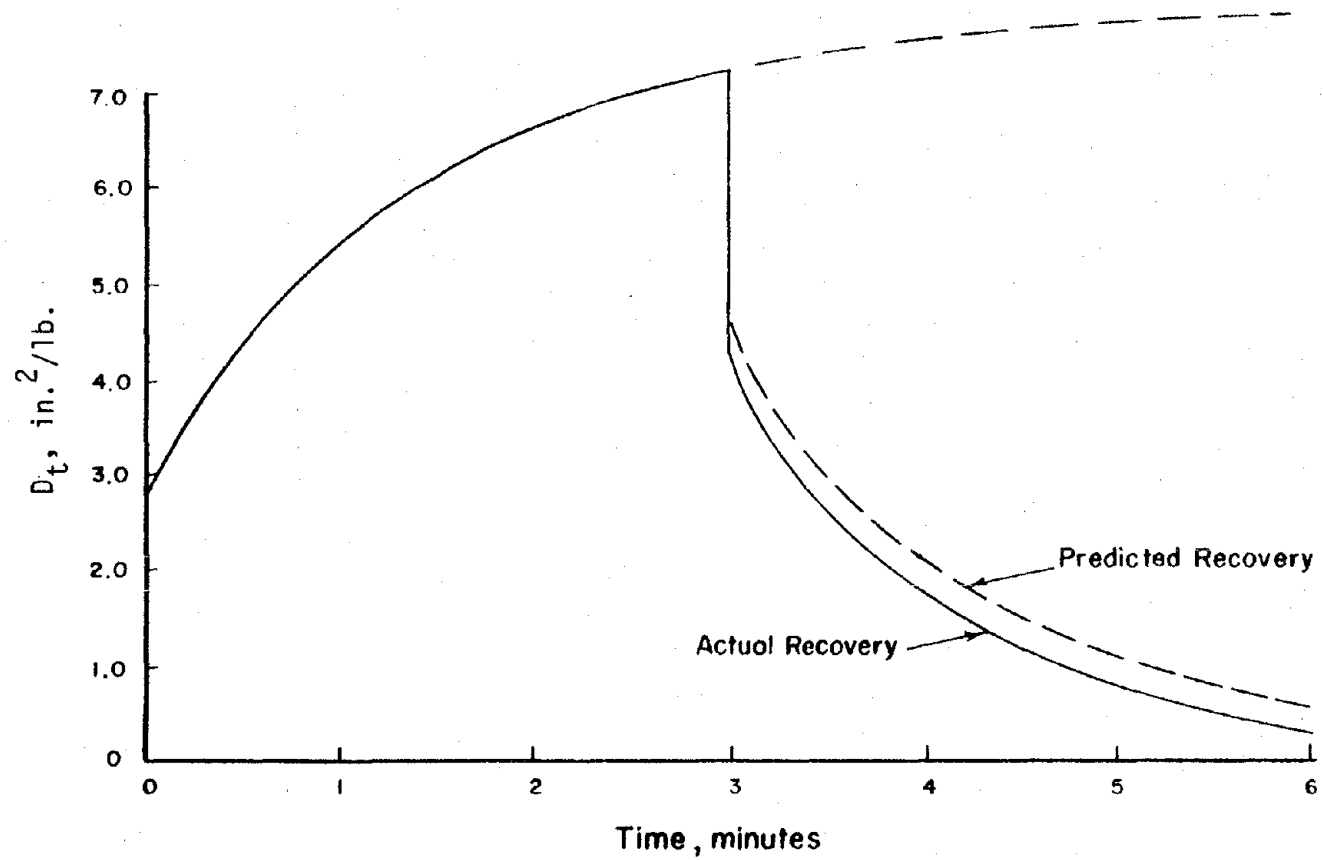


Figure 52. Creep and Recovery Test for a Sulphlex CR1 - Crushed Limestone Mix.

be repeated here as they are well-documented in reference 12. However, facets of the testing program which were either unique to SULPHLEX or to this study in general are discussed in Chapter II.

One particularly interesting and critically important facet of laboratory creep testing which deserves consideration at this point is specimen conditioning. The VESYS User's Manual (12) dictates a substantial period of conditioning prior to static creep compliance testing.

In an extensive evaluation of the sensitivity of the VESYS II structural model, Rauhut et al. (57) identified creep compliance determined under static loading condition as being a primary source of error. More specifically, it was determined that the vertical and radial strains calculated from the VESYS IIM analyses were too large, resulting in extravagant prediction of rutting and cracking. This was attributed to the high values of creep compliance obtained from static test data in the literature. The creep compliances computed from static laboratory testing were simply much higher than the correctly transformed reciprocals of dynamic or resilient moduli testing at like temperatures and durations of loading.

The difference was determined to be due to conditioning effects. To verify this creep compliance testing was performed immediately following the extraction of field cores from sections of the AASHTO Road Test site. These samples were affected by years of wheel loads. The measured compliances were much lower than for similar unconditioned laboratory-fabricated specimens. Thus, the hypothesis was that the problem was not a need to obtain data during a dynamic test to represent modulus, but that materials need to be conditioned dynamically prior to creep compliance testing. This hypothesis was well substantiated in the Rauhut et al. (57) study.

Creep specimens used in this study were conditioned in accordance with specifications of reference 12.

Figure 53 is a typical plot of creep compliance data. The bold curve represents the mean compliance from cores taken from the AASHTO Road site (preconditioned by years of traffic). In comparison are plotted compliance curves from laboratory statically loaded specimens.

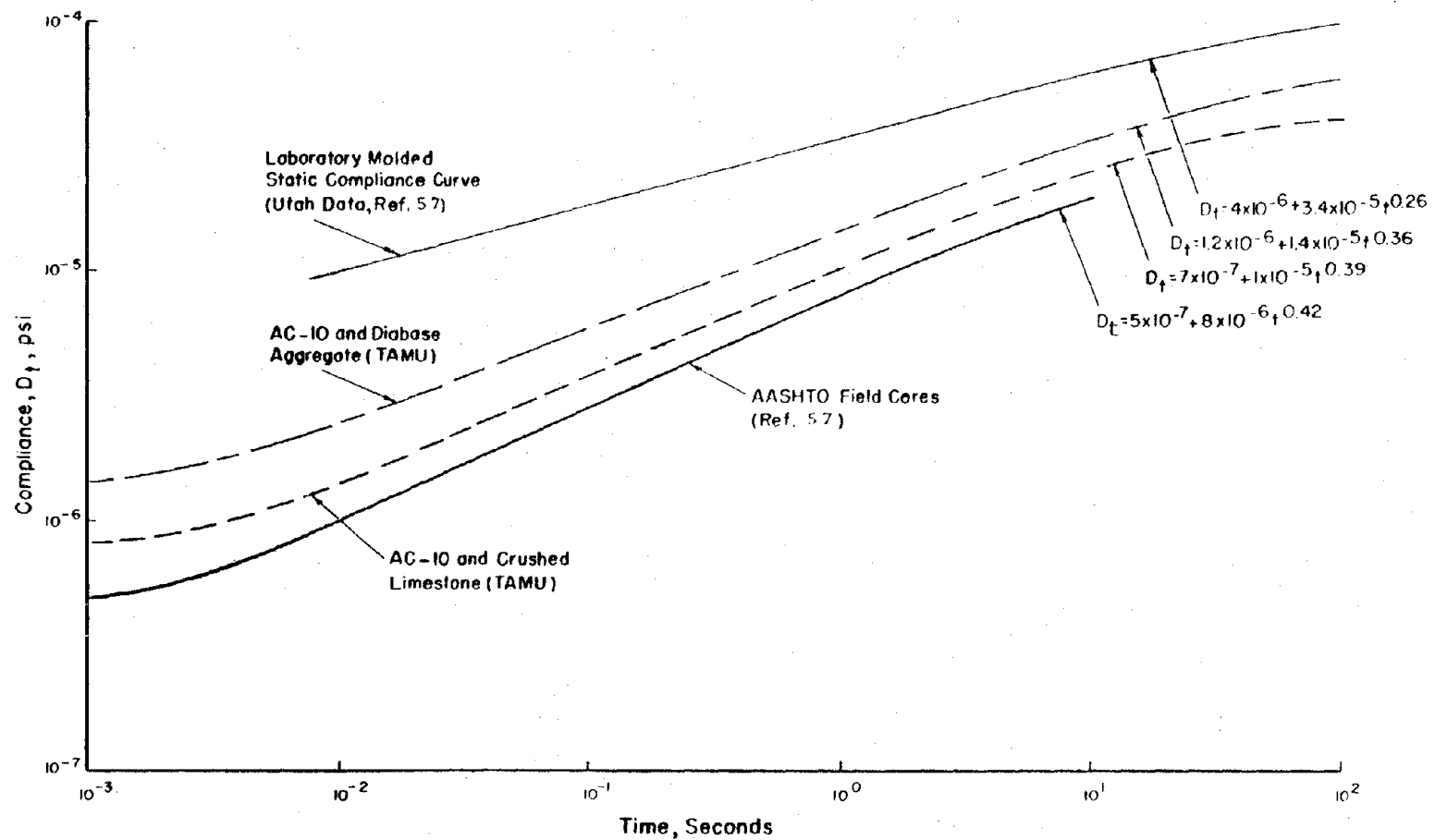


Figure 53. Comparison of Compliance Curves and the Effects of Load Conditioning.

The curve with the very high compliance is representative of the Utah data used in the VESYS sensitivity study (57). These data result in unrealistically poor fatigue and rutting life predictions for the pavements. Also plotted in Figure 53 are compliance curves for AC-10 mixtures (with crushed limestone and diabase aggregates) prepared and tested as the control mixtures for this study. Note that these curves compare favorably with the AASHTO core data and are considered realistic as control data for the VESYS analysis.

There are numerous ways to represent creep compliance, D_t , as a function of time. One of the most useful is by the power law:

$$D_t = D_0 + D_1 t^n$$

where D_0 is the glassy compliance,

D_1 is the intercept of the straight line portion of the creep compliance curve on log-log paper with the one second time line and

n is the slope of the logarithmic creep compliance curve.

This assumes that the material behaves in a Maxwellian manner. Of course, this is not an entirely valid assumption. The compliance curve could be more accurately modeled by a Prony series ($D_t = D_0 + D_1 e^{t/t_1} + \dots + D_i e^{t/t_i}$). However, the simple power law is useful in evaluating the transition portion of the compliance curve. It will be used only as a means of comparison among compliance curves. Using the power law to describe creep compliance data, the curves in Figure 53 are defined.

A second useful way to characterize viscoelastic responses is by means of stress relaxation plots. A sample of unit cross-sectional area is subjected to an instantaneous tensile strain, ϵ_0 , which is thereafter maintained constant. The stress is monitored as a function of time and the stress relaxation modulus is obtained as:

$$E_t = \frac{\sigma_t}{\epsilon_0}$$

Stress relaxation testing was primarily used to evaluate the aging properties of SULPHLEX. This will be discussed under the section dealing with aging. Stress relaxation data are presented in a similar

manner to compliance data, and, once again, a power law equation can be effectively used to compare data.

Molecular mobility and the probability of rotational movements in amorphous polymers is governed by a relationship involving free volume. The greater the fractional free volume, f , the easier the movement will be. Since molecular movement is governed by not only free volume but also by probability and the time scale of the experiment, it is not surprising that a relationship has been developed between free volume and time scale. Through the normal law of thermal expansion, this relationship can be modified to incorporate temperature. The resulting relationship is called the WLF (William-Landel-Ferry) equation in honor of those who developed it:

$$\Delta \log t = B (1/f - 1/f_0) = \frac{-(B/f_0)\Delta T}{(f_0/\alpha_f) + \Delta T}$$

where t is time, α_f is coefficient of expansion of free volume, ΔT is change in temperature, and B is a constant.

This equation signifies a shift in time scale which will produce the same mechanical properties (at least in those dependent upon the rotational movement of molecular segments) as will a related change in temperature given by the WLF equation.

The WLF equation is normally used to shift compliance data of amorphous polymers taken at various temperatures over short periods of time to form a master compliance curve. This is necessary because it is not practical, due to the viscoelastic nature of the amorphous polymers, to directly measure the complete behavior of the compliance as a function of time at a constant temperature. This would take too long and would make accurate measurement of compliances very difficult at both extremely small and extremely long times of loading.

A thermorheologically simple material possesses a unique capability. The compliance or modulus curves developed over a select range of times at a series of temperatures can be physically shifted horizontally to form a master curve. This horizontal shift should be consistent with that calculated by means of the WLF equation. In this

study compliance and/or modulus data are presented in the form of a master curve at a selected temperature. Time-temperature shift factors for various other temperatures will also be presented which allow the master curve to be shifted to account for temperature effects on compliance and/or modulus. This may be accomplished by simply transforming the time axis of the compliance curve to an axis of reduced times, ξ , defined as:

$$\xi = te^{[f(T)]}$$

where ξ is reduced time corresponding to a real time, t , at a constant temperature, T , and $f(T)$ is a function of temperature giving the shift of the compliance or modulus along the $\log t$ axis for temperature.

This function of temperature has been termed the shift factor and is often represented by the symbol a_T . For a particular reference temperature, the reduced time scale is a plot of t/a_T .

Physically the shift factor may be defined as:

$$a_T = \frac{t_T}{t_0}$$

in which t_t is the time required to observe a phenomenon at temperature T , and t_0 is the time required to observe the same phenomenon at some reference temperature, T_0 . Using the physical definition, it is easy to understand how a graphical approach to develop the shift factor is the most effective procedure.

As with compliance and relaxation modulus, the temperature dependence of mixtures is strongly related to the physical properties and temperature susceptibility of the binder. However, direct determinations based on binder properties, such as viscosity, alone are not satisfactory. Total mixture properties must be considered. Pagen has illustrated this concept quite dramatically in reference 86.

Davis et al. (91) has shown that the type of mineral filler influences the response of asphalt mixtures at different temperatures. In particular Davis et al. showed a dramatic effect of mineral filler on the shift factor, a_T . The effects of aggregate type, gradation, and mineral filler were carefully evaluated for each SULPHLEX binder

type. The combination effects of aggregate on compliance curves and time-temperature shift factors can drastically affect pavement performance in terms of such diverse responses as low temperature fracture and permanent deformation.

The rheological properties of SULPHLEX were compared in this study primarily based on the master curve of stiffness (the reciprocal of compliance but not to be confused with relaxation modulus) at a selected reference temperature together with time-temperature shift factors, a_T .

Results of Rheological Testing

In the following paragraphs creep compliance data and the reciprocal of compliance, creep stiffness, versus temperature, and time of loading are used to characterize SULPHLEX binders CR1, CR2, CR3, CR5 and 233A. As always, these binders are compared to the control binder AC-10. The effects of aggregate type and gradation on these rheological mixture properties are also evaluated. Finally, expected values of compliance versus temperature for each mixture type studied are recommended for use in the structural pavement design and optimization section of this report.

Table 31 presents the experiment design. The experiment is labeled a factorial experiment as it considers the effects of the variables listed in Table 31. However, due to practical limitations, the number of replicates for each test was limited to two. Thus, the intent of the experiment was not to statistically account for the effects of the variables nor to meet the qualifications of a rigorous analysis of variance but instead to orderly evaluate the rheological properties of SULPHLEX binders over a range of conditions.

The effect of three aggregate types were evaluated: crushed limestone (CLS), rounded river gravel (RG), and basalt. Two gradations were used. These gradations are very similar, but gradation A provides a mix with slightly lower air voids and lower VMA than gradation B.

Table 31. Partial Factorial Experiment For the Evaluation of Factors Influencing Creep Compliance.

Binder Air Voids, % Gradation Type ** Aggregate Type			CR1	CR2	CR3	CR5	233	AC-10
C L S	A	6-8 3-5 2-3	x	x	x	x*		x x*
	B	6-8 3-5 2-3	x				x	x
R G	A	6-8 3-5 2-3	x	x	x	x		x
	B	6-8 3-5 2-3						
B A S A L T	A	6-8 3-5 2-3						
	B	6-8 3-5 2-3	x	x		x	x	x

* Creep tests performed before and following one cycle Lottman conditioning.

** A is gradation shown in Figure 3.
B is a slightly more open gradation.

Note: The abbreviations CLS and RG refer to crushed limestone and river gravel aggregate, respectively.

The compaction effort was varied as required, by reducing the number of blows per layer of the Marshall compaction hammer to provide the appropriate variation in air void content for the mixtures in questions.

In the presentation of creep test data in the following paragraphs, the master stiffness versus duration of loading plots at 70°F are presented for each aggregate. This will be followed by plots of the time-temperature shift factors and finally the power law form of the creep compliance data for each binder-aggregate combination.

Figures 54 through 56 present the master stiffness curves for SULPHLEX and control mixtures for the three different aggregates. Stiffness plots versus duration of loading instead of creep compliance plots are presented because it is believed that the concept of stiffness is more recognizable and meaningful to highway engineers than is the term compliance or the magnitudes of compliance values. Of course, stiffness was computed directly from creep data and in this case, is simply the reciprocal of compliance.

Figure 54 compares the stiffness versus load duration curves for CR1, CR2, CR3, CR5, and the control mixture made with AC-10. At short load durations SULPHLEX is substantially stiffer than the asphalt concrete control mixtures. However, at long durations of load, the stiffness values converge rapidly. In fact, at load durations in the range of 10^4 to 10^5 seconds, the stiffness of SULPHLEX becomes lower than that of the control mixture. The obvious indication is that SULPHLEX under moving wheel loads should be less susceptible to deformation problems than asphalt concrete, but under stationary traffic SULPHLEX may exhibit continued creep.

Binder CR2 at long load durations exhibits substantial "linear amorphous polymer behavior." If an amorphous polymer is well cross-linked the long cooperative motion of chains which would result in translational motions of complete molecules is still greatly restricted by the presence of strong local interactions between neighboring chains. These interactions consist of primary chemical bonds. In the linear polymer, they are known as entanglements, and their precise nature is not clear. To a first approximation, the

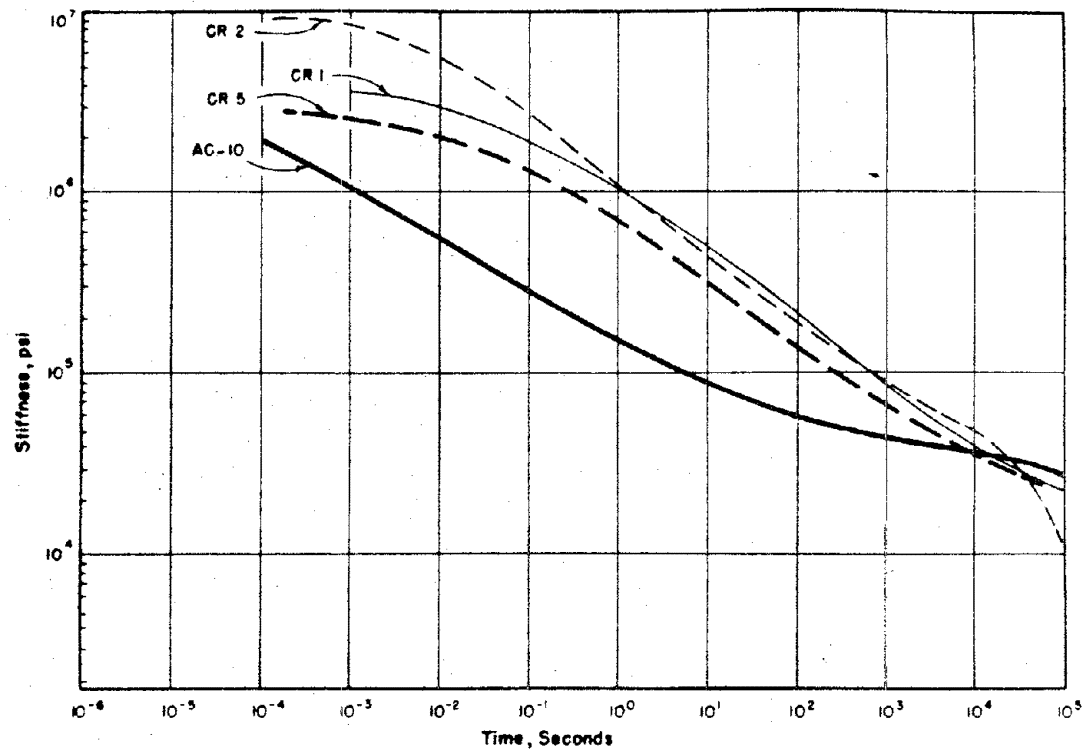


Figure 54. Stiffness Curves for All Mixtures Fabricated with Crushed Limestone.

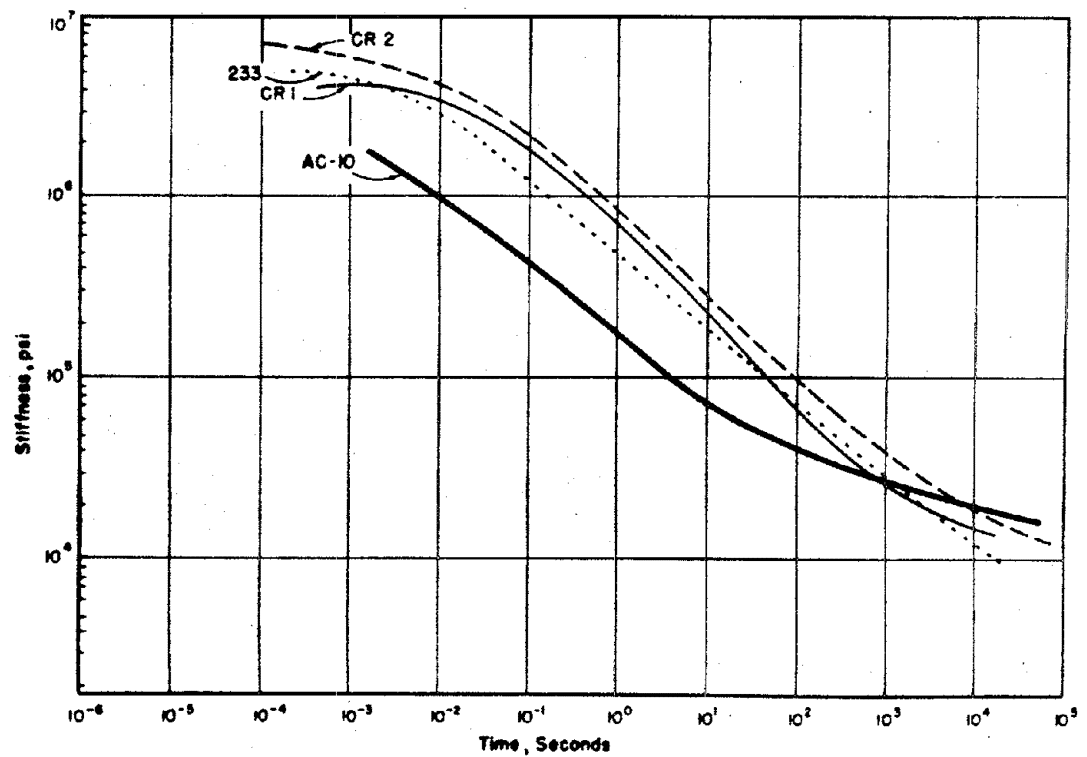


Figure 55. Stiffness Curves for All Mixtures Fabricated with Basaltic Aggregate.

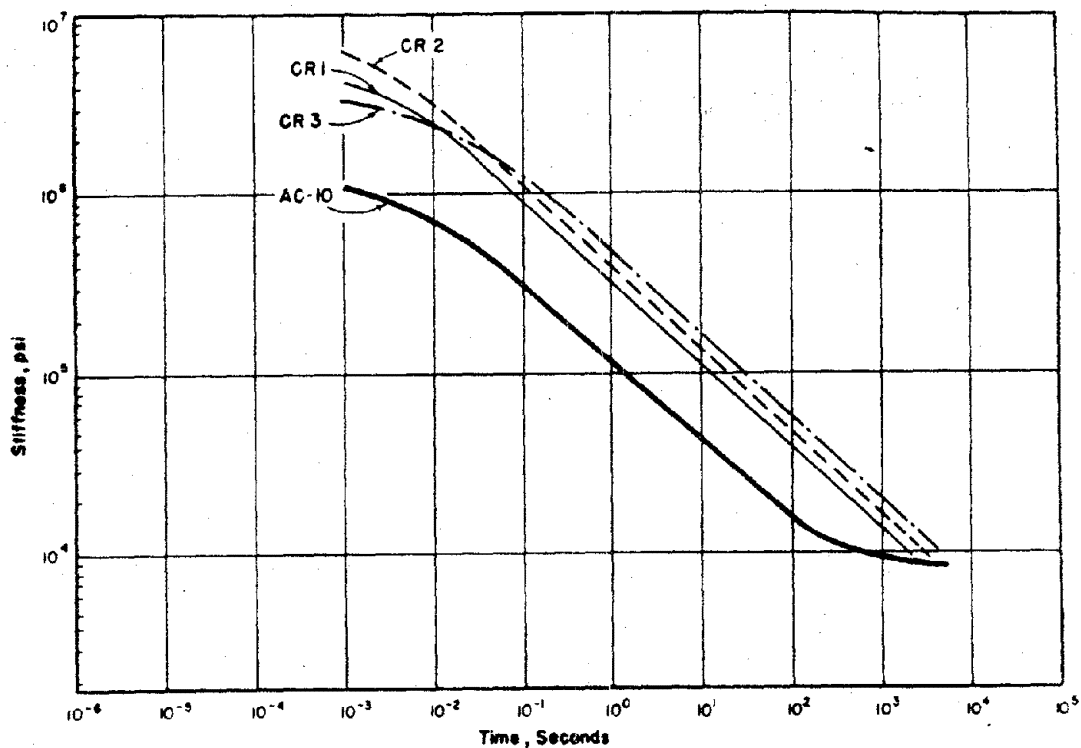


Figure 56. Stiffness Curves for All Mixtures Fabricated with Gravel Aggregate.

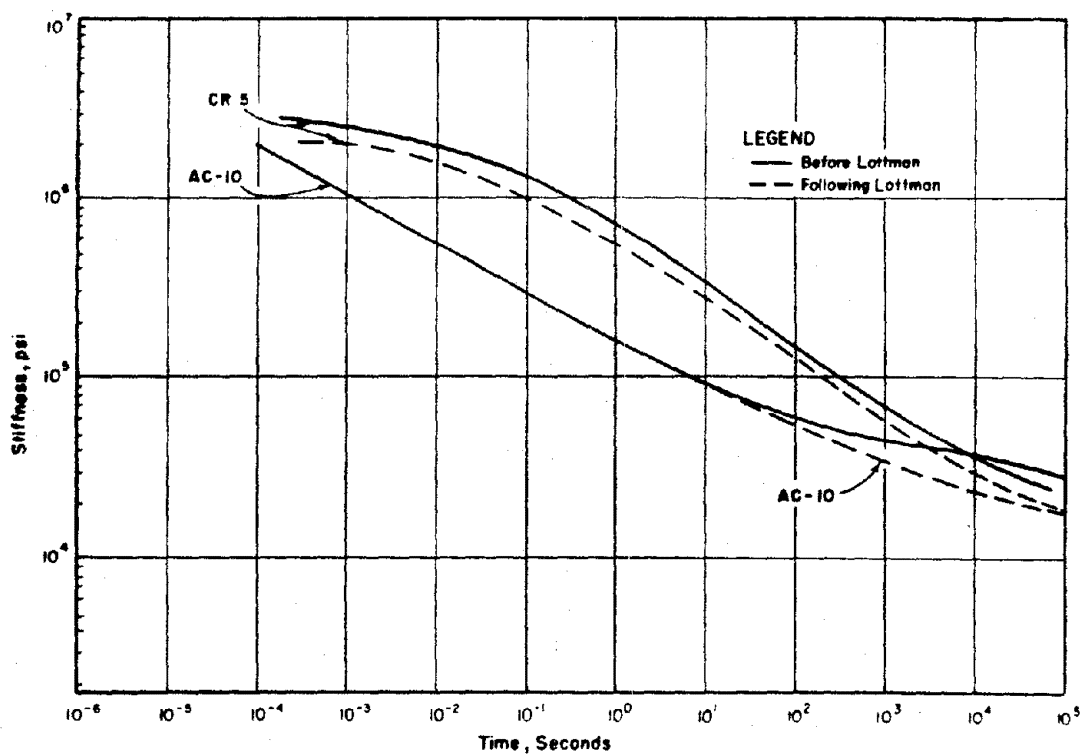


Figure 57. Stiffness Curves for Mixtures Fabricated with AC-10 and CR5 and Crushed Limestone Before and Following 1 Cycle Lottman Conditioning.

modulus will remain constant for a cross-linked polymer up to temperatures where chemical degradation begins to occur. The situation is quite different for a linear polymer. In this case, increasing temperature causes molecular motions to become more and more large-scale until eventually whole polymer molecules begin to translate.

Perhaps all the SULPHLEX binders show effects of linear behavior at the long durations of load. The consequences of this will be investigated in the chapter on structural design.

A second noticeable difference between SULPHLEX and the control mixture based on creep test data is the location of the glassy modulus plateau. The plateau occurs for all SULPHLEX binders at a longer load duration than for the control mixture. This is expected as the glass transition temperature of the basic SULPHLEX 233 formulation is approximately 30°F higher for SULPHLEX than for asphalt concrete.

Mixtures employing binders CR1 and CR2 behave substantially the same in the transition region as is substantiated by the power law representation of their creep curves in Table 32. Binder CR5 has a slightly lower slope in the transition region and behaves more like the control mixture than do the other binders.

Mixtures using binder CR3 possessed a virtually identical stiffness curve to CR1. The data for CR3 were not plotted as the CR1 curve represents the relationship adequately.

In general the SULPHLEX mixtures with crushed limestone aggregate possess high stiffnesses under load durations which represent moving traffic. SULPHLEX may possess desirable characteristics at intermediate temperatures and under moving traffic. However, their high glass transition temperature coupled with high mixture stiffness across the spectrum of load durations indicate low temperature cracking potential. A potential problem associated with continued deformation at long load rates exists at the other end of the spectrum.

Figure 57 presents the stiffness curves for CR5 and AC-10 specimens with crushed limestone before and following Lottman one

Table 32. Power Law Representations of Creep Compliance Data for SULPHLEX and Control Mixtures.

Binder	Aggregate	Gradation Type	Air Voids, Percent	$D_t = D_0 + D_1 t^n$
AC-10	CLS	A	3-5	$5.0 \times 10^{-7} + (7.1 \times 10^{-6})t^{0.26}$
	RG	A	2-3	$8.3 \times 10^{-7} + (8.3 \times 10^{-6})t^{0.45}$
	Basalt	B	3-5	$4.0 \times 10^{-7} + (5.2 \times 10^{-6})t^{0.32}$
	CLS*	A	3-5	$4.2 \times 10^{-7} + (1.0 \times 10^{-5})t^{0.33}$
CR1	CLS	A	3-5	$2.5 \times 10^{-7} + (1.0 \times 10^{-6})t^{0.47}$
	RG	A	2-3	$2.4 \times 10^{-7} + (3.3 \times 10^{-6})t^{0.43}$
	Basalt	B	3-5	$2.5 \times 10^{-7} + (1.2 \times 10^{-6})t^{0.44}$
	CLS*	A	3-5	$1.2 \times 10^{-7} + (1.7 \times 10^{-6})t^{0.47}$
CR2	CLS	A	3-5	$2.0 \times 10^{-7} + (9.0 \times 10^{-5})t^{0.45}$
	RG	A	2-3	$1.2 \times 10^{-7} + (2.5 \times 10^{-6})t^{0.46}$
	Basalt	B	3-5	$1.2 \times 10^{-7} + (1.1 \times 10^{-6})t^{0.40}$
CR5	CLS	A	3-5	$3.3 \times 10^{-7} + (1.4 \times 10^{-6})t^{0.34}$
	Basalt	B	3-5	$3.0 \times 10^{-7} + (1.3 \times 10^{-6})t^{0.42}$
	CLS*	A	3-5	$1.8 \times 10^{-7} + (1.6 \times 10^{-6})t^{0.37}$
233A	Basalt	B	3-5	$2.7 \times 10^{-7} + (1.2 \times 10^{-6})t^{0.49}$

* Lottman conditioning (1 cycle).

cycle conditioning. A deterioration in the stiffness response is noticed at the longer load durations for both mixtures.

The SULPHLEX and control mixture stiffness versus load duration curves for rounded river gravel and basalt aggregates are presented in Figures 55 and 56, respectively. These data show generally the following trends:

1. SULPHLEX binders generally have similar slopes in the transition zone for a given aggregate, Table 32.
2. The glassy modulus occurs at a much higher temperature than for the asphalt concrete.
3. Stiffnesses are much higher for SULPHLEX than for asphalt concrete for durations of load which would represent any type of moving wheel load.
4. At long durations of load, $> 10^4$ sec, SULPHLEX binders exhibit a linear amorphous polymeric degradation in stiffness.
5. The slope of the transition portion of the stiffness versus load duration master curves is statistically significantly less for the control mixture than for the SULPHLEX mixtures. This is illustrated by the n values in Table 32.
6. The glassy modulus of CR5 mixture is statistically significantly less than that of other SULPHLEX mixtures but significantly greater than the glassy modulus for the control mixtures of asphalt concrete, Table 32.

By comparing the time-temperature shift factors, a_T , for SULPHLEX and asphalt mixtures with various aggregates and gradations, Figures 58 through 60, it is apparent that:

1. Shift factors for asphalt concrete and SULPHLEX for each mixture evaluated were similar. In fact, the effect of binder on a_T was not statistically significant.
2. Ranges of shift factors between 100°F and 40°F are typical of those found in the literature for asphalt concrete (56) and sulfur-extended asphalt mixtures.

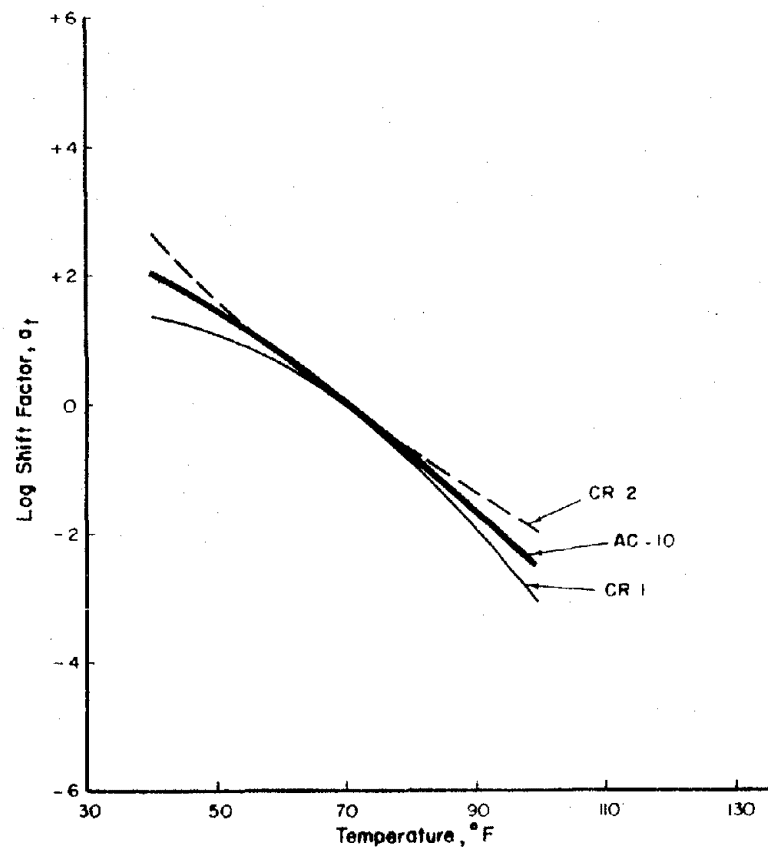


Figure 58. Time-Temperature Shift Factor for Mixtures with Crushed Limestone Aggregate.

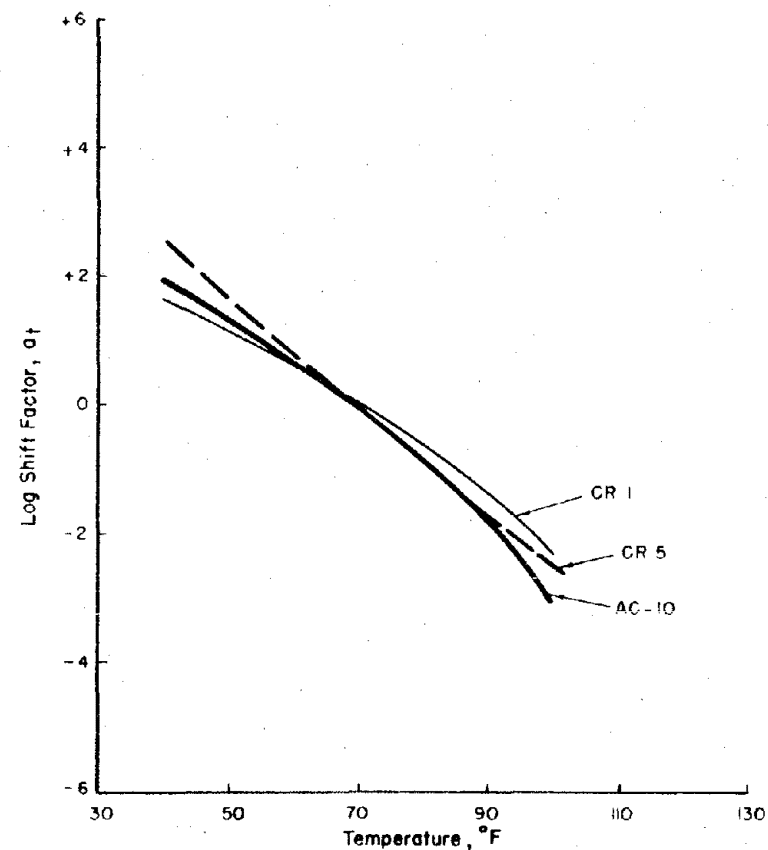


Figure 59. Time-Temperature Shift Factor for Mixtures with Basalt Aggregate.

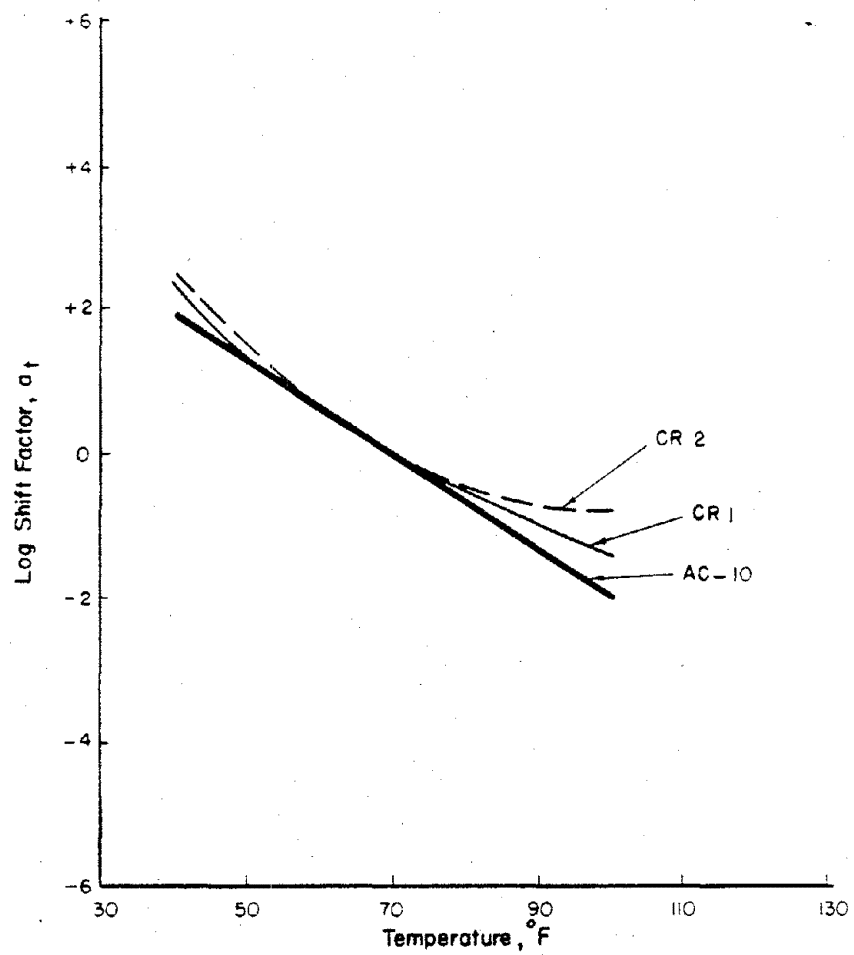


Figure 60. Time-Temperature Shift Factor for Mixtures with River Gravel Aggregate.

3. The effects on the shift factor of aggregate type, percent air voids and gradation were as great as was the effect of binder type.
4. Variation in binder content and/or variation in air voids content had no statistically significant or noticeable effects of the shift factor.

Although it has been established that for practical engineering purposes both SULPHLEX and asphalt concrete can be considered to be linearly viscoelastic, the application of a horizontal shift factor along the log time abscissa to produce a master curve is quite subjective. The value becomes even more subjective when the shift factor is described in terms of BETA. The term BETA is defined as the ratio of the change in $\log_{10} a_T$ over a change in temperature or a temperature interval

$$BETA = \frac{\Delta (\log_{10} a_T)}{\Delta T}$$

This value assumes a linear relationship between $\log_{10} a_T$ and temperature. As can be seen from Figures 58 through 60, this is not the case. The values of BETA which were used in the Structural Design chapter are presented in Table 33.

The master compliance curve at 70°F for the SULPHLEX and control mixtures was used in the VESYS structural subsystem in Chapter VII. By applying the shift factor or BETA factor to the compliance data (or stiffness data), the compliance (or stiffness) at any pavement temperature and any load duration can be determined.

VESYS Deformation Parameters

General

The VESYS structural pavement subsystem uses two parameters in the prediction of permanent deformation. They are called ALPHA and GNU and simply represent convenient mathematical parameters for fitting the relation of permanent strains to cycles of load on a log-log plot.

Table 33. Summary of BETA Values.

Binder	Aggregate	Gradation Type	Air Voids Content, %	BETA
AC-10	CLS	A	6-8	0.080
			3-5	0.070
		B	3-5	0.090
	RG	A	2-3	0.095
	Basalt	B	3-5	0.089
CR1	CLS	A	6-8	0.092
			3-5	0.089
		B	3-5	0.080
	RG	A	2-3	0.065
	Basalt	B	3-5	0.060
CR2	CLS	A	3-5	0.075
	RG	A	2-3	0.070
	Basalt	B	3-5	0.091
CR3	CLS	A	3-5	0.090
	RG	A	2-3	0.062
CR5	CLS	A	3-5	0.075
	Basalt	B	6-8	0.070
	RG	A	2-3	0.080

In developing ALPHA and GNU, researchers (12) decided that it was important to develop a method of representing permanent deformation that was most accurate and sensitive in the region of interest. This region was well past the number of cycles applied during laboratory testing. Also it was important to relate the amount of deformation that occurred during a single cycle to the number of previous load cycles so that the permanent strain during any load cycle could be predicted.

The method selected to represent permanent deformation characteristics, ϵ_a , of material for VESYS IIM involves a linear curve-fit on a log-log plot. This line may be defined by its intercept, I, at one load cycle and its slope, S. Thus,

$$\log \epsilon_a = \log I + S \log N$$

or

$$\epsilon_a = IN^S$$

The desired permanent strain due to the N^{th} loading is then

$$\epsilon_p(N) = \epsilon_a(N) - \epsilon_a(N-1)$$

or converting the right side of the equation to a continuous variable

$$\epsilon_p(N) = \frac{d\epsilon_a(N)}{dN} = \frac{d(IN^S)}{dN}$$

$$\epsilon_p(N) = ISN^{S-1}$$

The resilient or elastic strain, ϵ_r , is essentially a constant after relatively few cycles and is large compared to the permanent strain. Therefore, the fraction of the total strain $F(N)$, that is permanent may be considered to be

$$F(N) = \frac{\epsilon_p(N)}{\epsilon_r(N)} = \frac{\epsilon_p(N)}{\epsilon_r} = \frac{ISN^{S-1}}{\epsilon_r}$$

For convenience, arbitrary definitions were made for mathematical simplification:

$$\mu = IS/\epsilon_r \quad (\text{GNU})$$

$$\alpha = I - S \quad (\text{ALPHA})$$

As $F(N)$ is the fraction of permanent strain during cycle N , the permanent strain in a compression specimen during cycle N is $F(N)$ multiplied by ϵ_r . The increment of permanent strain, ϵ_a , may also be calculated during the interval of loading, N_1 to N_2 , by integrating $\epsilon_r F(N)$ as follows:

$$\Delta\epsilon_a = \int_{N_1}^{N_2} \epsilon_r F(N) dN = \frac{\epsilon_r \mu}{1-\alpha} [N_2^{1-\alpha} - N_1^{1-\alpha}]$$

The total height (H) reduction of a specimen would be $H \cdot \Delta\epsilon_a$ during the increments of repetitive load N_1 to N_2 .

Both μ and α are considered by VESYS to be constant for a layer of material. In reality they are quite stress dependent. Thus μ and α vary with depth in the layer as well as laterally from the center of load.

ALPHA and GNU are difficult parameters to which one may attach physical significance. However, the extensive sensitivity analysis of the VESYS structural subsystem by Rauhut et al. (57) provided a great step toward understanding the significance of these values. The most important findings in the Rauhut study with respect to this research in terms of ALPHA and GNU are summarized as follows:

1. The ALPHA parameter for asphalt concrete normally occurs within a range of from 0.63 to 0.07.
2. GNU of the surface layer (asphalt concrete) is quite variable and may be as high as 1.5, 2.0 or even higher.
3. ALPHA and GNU are used in VESYS IIM as if they were invariants, but they are actually vary with stress, temperature, mix, etc.
4. ALPHA and GNU are very stress-sensitive. Both decrease with increasing deviatoric stress, but at different rates.
5. Temperature should be an important parameter in testing for ALPHA and GNU for the surface layer (asphalt or SULPHLEX), but it is apparently introduced in VESYS IIM in a different manner. ALPHA and GNU define the fraction of the elastic

response to load that will remain when the load is removed. This elastic response is dependent on the stiffness or compliance. For asphalt concrete or SULPHLEX, a time-temperature shift function revises the master 70°F curve to account for actual temperatures. The assumptions of VESYS IIM are that the effects of varying layer stiffness with temperature will represent the somewhat different effects of varying permanent deformation with temperature. The proper test temperature for ALPHA and GNU is that used for the master creep-compliance curve (70°F).

6. Both ALPHA and GNU are much more heavily dependent on stress level than upon temperature.
7. A low ALPHA or a high GNU indicate increased rutting and vice versa.
8. Although quite variable, a low ALPHA is usually associated with a low GNU.
9. There is virtually no rutting, slope variance, or deterioration for ALPHA greater than 0.90.
10. Values of ALPHA and GNU falling within the bounds of the plots in Figure 61 may be considered consistent with asphalt concrete mixtures in practice. As a counter example, an ALPHA of 0.65 and GNU of 1.5 might define an unstable mixture with the potential for rutting, high slope variance, and rapid deterioration of serviceability. At the other extreme, an ALPHA of 0.88 and GNU of 0.2 might define a stiff mixture that would rut negligibly and suffer virtually no serviceability loss.
11. ALPHA and GNU values outside of the bounds of the plot of Figure 61 are not impossible but highly unlikely for modern asphalt concrete mixtures.

Measuring ALPHA and GNU

ALPHA and GNU are obtained by conducting incremental static-dynamic load tests on four-inch diameter by eight-inch tall cylindrical specimens. Since these parameters are sensitive to the in

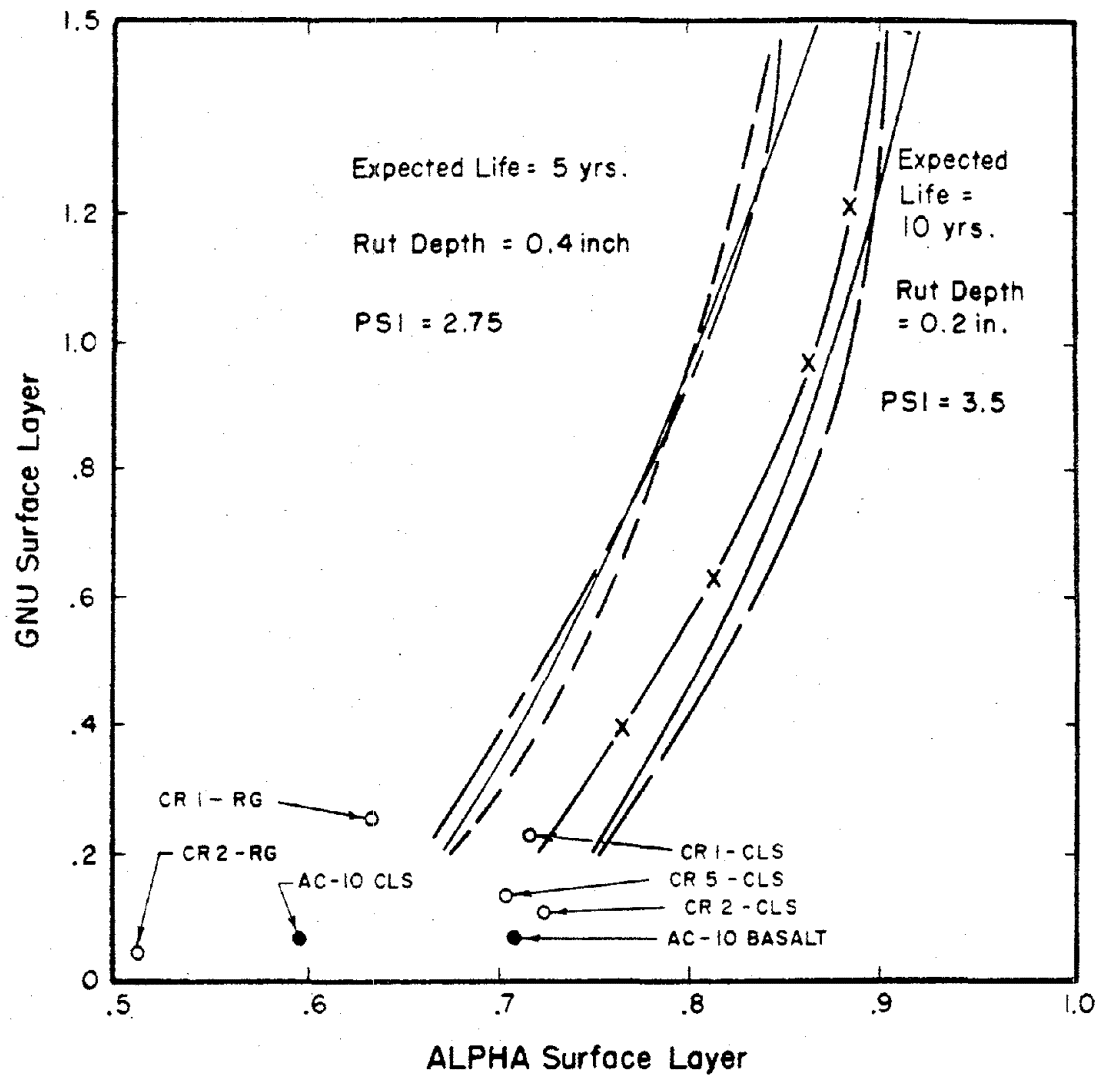


Figure 61. Typical Ranges of ALPHA and GNU Permanent Deformation Parameters. (The various lines represent data on asphalt concrete developed by Rauhut (57), and the area between the extreme lines represents a region of "typical" ALPHA and GNU values.)

situ state of stress and local environments, they should be determined on specimens subjected to realistic in situ stress states and average moisture contents and temperatures expected in the field.

ALPHA and GNU were measured at three temperature levels: 40°F, 70°F, and 100°F. Stress levels of 10 and 30 psi at 100°F, 10, 20, and 30 psi at 70°F and 30 and 50 psi at 40°F were applied in the deformation testing. Table 34 presents the experimental design for the permanent deformation testing.

Straight lines on log-log paper of accumulative strain versus number of load applications were fitted to the data to define the slope, S, and intercept, I. Dynamic, resilient strains were measured at the 200th repetition and were used in the computation of GNU.

Results of VESYS Pavement Deformation Testing

Table 35 presents the VESYS permanent deformation properties for each binder at the three temperature levels. These parameters are averages of those found at the stress levels tested. These average values were used to plot accumulated strain versus number of load repetitions, and these relationships are presented in Figures 62 through 69. The dynamic strains computed at the 200th load repetition were computed for each binder and temperature using the moduli from the stiffness versus load duration data previously discussed.

A number of general assumptions may be drawn from the VESYS permanent deformation data and a number of general observations made. First, the values of ALPHA in the total experiments ranged from 0.45 to 0.80. The values of GNU ranged from 0.015 to 0.26. It is difficult to label these values as being either good or bad, typical or atypical. Generally, the ALPHA value hovered within the range considered typical of asphalt concrete, while GNU values were generally much lower than would be expected for the magnitude of concomitant ALPHA values.

Second, by simply viewing the ALPHA and GNU data, variation from binder to binder at a selected temperature level and for a given aggregate is reasonably low. This indicates a basic similarity among binders in terms of permanent deformation.

Table 34. Experiment Design for Determination of Permanent Deformation Parameters.

Binder Stress Level, psi Temperature, °F Aggregate Type			CR1	CR2	CR3	CR5	233	AC-10
C L S	40	30	x	x		x		x
		50	x	x		x		x
	70	10	x	x	x	x		x
		20	x	x	x	x		x
		30	x	x	x	x		x
	100	10	x	x		x		x
B A S A L T	40	30					x	x
		50					x	x
	70	10					x	x
		20					x	x
		30					x	x
	100	10					x	x
R G	70	10	x					
		20	x					
		30	x					

Table 35. VESYS Deformation Parameters for SULPHLEX and Control Mixtures
(From Log-Log Plot of Accumulated Permanent Strain Versus
Load Application).

Binder	Aggregate	Test Temperature, °F	Slope, S	Intercept, I	Alpha	GNU
AC-10	CLS	40	0.20	2.0×10^{-6}	0.80	0.015
		70	0.42	9.0×10^{-6}	0.58	0.050
		100	0.50	3.0×10^{-5}	0.50	0.090
	Basalt	40	0.46	3.0×10^{-6}	0.54	0.040
		70	0.28	6.0×10^{-6}	0.72	0.052
		100	0.40	2.8×10^{-5}	0.60	0.099
CR1	CLS	40	0.20	1.5×10^{-6}	0.80	0.049
		70	0.26	9.0×10^{-6}	0.73	0.21
		100	0.33	3.9×10^{-5}	0.67	0.22
	RG	40	0.25	2.0×10^{-6}	0.75	0.100
		70	0.36	6.0×10^{-6}	0.64	0.25
		100	0.40	5.0×10^{-5}	0.60	0.29
CR2	CLS	40	--	---	----	----
		70	0.27	3.5×10^{-6}	- .73	0.070
		100	0.30	1.2×10^{-5}	0.70	0.067
CR5	CLS	40	0.20	2.0×10^{-6}	0.80	0.182
		70	0.30	7.0×10^{-6}	0.70	0.091
		100	0.42	3.0×10^{-5}	0.58	0.26
233	Basalt	40	0.55	2.9×10^{-6}	0.45	0.035
		70	0.49	2.5×10^{-6}	0.51	0.024
		100	0.43	1.0×10^{-5}	0.57	0.139

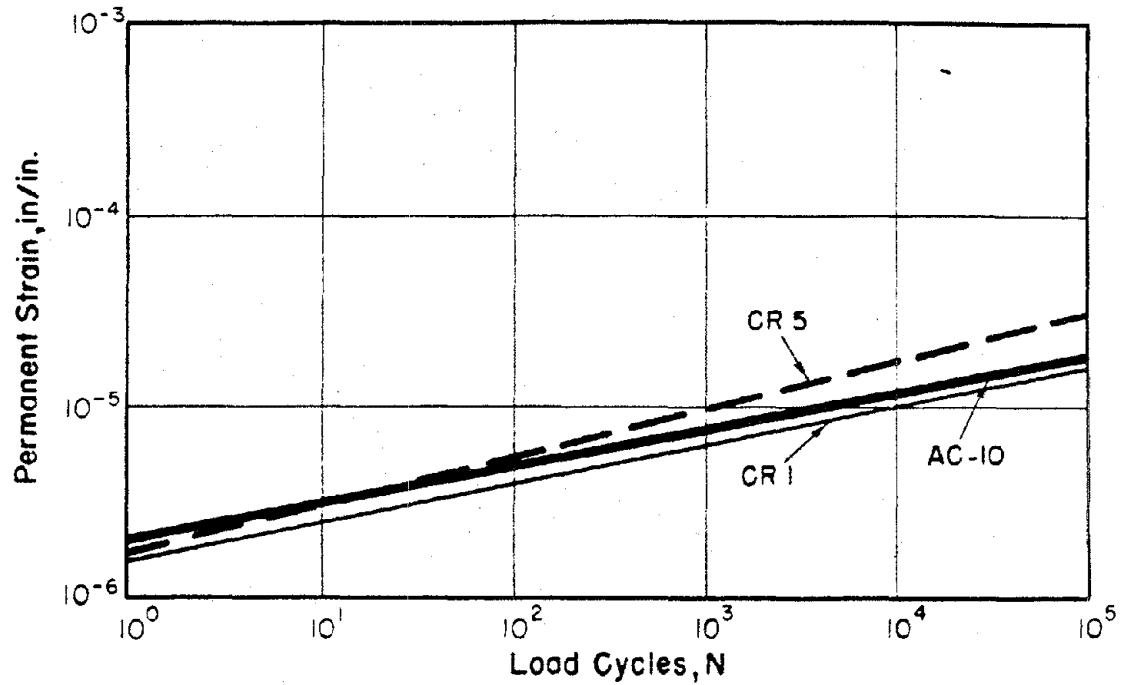


Figure 62. VESYS Permanent Deformation Plots for SULPHLEX and Asphalt Concrete Mixtures with Crushed Limestone Aggregate (40°F).

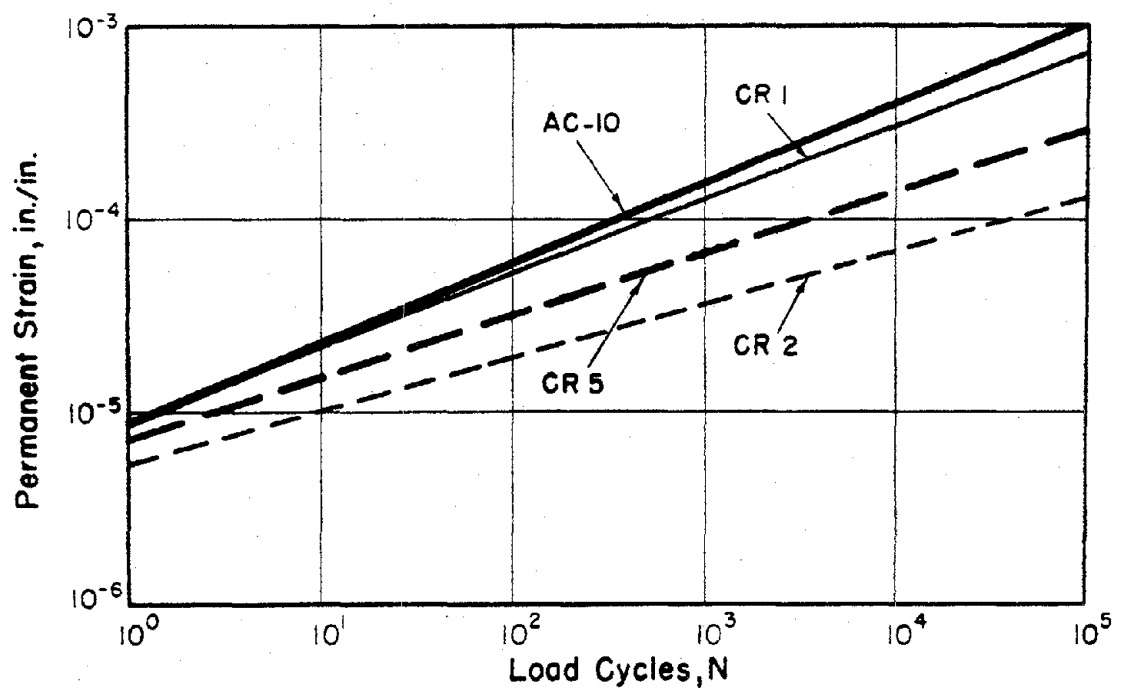


Figure 63. VESYS Permanent Deformation Plots for SULPHLEX and Asphalt Concrete Mixtures with Crushed Limestone Aggregate (70°F).

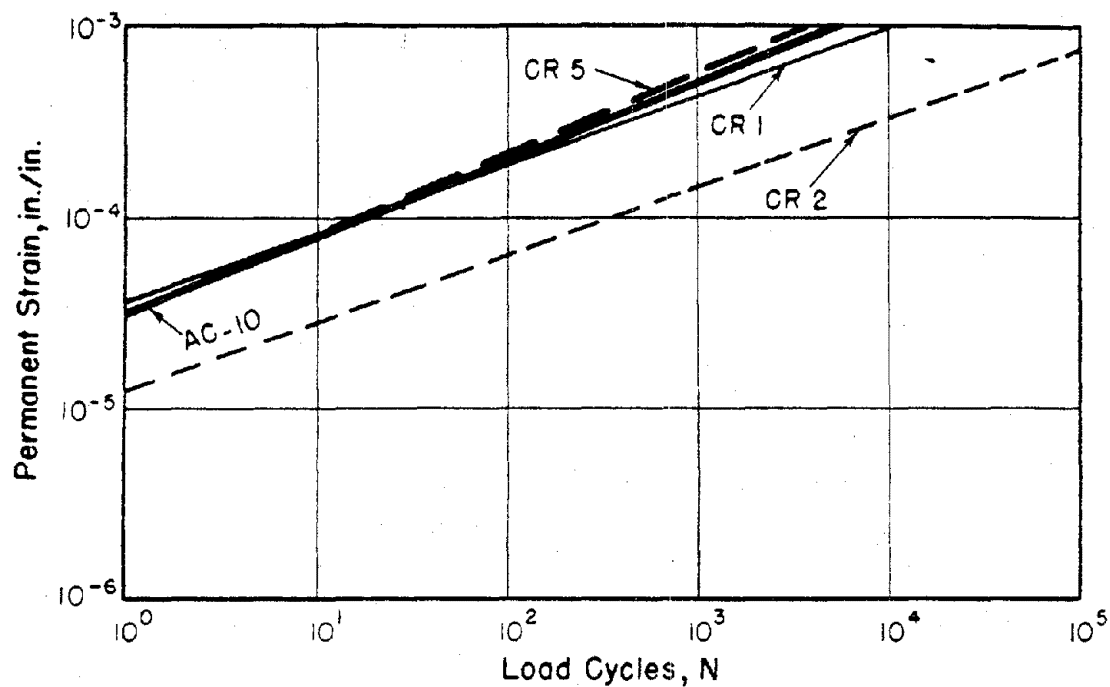


Figure 64. Permanent Deformation Plots for SULPHLEX and Asphalt Concrete Mixtures with Crushed Limestone Aggregate (100°F).

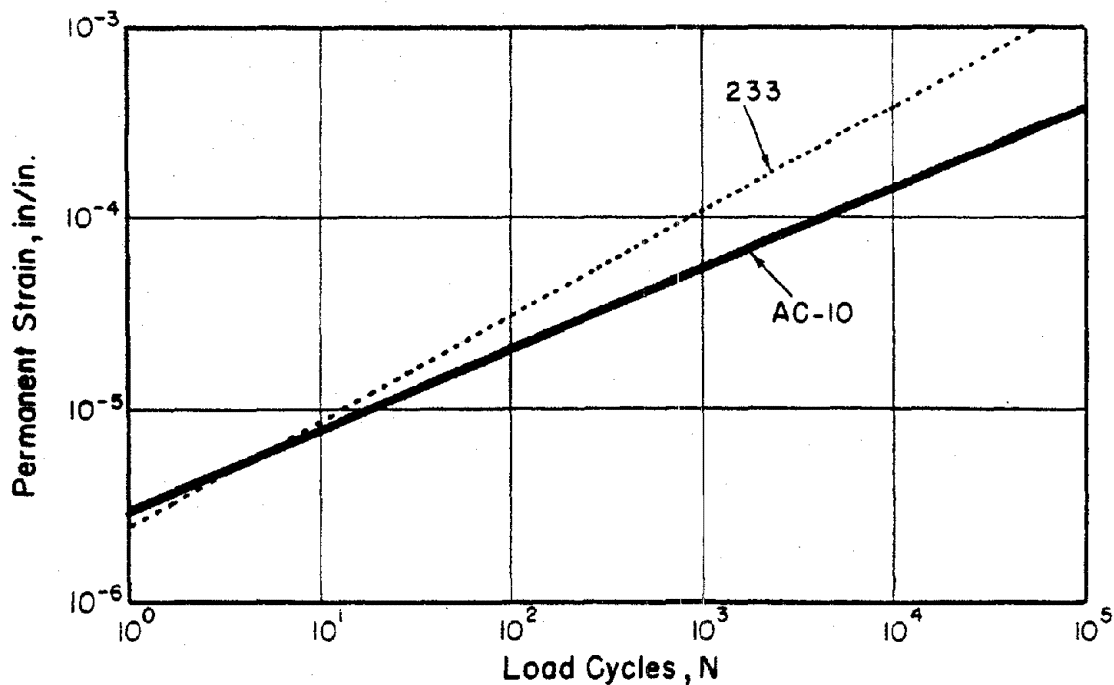


Figure 65. VESYS Permanent Deformation Plots for SULPHLEX and Asphalt Concrete Mixtures with Basaltic Aggregate (40°F).

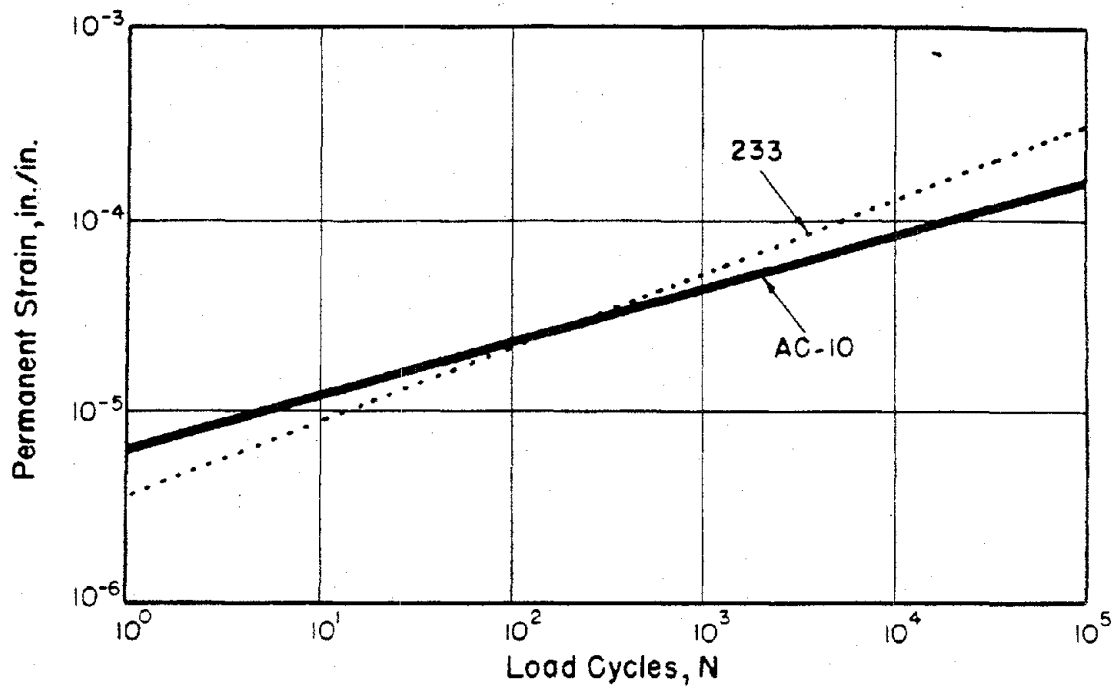


Figure 66. VESYS Permanent Deformation Plots for SULPHLEX and Asphalt Concrete Mixtures with Basaltic Aggregate (70°F).

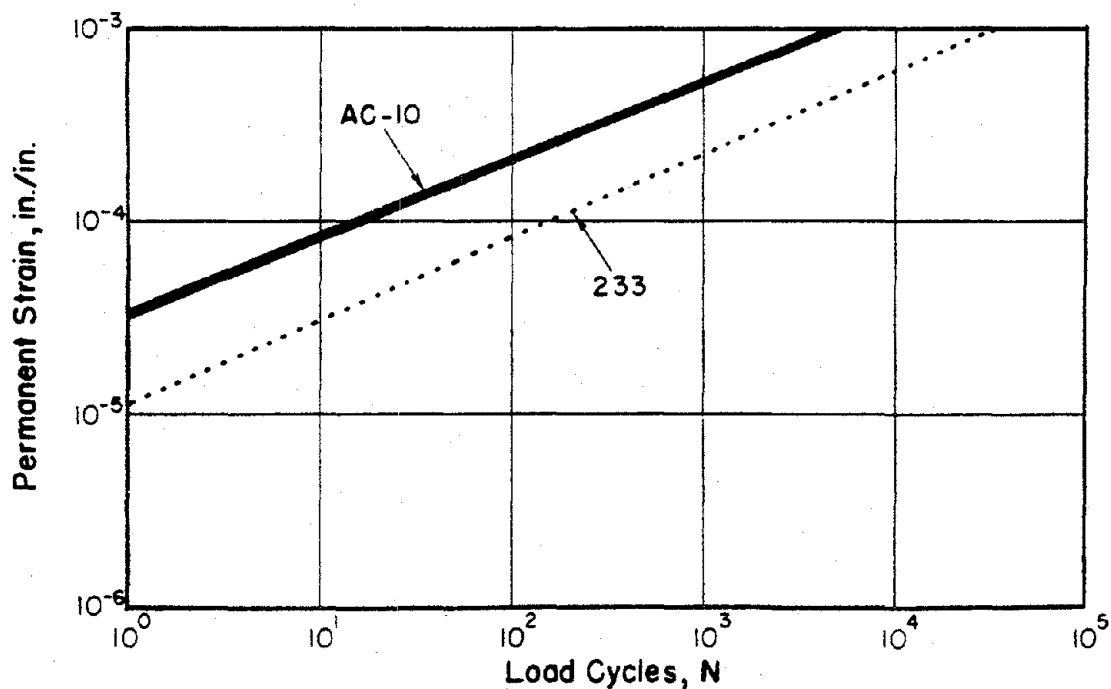


Figure 67. VESYS Permanent Deformation Plots for SULPHLEX and Asphalt Concrete Mixtures with Basaltic Aggregate (100°F).

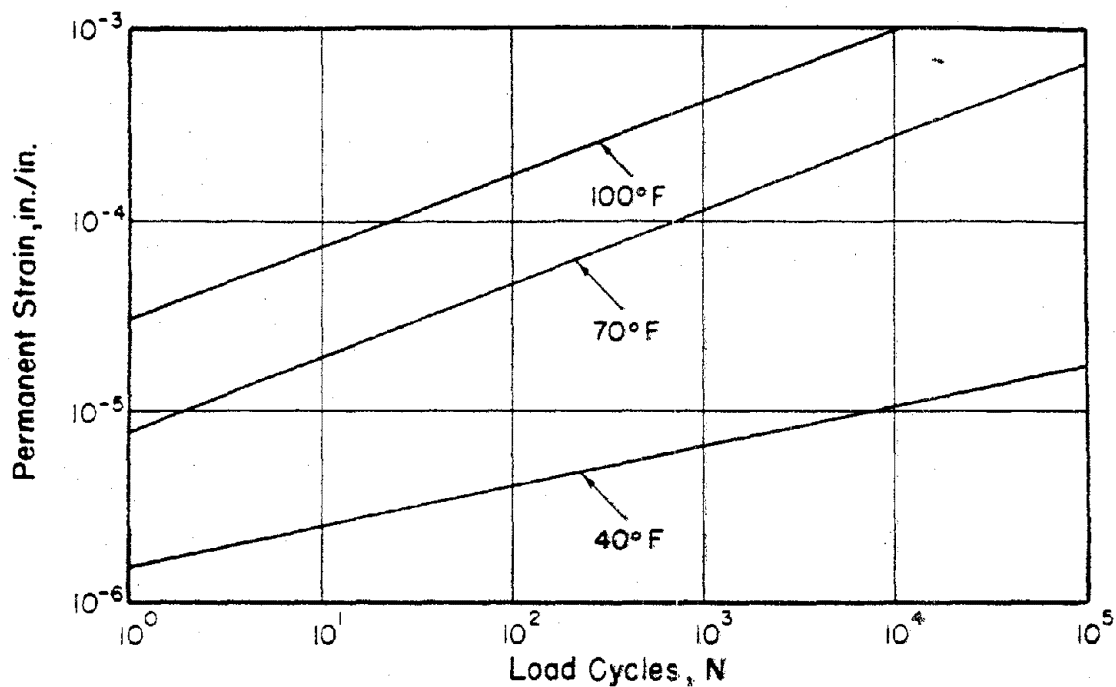


Figure 68. Permanent Deformation Characteristics of CR1 - Crushed Limestone Mixtures.

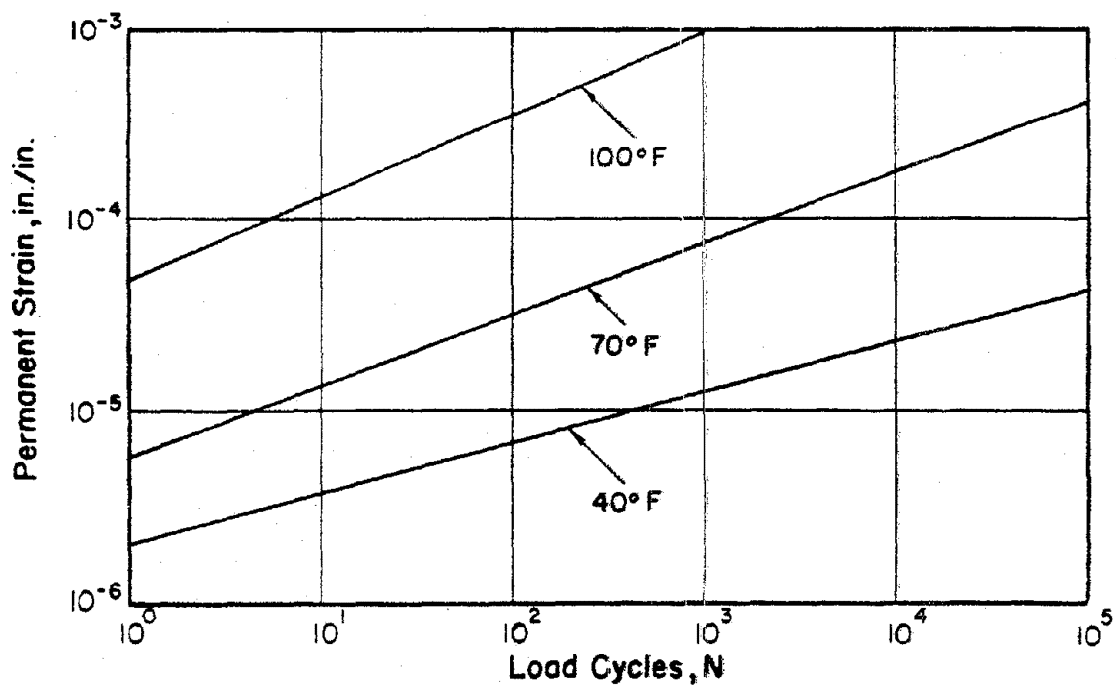


Figure 69. Permanent Deformation Characteristics of CR1 - River Gravel Mixtures.

Third, the regularity of the data and potential for the mixture to produce excess field deformation can be estimated from Figure 61. Here the locus of ALPHA and GNU are plotted for each binder at 70°F. The conclusion is that the combination of average to high-ALPHA values with low GNU value is somewhat unusual (57). The assumption is that these combinations of ALPHA and GNU will not produce excessive serviceability loss due to deformation (57). Little (92) and Pickett (56) (see Table 36) have also presented similar combinations of moderate to high ALPHA values coupled with low GNU values for recycled asphalt concrete and sulfur-extended asphalt mixtures, respectively. This combination of high ALPHA values and low GNU values may be typical of stiffer mixtures.

Finally, Table 36 compares ALPHA and GNU values obtained on sulfur-extended asphalt mixtures, recycled asphalt concrete mixtures and SULPHLEX. All testing was performed at Texas A&M. VESYS analyses were carried out for each material. Table 36 summarizes the results. The ALPHA and GNU values of SULPHLEX binders are similar to the other binders which are predicted to perform well under repeated short term load applications.

By plotting the accumulated permanent strain versus load cycle data, Figures 62 through 69, the following observations were made:

1. Binders CR1, CR5, and AC-10 respond essentially the same when used with the crushed limestone aggregate.
2. The CR2-crushed limestone mixture shows substantially less accumulated strain at 70°F and 100°F.
3. The basalt aggregate and binder 233A mixture responds very similar to AC-10, except at the 100°F temperature where the 233A-basalt mixture performs better.
4. Aggregate type affects the accumulated strain versus cycles of load plot, as would be expected.

Table 36. Comparison of VESYS Permanent Deformation Parameters at 70°F for SULPHLEX, Sulfur-Extended Asphalt and Recycled Asphalt.

Category	Material	ALPHA	GNU	Deformation Performance Potential
Sulfur- Extended Asphalt	Sulfur AC with limestone aggregate (50% sulfur)	0.80	0.156	
	Sulfur AC with limestone aggregate (25% sulfur)	0.76	0.15	Less than 0.25 inches of rutting in 20 years of 6,000 VPD traffic (6 inch surface).
	Sulfur AC with limestone aggregate (50% sulfur)	0.79	0.057	
	Recycled AC mix with 25% sulfur	0.56	0.023	
Recycled Asphalt Concrete	California Valley Recycled Mix with Recycling Agent C.	0.82	0.182	0.30 inches of rutting in 20 years 6,000 VPD traffic (6 inch surface).
	California Valley Recycled Mix with Recycling Agent B	0.67	0.086	Less than 0.1 inches of rutting in 20 years of 6,000 VPD traffic (6 inch surface).
	Oregon Recycled Mix with Recycling Agent C	0.72	0.168	Less than 0.29 inches of rutting in 20 years of 6,000 VPD traffic (6 inch surface).

Table 36. Comparison of VESYS Permanent Deformation Parameters at 70°F for SULPHLEX, Sulfur-Extended Asphalt and Recycled Asphalt (continued).

Category	Material	ALPHA	GNU	Deformation Performance Potential
SULPHLEX	CR1 and Crushed Limestone	0.73	0.21	-----
	CR2 and Crushed Limestone	0.73	0.070	-----
	CR5 and Crushed Limestone	0.70	0.091	-----
	233A and Basalt	0.51	0.024	-----
Control Mixtures	AC-Crushed Limestone (Control for Sulfur Extended Asphalt)	0.71	0.127	-----
	AC-Crushed Limestone (Control for Recycled Study)	0.66	0.115	0.34 inches of rutting in 20 years of 6,000 VPD traffic (6-inch surface).
	AC-Crushed Limestone (Control for Sulphlex Study)	0.58	0.050	-----
	AC-Basalt (Control for Sulphlex Study)	0.72	0.052	-----

The Shell Method of Estimating Deformation Potential

General

The development of the Shell method is discussed extensively in References 93, 94, and 95; therefore, only a brief background and description of the method is given here.

The Shell procedure is based on the static creep test in which a constant force is applied perpendicularly to the parallel end faces of a cylindrical specimen. The axial deformation is measured as a function of the loading time for a constant temperature. If the test is conducted over a range of temperatures, a master stiffness curve may be constructed.

In a long-term loading test such as the creep test or an actual pavement layer, the structure of the paving mix undergoes a change. Under the applied load the binder between the mineral aggregate is squeezed into the voids. As a result more particle-to-particle contacts are formed and a transfer of force from the binder to the aggregate system occurs. Hills (96) developed a theoretical physical model to describe creep behavior mathematically. In his approach the relative displacement of a pair of adjacent mineral aggregate particles in a viscoelastic matrix is calculated. He characterizes the deformation of asphalt mixes as

$$\frac{\epsilon_{mix}}{F_y} = 2^q \left[\left(1 + \frac{\epsilon'_{binder}}{F_x} \right) 2^{\frac{1}{q}} - 1 \right]$$

where

ϵ_{mix} is the strain in the asphalt mix,

$\frac{1}{F_y}$, $\frac{1}{F_x}$ are factors which are constant for one particular creep test,

q is an integer greater than or equal to one, being determined by the grading of the mineral aggregate, and ϵ'_{binder} is the calculated strain in the binder.

It can be seen from this model that the strain, or deformation, of a given paving mix under a constant load is dependent only on the strain in the binder. This led Hills to plot the stiffness modulus of the mix (S_{mix}) against the stiffness modulus of the binder (S_{binder}). The result was a curve which fit the theoretical model. Thus an S_{mix} vs. S_{binder} curve is a basic way of characterizing creep behavior which is independent of loading time, temperature, or stress level. The S_{mix} - S_{binder} curve is the basis of the Shell method for predicting rut depth; it allows a value of S_{mix} derived from a creep test to be predicted from a value of S_{binder} calculated on the basis of binder viscosity, traffic, and climatic conditions. Since S_{mix} is determined from a creep test, it actually represents only the irreversible or viscous portion of the stiffness modulus and so can be used to calculate rut depth.

In the creep test an equal relative reduction in layer thickness, $\Delta h/h$, is attained at a lower stress than in an actual pavement layer. This is due to a uniform stress distribution caused by no lateral confinement. Therefore an effective stress, σ_{eff} , which is lower than the contact stress, σ_0 , is defined as

$$\sigma_{eff} = Z\sigma_0$$

where Z is the ratio of stress in a creep sample to the contact stress causing an equal deformation in a pavement layer. The term Z can alternatively be defined as the relative reduction in layer thickness in an actual pavement to that of a specimen subjected to the creep test under the same loading conditions. Since traffic loading times are short, it can be assumed that the pavement structure behaves elastically. For an elastic multilayer pavement system, Z becomes a function of the ratio of elastic moduli, the radius of loading and the paving layer height. Many values of Z for different combinations of moduli and layer thickness have been calculated using BISTRO and are tabulated in the Shell Pavement Design Manual (93).

The deformation of a pavement layer can be calculated by

$$\epsilon_{mix} = \frac{\sigma_{eff}}{S_{mix}} = \frac{Z \cdot \sigma_o}{S_{mix}}$$

or

$$\Delta h = h \cdot \epsilon_{mix} = \frac{Z \cdot \sigma_o}{S_{mix}}$$

where ϵ_{mix} is the permanent mix strain, and S_{mix} is derived from the creep test. Many calculated permanent deformations were compared to actual rut depths developed in a wheel tracking test at the Koninklijke Shell Laboratory (94). The actual and calculated rut depths always differed by a factor of less than two. The Shell researchers attributed this to the difference in deformation between dynamic and static loading. It was found that the permanent deformation attained in a dynamic test is greater than that in a static test due to the effects of plastic deformation. A large part of plastic deformation takes place immediately after a load application. For this reason an empirical correction factor, C_m , ranging from 1.0 to 2.0 was introduced. Rut depth is now calculated as

$$\Delta h = C_m \cdot h \cdot \epsilon_{mix} = C_m \cdot h \cdot \frac{Z \cdot \sigma_o}{S_{mix}}$$

In order to determine S_{mix} , an expression must be developed to calculate S_{binder} . When a sample is deformed, the strain in the binder can be expressed as

$$\epsilon_{bit} = \epsilon_{elastic} + \epsilon_{viscoelastic} + \epsilon_{viscous}$$

The stiffness modulus of the binder can be expressed as

$$\frac{1}{S_{binder}} = \frac{\epsilon_{binder}}{\sigma} = \frac{1}{S_{binder, el.}} + \frac{1}{S_{binder, visc. - el.}} + \frac{1}{S_{binder, visc.}}$$

The irreversible, or permanent deformation, portion of S_{binder} is the viscous component, $S_{binder, visc.}$ or

$$S_{binder, visc.} = \frac{\sigma}{\epsilon_{visc.}}$$

For a purely viscous material

$$\frac{d\epsilon}{dt} = \sigma/\lambda$$

and for a incompressible fluid

$$\epsilon = \frac{\sigma}{3\eta} \cdot t$$

where η is the dynamic viscosity of the binder at temperature T and loading time t . For static conditions,

$$S_{\text{binder, visc.}} = \frac{3}{t} \eta$$

In order to relate deformation behavior to number of wheel passes, it is assumed that the permanent deformation of the mix is a function of the viscous component of S_{binder} . The irreversible deformation of the binder proceeds linearly in relation to time at constant temperature; for a cyclic loading test the loading times are allowed to be superimposed. Total loading time, t , is then

$$T = N \cdot t_w$$

where N is the number of standard wheel load passes, and t_w is the loading time per pass. If the temperature is varied, the number of wheel passes at different temperatures or viscosities would have to be summed as

$$S_{\text{binder, visc.}} = \frac{3}{K \cdot t_w \cdot \sum_{i=1}^N \left(\frac{N}{\eta} \right) T_i}$$

Rut depth may now be calculated through a simple procedure. Using data from the creep test an $S_{\text{mix}}-S_{\text{binder}}$ diagram may be plotted. $S_{\text{binder, visc.}}$ may be calculated knowing climatic conditions, binder viscosity and the number of standard wheel loads expected in the life of the pavement. Entering the $S_{\text{mix}}-S_{\text{binder}}$ diagram with $S_{\text{binder, visc.}}$, a value of S_{mix} is found. Now knowing S_{mix} , the contact stress, the layer height, C_m and Z , the rut depth, may be calculated. This

calculated rut depth is only the permanent deformation occurring in the paving mix. The total (actual) rut depth must include the permanent deformation of the base and subgrade.

S_{mix} Versus S_{binder} Curves

Using the principles discussed above, S_{mix} versus S_{bit} curves were plotted for the SULPHLEX mixtures and the control mixture. This analysis is presented both for CR1 and AC-10 with crushed limestone. The results are typical of other SULPHLEX mixtures. Since the S_{mix} versus S_{bit} plot is the key to the deformation analysis, it is valuable to carefully scrutinize these plots.

The S_{mix} - S_{bit} curves were plotted using viscosity versus temperature relationships for the binders and creep stiffness relationships for the mixtures. For each value of S_{mix} based on the creep stiffness curves (a function of duration of loading and temperature), a value of $S_{bit, visc.}$ was computed ($3\eta/t$), where η is the binder viscosity at the same temperature stiffness. Of course these relationships are only valid for conditions under which the binder is purely viscous and the load is of long duration (95).

Figure 70 presents S_{mix} versus S_{bit} data for CR1 and AC-10 mixtures using crushed limestone aggregate. Binder contents at and above optimum were used. For each binder content of AC-10 an equal-by-volume binder content of SULPHLEX was evaluated.

The effect of binder content is as would be expected at these low stiffnesses of the binder. The SULPHLEX mixture is stiffer than asphalt concrete as the duration of loading is reduced and/or the temperature of testing is lowered. However, at low S_{bit} values (below about 10^{-1} psi) the SULPHLEX S_{mix} becomes lower than that of asphalt concrete. This is not surprising following the analysis of the creep stiffness curves, where a "linear type" response has been found to occur. However, this lower S_{mix} for CR1 at low S_{bit} will not normally affect computation of rutting as the combination effects of viscosity, as influenced by temperature and $t = N \cdot t_w$, will simply not bring S_{bit} into the critical range (below approximately 10^{-1} psi).

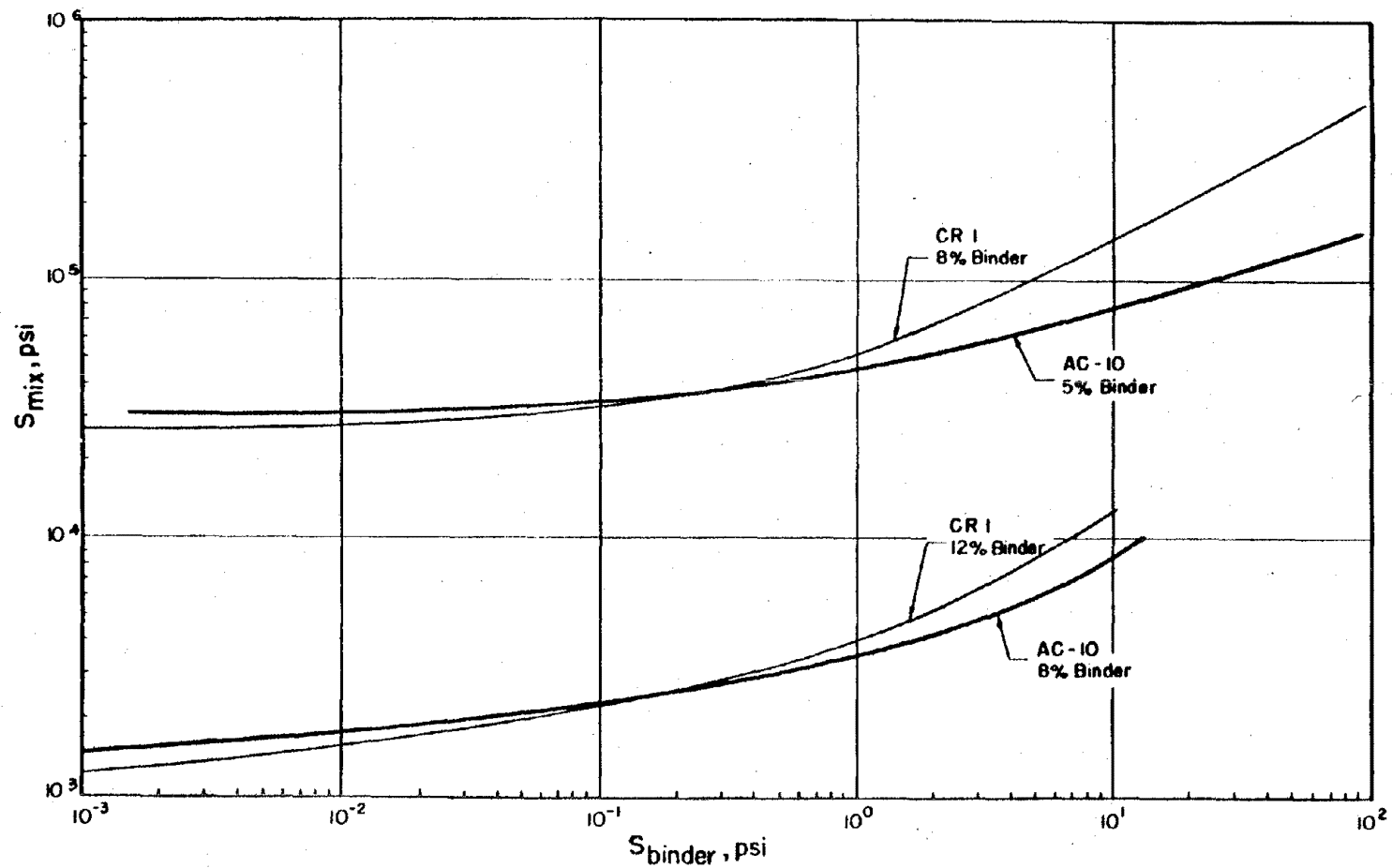


Figure 70. Plot of S_{binder} Versus S_{mix} for Mixtures of CR1 or AC-10 with Crushed Limestone Aggregate.

Deformation Analysis

A permanent deformation analysis was performed using the Shell method for the CR1 and AC-10 mixtures whose stiffness characteristics are represented in Figure 70. Three climatic regions were studied: a warm climate, typical of Mobile, Alabama; a moderate climate, typical of Dallas, Texas; and a cold climate, typical of Chicago, Illinois.

An effective viscosity was calculated for each climatic region and binder as shown in the Shell Pavement Design Manual (93).

$$\eta_{\text{eff}} = \frac{12}{\sum_{i=1}^3 \left(\frac{1}{\eta_i} \right)}$$

where η_i is the viscosity at the mean monthly air temperature. The paving mix was divided into three sublayers and the effective viscosity of each sublayer was adjusted according to its depth below the surface. Assuming the load duration of a moving wheel to be 0.02 seconds, the binder stiffness is

$$S_{\text{binder, viscous}} = \frac{3\eta_{\text{eff}}}{N (0.02 \text{ sec.})}$$

where N is the number of equivalent 18-kip axle loads (which are assumed to be uniformly distributed through the year). A value of S_{mix} can be found using the $S_{\text{mix}}-S_{\text{binder}}$ diagram. The relative reduction in layer height is then

$$\Delta h = 1.6h \frac{Z(100 \text{ psi})}{S_{\text{mix}}}$$

where C_m is 1.6 and the tire pressure is assumed to be 100 psi. The appropriate Z -factor can be found in the Shell Manual (93).

Rut depths were negligible for every case even at traffic levels of 100 million applications.

CHAPTER VIII

STRUCTURAL ENGINEERING PROPERTIES (4): MODULUS PROPERTIES

General

The modulus properties of the materials which make up flexible pavement layers are an indispensable part of most up-to-date structural pavement design techniques. In fact the most commonly used failure criteria in flexible pavement design are tensile strain in the stiffest layer and vertical compressive strain in the subgrade layer. These criteria are extremely sensitive to the respective modulus properties of the pavement layers. Thus the pavement engineer must not only seek an accurate estimate of the modulus but also the proper definition of modulus for the intended purpose.

Of course, viscoelastic materials such as SULPHLEX and asphalt concrete add another dimension of difficulty to the task of selecting the correct modulus. These materials have modulus properties which are affected by time (duration of loading) and temperature.

Van der Poel (97) has defined the modulus of asphalt cement as stiffness:

$$S(t,T) = \sigma/\epsilon$$

where t = time of loading and T = temperature.

Figure 71 is a simplified illustration of the time of loading dependency of idealized asphalt concrete at a selected temperature. It is easy to trace the change in behavior from an elastic response at short loading times, through a delayed elastic behavior zone and finally to a region where the stiffness is totally a function of the viscous properties of the binder. This representation is helpful in analyzing the creep stiffness data presented previously. Due to the time-temperature superposition properties of asphalt and SULPHLEX the abscissa in Figure 71 could be changed to temperature if stiffness were measured at a selected duration of loading.

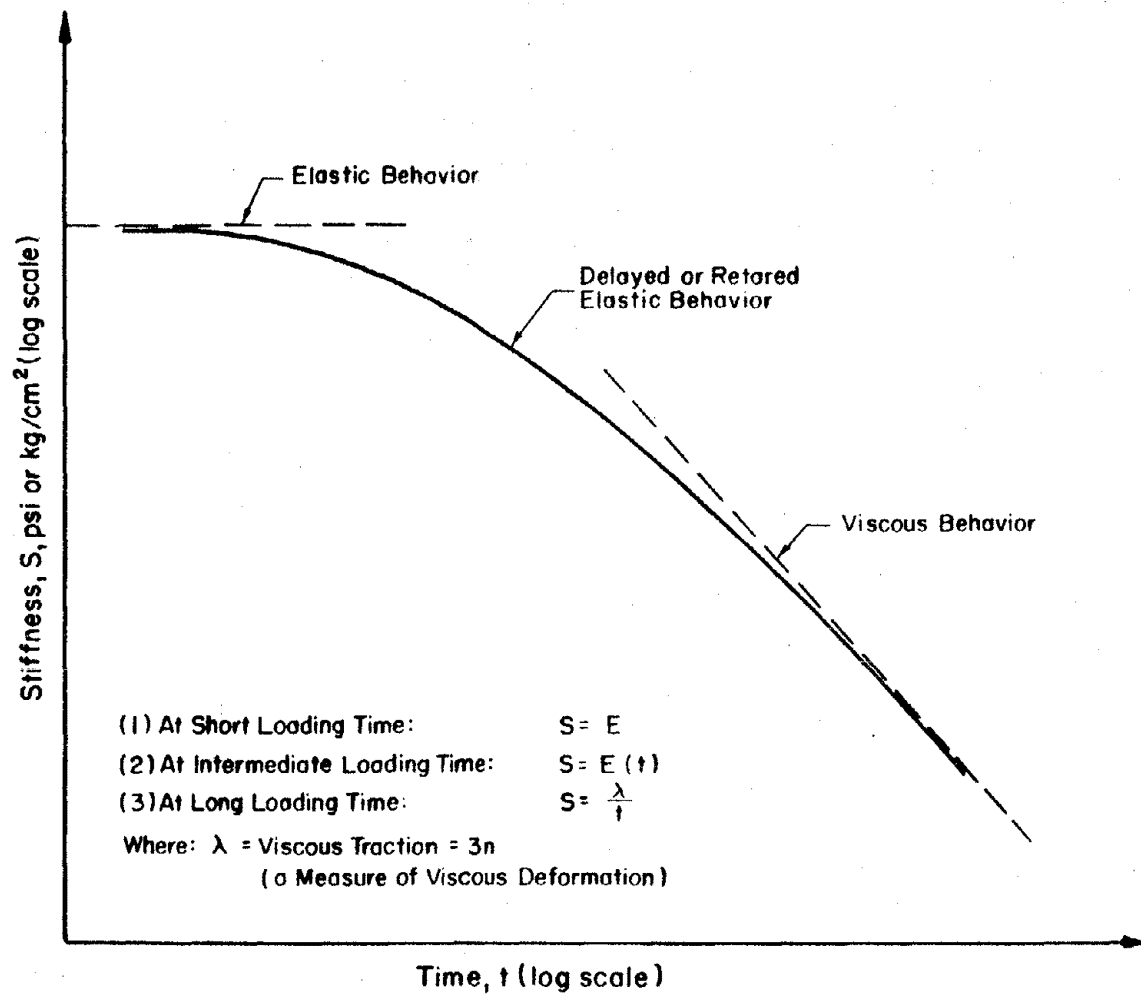


Figure 71. Simplified Illustration of Components of Stiffness: Elastic, Viscoelastic, and Viscous.

In this study the modulus properties of SULPHLEX were measured in five forms:

1. Resilient modulus, M_r .
2. Creep Stiffness.
3. Dynamic modulus, E^* .
4. Flexural modulus.
5. Relaxation modulus.

Resilient Modulus

The resilient moduli, defined as the ratio of induced stress to recoverable strain, were measured by the Mark IV device developed by Schmidt (10). The device applies a 0.1-second load pulse once every three seconds across the vertical diameter of a cylindrical specimen (Marshall type specimen) and senses by linear variable transformers the resultant deformation across the horizontal diameter. The shape of the load impulse is shown in Figure 72.

The resilient modulus was used throughout this research as a quality assurance measure. Resilient moduli data were recorded from aging studies, water susceptibility studies, and mixture design studies. The results of these data will be reported under the proper category. In this section laboratory mixtures prepared with binders CR1, CR2, CR3, CR5, 233A, AC-10 were aged for six days at 50°F and tested at four temperatures: -10, 32, 73, and 104°F. The 6-day cure period was selected based on an aging study which revealed that the resilient modulus does not appreciably change in the laboratory following six days of curing at 50°F.

In addition to the laboratory-molded specimens, field cores from a SULPHLEX demonstration project in San Antonio, Texas, (Loop 1604) were tested over the same temperature range. These data are plotted in Figure 73 and summarized in Table 37.

The resilient modulus versus temperature relationship is very similar for SULPHLEX binders CR1, CR2, CR3, and the field cores from Loop 1604, San Antonio, Texas. These cores were 2 months old at the date of testing.

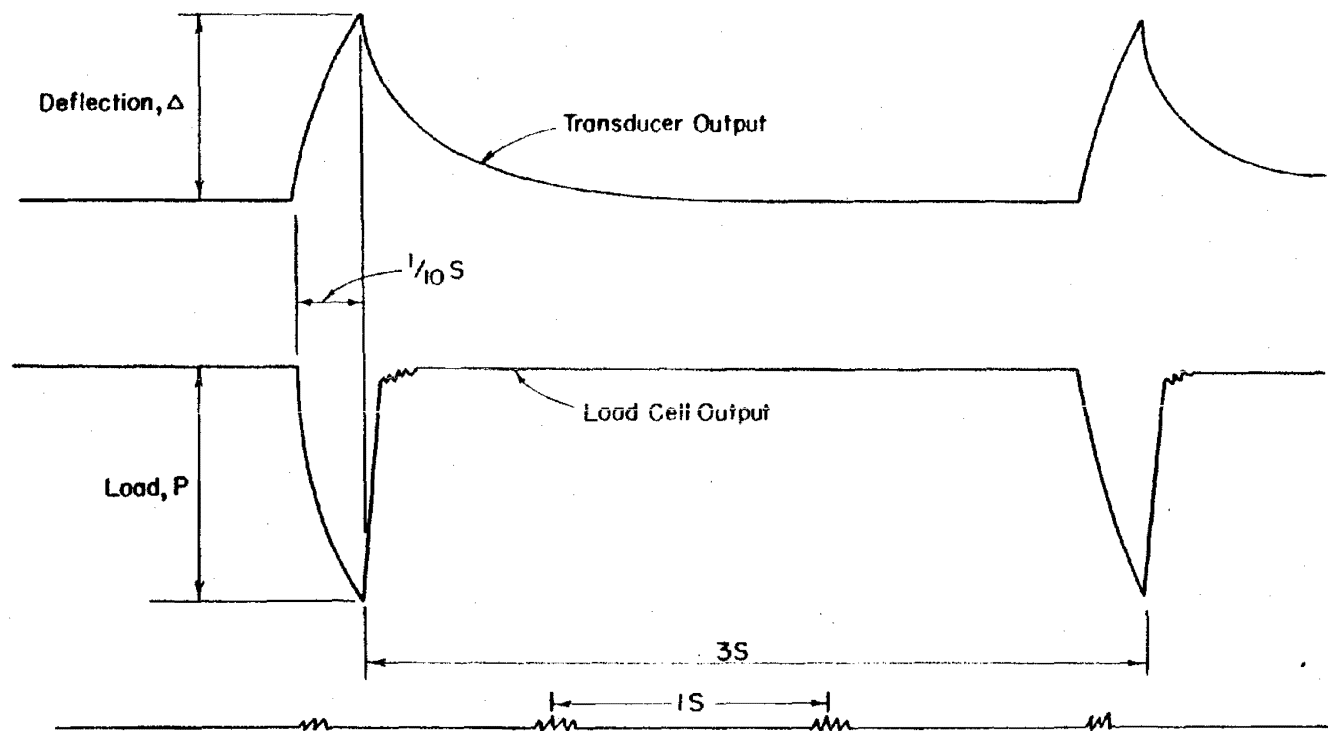


Figure 72. Load Pulse of the Resilient Modulus Device.

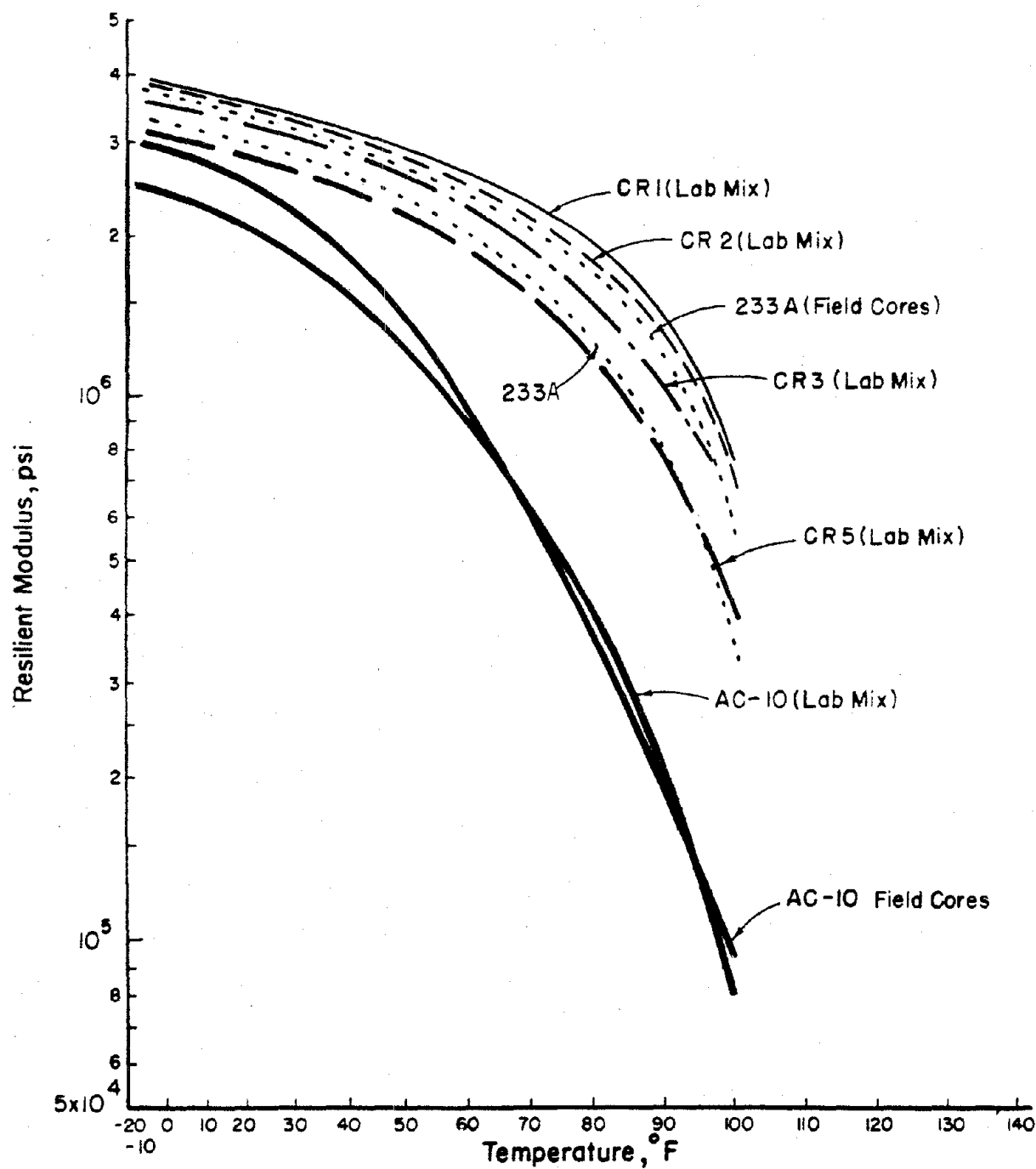


Figure 73. Resilient Moduli Versus Temperature for SULPHLEX and Asphalt Concrete Fabricated with Crushed Limestone.

Table 37. Summary of Resilient Moduli of SULPHLEX and Control Mixtures.

Binder	Aggregate	Type Mixture	Mean Resilient Modulus, psi x 10 ⁶			Number of Samples, n
			-10°F	73°F	104°F	
CR1	CLS	Lab	4.01	2.22	0.790	50
CR2	CLS	Lab	4.00	2.16	0.699	50
CR3	CLS	Lab	3.62	1.82	0.670	20
CR5	CLS	Lab	3.19	1.29	0.540	20
233	Basalt	Lab	3.29	1.50	0.300	9
233A	CLS	Field	3.81	2.01	0.710	20
AC-10	CLS	Lab	2.66	0.489	0.077	20
AC-10	Basalt	Lab	2.51	0.321	0.102	9
AC-20	CLS	Field	3.00	0.501	0.092	20

The mixtures with CR5 and the original 233A proved to have significantly lower resilient moduli than the other SULPHLEX binders across the test temperature range.

Both the laboratory mixture of AC-10 plus crushed limestone and the field cores from Loop 1604 of AC-20 and crushed limestone produced similar M_R versus temperature relationships. It is clear that the SULPHLEX mixtures are substantially stiffer across the temperature range. Obviously, resilient moduli will vary based on the effects of aggregate type, gradation, void content, etc.; but the unmistakable trend is that SULPHLEX mixtures under rapid load rates are much stiffer than asphalt concrete. However, SULPHLEX binders display a very definite temperature susceptibility and viscoelastic response.

Figure 73 indicates that the viscoelastic behavior of SULPHLEX actively begins at about 32°F. Below about 32°F the modulus is probably very nearly linearly elastic. However, the accuracy of diametral resilient moduli determinations at low temperatures (32°F) is poor (10). The resilient modulus data in Figure 73 coupled with creep stiffness data in Figures 54 through 57 indicates a dominating viscous response at high temperatures, perhaps above 100°F.

The argument has often been put forth that perhaps SULPHLEX layers should be designed as rigid pavement layers as they probably crystallize rapidly in the thin film arrangement found in mixtures, and they are probably very nearly linearly elastic in normal pavement conditions. However, the pronounced viscous effects at higher temperatures and longer loading rates and especially a combination of the two effects demands thoughtful consideration of the consequences of these effects in pavement design applications.

Creep Stiffness

The diametral resilient modulus is often subjected to criticism because of the light load used, the conditions of biaxial stressing and the rigid assumptions which must be closely adhered to, but are not, in order for the cylindrical, diametrically loaded specimen to respond elastically. In order to more precisely establish the modular

properties of SULPHLEX under different conditions of loading and different states of stress, other forms of moduli were computed.

Creep stiffness is simply the inverse of the creep compliance. For purposes of comparison creep stiffness was calculated at 0.1 seconds of load duration at 40°F, 70°F, and 100°F during the compressive creep test. The resulting values are tabulated in Table 38.

As expected these moduli do not closely agree with the resilient moduli. However, the same trends are evident as were established with resilient moduli data. These moduli are plotted in Figure 74.

Dynamic Modulus and Flexural Modulus

The dynamic moduli and flexural moduli are also presented in Table 38. The dynamic modulus is defined here as the ratio of stress applied during repeated load permanent deformation testing to the dynamic strain at the 200th load application. The flexural modulus is defined as the modulus of the flexural fatigue beams at the 200th load application. The modulus is more clearly defined as

$$E_{\text{flex.}} = \frac{Pa(3l^2 - 4a^2)}{48I\Delta}$$

where P is dynamic load applied to deflect the beam

a is 1/2(-4)

R is reaction span length

I is specimen moment of inertia

Δ is dynamic beam deflection at the center point

The dynamic moduli are plotted in Figure 75.

Relaxation Moduli

The relaxation modulus was measured by applying a compressive stress which induced an initial strain of 100 micro inches per inch in specimens 4 inches in diameter and 8 inches high. Strains were

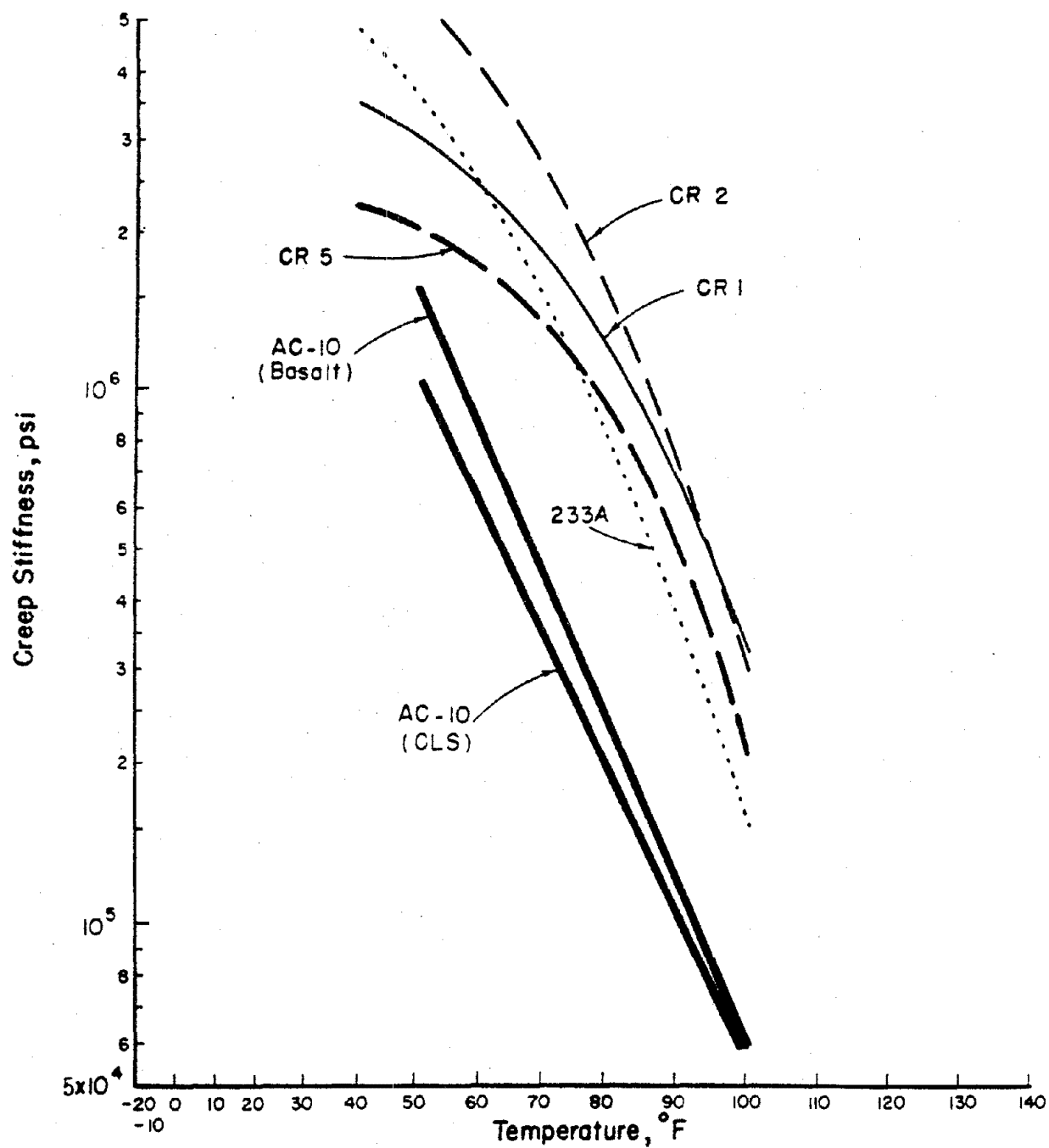


Figure 74. Creep Stiffness Versus Temperature for all Mixtures.

Table 38. Summary of Creep Stiffnesses, Dynamic Moduli and Flexural Moduli for all Mixtures.

Binder	Aggregate	Creep Stiffness, $\text{psi} \times 10^6$			Dynamic Modulus, $\text{psi} \times 10^6$			Flexural Modulus $\text{psi} \times 10^6$ 70°F
		40°F	70°F	100°F	40°F	70°F	100°F	
CR1	CLS	3.51*	1.90	0.320	4.00	2.69	0.290	0.350
CR2	CLS	8.00	2.90	0.300	4.76	2.22	0.495	0.675
CR5	CLS	2.20	1.30	0.210	2.75	1.30	0.190	0.330
233A	Basalt	5.00	2.00	0.150	4.00	1.02	0.200	-----
AC-10	CLS	1.10	0.310	0.060	2.10	0.397	0.086	0.056
AC-10	Basalt	1.50	0.400	0.059	2.50	0.700	0.090	-----

*Each value represents the mean of three data points.

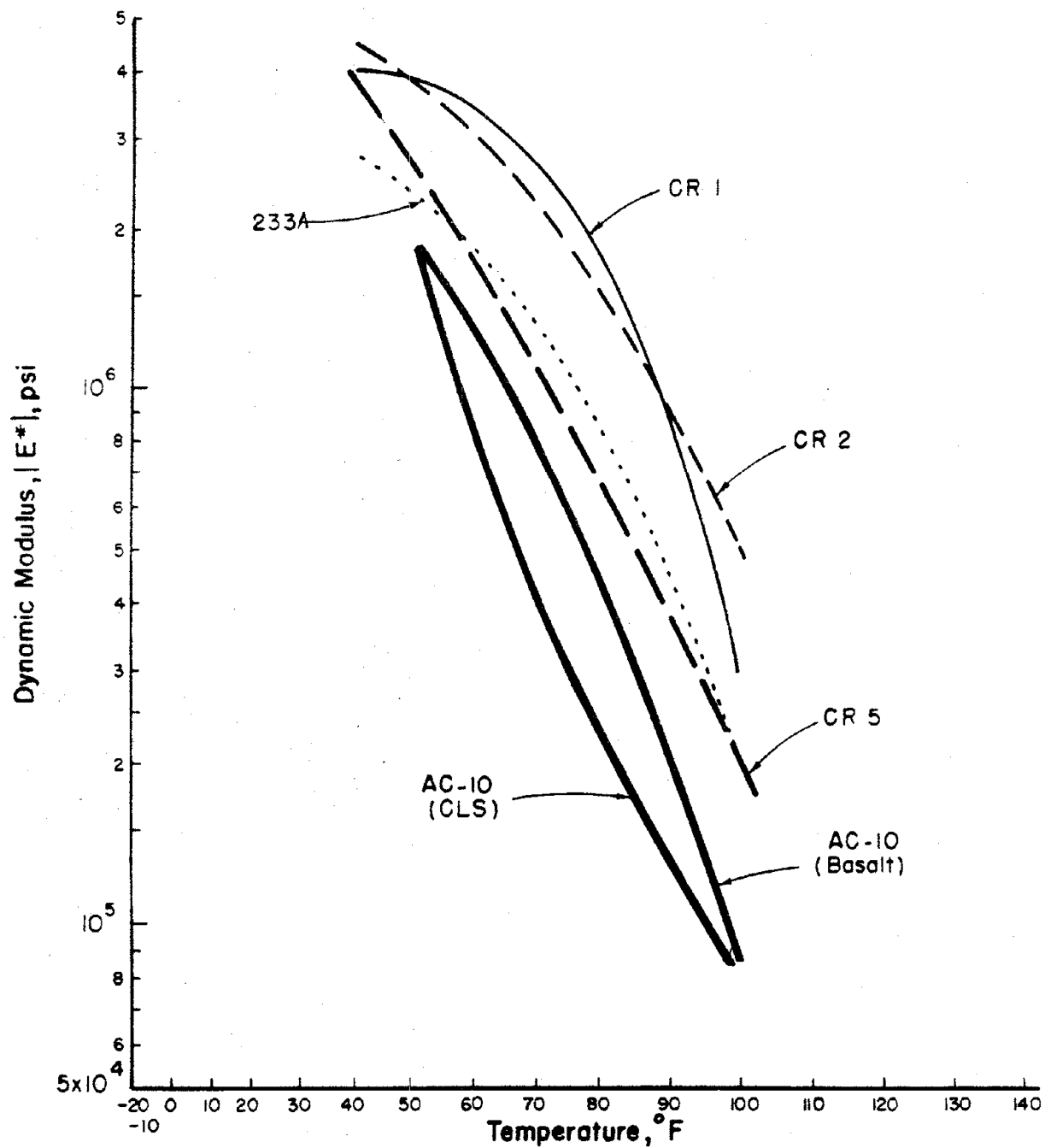


Figure 75. Dynamic Moduli Versus Temperature for all Mixtures.

measured with linear variable transformers. Strains were monitored across the middle four inches of the cylindrical specimens. The resulting relaxation moduli are presented in Table 39.

Summary of Modulus Properties

From this study of modulus properties the following conclusions are established:

1. SULPHLEX binders CR1, CR2, and CR3 generally exhibit very similar modulus properties over the temperature range that a typical pavement is expected to experience.
2. Although substantially stiffer than asphalt concrete over the normal pavement temperature range, all SULPHLEX binders exhibit well-defined viscoelastic response above the T_g as well as a dominant viscous response at higher temperatures. These properties must be accounted for in structural pavement design considerations.
3. Binder CR5 is significantly softer than other SULPHLEX binders across the temperature range to which pavements are normally subjected.
4. Resilient moduli, stiffness moduli, dynamic moduli, flexural moduli, and relaxation moduli were evaluated for each binder and the conclusions stated above consistently substantiated by each of the moduli versus temperature data.

Table 39. Relaxation Moduli at 73°F, 0.1 Second Load Duration
for SULPHLEX and Control (Asphalt Concrete) Samples.
(All Specimens Contain Crushed Limestone Aggregates).

Relaxation Modulus, psi x 10 ⁶			
Binder	Mean Value	Standard Deviation	Number of Samples
CR1	1.129	0.180	3
CR2	0.637	0.010	3
CR3	1.449	0.023	3
CR5	0.557	0.158	3
AC-10	0.433	0.095	3

CHAPTER IX MOISTURE DAMAGE AND THERMAL AGING

Moisture Damage of SULPHLEX Mixtures

Background

Lentz and Harrigan (21) performed a detailed water damage study on SULPHLEX 233 and an asphalt concrete control mixture. In summary Lentz and Harrigan state that although acceptable mixtures of SULPHLEX can be obtained, with respect to Marshall criteria, at the same weight percentage of SULPHLEX as asphalt, a higher binder content may be required to provide resistance to moisture damage. Furthermore, the addition of antistripping agents, such as hydrated lime or tall oil, was found to increase the retained strength of SULPHLEX mixtures substantially.

The objectives of this study were to: (1) evaluate the moisture damage susceptibility of SULPHLEX binders CR1, CR2, CR3, and CR5 as compared to the asphalt concrete control mixture; (2) be able to recommend steps to be taken in the mixture design process to reduce moisture damage susceptibility to an acceptable level, if possible, and (3) be able to predict the effects of moisture damage on the engineering properties of SULPHLEX.

Basic Mechanisms

Lee (98) points out that two basic mechanisms of moisture damage on asphalt mixture exist: stripping and softening. Stripping is the loss of adhesion between the binder and the aggregate surface caused primarily by the action of water or water vapor. Softening is a general loss of stability of a mixture that is caused by a low level of cohesion due to the action of moisture within the binder or binder matrix.

Moisture-induced damage produces several forms of distress in a pavement such as shoving, rutting, or bleeding.

It is generally assumed that moisture damage will not occur without some level of stripping or deterioration of the aggregate-binder bond. No single stripping mechanism has been accepted, and it is unlikely that a single mechanism produces stripping even under controlled conditions. Stripping is likely to be due to the interaction of a number of mechanisms including:

1. Displacement.
2. Detachment.
3. Chemical debonding.
4. Blistering and pitting.
5. Emulsion formation.
6. Pore pressure.

Numerous attempts at developing tests which can aid the engineer in identifying asphalt concrete mixtures that are susceptible to moisture damage have been made. These procedures include:

1. ASTM D 1664 Stripping Test.
2. California Swell Test.
3. Texas Film Stripping Test.
4. Texas Freeze-Thaw Pedestal Test.
5. Boiling Test.
6. Thin-Film Chromatography.
7. Compression Strength Test on Dry and Wet Specimens.
8. Indirect Tensile Test on Dry and Wet Specimens.

Although the stripping tests based on amounts of aggregate surface successfully coated or visual observations are quite valuable, the compression test before and following moisture conditioning and the indirect tension test before and following moisture conditioning were selected for this study. These test methods were selected for three reasons. First, Region 15 of FHWA uses the immersion-compression test method (ASTM D 1075 or AASHTO T165) in their mixture design procedures. Second, Lottman (16, 17) in his extensive studies on moisture damage suggests a strength analysis before and following moisture conditioning. Finally, the effect of moisture damage on the engineering response of SULPHLEX and asphalt concrete mixtures is the

primary impetus of this work. This effect can best be measured by a change in stiffness, softening, or loss of strength of the mixture due to moisture conditioning.

Testing Approach

Figure 76 illustrates the laboratory procedures used to establish the moisture susceptibility of the SULPHLEX mixtures. Leg 1 was performed in accordance with AASHTO T165 (ASTM D 1075).

Leg 2 specimens were tested in indirect tension following a one-cycle Lottman procedure and the resilient moduli were recorded prior to and following the one-cycle Lottman procedure. The Lottman procedure is explained in detail in Appendix A of Reference 17.

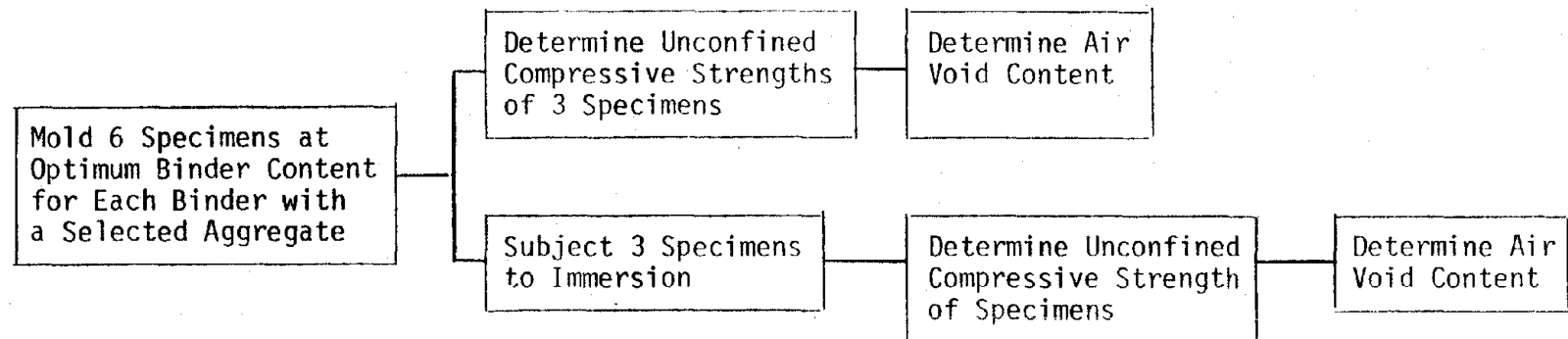
Leg 3 specimens were prepared and tested in accordance with ASTM D 1559, Test for Resistance to Plastic Flow of Bituminous Mixtures Using the Marshall Apparatus. The accelerated Lottman conditioning was performed in accordance with Appendix A of Reference 17.

Leg 4 specimens were fabricated and tested in accordance with the VESYS IIM User's Manual procedure.

In general, crushed limestone was used as the aggregate for each mixture. However, in Leg 3, the effects of a second aggregate, a silicious river gravel, were tested. In Leg 1, the effects of hydrated lime and tall oil as antistripping agents were observed. Lentz and Harrigan (21) performed a more thorough study of the effects of antistripping agents on the moisture damage potential of SULPHLEX.

Based on the test procedures discussed in the preceding paragraphs, the objective of this research was to evaluate the relative potential of SULPHLEX mixtures to sustain softening or weakening due to moisture damage. A prediction of the effects of moisture damage on the performance life of SULPHLEX layers in pavements is beyond the scope of this study.

Leg 1: Moisture Effects on Unconfined Compressive Strength.



Leg 2: Moisture Effects on Indirect Tensile Strength and Resilient Modulus.

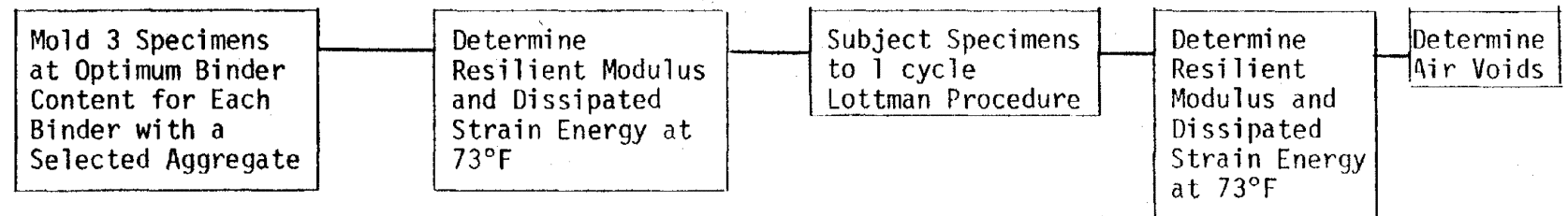
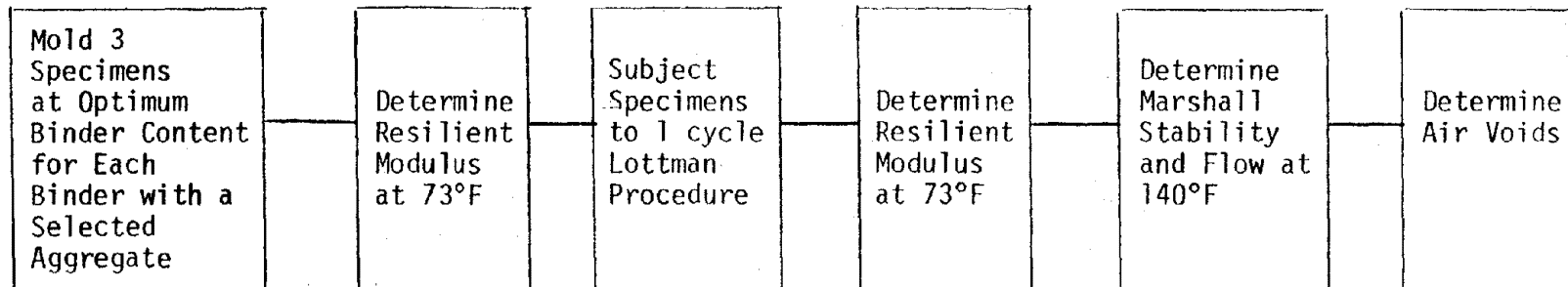


Figure 76. Sequence of Testing for Moisture Effects.

Leg 3: Moisture Effects on Marshall Stability and Resilient Modulus.



Leg 4: Moisture Effects on Creep Compliance.

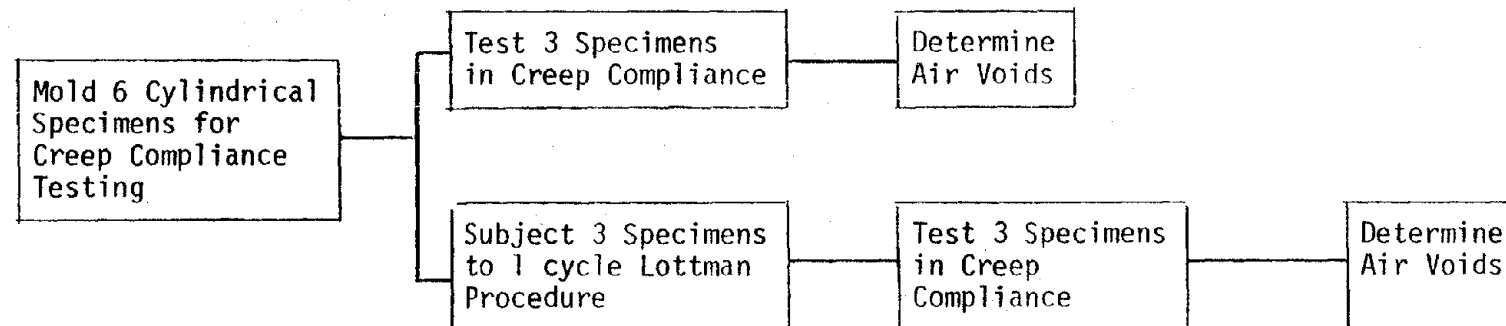


Figure 76. Sequence of Testing for Moisture Effects (continued).

Results

Table 40 presents the results of Leg 1 of the moisture effects study. Dry strengths of the SULPHLEX mixtures were greater than those of the control asphalt concrete mixtures. Both the control mixtures and the SULPHLEX mixtures are dense, high stability mixtures and are expected to develop relatively high compressive strengths as shown in Table 40. Compressive strengths following moisture conditioning (AASHTO T165) for untreated SULPHLEX vary greatly but are, except for binder CR3, generally lower than the wet compressive strength for the asphalt mixtures. A striking difference between asphalt and SULPHLEX mixtures exists in the percent of retained strength following moisture conditioning. All SULPHLEX binders fall short of the 70 percent level normally considered an acceptable residual strength when the optimum binder content is used in the mixture. (See Chapter III).

The effects of binder content variation and additives were partially evaluated in Leg 1 of this study. When the SULPHLEX mixtures were fabricated at equal percentages of binder by weight as compared to asphalt, dry compressive strengths were high but wet strengths were drastically reduced, and percentages of retained strength fell below 10 percent. This establishes the importance of the equal volume concept in mixture design despite the fact that adequate stabilities of SULPHLEX mixtures can be achieved at lower, equal on the basis of weight of asphalt binder, percentages.

The effects of two antistripping additives were partially evaluated. It has been hypothesized that the nonpolarity of SULPHLEX may present a problem in terms of its ability to adhere to aggregate surfaces in the presence of moisture and heat. To improve the adhesion between binder and the aggregate, the aggregate surface may be coated with an agent that will reverse the predominant electrical charges and reduce the surface energy of the aggregate. A second, more practical approach is to reduce the surface tension of the binder, and at the same time, give the binder an electrical charge opposite to that of the aggregate surface. These chemical

Table 40. Effect of Moisture Damage of Unconfined Compressive Strength.

Binder	Compressive Strength, psi @ 77°F			
	As Molded Percent Air Voids	Dry	Wet*	Percent Retained Strength
CR1**	5	1,232	310	25
	(1 of 3 specimens fell apart in Lottman cycle)			
CR1	8	800	50	6
CR1 + 1/2% Hydrated Lime	6	969	650	67
CR2	6	650	320	49
CR2	8***	600	60	10
CR2 + 1/2% Tall Oil	6	610	400	66
CR3	4	1,075	650	60
CR5	6	605	305	50
CR5 + 1/2% Tall Oil	4	810	690	85
AC-10	6	530	395	74

* 24 hours immersion in 140°F water followed by 2 hours immersion in 77°F water.

** Each data point is the average of 3 specimens - all specimens fabricated at optimum binder content unless otherwise noted.

*** Fabricated with same weight percent binder as the asphalt mixture.

antistripping additives act as surfactants to reduce the surface tension and allow the asphalt in the presence of mechanical agitation to more evenly coat the aggregate particles.

Hydrated lime has been used successfully in the past as an antistripping agent. Hydrated lime is a strongly alkaline substance that has great neutralizing power. The calcium from the lime replaces lower valence and smaller cations on the surface of the aggregate. This results in a calcium-rich surface of the aggregate. This calcium-rich surface may react with long chain organic acids to form water resistant surfaces (98). Amines, diamines and tall oil showed good potential in terms of retained unconfined compressive strength for SULPHLEX mixtures in the Lentz and Harrigan study (21).

As shown in Table 40, both tall oil and hydrated lime when used at 1/2 weight percent of total aggregate greatly increased the retained unconfined compressive strengths of CR1, CR2, and CR5 mixtures. Tall oil was added to the aggregate prior to mixing.

On the basis of Leg 1 of this study, moisture resistant mixtures of SULPHLEX can only be obtained by using a high enough binder content to reduce voids to the normally acceptable level of three to five percent. This apparently requires at least an equal volume percentage of SULPHLEX as would be required for asphalt. An antistripping agent is suggested based on this research and that done by Lentz and Harrigan (21). Further research with various aggregate types will be required to establish the moisture susceptibility of SULPHLEX mixtures.

Leg 2 of the moisture effects study uses the accelerated Lottman conditioning procedure described in detail in Appendix A of Reference 17. In the Lottman procedure, internal pressures in the mixture are produced by vacuum saturation followed by a freeze and warm-water soaking cycle. This procedure was selected as it has been identified by a National Cooperative Highway Research Program (16, 17) as being an excellent predictor of moisture damage susceptibility. This was based on a five-year study which monitored the performance of eight pavement sections following the characterization of their moisture damage potential by the Lottman procedure.

Lottman (17) describes a detailed test procedure for which a short-term and long-term damage index is computed. The damage index is a ratio of pre-conditioning to post-conditioning indirect tensile strengths or resilient moduli. In the case of the short-term factor the objective is to produce a saturated specimen which will simulate saturation in the field. A vacuum saturation procedure is used to produce this condition. The long-term factor is supposed to represent an "ultimate" damage condition. The Lottman accelerated procedure is used, in this case, in the conditioning process.

The tests results summarized in Table 41 are for mixtures using the crushed limestone aggregate. In each case the mixture was subjected to the most deleterious, long-term type moisture conditioning. It is curious that very little loss of structural capability is reflected in the comparison of before and after resilient moduli (the ratios of residual to before moisture conditioning resilient moduli ranged from 76 to 92 percent). On the other hand, the residual tensile strengths are quite low for all SULPHLEX mixtures. From extensive previous indirect tensile testing at 77°F and, 0.02 inches per minute stroke rate, the approximate level of retained strength following moisture conditioning was from 5 to 10 percent for the SULPHLEX mixtures and about 25 percent for the control mixture.

In Leg 3 of the moisture effects study, seven day soaking was used in lieu of either vacuum saturation or the accelerated Lottman procedure. The effects of aggregate type (river gravel and crushed limestone) and percent air voids were partially evaluated. The results, Table 42, reflect a substantial deterioration in structural response as reflected by the resilient modulus for the CR1 - crushed limestone mixture. Air void contents ranged from 4.1 to 7.2 percent. On the other hand, the retained moduli for the CR1 - river gravel mixtures were very high, probably due to the very low air void content of these mixtures and the consequent inability of the specimens to imbibe water during the 7-day soak period. The same aggregate effect on the resilient moduli results was seen in the asphalt concrete data.

Table 41. Effects of One Cycle Lottman Conditioning on Mixtures of SULPHLEX and Asphalt Cement (Control) with Crushed Limestone.*

Binder	Percent Air Voids	Before Lottman Conditioning		After Lottman Conditioning		Indirect Tensile Test* After Lottman Conditioning	
		M_R @ 73°F, psi	DSE* psi in/in	M_R @ 73°F, psi	DSE*, psi in/in	σ_{ult} , psi	ϵ_{ult} , in/in
CR1	6	1,630,000	27.8	1,460,000	49.0	55	0.00529
CR2	7	1,200,000	92.3	1,320,000	62.3	42	0.00509
CR3	6	1,590,000	19.0	1,210,000	82.4	33	0.00760
CR5	6	1,550,000	32.9	1,340,000	74.3	49	0.00472
AC Control	6	810,000	150.4	610,000	244.9	55	0.00506

Each data point is the average of three specimens - all specimens fabricated at optimum binder content.

* @ 77°F and 0.02 in/min stroke rate.

** DSE - Disipated strain energy.

Table 42. Effect of 7 - Day Soak on Mixtures of SULPHLEX and Asphalt Cement (Control) and Crushed Limestone.

Before Soaking				After Soaking		
Binder	Aggregate	Percent Air Voids	M _R @ 73°F, psi	M _R @ 73°F, psi	Marshall Stability, lbs	Flow 1/100 in
CR1*	Crushed Limestone	7	1,400,000	165,000	1,000	24
CR1	Crushed Limestone	4	1,960,000	189,000	1,200	27
CR1	River Gravel	3	1,510,000	1,128,000	1,400	19
CR1	River Gravel	2	1,550,000	1,630,000	1,500	18
AC-10	Crushed Limestone	6	275,000	102,000	1,500	15
AC-10	Crushed Limestone	4	495,000	241,000	2,000	14
AC-10	River Gravel	3	252,000	200,000	400	14
AC-10	River Gravel	1	410,000	521,000	1,000	12

* Each data point is the average of 3 specimens - all specimens fabricated at optimum binder content.

The Marshall stability and flow data following the 7-day soak are indicative of substantial strength loss for all SULPHLEX specimens, without regard to the effect of the type of aggregate. Based on the results of extensive Marshall stability testing previously in this study on specimens fabricated in an identical manner, a stability loss of approximately 50 percent occurred. Although Marshall Stability testing showed substantial strength losses for all aggregates tested, i.e., river gravel and crushed limestone, the average strength loss for the crushed limestone mixtures was again statistically significantly greater than for the river gravel mixtures. This was in part due to the lower air void contents of the river gravel mixtures.

On the basis of the results of Legs 1 through 3, it is apparent that SULPHLEX is substantially more susceptible to moisture effects than asphalt; and that a tight, low air void content mixture is required for acceptable performance with respect to moisture susceptibility. The resilient modulus is questionable in its ability to monitor moisture deterioration effects alone. A strength test such as the indirect tensile test, compression test or Marshall stability test is necessary in addition.

A very recent study (99) and some current and ongoing research (100) indicate that a deleterious reaction may occur between sulfur, polysulfides, and calcium. It has been hypothesized that a water soluble precipitate (calcium sulfate) may be produced by this reaction. If such a reaction is verified by further research, the use of SULPHLEX with limestone aggregate and especially with hydrated lime (as an antistripping agent) will require an extended evaluation.

Effects of Aging on SULPHLEX Mixtures

Background

Durability of paving mixtures is defined as their resistance to weathering and to the abrasive action of traffic (20). Included under the effects of weathering are changes in the characteristics of

asphalt due to any or all of the following factors: (1) oxidation, (2) volatilization, (3) polymerization, (4) thixotropy, (5) separation and (6) syneresis. In addition, one must consider the changes in the mixture due to the action of water. The effects of water action have been discussed with respect to the way they alter the engineering properties of SULPHLEX. This chapter deals with the effects of aging due to elevated temperatures.

A detailed explanation of the thermal stability of SULPHLEX is presented in a companion report from this study (1). Briefly summarized, the thermal stability study revealed that substantial changes in mixture properties occur when the SULPHLEX binder exists in a thin film. Loss of volatiles and changes in rheological properties can be determined and used as a measure of the reproducibility of the preparation of SULPHLEX. SULPHLEXES are quite sensitive to thermal exposure and vary in sensitivity among different lots.

Ludwig et al. (101) reported 4- to 5-percent weight losses in thin film oven testing for four SULPHLEXES; 230, 126, 233, and 433; compared with no loss for AC-20 asphalt. As a consequence Matrecon, Inc. undertook two series of tests:

1. Rolling thin film oven tests and
2. Hot oven storage of SULPHLEX in cans.

The results of the rolling thin film oven test confirmed those of Ludwig et al. with respect to the volatile loss and also showed the significant hardening of SULPHLEX that occurs during exposure of thin films to high temperature. The results also indicated a significantly lower volatility of SULPHLEX prepared at lower temperatures, i.e., 302°F, compared with that prepared at higher temperatures, i.e., 338°F.

In a second series of tests, Matrecon, Inc. exposed small cans of SULPHLEX 233 to elevated temperatures to determine the effect on its properties. Most tests were conducted at 275°F since this is a common storage and handling temperature for asphalt binders.

In order to simulate tank storage at 275°F, samples of SULPHLEX in covered, but unsealed, containers were aged in an oven for 42 days and the changes in penetration, viscosity, and density were monitored. The

results revealed substantial increases in viscosity and decreases in penetration. The conclusion was that SULPHLEX cannot be routinely stored at 275°F as can be done with conventional asphalts.

In order to eliminate any effects of oxygen on thermal stability, SULPHLEX was also aged at 275°F under an inert gas atmosphere (nitrogen). The resulting viscosity increase in the nitrogen atmosphere was greater than that which occurred with the samples exposed to air. The data from both exposures suggest degradation may be inhibited by the oxygen in the air.

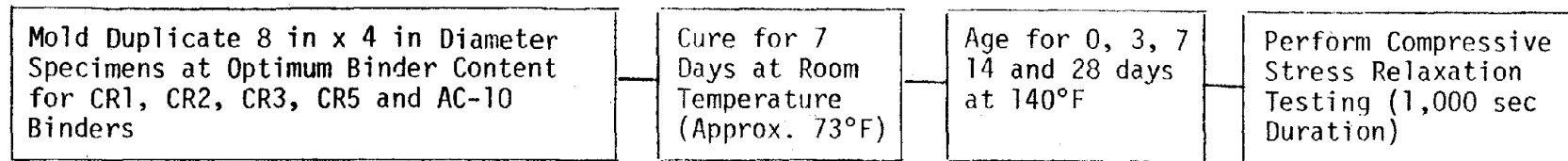
An analysis of the residue of the SULPHLEXES following storage at 275°F revealed that residues contained more sulfur than the initial changes. The calculated average sulfur contents of the total volatiles were in the range of 35 to 45 percent. Approximately 17 percent of the volatile loss consisted of hydrogen sulfide while the remainder of the recoverable volatile fraction consisted of a liquid fraction of which approximately 84 percent was carbon, 10 percent was hydrogen and 1.5 percent was sulfur.

This background information makes it imperative to consider the thermal stability or elevated temperature aging of SULPHLEX mixtures in this study.

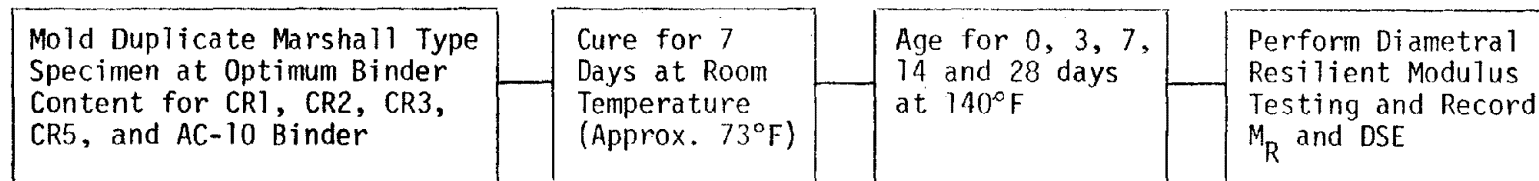
Research Approach

Ideally preparation of laboratory mixtures of SULPHLEX or asphalt concrete simulate the operation of a hot mix plant and thus simulate the aging which will occur in the binder of a mixture subjected to hot mix plant action. Perhaps the most severe, realistic temperature that a mixture will be subjected to in the field is 140°F. This represents a high nominal summer day pavement temperature. Thus, laboratory mixtures subjected to aging at 140°F following conventional fabrication techniques, should resemble the worst conditions of thermal aging that may normally occur in situ. All mixtures in this study, consequently, were aged at 140°F following molding for varying periods of time. Figure 77 illustrates the testing sequence.

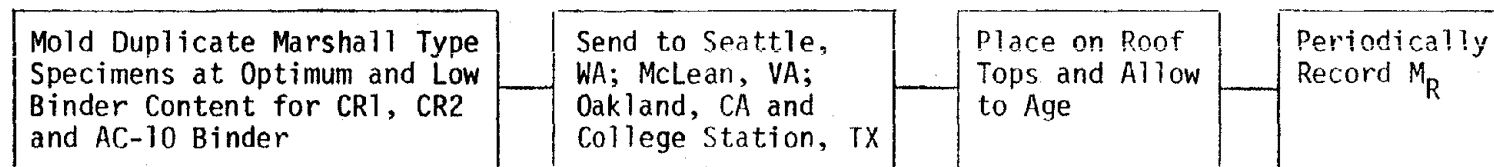
Leg 1: Stress Relaxation Testing.



Leg 2: M_R and DSE Testing.



Leg 3: In Situ Aging of Lab Molded Specimens.



Leg 4: Loop 1604 Field Core Structure.

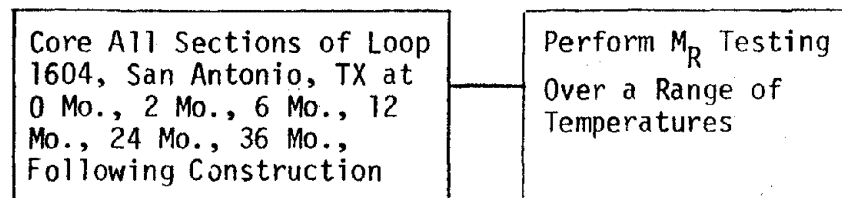


Figure 77. Evaluation of Changes in Material Response with Aging.

Effect of Aging on Stress Relaxation Modulus

The compressive stress relaxation modulus was used as an index of aging for the mixtures of SULPHLEX. Specimens eight inches in height and four inches in diameter were fabricated in accordance with fabrication instructions for creep compliance specimens for asphalt concrete in the VESYS IIM User's Manual (12).

The specimens were then subjected to a constant strain, 100 micro inches per inch, for a period of 1000 seconds. The decay in stress was recorded on an MTS servohydraulic system. Stress relaxation tests for all mixtures were performed at 0, 3, 7, 14, and 28 days. Two replicates were tested for each mixture.

Initially it was hoped that the Maxwell model could be used to approximate the relaxation of the specimens in question. The idea was to compute the relaxation time for each experiment and compare the relaxation times as an index of aging. This idea was abandoned for several reasons. One was that the relaxation time for most of the experiments turned out to be very small and insensitive to the phenomenon which we wished to test. Second, the Maxwell model is no doubt too simple to explain SULPHLEX or asphalt concrete stress relaxation.

As an alternative to the relaxation time, the stress relaxation modulus versus time for each condition of testing was computed. Therefore, a stress relaxation modulus versus time of loading plot was developed for each mixture of binder (SULPHLEX or asphalt) and crushed limestone aggregate. The relative shift in the relaxation modulus curve was then used as the index of comparative aging, a simple but quite revealing approach.

Effect of Aging on Strain Energy and Resilient Modulus

A second approach used to monitor the aging of the mixtures of SULPHLEX and the control mixture of asphalt concrete was the change in resilient modulus with aging. As has been discussed, the resilient modulus is measured using the Schimdt device, Mark IV, (10). This

device was modified so that a trace of the load versus deformation response could actually be recorded. The modification of the Mark IV device was not a trivial task as considerable effort was required to eliminate the "noise" and record meaningful responses. Figure 78 presents a typical load versus deformation response which exemplifies the type of plot used to determine the dissipated strain energy.

The "hysteresis loop", which is the shaded portion of the plot in Figure 78, is the point of interest. The "hysteresis loop" is considered to represent a dissipation of energy as heat in the stress-strain cycle. Very close to a crack tip the presence of mechanical hysteresis will undoubtedly affect the propagation of the crack. Of course hysteresis can result from plastic as well as viscous deformations. However, based on the low stress level applied to the specimens tested in this manner, approximately 10 psi, and due to the long recovery period between test periods, it is believed that the hysteresis loop is due to recoverable viscoelastic responses. The Mark IV resilient modulus device is highly repeatable. One load pulse is generated approximately three seconds following the previous pulse. These three seconds represent thirty times the time of loading applied to the sample. During the monitoring of the resilient modulus test it is evident that the plastic, nonrecoverable, deformation decreases greatly after about 30 to 40 cycles. In fact, the magnitude of plastic deformation after this point becomes so small as to be considered unimportant. At this point the "hysteresis loop" is continually retraced with each loading cycle. Thus the recoverable deformation is somewhat arbitrarily defined because of the time of recovery allowed by the test apparatus and because of the test temperature, always 73°F. However, since these variables are held constant for each test, a relative value of dissipated strain energy due to viscoelastic, recoverable deformations can be determined.

The dissipation of energy in this manner would hypothetically be beneficial from a fracture standpoint as the elastic stored energy, needed to drive the crack, due to a loading cycle, would be correspondingly reduced. Furthermore, as aging leads to brittle pavements susceptible to cracking, the ability to maintain a

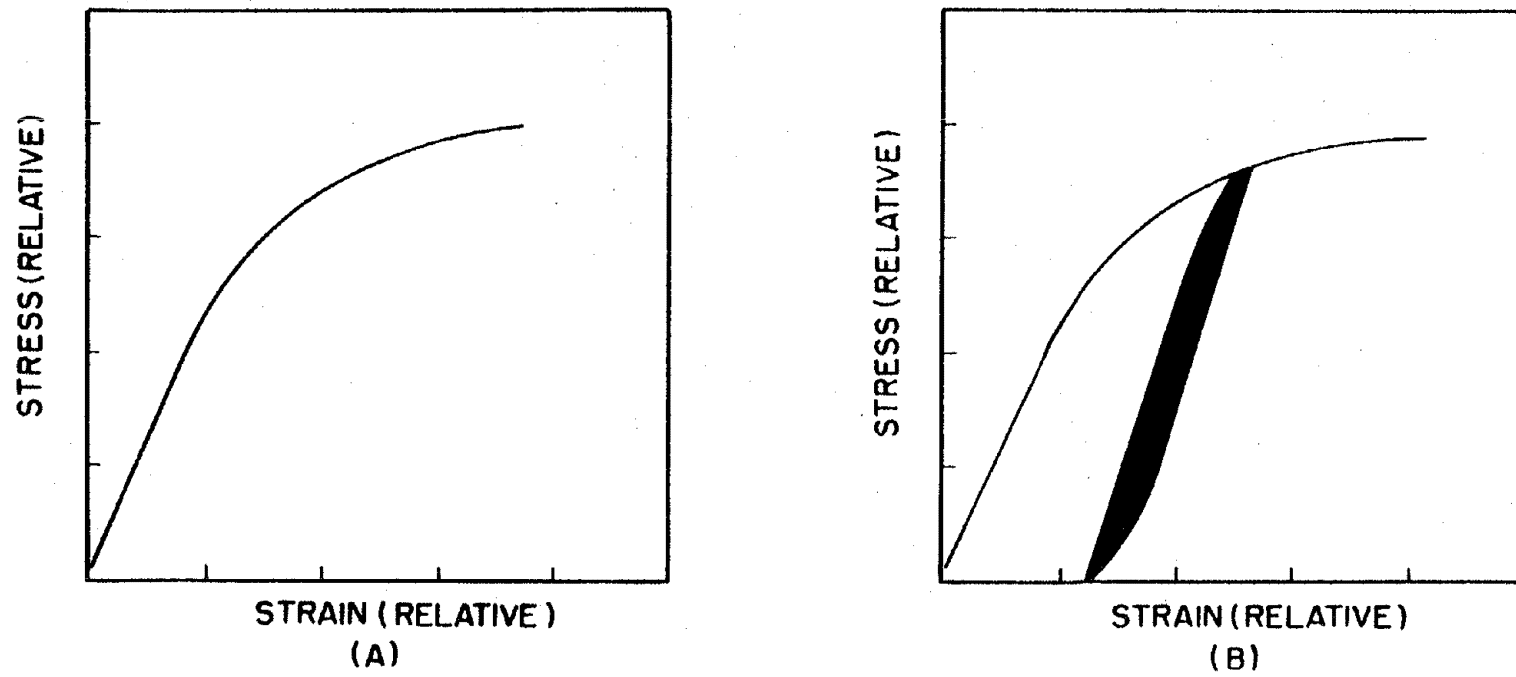


Figure 78. Hysteresis Loop and the Dissipated Strain Energy Concept.

"hysteresis loop" of this type with aging would seem to be an indicator of low aging potential while rapid loss of the "hysteresis loop" coupled with an increase in resilient modulus represents embrittlement and susceptibility to aging.

Materials Subjected to In Situ Aging

Specimens were prepared for resilient modulus testing in January of 1982 and shipped to Seattle, Washington; Mclean, Virginia, and Oakland, California. In addition, a set of specimens were retained in College Station, Texas. These specimens were placed in the unguarded environment at these locations and allowed to age for two years. The resilient modulus was recorded periodically for each specimen. A total of six specimens were sent to each location: one specimen each of CR1 and CR2 at six percent binder, CR1 and CR2 at eight percent binder and asphalt concrete at four and six percent binder. The objective of this evaluation was to determine the comparative aging of the two binders in the various environments.

Loop 1604 around the city of San Antonio, Texas, was overlaid with one inch of SULPHLEX in August 1980. This overlay was periodically cored, and the cores were tested at Texas A&M. Not only were the SULPHLEX sections (which consisted of SULPHLEX 233A and crushed limestone) cored but also the control section consisting of AC-20 and crushed limestone. Varying percentages of all binders were used in the Loop 1604 project. Sections containing each percentage of binder were cored and tested at Texas A&M providing valuable information on the comparative aging of SULPHLEX in actual environments.

Results of Stress Relaxation Analysis

From Figure 79 through 83 it is apparent that:

1. The relaxation moduli of asphalt concrete (AC-10 and crushed limestone) are an order of magnitude less than those of the

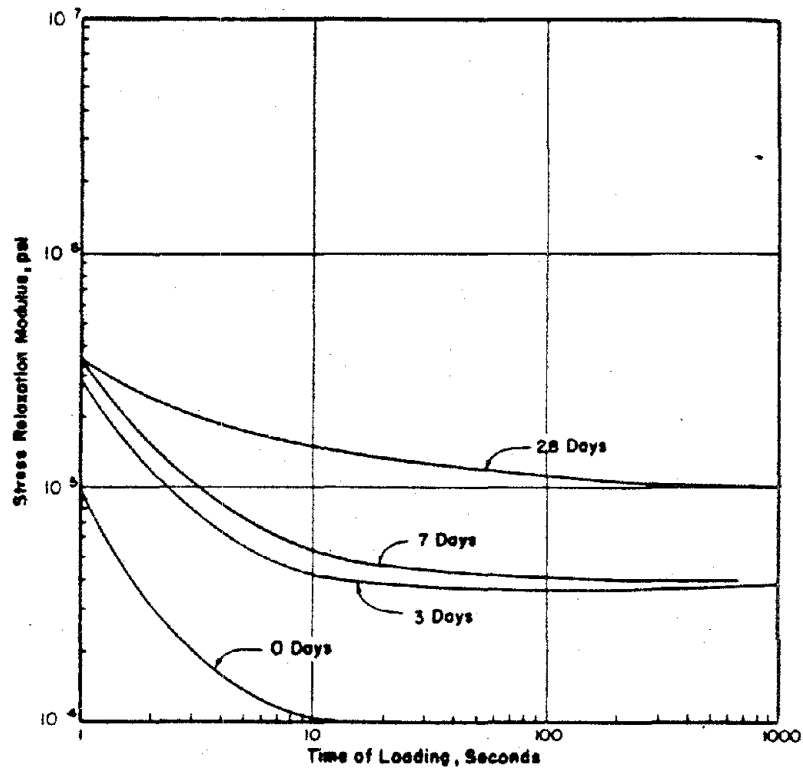


Figure 79. Effects of Aging at 140°F on the Compressive Stress Relaxation Modulus Versus Duration of Loading for AC-10 - Crushed Limestone Mixtures.

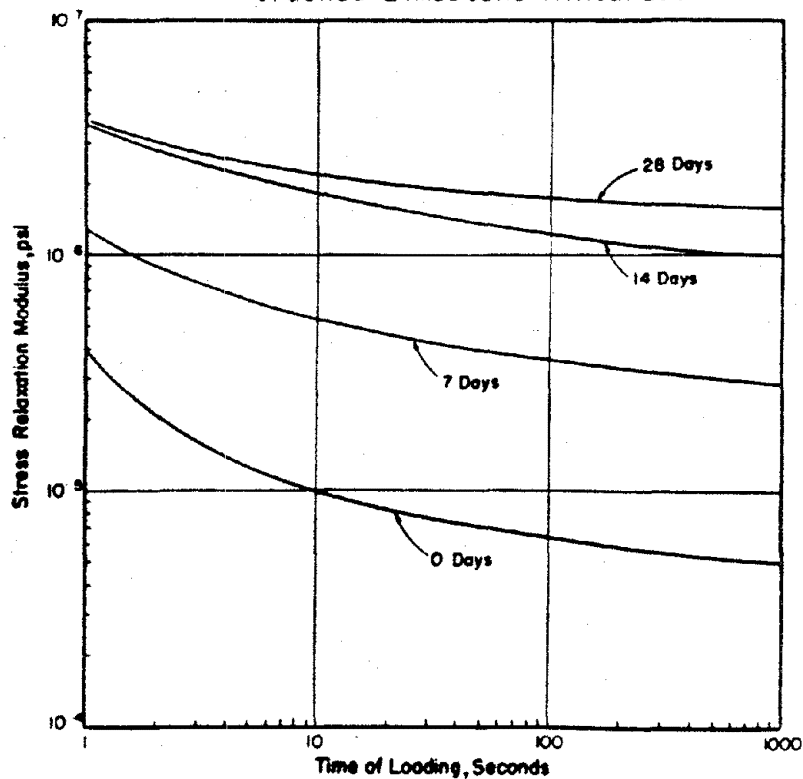


Figure 80. Effects of Aging at 140°F on the Compressive Stress Relaxation Modulus Versus Duration of Loading for CR1 - Crushed Limestone Mixtures.

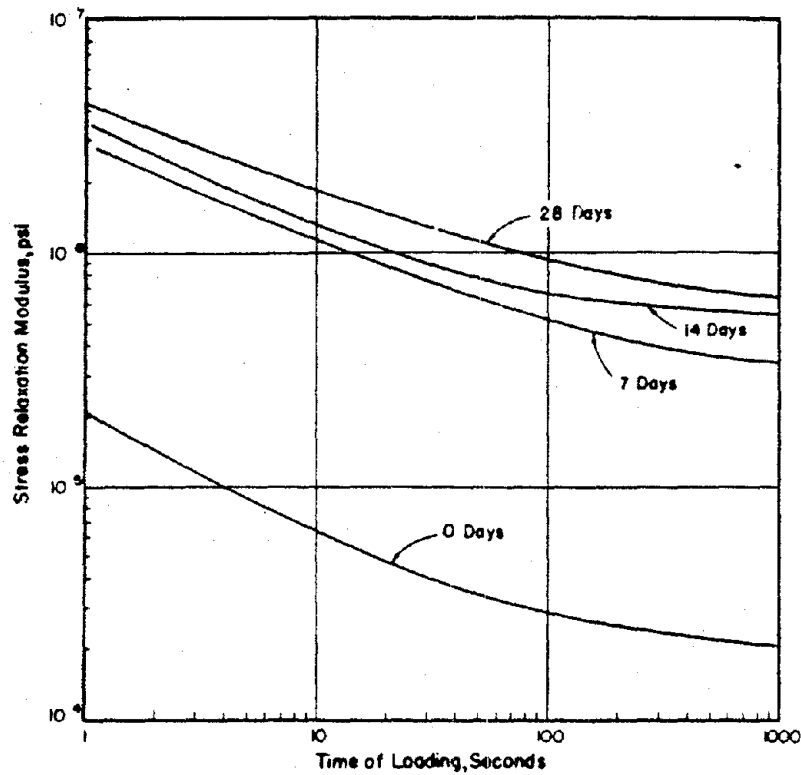


Figure 81. Effects of Aging at 140°F on the Compressive Stress Relaxation Modulus Versus Duration of Loading for CR2 - Crushed Limestone Mixtures.

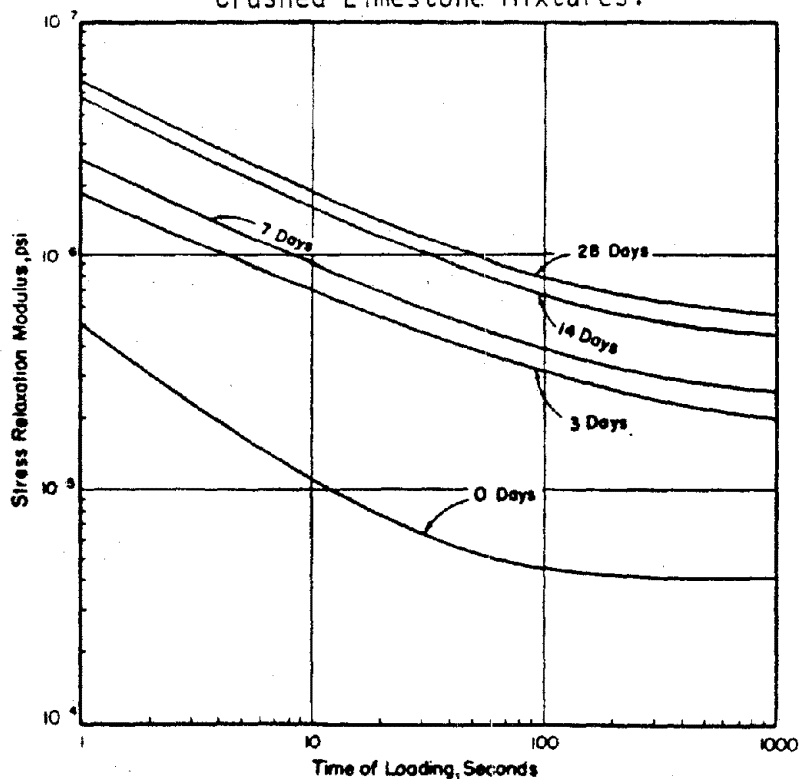


Figure 82. Effects of Aging at 140°F on the Compressive Stress Relaxation Modulus Versus Duration Loading for CR3 - Crushed Limestone Mixtures.

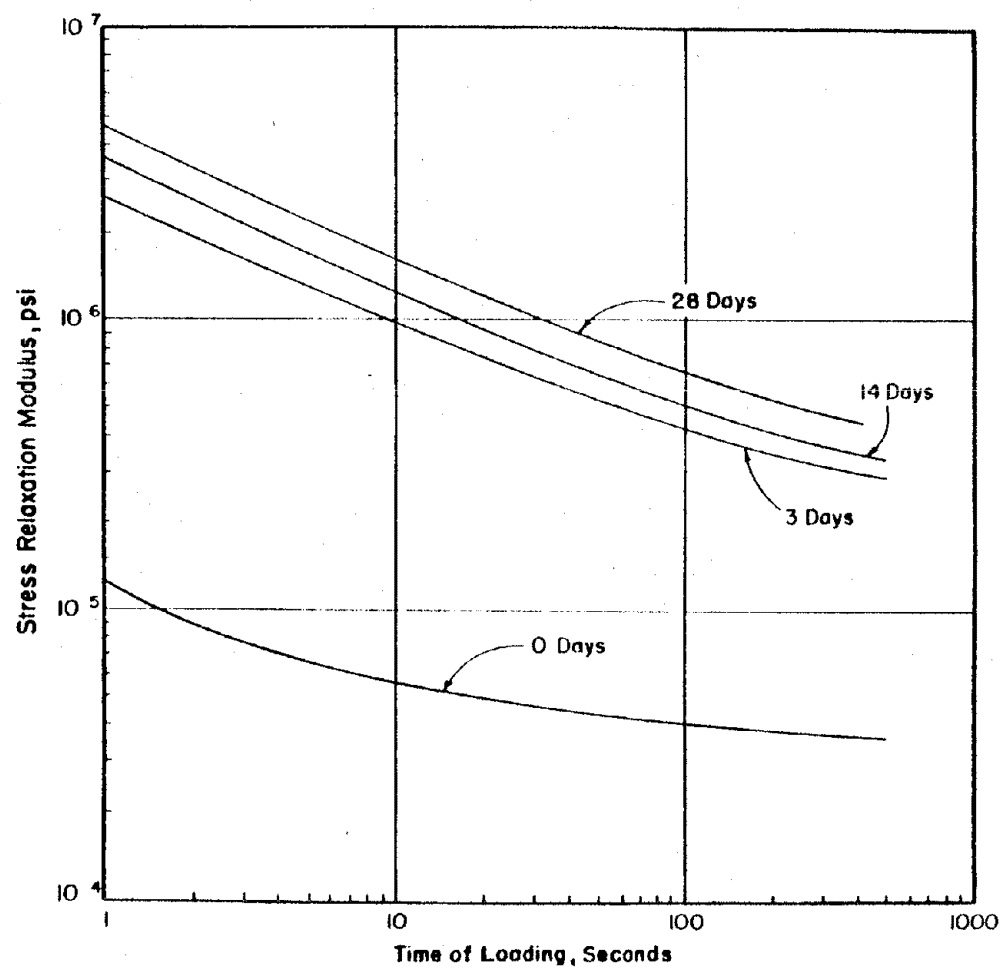


Figure 83. Effects of Aging at 140°F on the Compressive Stress Relaxation Modulus Versus Duration of Loading for CR5 - Crushed Limestone Mixtures.

SULPHLEX binders throughout the aging process.

2. The SULPHLEX binders, in general, exhibit the majority of hardening during the first three days of aging at 140°F. The asphalt mixture hardens more uniformly over the aging period.
3. The asphalt concrete mixtures reach an approximate asymptotic modulus value over a much shorter time of relaxation than do the SULPHLEX mixtures. In most cases the SULPHLEX mixtures have not reached the "equilibrium modulus" or constant modulus at the end of the 1000-second period.

These observations most certainly substantiate the previous data which have established that SULPHLEX mixtures are stiffer than asphalt concrete and hence respond in a substantially different manner structurally than does asphalt concrete.

The rapid hardening or the fact that the large portion of hardening occurs during the first three days for SULPHLEX mixtures is consistent with the notion that SULPHLEX, in thin films, crystallizes rapidly. One may note further from Figures 79 through 83 that the approximate slope of the relaxation curves for three through 28 days are, for a given binder, nearly equal. Furthermore, these curves suggests a much slower relaxation than for the initial or zero day curves. In contrast, the relaxation curves for asphalt concrete, Figure 79, show a continuous increase in time of relaxation with age.

Results of DSE and Resilient Modulus Analysis

The results of the aging study based on the indices of dissipated strain energy, DSE, and resilient moduli are presented in Table 43. The data can be effectively summarized into a manageable form as is shown in Figures 84 and 85.

From Figure 85 it is once again apparent that SULPHLEX mixtures develop most of their stiffness within only about three days of aging. The stiffnesses remain relatively constant throughout the remainder of the aging period. It is interesting that the SULPHLEX binder CR5 does not age as severely beyond the initial crystallization as do the other SULPHLEX binders.

Table 43. Summary of Effects of Aging at 140°F as Reflected by Resilient Modulus and Dissipated Strain Energy.*

Binder	Testing Temperature, °F	Specimen Age, Days	Resilient Modulus, psi x 10 ⁶	DSE, in-lb/in ³
CR1	32	0	--	--
		28	2.59	9.70
		56	2.51	13.7
	77	0	1.47	46.6
		3	2.31	15.4
		7	2.12	12.4
		14	2.24	9.10
		28	2.23	3.80
		56	2.32	8.70
	104	0	--	--
		28	1.70	18.6
		56	1.99	20.6
CR2	32	0	--	--
		28	2.73	16.5
		56	2.48	12.7
	77	0	1.05	161
		3	1.89	19.0
		7	1.87	21.2
		14	1.92	6.10
		28	2.15	11.8
		56	2.38	6.80
	104	0	--	--
		28	1.46	28.8
		56	1.82	32.5
CR3	32	0	--	--
		28	2.56	8.30
		56	2.35	12.6
	77	0	1.43	56.3
		3	1.74	18.9
		7	1.81	6.60
		14	1.84	6.20
		28	2.06	4.90
		56	2.30	10.0

Table 43. (Continued).

Binder	Testing Temperature, °F	Specimen Age, Days	Resilient Modulus, psi x 10 ⁶	DSE, in-lb/in ³
CR3	104	0	--	--
		28	1.30	89.5
		56	1.45	73.1
CR5	32	0	--	--
		28	2.82	5.90
		56	2.61	12.4
	77	0	1.16	104
		3	1.60	20.0
		7	1.96	17.0
		14	1.85	7.70
		28	2.09	14.5
		56	2.10	18.7
	104	0	--	--
		28	1.20	88.0
		56	1.52	46.9
AC-10	32	0	--	--
		28	1.97	8.70
		56	1.78	12.9
	77	0	0.53	271
		3	0.66	235
		7	0.70	197
		14	0.67	210
		28	0.71	194
		56	0.78	179
	104	0	--	--
		28	0.20	1,330
		56	0.19	1,340

* Note: Each data point is the average of 3 specimens.

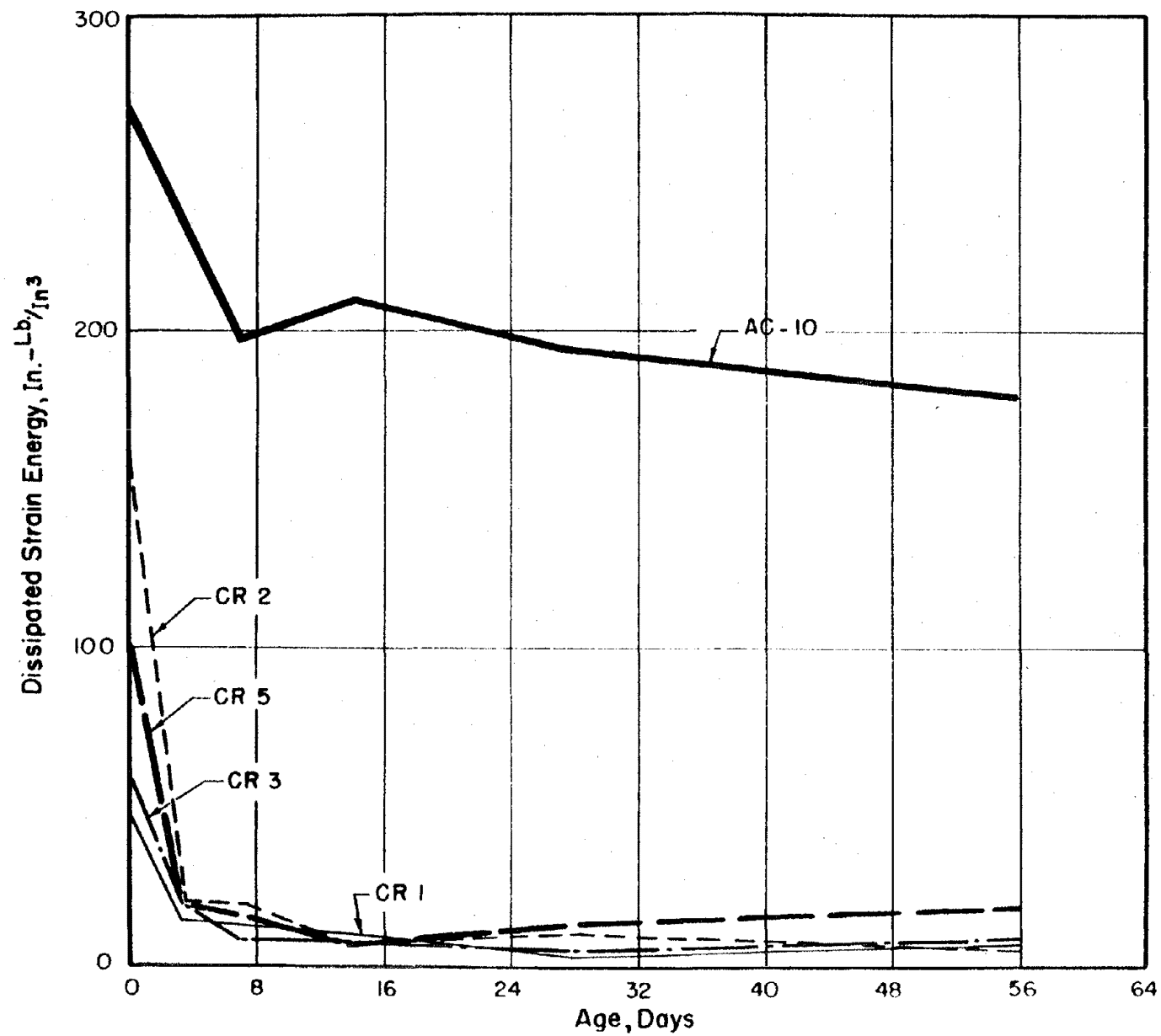


Figure 84. Change in Dissipated Strain Energy with Aging at 140°F for all Mixtures.

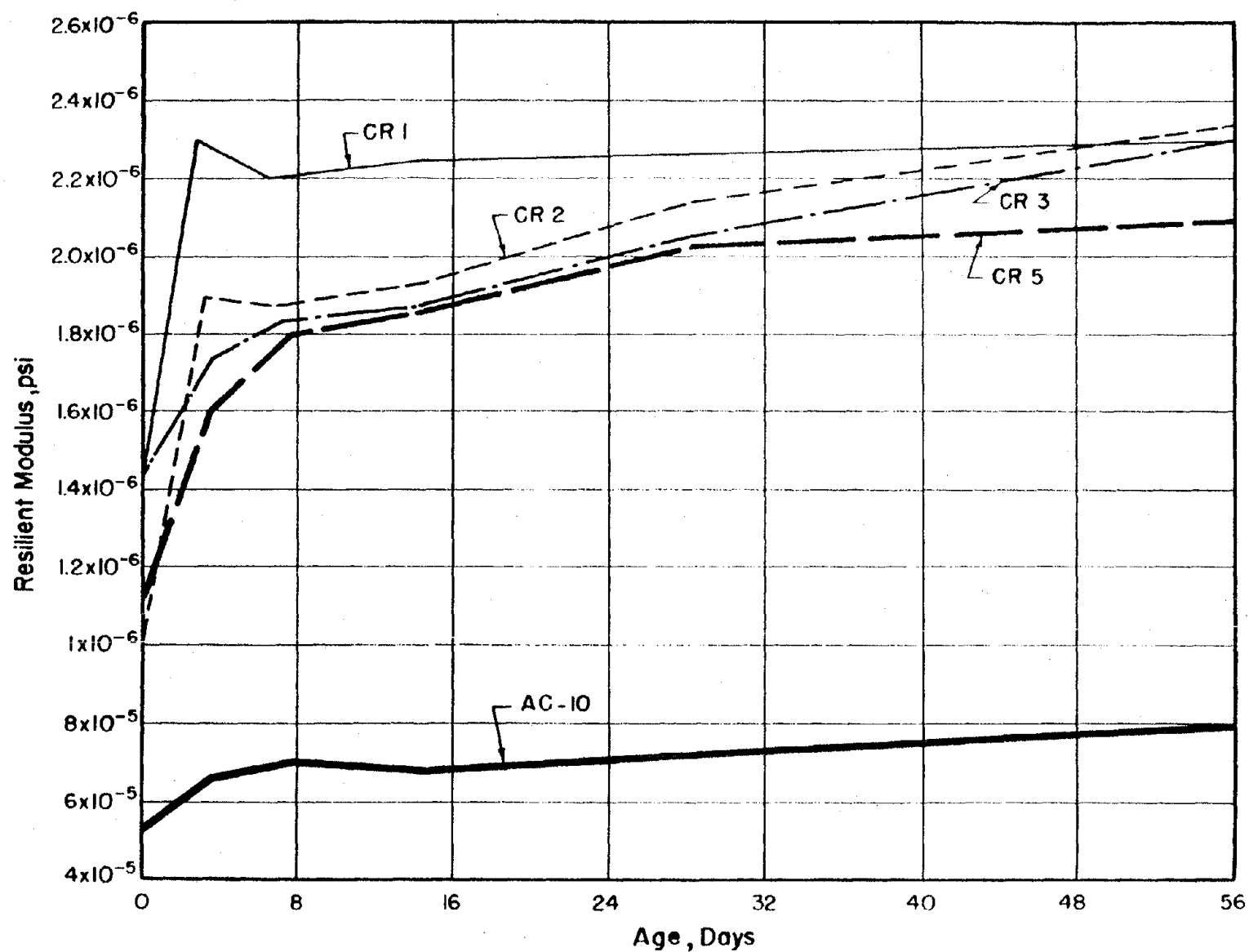


Figure 85. Change in Resilient Modulus with Aging at 140°F for all Mixtures.

In Figure 85 the DSE is plotted against the time of aging. Once again the rapid loss in DSE is apparent within the initial three days of aging as opposed to the relatively constant level of DSE following the 3-day mark. Asphalt concrete as well experiences the vast majority of its DSE loss during the initial week of aging. However, the asphalt mixture still retains an order of magnitude higher DSE than SULPHLEX mixtures.

The comparative magnitudes of the DSE's for asphalt concrete and SULPHLEX mixtures throughout the period of aging, Figure 84, is a clear indication of the greater potential of asphalt concrete to dissipate energy in the form of viscoelastic deformations as opposed to storing the energy which is available for crack propagation. Although SULPHLEX possesses high toughness in terms of load to failure test, such as indirect tension, due to its great stiffness, it does not have the energy dissipation potential of asphalt cement.

Results of In Situ Aging

The aging data as reflected by resilient moduli at 32, 77, and 104°F are summarized in Table 44. These data substantiate previous trends that the SULPHLEX binder crystallizes rapidly. In this case during the first week of service the vast majority of hardening occurred. Secondly, these data show that even following hardening by crystallization, the resilient modulus still maintains approximately the same level of sensitivity to temperature as it possessed before aging. This, of course, indicates a retention of viscous or viscoelastic behavior during and/or following periods of aging but at a drastically different level of stiffness.

Table 45 summarizes the resilient modulus testing of SULPHLEX in four environments. This stiffness increase is consistent for all environments. The end product stiffness, December 1983, is approximately the same for all environments except Seattle. Resilient modulus testing was performed at Texas A&M for specimens aged in College Station, Texas; Mclean, Virginia, and Oakland, California. The

Table 44. Changes in Resilient Modulus with Age on Field Cores from Loop 1604, San Antonio, Texas.

Binder	Percent Binder Content By Weight of Mixture	Age of Specimen, Months	Resilient Modulus, psi x 10 ^{6*}		
			@ 32°F	@ 77°F	@ 104°F
233A	7.0	0	4.210	2.250	0.430
		0.25	4.000	1.6000	0.290
		2	4.500	2.500	0.590
		12	4.500	2.600	0.500
		24	4.200	2.500	0.540
	7.5	0	5.200	2.210	0.590
		0.25	4.500	1.900	0.400
		2	4.950	2.200	0.780
		12	5.200	2.400	0.800
		24	5.200	2.350	0.810
	8.0 (Section A)	0	4.200	1.610	0.460
		0.25	3.200	0.800	0.300
		2	4.000	1.600	0.420
		12	3.900	1.400	0.350
		24	3.500	1.450	0.484
	8.0 (Section B)	0	5.210	1.900	0.490
		0.25	4.900	1.400	0.400
		2	5.200	2.510	0.790
		12	5.100	1.960	0.780
		24	5.100	1.950	0.775
AC-20	5.5	0	2.400	0.340	0.040
		0.25	2.900	0.350	0.039
		2	3.00	0.525	0.070
		12	2.600	0.638	0.125
		24	2.650	0.675	0.135

* Note: Each data point is the average of 6 specimens.

Table 45. Summary of Resilient Modulus Testing of SULPHLEX Specimens Aged In Situ in Four Environments.

Location of Specimen Aging	Binder	Date of Test	Resilient Modulus,* psi, @ 77°F
College Station, Texas	6% CR1	Apr '82	1,760,000
		Sep '82	2,100,000
		Dec '83	2,250,000
	8% CR1	Apr '82	1,000,000
		Sep '82	1,670,000
		Dec '83	2,200,000
	6% CR2	Apr '82	1,410,000
		Sep '82	2,280,000
		Dec '83	2,400,000
	8% CR2	Apr '82	1,150,000
		Sep '82	2,100,000
		Dec '83	2,250,000
	6% AC-10	Apr '82	400,000
		Sep '82	575,000
		Dec '83	740,000
McLean, VA	6% CR1	Apr '82	1,360,000
		Dec '83	2,000,000
	8% CR1	Apr '82	1,000,000
		Dec '83	1,750,000
	6% CR2	Apr '82	1,410,000
		Dec '83	2,100,000
	8% CR2	Apr '82	1,150,000
		Dec '83	1,490,000
Oakland, CA	6% CR1	Apr '82	1,360,000
		Dec '83	2,100,000
	8% CR1	Apr '82	1,000,000
		Dec '83	2,010,000
	6% CR2	Apr '82	1,410,000
		Dec '83	2,250,000
	8% CR2	Apr '82	1,150,000
		Dec '83	1,900,000

Table 45. (Continued).

Location of Specimen Aging	Binder	Date of Test	Resilient Modulus, psi, @ 77°F
Seattle, WA	6% CR1	Apr '82	2,180,000
		Sep '82	3,110,000
		Dec '83	3,480,000
	8% CR1	Apr '82	1,010,000
		Sep '82	2,510,000
		Dec '83	2,980,000
	6% CR2	Apr '82	1,420,000
		Sep '82	2,170,000
		Dec '83	2,950,000
	8% CR2	Apr '82	1,100,000
		Sep '82	1,580,000
		Dec '83	2,090,000

* Note: Each data point is the average of 2 specimens (4 tests).

specimens aged in Seattle, Washington, were tested at the University of Washington.

The difference in test laboratories could well account for the differences in stiffness levels between the Seattle-aged specimens and all others.

CHAPTER X

PAVEMENT DESIGN AND STRUCTURAL ANALYSIS

General

The primary purpose of this chapter is to evaluate SULPHLEX as a surface or full depth (surface and base) pavement course in a variety of climates. In every case SULPHLEX is compared to a comparable asphalt concrete pavement. Four pavement layer combinations were considered: (1) a conventional pavement with a surface course of SULPHLEX or hot-mixed asphalt concrete, (2) a full depth section, (3) a surface course over a lime-treated clay subgrade, and (4) a surface course over a portland-cement-treated subgrade.

Table 46 summarizes the partial factorial combinations considered. The structural engineering properties of binders CR1, CR2, and CR3 were considered to be similar enough so that they could be characterized as a single binder with nominal or typical engineering properties of all three SULPHLEX binders. Binder CR5 was different than the other three SULPHLEX binders and performed more like asphalt concrete. Therefore, binder CR5 was evaluated separately. Asphalt concrete composed of AC-10 and crushed limestone was the control mixture. Of course, all SULPHLEX mixtures used the identical crushed limestone aggregate.

In addition to the 48 combinations (four pavement layer combinations x three climates x two traffic levels x two binders) of factors, nine additional interactions were considered. These interactions were studied in order to evaluate the effects of: (1) excessively long load duration and/or extremely high pavement temperatures and (2) the effects of using CR5 versus CR1, CR2, or CR3.

A pavement systems approach involving FPS-BISTRO and the VESYS structural pavement subsystem was used in the analysis of these factors, shown in Table 46. The approach is explained in the following paragraphs.

Table 46. Organization of Structural Design and Analysis Study.

Pavement Combinations 1	Regions 2	Traffic Levels 3	Load Duration 4	Binder Type	Sur-CSB			Full Depth			Sur-LT Subg.			Sur-CT Subg.		
					C	M	H	C	M	H	C	M	H	C	M	H
					SH	IH	SH	IH	SH	IH	SH	IH	SH	IH	SH	IH
					SH	IH	SH	IH	SH	IH	SH	IH	SH	IH	SH	IH
CR1-	CR3	Normal	Very s Long													
CR5	Normal	Very s Long														
AC-10	Normal	Very s Long														

Notes: 1. Sur - Surface Course (AC or Sulphlex); CSB - Crushed Limestone Base; LT Subg. - Lime Treated Subgrade; CT Subg. - Cement Treated Subgrade.

2. C - Cool; M - Moderate; H - Hot.

3. SH - State Highway and IH - Interstate Highway.

4. Normal - 55-60 mph; Very Long - Approximately 10^3 - 10^6 seconds.

5. Very high temperature may be substituted for long duration, i.e., 120-140°F pavement temperature.

Approach

Pavement System

A pavement design system is a computer system that is capable of investigating a large variety of pavement design strategies and determining the economically optimum combination of materials and layer thicknesses which will provide an acceptable level of riding quality over a specified analysis period. A structural design subsystem forms a part of this overall design. It has the capability of predicting the performance (as measured by the serviceability index in this particular case) of a specified pavement and also evaluates pavement materials on a structural basis. FPS-BISTRO is a combination of a pavement design system and structural subsystem. VESYS, a structural design subsystem, also predicts performance on the basis of serviceability index but utilizes material properties different than those used in FPS-BISTRO for a mechanistic evaluation. Obviously, use of each program has a place in the generation of an optimum, structurally adequate pavement design scheme.

For this analysis a slightly modified version of FPS-BISTRO was used as a screening tool whereby optimum designs were determined for each of 48 possible combinations of material, climate, and traffic. Optimum designs for each of these conditions were further analyzed by VESYS. Figure 86 is a schematic of the design process. Table 47 lists the variables considered in the pavement design procedure. Figure 87 is a concise summary of the pavement cross sections considered.

FPS-BISTRO

As its name implies, this system is a combination of the Flexible Pavement System (FPS-13) used by the Texas State Department of Highways and Public Transportation (102) and BISTRO (103), a linear elastic structural analysis program developed by Shell. Initially, trial designs for the materials under consideration were evaluated on the basis of Present Serviceability Index.

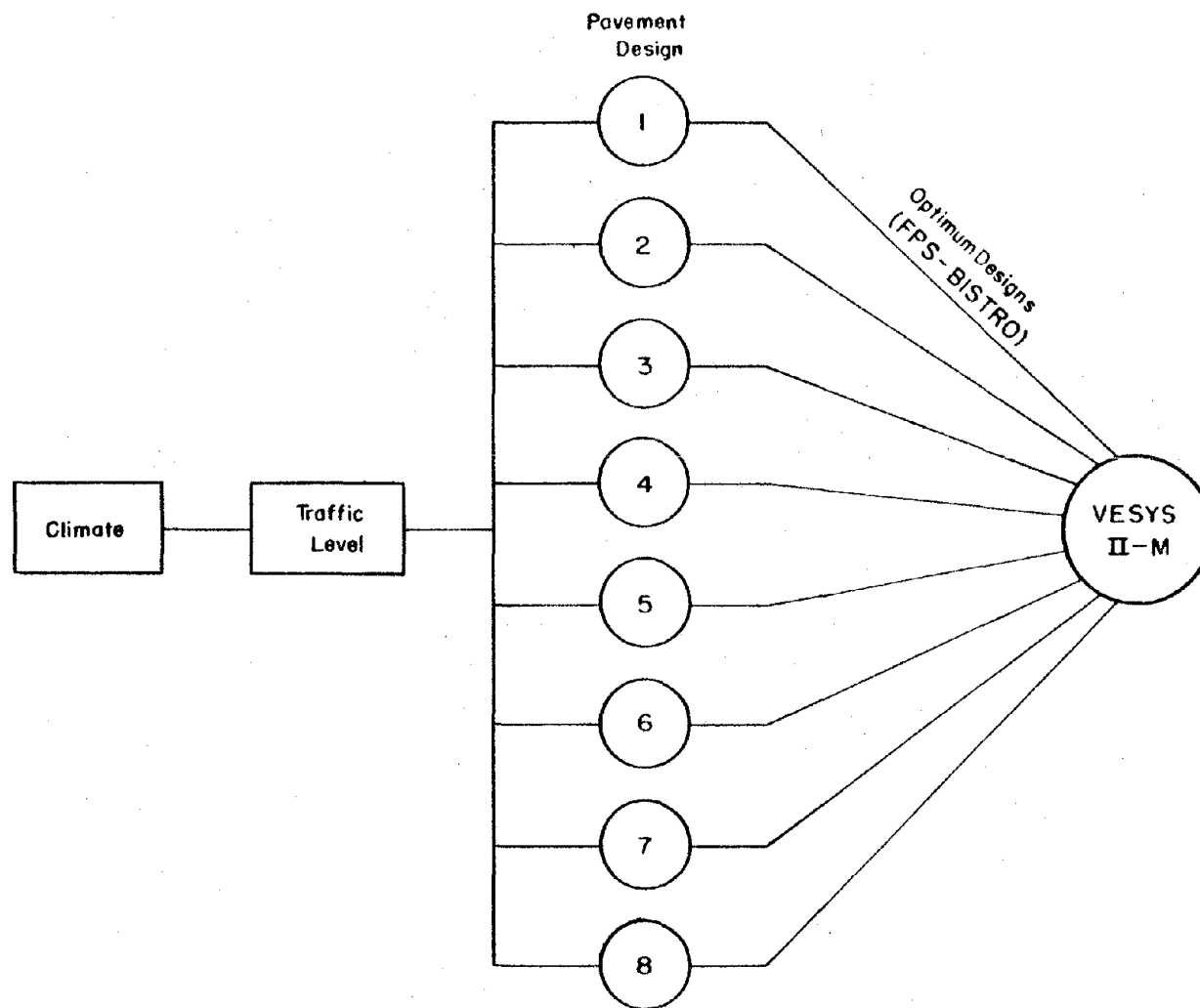
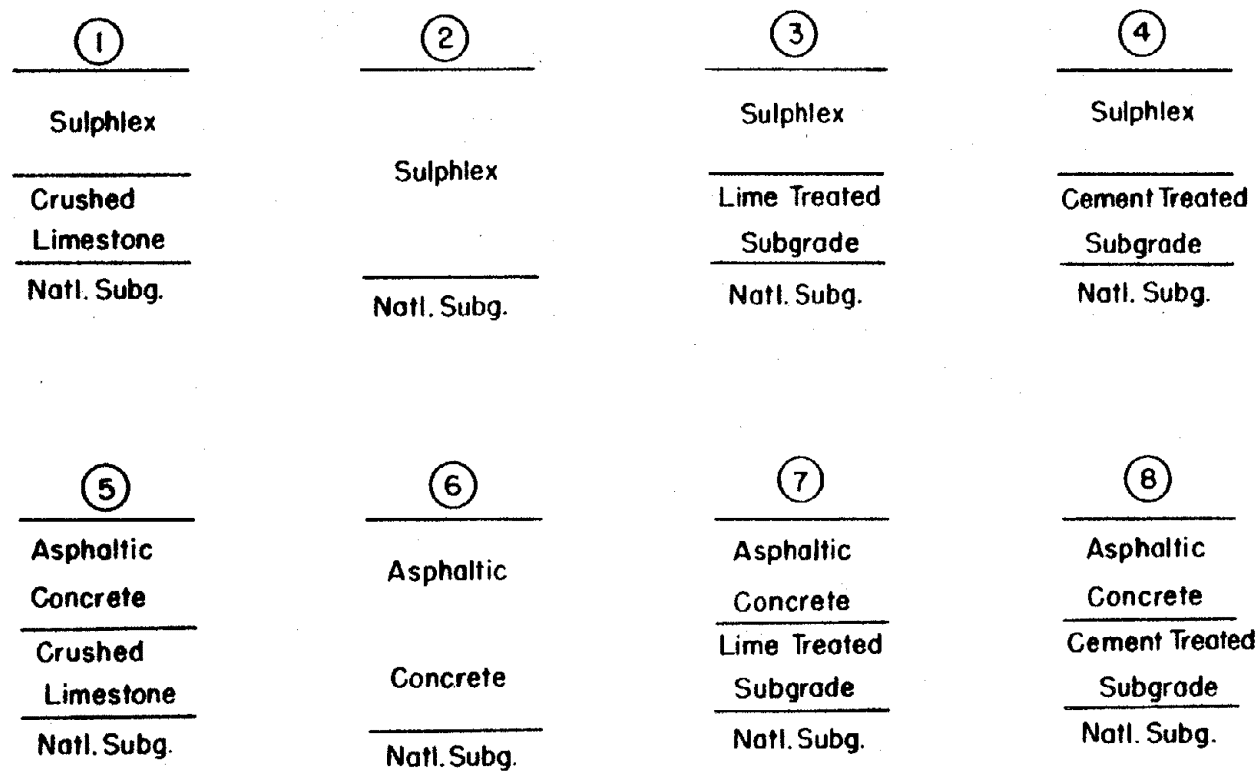


Figure 86. Schematic of Pavement Design Procedure.

Table 47. List of Variables Considered in Pavement Design Procedure.

Variable	Level
Climate	Extreme Northern (Cool) Northern (Moderate) Southern (Hot)
Traffic	State Highway Interstate Highway
Pavement Materials	Surface Course Sulphlex Asphaltic concrete Base Course Sulphlex Asphaltic concrete Crushed limestone Lime treated subgrade Cement treated subgrade Subgrade Fine grained



Sulphlex - 2-12 in (2-24 in for design ②)

Asphaltic Concrete - 2-12 in (2-24 in for design ⑥)

Crushed Limestone - 4-10 in

Lime Treated Subgrade - 4-10 in

Cement Treated Subgrade - 4-10 in

Figure 87. Pavement Section Analyzed by FPS-BISTRO.

The Present Serviceability Index (PSI) is based upon a rating scale that designates the condition of the pavement at any time. A rating of 5.0 indicates a "perfect" pavement, whereas a rating of 0 indicates an "impassible" pavement (104). The concept of PSI was developed at the AASHO Road Test (105). Here it was found that new pavements had an average PSI of 4.2. Terminal serviceability index is the PSI of a pavement when riding quality has dropped to a certain minimum acceptable level. Values typically used for terminal serviceability indices are 2.0 and 2.5. Serviceability loss over time has been defined by Scrivner (105) as a function of surface curvature index, temperature and the number of 18-kip single axle loads. Using data from the AASHO Road Test, Scrivner developed the following relationship:

$$P = 5 - \left(\sqrt{5 - P_1} + 53.6 \frac{NS^2}{\bar{\alpha}} \right)^2$$

where P is the serviceability index at time t,

P_1 is the initial serviceability index immediately after construction or after an overlay,

N is the total number of 18-kip equivalent single axle loads, in millions, applied during a period for which S is relatively constant,

$\bar{\alpha}$ is the harmonic mean of daily temperature values above 32°F, and

S is the surface curvature index, 1/20th of the difference between deflections at point A and point B, Figure 88, in milli-inches (see Ref. 105).

Obviously, serviceability loss increases with increased load repetitions, N, and increased surface deflection as reflected by S, and is affected by temperature as accounted for by $\bar{\alpha}$. The effect of $\bar{\alpha}$ on serviceability loss is partially accounted for by an increased susceptibility to fatigue cracking at colder temperatures as well as increased susceptibility to deformation at higher temperatures. Figure 88 depicts the load geometry and points of analysis within the pavement cross section.

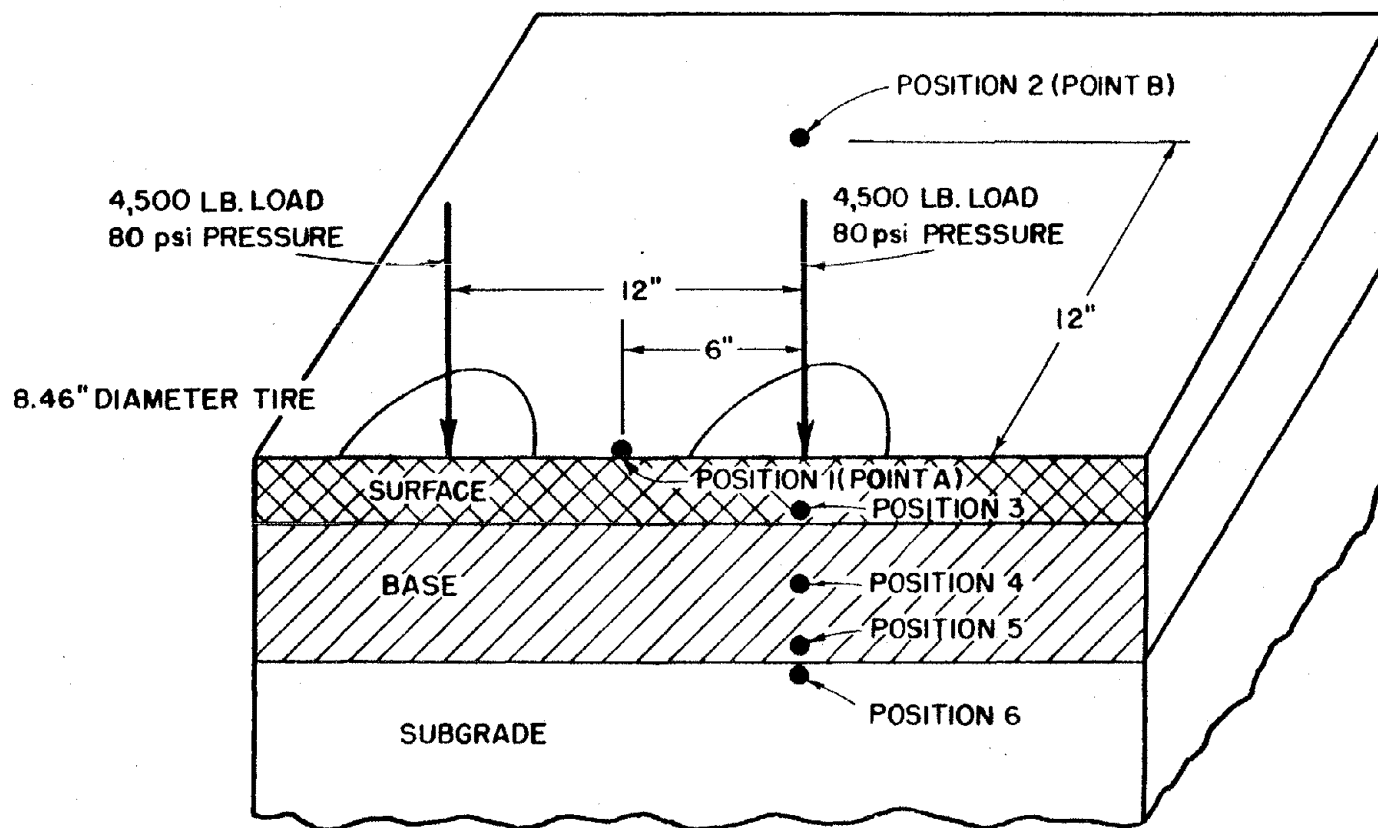


Figure 88. Load Geometry in Surface Curvature Index Calculations.

The PSI deteriorates with time (and load repetitions) to a terminal serviceability thereby resulting in the need for an overlay. Program inputs allow for specific values of initial and terminal PSI and minimum time to first overlay. Designs meeting serviceability requirements are then checked against structural failure criteria. The structural failure criteria of the initial program were based on the Texas Triaxial Test. Actual principal stresses and strains, computed by BISTRO, were compared to allowable values calculated from relationships developed by the Texas Highway Department. While this was functionally adequate, Texas Transportation Institute (106) replaced these structural criteria by a more "rational" criteria based on layered elastic analysis.

The new failure criteria include the following:

1. Flexural fatigue at the bottom of the surface course,
2. Permanent deformation at mid-depth of the granular base course,
3. Flexural fatigue at the bottom of stabilized base layers and
4. Permanent deformation at top of subgrade.

Flexural Fatigue at the Bottom of the Surface Course

The following fatigue relationship was utilized for the surface course:

$$N = K_1 \left(\frac{1}{\epsilon_t} \right)^{K_2}$$

where N is number of 18-kip equivalent single axle loads, and

ϵ_t is maximum tensile strain at bottom of surface course.

The terms K_1 and K_2 are constants developed at various temperatures for both SULPHLEX and asphaltic concrete. This equation can be rewritten as:

$$\epsilon_t = \left(\frac{K_1}{N} \right)^{1/K_2}$$

The term ϵ_t becomes an allowable strain for a given N and is compared to that actually developed in the pavement. Parameters K_1 and K_2 are shifted from laboratory to field values as discussed in Chapter V.

Permanent Deformation - Mid-depth of Granular Base Course

Duncan and Chang (107) developed a general hyperbolic expression for sands and clays that expresses strain as measured in the static triaxial test as a function of the deviator stress and confining pressure. Barksdale (108) performed a similar analysis using a repeated load triaxial testing apparatus and found an equation analagous to that developed by Duncan and Chang. The Duncan-Chang expression is

$$\epsilon_a^P = 1 - \frac{\frac{(\sigma_1 - \sigma_3)/K\sigma_3^n}{(\sigma_1 - \sigma_3)R_f}}{\frac{2(c - \cos \phi + \sigma_3 \sin \phi)}{(1 - \sin \phi)}}$$

where ϵ_a^P is permanent axial strain after a particular number of load applications,

$(\sigma_1 - \sigma_3)$ is deviator stress,

$K \sigma_3^n$ is initial tangent modulus of the stress-strain curve as a function of confining pressure (K and n are constants),

c is cohesion,

ϕ is angle of internal friction, and

R_f is ratio of compressive strength to asymptotic stress difference; $(\sigma_1 - \sigma_3)_f$; for granular bases usually between $\frac{(\sigma_1 - \sigma_3)_f}{(\sigma_1 - \sigma_3)_{ult.}}$

0.70 and 1.00.

Based on data reported by Barksdale, Lytton and others (109) developed the following equation which predicts permanent strain in granular materials at a higher number of load repetitions.

$$\epsilon_{ND}^P = \epsilon_{NK}^L + \{ \log_{10} (ND) - \log_{10} (NK) \} \cdot (\text{Slope})$$

where ϵ_{ND}^P is permanent strain at a desired large number of load applications, percent

ϵ_{NK}^P is permanent strain at a known number of load applications

ND is desired large number of load applications at which ϵ_{ND}^P is required

NK is number of load applications which produces ϵ_{NK}^P

Slope is $1.3507 \times 10^{-3} (\sigma_1 - \sigma_3)^{1.2623}$ for $0 < (\sigma_1 - \sigma_3) < 30$ psi

is $1.0543 \times 10^{-4} (\sigma_1 - \sigma_3)^{2.0191}$ for $(\sigma_1 - \sigma_3) > 30$ psi

Each of these relationships was incorporated in the program. Strain as defined by Duncan's equation, ϵ_a^P , was used as ϵ_{NK}^P in Lytton's relationship ($NK = 10,000$). The resulting permanent deformation was compared to an allowable value of 0.5 inches.

Flexural Fatigue at Bottom of Course

When SULPHLEX was used as a surface or base, the same fatigue criteria were used as for AC surfaces. The failure criterion for lime- and portland-cement-treated bases was the typical relationship between stress ratio and allowable number of repetitions:

$$SR = 1.037315(1/N)^{0.05323}$$

(ratio of actual induced stress to flexural stress causing failure)

where SR is stress ratio at failure for a given N, and

N is number of 18-kip equivalent single axle loads.

The criterion, then, is based on an allowable stress, which is related to SR in the following manner:

$$\sigma_a = SR (\sigma_t)$$

where σ_a is allowable flexural tensile stress

σ_t is flexural tensile strength

SR is as defined above

Permanent Deformation at the Top of Subgrade

Again, a relationship involving ϵ_v , N, K_3 , and K_4 was developed

$$\epsilon_v = K_3 (1/N)^{1/K_4}$$

where ϵ_v is allowable permanent strain at a given N ,
 N is as defined previously, and K_3 and K_4 are regression constants.

The terms K_3 and K_4 were based on data presented by Santucci (110) at the 4th International Conference on the Structural Design of Asphalt Pavements.

All pavement cross sections that meet both serviceability and structural requirements are considered feasible and are prioritized on the basis of cost. Factors include construction costs (both initial and overlay), material costs, maintenance costs, and salvage value of the material. All costs incurred at future times (i.e., overlay construction costs, yearly maintenance) are discounted to present value for comparison. The optimum design is the design that has the lowest total cost. Typical design schemes consist of an initial design followed by two or three overlays over a 20-year life span.

Preparation of Input for FPS-BISTRO

Input data were compiled for each of eight (8) pavement systems, three (3) climatic conditions, and two (2) traffic levels. Items required for the FPS-BISTRO program include the following:

1. Climatic data,
2. Material costs,
3. User costs,
4. Maintenance costs,
5. Traffic data,
6. Construction data and
7. Material properties.

A typical set of input data is given in Table 48. The length of analysis period was chosen as 20 years. This is the value recommended for interstate highways. For the sake of comparison, a 20-year analysis period was also used for State highway analysis. A minimum time to first overlay was chosen as three years. A minimum serviceability index of 2.5 was used for both State and interstate analyses. A design confidence level of 99.99 percent (F) was chosen

Table 48. Summary of Texas FPS-BISTRO Input Data

BASIC DESIGN CRITERIA

Length of the Analysis Period (Years)	20.0
Minimum Time of First Overlay (Years)	3.0
Minimum Time Between Overlays (Years)	3.0
Minimum Serviceability Index P2	2.5
Design Confidence Level	
Interest Rate or Time Value of Money (Percent)	12.0

PROGRAM CONSTRAINTS

Max Funds Available Per Sq. Yd. for Initial Design (Dollars)	60.00
Maximum Allowed Thickness of Initial Construction (Inches)	24.0
Accumulated Max Depth of all Overlays (Inches) (Excluding Level-Up)	5.0

TRAFFIC DATA

ADT at Beginning of Analysis Period (Vehicles/Day)	8000.
ADT at End of Twenty Years (Vehicles/Day)	16000.
One-Direction 20.-Year Accumulated No. of Equivalent 18-KSA	5,000,000 & 6,500,000
Average Approach Speed to the Overlay Zone (MPH)	55.0
Average Speed Through Overlay Zone in Overlay Direction (MPH)	30.0
Average Speed Through Overlay Zone in Nonoverlay Direction (MPH)	55.0
Proportion of ADT Arriving Each Hour of Construction (Percent)	7.0
Percent Trucks in ADT	15 & 20.0

ENVIRONMENT AND SUBGRADE

District Temperature Constant	8, 19, 38
-------------------------------	-----------

Table 48. Summary of Texas FPS-BISTRO Input Data (continued).

Swelling Probability	0.0
Potential Vertical Rise (Inches)	0.0
Swelling Rate Constant	0.0

CONSTRUCTION AND MAINTENANCE DATA

Serviceability Index of the Initial Structure	4.2
Serviceability Index After an Overlay	4.2
Minimum Overlay Thickness (Inches)	2.0
Overlay Construction Time (Hours/Day)	10.0
Asphaltic Concrete Compacted Density (Tons/C.Y.)	1.95 & 2.00
Asphaltic Concrete Production Rate (Tons/Hour)	200.0
Width of Each Lane (Feet)	12.0
First Year Cost of Routine Maintenance (Dollars/Lane-Mile)	75.00
Annual Incremental Increase in Maintenance Cost (Dollars/Lane-Mile)	30.00

DETOUR DESIGN FOR OVERLAYS

Traffic Model Used During Overlaying	3
Total Number of Lanes of the Facility	4
Number of Open Lanes in Restricted Zone (Overlay Direction)	1
Number of Open Lanes in Restricted Zone (Nonoverlay Direction)	2
Distance Traffic is Slowed in Overlay Direction (Miles)	0.50
Distance Traffic is Slowed in Nonoverlay Direction (Miles)	0.50
Detour Distance Around the Overlay Zone (Miles)	0.0

for this analysis. This input affects the level of traffic variability. A higher confidence level would result in a more conservative pavement design. The time value of money, in this case 12 percent, was used to discount material costs (for overlays), user costs, maintenance costs, and construction costs (for overlays) to a present worth amount.

The maximum funds available for initial construction depend on two factors: material costs and material thicknesses. A value of \$60/SY provided enough money for complete analysis of each pavement system. The maximum allowed thickness of initial construction was set at 24 inches, the sum of the thickest surface and base layers. Accumulated maximum depth of all overlays (excluding level-up) was set at five inches.

Two traffic levels were used in this analysis: State highways and interstate highways. For each highway condition, it was assumed that traffic increased linearly from an average daily traffic level (ADT) of 8,000 vehicles per day to 16,000 vehicles per day at the end of the 20-year analysis period. These values are used in the traffic equation to determine the distribution of equivalent 18-kip single axle loads as a function of time, and are used for the calculation of traffic delay costs during overlay construction. For State highway traffic the one directional 20-year accumulated number of 18-kip single axle loads was set at five million. For interstate highways, this value was set at 6.5 million. The percent trucks in the ADT was set at 15 percent for State highway analysis and 20 percent for interstate highway analysis. Highways with higher percentages of trucks have higher user costs due to the greater costs of delaying trucks than cars during overlay operations. For each traffic level, a four-lane highway was chosen. This affects the extent of traffic delay through the overlay zone. The average speed through the zone, in the overlay direction, was set at 30 mph. Because of the four-lane design, the traffic moving in the direction opposite the overlay would probably not be affected and could move at its original speed of 55 mph. The proportion of ADT arriving each hour during construction was set at seven percent. This value contributes to the magnitude of user costs incurred during overlay construction.

As discussed earlier, the district temperature constant, $\bar{\alpha}$, is a constant based upon mean monthly temperature above 32°F. Three climatic regions were chosen for analyses. The regions represented are listed below:

<u>Climate</u>	<u>Representative City</u>	<u>$\bar{\alpha}$, °F</u>
Extreme northern	Ontario, Canada	8
Northern	Ottawa, Illinois	19
Southern	Brownsville, Texas	38

For each pavement, the subgrade was assumed to be a fine-grained relatively nonexpansive material. Therefore, the swelling probability, potential vertical rise, and swelling rate constant were all assigned values of zero.

The serviceability index for a new pavement and a pavement immediately after an overlay was set at 4.2. This is a typical value developed at the AASHO Road Test (104), Ontario Ministry of Transportation and Communications (111) and in Texas (112). Minimum overlay thickness, a function of maximum aggregate size, was set at two inches. Typically, contractors work an average of 10 hours per day during overlay construction. Compacted density values are based on laboratory densities of SULPHLEX and asphaltic concrete. A value of two tons per cubic yard was used for SULPHLEX, whereas asphaltic concrete was assigned a value of 1.95 tons per cubic yard for in-place density. A typical production rate of 200 tons per hour was chosen for each surface material. This value is used within the program to calculate traffic delay costs. Each lane width was set at 12 feet. A value of \$75 per lane mile was used for routine maintenance costs with an annual incremental increase of \$30 per lane mile.

Detour design for overlays depends on the highway geometrics and the surrounding roadsides. The choice of detour design is incorporated in the program as it affects user costs. A four-lane model, was used in this analysis in which one lane at a time could be closed for overlay construction. The traffic would be routed to the adjacent lane traveling in the same direction. Consequently, the

number of open lanes in the overlay and nonoverlay directions were set at one and two, respectively. It was assumed that traffic would be slowed for about 0.5 miles in each direction. This accounts for the possibility of a four-lane highway with no median in which the oncoming traffic might naturally decrease in speed. The detour design around the overlay zone was set at zero miles.

In-place material costs, depths, and salvage values are all incorporated in the program. Each of the materials considered were listed earlier. Minimum and maximum layer depths are shown in Figure 87. Salvage percentages are as listed below:

<u>Material</u>	<u>Salvage %</u>
SULPHLEX	10
Asphaltic concrete	25
Crushed limestone	70
Lime treated subgrade	70
Cement treated subgrade	70

In place cost of the SULPHLEX mixture was based on formulation No. 233 (eight percent by weight), January 1984 chemical prices and crushed limestone aggregate costs. It was assumed that ratio of material (binder + aggregate) cost to in-place cost was the same for SULPHLEX and asphaltic concrete. In-place material costs for all other materials were developed by adjusting published prices for inflation. All costs are listed below:

<u>Material</u>	<u>In-Place Cost \$/CY</u>
SULPHLEX mixture	148.00
Asphaltic concrete	78.00
Crushed limestone	25.20
Lime-treated subgrade	12.60
Cement-treated subgrade	15.10

All other material properties used in this analysis are given in Table 49.

Table 49. Material Properties Used in Texas FPS-BISTRO program.

Temperature (°F)	40	51	70
Stiffness (psi):			
Sulphlex	3,000,000	2,700,000	2,100,000
Asphaltic concrete	1,500,000	1,100,000	600,000
Crushed limestone	35,000	35,000	35,000
Lime-treated subgrade	100,000	100,000	100,000
Cement-treated subgrade	500,000	500,000	500,000
Fine-grained subgrade	10,000	10,000	10,000
Poisson's Ratio:			
Sulphlex	.30	.30	.30
Asphaltic concrete	.35	.35	.35
Crushed limestone	.40	.40	.40
Lime-treated subgrade	.20	.20	.20
Cement-treated subgrade	.15	.15	.15
Fine-grained subgrade	.40	.40	.40
Fatigue Parameter K_1 :			
Sulphlex	2.61×10^{-4}	1.42×10^{-3}	1.42×10^{-3}
Asphaltic concrete	1.29×10^{-6}	4.10×10^{-5}	4.10×10^{-5}
Fatigue Parameter K_2 :			
Sulphlex	2.21	2.24	2.24
Asphaltic concrete	2.93	2.80	2.80
Other Base Course Material Properties:			
Crushed Limestone $K = 300$ $n = 0.40$ $\phi = 36^\circ$ Allowable Permanent Deformation = 0.5 inches			
Lime-treated subgrade		Flexural tensile strength = 25 psi	
Cement-treated subgrade		Flexural tensile strength = 160 psi	

Other Natural Subgrade Properties

Permanent Deformation Parameters:

$$K_1 = 0.222 \times 10^{-8}$$

$$K_2 = 4.420$$

VESYS Analysis

The 48 optimum designs as established by FPS-BISTRO are shown in Tables 50 through 52. These designs were further evaluated by the use of VESYS IIM (12). The climates and traffic levels chosen were similar to those used in the FPS-BISTRO analysis. This probabilistic design procedure uses the following inputs along with their variabilities, for computational analysis:

1. Traffic.
2. System Geometry.
3. Environment.
4. Material Properties.
5. System Properties.
6. System Performance Bounds.

Using these values, the computer program determines the pavement response to a defined wheel load, both stationary and moving. These responses, called primary and general, are then used as inputs in the calculation of three damage indicators: rut depth, roughness, and cracking. These distress mechanisms are components of the AASHTO equation which predicts pavement performance on the basis of Present Serviceability Index (PSI). When used as a design tool, the values of rut depth, roughness, cracking, and PSI are compared to allowable criteria. In this case, these results were used to compare the optimum SULPHLEX and asphaltic concrete pavements at a given climate and traffic level. In addition, the SULPHLEX binder CR5 was analyzed under several conditions. Also, the effects of prolonged loading at high temperatures were evaluated for certain designs of CR1, CR5, and AC-10.

Traffic

VESYS provides several inputs that describe the expected traffic. They are traffic level, load intensity, configuration, and duration.

Table 50. Optimum design schemes as determined by Texas FPS-BISTRO (70°F).

		Section # [*]															
		State Highway Traffic								Interstate Highway Traffic							
		1	2	3	4	5	6	7	8	1	2	3	4	5	6	7	8
Initial Const. Cost	\$/SY	31.58	28.78	24.06	12.42	24.47	21.67	20.83	8.11	27.47	24.67	24.06	12.42	26.63	23.83	23.00	8.53
Overlay Const. Cost	\$/SY	3.71	3.31	6.88	3.31	3.99	4.69	3.56	4.13	9.17	9.49	8.19	5.65	4.19	4.69	3.56	4.69
User Cost	\$/SY	0.01	0.01	0.02	0.01	0.02	0.03	0.02	0.03	0.03	0.03	0.03	0.02	0.03	0.03	0.02	0.03
Routine Maintenance Cost	\$/SY	0.21	0.22	0.18	0.22	0.17	0.17	0.18	0.17	0.17	0.17	0.17	0.19	0.18	0.17	0.18	0.17
Salvage Value	\$/SY	-0.59	-0.38	-0.64	-0.47	-0.99	-0.84	-0.93	-0.61	-0.63	-0.43	-0.64	-0.56	-1.10	-0.90	-0.98	-0.70
TOTAL COST	\$/SY	34.92	31.93	30.51	15.48	27.66	25.71	23.67	11.83	36.21	33.92	31.80	17.72	29.92	27.83	25.78	12.72
NUMBER OF LAYERS		2	2	2	2	2	2	2	2	2	2	2	2	2	2	2	2
LAYER DEPTHS (inches)																	
D(1)		7.0	2.0	5.0	2.0	10.0	3.0	8.0	2.0	6.0	2.0	5.0	2.0	11.0	8.0	9.0	2.0
D(2)		4.0	5.0	10.0	10.0	4.0	7.0	10.0	9.0	4.0	4.0	10.0	10.0	4.0	3.0	10.0	10.0
NO. OF PERF. PERIODS		2	2	3	2	3	3	3	3	3	3	3	3	3	3	3	3
PERFORMANCE TIME (YEARS)																	
T(1)		8.8	9.7	6.4	10.3	6.2	5.7	7.0	6.1	4.1	3.6	5.1	8.2	6.5	5.8	7.4	6.2
T(2)		22.0	22.5	16.4	20.8	12.5	11.6	13.5	12.5	11.6	11.0	13.4	17.1	12.7	11.6	13.9	12.2
T(3)				32.1		20.5	20.5	21.6	20.3	27.0	24.0	26.7	30.2	21.0	20.2	21.0	20.5
OVERLAY POLICY (INCH)																	
(Including Level up)																	
O(1)		2.5	2.5	2.5	2.5	2.5	2.5	2.5	2.5	2.5	2.5	2.5	2.5	2.5	2.5	2.5	2.5
O(2)				2.5		2.5	3.5	2.5	2.5	2.5	2.5	2.5	2.5	3.5	3.5	2.5	3.5
O(3)																	

* Sections are identified in Figure 87.

Table 51. Optimum design schemes as determined by Texas FPS-BISTRO (51°F).

		Section # *															
		State Highway Traffic								Interstate Highway Traffic							
		1	2	3	4	5	6	7	8	1	2	3	4	5	6	7	8
Initial Const. Cost	\$/SY	35.69	32.89	32.28	12.42	20.13	19.50	18.67	10.69	35.69	32.89	34.29	12.42	24.47	21.67	20.83	12.86
Overlay Const. Cost	\$/SY	3.31	2.64	2.95	7.56	6.56	5.25	5.69	3.99	4.15	3.31	3.31	11.16	3.99	4.46	5.69	3.99
User Cost	\$/SY	0.01	0.01	0.01	0.02	0.04	0.03	0.03	0.02	0.01	0.01	0.01	0.04	0.02	0.03	0.03	0.02
Routine Maintenance Cost	\$/SY	0.22	0.23	0.22	0.17	0.17	0.17	0.17	0.17	0.21	0.22	0.22	0.17	0.17	0.17	0.17	0.17
Salvage Value	\$/SY	-0.63	-0.43	-0.64	-0.56	-0.93	-0.79	-0.93	-0.70	-0.63	-0.43	-0.53	-0.60	-0.99	-0.79	-0.98	-0.75
TOTAL COST	\$/SY	38.60	35.34	34.83	19.62	25.97	24.17	23.63	14.18	39.43	36.00	37.30	23.18	27.66	25.54	25.74	16.29
NUMBER OF LAYERS		2	2	2	2	2	2	2	2	2	2	2	2	2	2	2	2
LAYER DEPTHS (inches)																	
D(1)		8.0	2.0	7.0	2.0	8.0	7.0	7.0	3.0	8.0	2.0	8.0	2.0	10.0	8.00	8.00	4.0
D(2)		4.0	6.0	10.0	10.0	4.0	2.0	10.0	10.0	4.0	5.0	4.0	10.0	4.0	2.00	10.00	10.0
NO. OF PERF. PERIODS		2	2	2	3	3	3	3	3	2	2	2	3	3	3	3	3
PERFORMANCE TIME (YEARS)																	
T(1)		10.2	11.9	11.1	5.7	3.5	4.7	4.7	6.3	8.1	9.6	9.8	4.5	6.0	5.4	5.2	6.5
T(2)		26.0	25.3	23.5	12.5	10.4	10.6	11.8	12.5	21.5	20.8	21.8	10.1	12.8	11.6	12.2	12.7
T(3)					23.7	20.2	22.0	20.9	20.7				22.7	21.8	20.4	20.9	20.4
OVERLAY POLICY (INCH)																	
(Including Level Up)																	
O(1)		2.5	2.5	2.5	2.5	3.5	2.5	3.5	2.5	2.5	2.5	2.5	2.5	2.5	2.5	3.5	2.5
O(2)					2.5	2.5	3.5	2.5	2.5				3.5	2.5	2.5	2.5	2.5
O(3)																	

* Sections are identified in Figure 87.

Table 52. Optimum design schemes as determined by Texas FPS-BISTRO (40°F).

		Section #*															
		State Highway Traffic								Interstate Highway Traffic							
		1	2	3	4	5	6	7	8	1	2	3	4	5	6	7	8
Initial Const. Cost	\$/SY	43.91	32.89	34.29	24.75	26.63	23.83	25.23	19.36	43.91	37.00	34.29	24.75	28.80	26.00	27.40	21.53
Overlay Const. Cost	\$/SY	2.64	8.79	8.47	7.85	3.99	5.25	4.69	3.69	3.71	7.56	9.84	11.16	3.69	5.08	4.13	4.19
User Cost	\$/SY	0.05	0.03	0.03	0.03	0.02	0.03	0.02	0.01	0.02	0.03	0.04	0.02	0.03	0.03	0.03	0.03
Routine Maintenance Cost	\$/SY	0.23	0.17	0.17	0.17	0.17	0.17	0.17	0.18	0.21	0.17	0.17	0.17	0.18	0.17	0.17	0.18
Salvage Value	\$/SY	-0.71	-0.51	-0.61	-0.69	-1.05	-0.90	-1.00	-0.92	-0.71	-0.55	-0.61	-0.73	-1.10	-0.95	-1.00	-1.03
TOTAL COST	\$/SY	46.08	41.36	43.34	32.10	29.77	28.39	29.12	22.33	47.13	44.21	43.71	35.39	31.59	30.33	30.73	24.88
NUMBER OF LAYERS		2	2	2	2	2	2	2	2	2	2	2	2	2	2	2	2
LAYER DEPTHS (inches)																	
D(1)		10.00	3.00	8.00	5.00	11.00	9.00	11.00	7.00	10.00	3.00	8.00	5.00	12.00	10.00	12.00	8.00
D(2)		4.00	5.00	4.00	10.00	4.00	2.00	4.00	10.00	4.00	6.00	4.00	10.00	4.00	2.00	4.00	10.00
NO. OF PERF. PERIODS		2	3	3	3	3	3	3	3	2	3	3	3	3	3	3	3
PERFORMANCE TIME (YEARS)																	
T(1)		11.8	4.5	4.8	5.7	6.0	5.0	5.9	6.7	9.5	5.7	3.8	4.5	6.7	5.5	5.7	6.7
T(2)		30.1	10.9	12.0	12.5	12.9	11.0	12.1	12.9	24.9	12.6	9.7	10.1	13.3	12.8	11.8	12.6
T(3)			20.9	24.3	22.2	21.0	20.2	20.5	20.4		22.5	20.0	20.5	20.0	20.6	20.1	20.3
OVERLAY POLICY (INCH)																	
(Including Level up)																	
O(1)		2.5	2.5	2.5	2.5	2.5	2.5	2.5	2.5	2.5	2.5	2.5	2.5	2.5	3.5	2.5	2.5
O(2)			2.5	2.5	2.5	2.5	3.5	3.5	2.5		2.5	2.5	3.5	2.5	2.5	2.5	3.5
O(3)																	

* Sections are identified in Figure 87.

Traffic levels reflect the expected heavy axle loads per day. They can be incorporated by use of either actual load distributions, or as in this case, 18-kip equivalents. Traffic levels simulating both state highway (5,000,000 accumulated loads after 20 years) and interstate highway (6,500,000 accumulated loads after 20 years) were evaluated. Initial levels were assumed to increase linearly to final 20-year values.

The design wheel load was 1/2 of an 18-kip single axle. For an 80 psi tire pressure, the contact radius of the load is six inches. Since equivalent axle loads were used, the variance of the load amplitude was set at zero. Load duration, a function of vehicle speed and contact radius, has a tremendous impact on pavement response especially in viscoelastic materials. A value of 0.1 seconds was used to simulate traffic operating in the 55-60 mile per hour speed range.

The variance of the load duration was set at 0.52×10^{-5} seconds. Longer loading conditions simulating those experienced at a busy intersection were affected by changing the load duration to 100 seconds.

System Geometry

System geometry is simply the thickness of each layer above the subgrade. VESYS IIM allows for analysis of pavement sections up to three layers. For pavements sections 1, 3-5, and 7-8, Figure 87, a three-layer system was modelled by using the original design thicknesses as chosen by FPS-BISTRO. For pavement sections 2 and 6, a two-layer system was modelled by setting the material properties for layers 1 and 2 equal.

Environment

The major environmental influences on pavement response are temperature and moisture (12). VESYS IIM handles temperature changes in the top pavement layer by use of a time-temperature shift factor (BETA) of pavement response. Fatigue constants also vary with temperature thereby affecting the damage due to cracking. Moisture

content of the granular and cement-stabilized base, lime-stabilized subgrade and natural subgrade are reflected in the creep properties of each material. As mentioned earlier, three climates were evaluated fully with limited evaluation at a very hot temperature.

Material Properties

The material properties for use in the structural analysis portion of the program can be broken into two categories: primary response properties and distress properties.

Primary response is defined as the time dependent state of stress, strain, or deformation existing in the pavement due to a stationary load applied to the surface of the pavement (12). The relationships built into the program allow the incorporation of stress dependency, load history, and plastic effects on pavement response (12). The pavement primary response properties are the creep compliance functions for both rate-independent and rate-dependent layer materials (12). The viscoelastic or rate dependent properties of SULPHLEX and asphaltic concrete are defined by the creep compliance relationships tabulated in Table 53. All other materials in this analysis were considered elastic (rate-independent) and are therefore characterized by a constant compliance value or creep compliance. The coefficients of variation of creep compliance for each material account for the variability of the creep properties for each material and in turn affect calculation of damage indicators. The effects of time and temperature on creep compliance are considered by the use of a time temperature shift factor (BETA). For a given loading time and temperature the program calculates the creep compliance of a material by using BETA and the master creep curve at 70°F.

The distress properties are composed of fatigue and permanent deformation characteristics. The phenomenological fatigue model used in VESYS IIM is that defined earlier which relates fatigue constants K_1 , K_2 and radial strain at the bottom of layer 1 to an allowable number of load applications, N , to failure or cracking. The values utilized for SULPHLEX and asphaltic concrete are listed for each

Table 53. Creep Properties Used In VESYS IIM Analysis.

Creep Compliance @ 70°F, psi^{-1}									
Time (Seconds)	AC-10	CR1	CR5	Crushed Limestone	Lime Treated Subgrade	Cement Treated Subgrade	Hard Clay Subgrade	Medium Clay Subgrade	Soft Clay Subgrade
0.03	2.00×10^{-6}	3.57×10^{-7}	7.00×10^{-7}	2.86×10^{-5}	1.0×10^{-5}	2.0×10^{-6}	6.6×10^{-5}	1.0×10^{-4}	4.0×10^{-4}
0.10	3.45×10^{-6}	5.00×10^{-7}	9.00×10^{-7}	2.86×10^{-5}	1.0×10^{-5}	2.0×10^{-6}	6.6×10^{-5}	1.0×10^{-4}	4.0×10^{-4}
0.30	3.70×10^{-6}	5.55×10^{-7}	1.10×10^{-6}	2.86×10^{-5}	1.0×10^{-5}	2.0×10^{-6}	6.6×10^{-5}	1.0×10^{-4}	4.0×10^{-4}
1.00	5.56×10^{-6}	9.09×10^{-7}	1.30×10^{-6}	2.86×10^{-5}	1.0×10^{-5}	2.0×10^{-6}	6.6×10^{-5}	1.0×10^{-4}	4.0×10^{-4}
3.00	7.14×10^{-6}	1.09×10^{-6}	1.66×10^{-6}	2.86×10^{-5}	1.0×10^{-5}	2.0×10^{-6}	6.6×10^{-5}	1.0×10^{-4}	4.0×10^{-4}
10.00	1.05×10^{-5}	1.89×10^{-6}	3.00×10^{-6}	2.86×10^{-5}	1.0×10^{-5}	2.0×10^{-6}	6.6×10^{-5}	1.0×10^{-4}	4.0×10^{-4}
30.00	1.27×10^{-5}	2.27×10^{-6}	4.30×10^{-6}	2.86×10^{-5}	1.0×10^{-5}	2.0×10^{-6}	6.6×10^{-5}	1.0×10^{-4}	4.0×10^{-4}
100.00	1.72×10^{-5}	4.76×10^{-6}	6.50×10^{-6}	2.86×10^{-5}	1.0×10^{-5}	2.0×10^{-6}	6.6×10^{-5}	1.0×10^{-4}	4.0×10^{-4}
1000.00	2.08×10^{-5}	1.05×10^{-5}	1.10×10^{-5}	2.86×10^{-5}	1.0×10^{-5}	2.0×10^{-6}	6.6×10^{-5}	1.0×10^{-4}	4.0×10^{-4}

climate in Table 54. Obviously, these fatigue relationships determine the level of damage index due to the load-related fatigue cracking. The permanent deformation characteristics of a material are described by two parameters, μ (GNU) and α (ALPHA). These parameters were discussed in Chapter IV.

The values of μ and α for a SULPHLEX and asphaltic concrete each change with temperature. VESYS IIM does not allow this variation with temperature, however. Therefore, values representing the average climatic regional temperature were used. These values are listed below:

Climate		ALPHA			GNU		
		AC-10	CR1	CR5	AC-10	CR1	CR5
Cold	(40°F)	0.80	0.80	0.80	0.015	0.049	0.152
Moderate	(51°F)	0.73	0.78	--	0.026	0.097	--
Hot	(70°F)	0.58	0.73	0.70	0.050	0.210	0.091
Very Hot	(100°F)	0.50	0.67	0.58	0.090	0.220	0.260

System Properties

Two pavement system properties are used in the computation of pavement roughness. The value of the correlation coefficient of the roughness model was set at 1.0 while the value of the exponent was 0.058.

System Performance Bounds

System performance bounds define acceptable limits of PSI and account for its variation. The initial serviceability index was chosen as 4.2 with a standard deviation of 0.20. The minimum acceptable level of serviceability was set at 2.5. The minimum acceptable reliability that the PSI was above the failure level was set at 70 percent.

Table 54 . Phenomenological Fatigue Constants Used in VESYS IIM Analysis.

Cool Climate	K_1			K_2		
Temp. °F	AC-10	CR1	CR5	AC-10	CR1	CR5
10	1.29×10^{-6}	2.61×10^{-4}	2.44×10^{-5}	2.93	2.21	2.59
13	1.29×10^{-6}	2.61×10^{-4}	2.44×10^{-5}	2.93	2.21	2.59
16	1.29×10^{-6}	2.61×10^{-4}	2.44×10^{-5}	2.93	2.21	2.59
35	1.29×10^{-6}	2.61×10^{-4}	2.44×10^{-5}	2.93	2.21	2.59
50	1.29×10^{-6}	2.61×10^{-4}	2.44×10^{-5}	2.93	2.21	2.59
56	4.10×10^{-5}	1.42×10^{-3}	2.00×10^{-4}	2.80	2.24	2.64
63	4.10×10^{-5}	1.42×10^{-3}	2.00×10^{-4}	2.80	2.24	2.64
65	4.10×10^{-5}	1.42×10^{-3}	2.00×10^{-4}	2.80	2.24	2.64
61	4.10×10^{-5}	1.42×10^{-3}	2.00×10^{-4}	2.80	2.24	2.64
57	4.10×10^{-5}	1.42×10^{-3}	2.00×10^{-4}	2.80	2.24	2.64
34	1.29×10^{-6}	2.61×10^{-4}	2.44×10^{-5}	2.93	2.21	2.59
22	1.29×10^{-6}	2.61×10^{-4}	2.44×10^{-5}	2.93	2.21	2.59

Table 54 . Phenomenological Fatigue Constants Used in VESYS IIM Analysis
(continued).

Moderate Climate	K_1			K_2		
Temp. °F	AC-10	CR1	CR5	AC-10	CR1	CR5
21	1.29×10^{-6}	2.61×10^{-4}	2.44×10^{-5}	2.93	2.21	2.59
24	1.29×10^{-6}	2.61×10^{-4}	2.44×10^{-5}	2.93	2.21	2.59
26	1.29×10^{-6}	2.61×10^{-4}	2.44×10^{-5}	2.93	2.21	2.59
45	1.29×10^{-6}	2.61×10^{-4}	2.44×10^{-5}	2.93	2.21	2.59
61	4.10×10^{-5}	1.42×10^{-3}	2.00×10^{-4}	2.80	2.24	2.64
69	4.10×10^{-5}	1.42×10^{-3}	2.00×10^{-4}	2.80	2.24	2.64
73	4.10×10^{-5}	1.42×10^{-3}	2.00×10^{-4}	2.80	2.24	2.64
75	4.10×10^{-5}	1.42×10^{-3}	2.00×10^{-4}	2.80	2.24	2.64
71	4.10×10^{-5}	1.42×10^{-3}	2.00×10^{-4}	2.80	2.24	2.64
68	4.10×10^{-5}	1.42×10^{-3}	2.00×10^{-4}	2.80	2.24	2.64
44	1.29×10^{-6}	2.61×10^{-4}	2.44×10^{-5}	2.93	2.21	2.59
39	1.29×10^{-6}	2.61×10^{-4}	2.44×10^{-5}	2.93	2.21	2.59

Table 54 . (continued).

Hot Climate	K_1			K_2		
Temp. °F	AC-10	CR1	CR5	AC-10	CR1	CR5
41	1.29×10^{-6}	2.61×10^{-4}	2.44×10^{-5}	2.93	2.21	2.59
43	1.29×10^{-6}	2.61×10^{-4}	2.44×10^{-5}	2.93	2.21	2.59
45	1.29×10^{-6}	2.61×10^{-4}	2.44×10^{-5}	2.93	2.21	2.59
60	4.10×10^{-5}	1.42×10^{-3}	2.00×10^{-4}	2.80	2.24	2.64
75	4.10×10^{-5}	1.42×10^{-3}	2.00×10^{-4}	2.80	2.24	2.64
87	1.21×10^{-4}	2.23×10^{-2}	1.90×10^{-3}	2.96	2.05	2.67
93	1.21×10^{-4}	2.23×10^{-2}	1.90×10^{-3}	2.96	2.05	2.67
95	1.21×10^{-4}	2.23×10^{-2}	1.90×10^{-3}	2.96	2.05	2.67
91	1.21×10^{-4}	2.23×10^{-2}	1.90×10^{-3}	2.96	2.05	2.67
87	1.21×10^{-4}	2.23×10^{-2}	1.90×10^{-3}	2.96	2.05	2.67
64	4.10×10^{-5}	1.42×10^{-3}	2.00×10^{-4}	2.80	2.24	2.64
59	4.10×10^{-5}	1.42×10^{-3}	2.00×10^{-4}	2.80	2.24	2.64

Results

VESYS Structural Analysis

The structural analysis portion of VESYS IIM uses the results from the primary and general responses as input into three damage models. These models are for rut depth, roughness and cracking.

Rut depth is the accumulation of permanent deformation with the increase in the number load applications. It is a function of the general moving load deflection response, the number of previous repetitions and the system permanent deformation properties (12).

Roughness of the pavement is measured by the slope variance of the pavement surface. It is a function of the magnitude and variability of rut depth, the variation in the primary deflection response and system roughness properties (12).

The dimensionless cracking damage index is a measure of the amount of fatigue life remaining in the pavement. When this index reaches a value of 1.0, the surface pavement layer cracks at the bottom. The cracking damage index is a function of the number of load repetitions, the mean, and variance of the general radial strain response at a given temperature and the mean and variance of the fatigue properties of the pavement (12).

Each of these distresses are calculated at certain specified intervals within the life of the pavement. Following each interval the distress parameters are input in the following AASHTO equation predicting PSI:

$$PSI' = PSI - 1.91(\log(1+SV)) - 0.01 \sqrt{C} - 1.38(RT)^2$$

where PSI' is present serviceability index after a given number of load applications.

PSI is initial serviceability index.

SV is slope variance (millionth radians).

C is area cracked (sq. ft/1000 sq. ft.).

RT is rut depth (in.).

Results of VESYS Analysis

The results from the pavement optimization portion of the VESYS analysis are presented in Tables 55 and 56. In essence, a comparison was made between optimum pavement schemes, not necessarily equal thicknesses of alternate materials. It is also important to remember that economic considerations play a major role in this evaluation due to their input in FPS-BISTRO, which was used to screen potential designs.

All pavements sections evaluated, with the exception of those listed below, met the serviceability requirements as determined by VESYS II-M.

Asphalt concrete with crushed stone base, warm climate,
Full-depth asphalt concrete for moderate and warm climate,
Asphalt concrete with lime-treated base, warm climate and
Full-depth CR1, warm climate.

Pavements with portland-cement-treated bases provided the highest level of serviceability throughout the analysis period for pavements containing both SULPHLEX and asphalt concrete surfaces. In fact, for every classification evaluated, the "optimum" pavement scheme was also the cheapest thereby providing a truly optimum condition. In other words, structural performance and optimum economics have combined to create an optimum pavement scheme.

The choice of cement-treated subgrade in every instance is primarily based on two factors: the required thickness and cost of cement-stabilized base. The cement-treated material is much stiffer than any other base material evaluated. Consequently, an adequately thick stiff layer contributes greatly to the overall structural response of a pavement. The ability of this material to withstand stress allows for thinner layers of the more expensive asphaltic concrete or SULPHLEX thereby reducing the total cost of the pavement. This is especially evident in warmer climates. For each traffic level in the warm climate, the thickness of the asphalt concrete surface

Table 55. Summary of VESYS IIM Results Using Optimum FPS-BISTRO Pavement Thicknesses. (Interstate Highway Traffic.)

Distress Type	Surface Course	Pavement Combinations 1 Climatic Regions 2	Sur-CSB			Full Depth			Sur-LT Subg.			Sur-CT Subg.		
			C	M	H	C	M	H	C	M	H	C	M	H
Cracking Index (yrs. to CI=1.0)	AC		20.0	6.0	16.0	>20.0	9.0	>20.0	>20.0	7.0	20.0	>>20.0	>>20.0	---
	CR1		13.0	7.0	6.0	< 0.5	<0.5	<0.5	7.0	8.0	6.0	11.0	12.0	>20.0
	CR5				9.0	1.5						>>20.0		>>20.0
Rut Depth, in. at 20 yr. Service Life	AC		0.023	0.060	0.617	0.138	0.381	3.331	0.012	0.039	0.544	0.010	0.023	---
	CR1		0.031	0.070	0.278	0.047	0.105	0.380	0.024	0.057	0.232	0.022	0.016	0.047
	CR5				0.206	0.196						0.075		0.032
Slope Variance Radians x 10 ⁶ at 20yr. Life	AC		0.018	0.126	13.27	1.708	13.12	10 ³	0.005	0.042	8.52	0.002	0.012	---
	CR1		0.032	0.164	2.61	0.072	0.357	4.70	0.019	0.107	1.31	0.011	0.010	0.084
	CR5				1.47	0.933						0.123		0.040
PSI at 20yr. Life	AC		3.96	3.78	1.20	3.33	1.61	---	4.19	3.85	1.67	4.19	4.19	---
	CR1		3.86	3.75	2.75	3.82	3.62	2.28	3.87	3.80	3.13	3.87	3.88	4.13
	CR5				3.10	3.30						4.10		4.17

- Notes: 1. Sur-CSB represents SULPHLEX or AC Surface over crushed stone base.
 Sur-LT Subg. represents SULPHLEX or AC Surface over lime treated subgrade.
 Sur-CT Subg. represents SULPHLEX or AC Surface over Portland Cement treated subgrade.
2. C - Cool
 M - Moderate
 H - Hot

Table 56. Summary of VESYS IIM Results Using Optimum FPS-BISTRO
Pavement Thickness (State Highway Traffic).

Distress Type	Surface Course	Climatic Regions 2	Pavement Combinations 1	Sur-CSB			Full Depth			Sur-LT Subg.			Sur-CT Subg.		
				C	M	H	C	M	H	C	M	H	C	M	H
Cracking Index (ys. to CI=1.0)	AC			18.0	5.00	15.0	20.0	10.0	20.0	>20.0	8.00	17.0	>>20.0	>>20.0	---
	CR1			16.0	10.00	8.0	0.5	7.0	1.0	10.0	10.0	7.0	14.0	16.0	>20.0
	CR5			>>20.0											
Rut Depth, in. at 20 yr. Service Life	AC			0.022	0.066	0.547	0.129	0.363	3.05	0.011	0.037	0.463	0.008	0.018	---
	CR1			0.030	0.066	0.247	0.036	0.100	0.360	0.023	0.054	0.218	0.019	0.015	0.044
	CR5			0.092											
Slope Variance Radiations x 10 ⁶ at 20yr. Life	AC			0.017	0.155	10.49	1.492	11.97	843.7	0.004	0.037	5.99	0.002	0.009	---
	CR1			0.03	0.148	2.06	0.016	0.322	4.19	0.017	0.080	1.16	0.008	0.009	0.075
	CR5			0.291											
PSI at 20yr. Life	AC			3.87	3.76	1.49	3.20	1.70	---	4.11	3.85	2.01	4.19	4.19	---
	CR1			3.86	3.76	2.90	3.87	3.64	2.38	3.87	3.82	3.19	3.88	3.88	4.13
	CR5			3.98											

- Notes: 1. Sur-CSB represents SULPHLEX or AC Surface over crushed stone base.
 Sur-LT Subg. represents SULPHLEX or AC Surface over lime treated subgrade.
 Sur-CT Subg. represents SULPHLEX or AC Surface over Portland Cement treated subgrade.
2. C - Cool
 M - Moderate
 H - Hot

layer was only 2 inches. This combined with the stiffness of the base created compressive strains at the bottom of the surface layer at temperatures above 80°F in the VESYS analysis. Consequently, the program was terminated at that point.

Considering the viscoelastic properties of both asphaltic concrete and SULPHLEX, two other conditions were evaluated with full-depth designs of AC, CR1, and CR5. Each section was analyzed by the use of VESYS under conditions simulating a busy intersection at 100°F and in a parking lot at 100°F. In each case, the permanent deformation parameters of α and μ at 100°F were used. The results of these analyses are given in Table 57.

The State highway traffic level was reduced to 1/5 its original value in order to simulate a proportion of heavy trucks moving through a given intersection. A load duration of 100 seconds was used to simulate traffic stopped at a signalized intersection. A comparison of the three materials generally shows that the performance of AC and CR1 are the extremes with CR5 somewhere between. This can especially be seen in the magnitudes of rut depth and slope variance. Because of excessive rut depths and slope variance, serviceability after 20 years was very low. Considering the combination of temperature, load level, and load duration, these results seem reasonable.

The PSI of the AC, CR5, and CR1 pavements fell below the allowable level of 2.5 at 0.30, 0.05, and 0.87 years, respectively. Again, note that the CR1 performed adequately for the longest period of time with the AC pavement having the shortest life. While actual climates may not produce constant 100°F pavement temperatures for such long periods, these results do depict the relative performance of these pavements at a given temperature, traffic level, and load duration. Considering this harsh combination, these results seem reasonable.

In the case of the parking lot, the pavement was subjected to one load of 3×10^4 seconds in length (eight hours) per day. Binders CR5 and AC generally performed similarly. This is especially evident when considering PSI after 20 years. Only the CR1 pavement remained above the acceptable level of serviceability. Obviously, this is a

Table 57. Effects of Load Duration on Performance of Full-Depth Pavements from FPS-BISTRO (100 F).

		Load Duration	
		100 sec ^a	3 X 10 ⁴ sec ^b
Cracking Index (Years to CI = 1.0)	AC	10.0	>>20.0
	CR1	1.5	>>20.0
	CR5	13.0	>>20.0
Rut Depth (in) (at 20 year life)	AC	3.09	0.39
	CR1	1.06	0.30
	CR5	2.46	0.31
Slope Variance (Radians X 10 ⁶ at 20 year life)	AC	866.0	13.6
	CR1	36.7	2.94
	CR5	137.7	3.03
PSI (at 20 year life)	AC	0.30	1.89
	CR1	1.10	2.97
	CR5	0.65	2.94

^a 1/5 of State Highway Traffic

^b 1 load per day

reflection of the lower levels of rut depth and slope variance. As would be expected, with this very low level of traffic, no cracking was observed within the first 20 years for every pavement.

Comparative Analysis with Crushed Limestone Base

An additional VESYS analysis was performed for pavement sections consisting of thin (2-inch) and thick (6-inch) surface layers of AC, CR1, and CR5 over a 6-inch crushed limestone base and both hard and soft subgrades. Each combination was evaluated at each of three climates and with State highway traffic. The results of this analysis are given in Table 58. Because of excessive cracking, no results from the thin pavements were graphed. Figures 89 through 92 show the worst case for each type distress for the thick pavements.

Thin Pavements Over Hard Subgrade

All pavement-climate combinations, with the exception of CR5 in the hot climate, cracked within the first 0.5 years. Based on all the other types of distress, the AC-10 and CR5 pavements performed similarly. This was especially evident at the cold and moderate climates. For a given binder, a warmer climate increased the rut depth and slope variance thereby decreasing the PSI. This increase is obviously a function of the permanent deformation properties of the materials. However, the serviceability level of each pavement did remain above the minimum level of 2.5. Maximum rut depths, slope variance, and minimum PSI all occurred with the AC pavement subjected to the hot climate.

Thin Surface Over Soft Subgrade

For these pavement combinations, all sections cracked within the first 0.5 years. The similarity of AC and CR5 was again evident especially in the cold and moderate climates. Again, the magnitudes

Table 58. Summary of VESYS IIM Analysis (6-Inch Crushed-Limestone Base).

Distress Type	Surface Course	Climatic Regions	Subgrade	Surface Thickness	THIN(2 in)						THICK(6in)					
					HARD			SOFT			HARD			SOFT		
					C	M	H	C	M	H	C	M	H	C	M	H
Cracking Index(yrs. to CI=1.0)	AC	< 0.5	< 0.5	< 0.5	< 0.5	< 0.5	< 0.5	3.0	3.0	4.0	1.5	1.5	2.0			
	CR1	< 0.5	< 0.5	< 0.5	< 0.5	< 0.5	< 0.5	5.0	6.0	7.0	3.0	3.0	4.0			
	CR5	< 0.5	0.5	1.5	< 0.5	< 0.5	< 0.5	9.0	9.0	14.0	5.0	5.0	8.0			
Rut Dept., in. at 20 yr. Service Life	AC	0.13	0.14	0.20	1.39	1.47	1.90	0.05	0.07	0.43	0.66	0.77	1.57			
	CR1	0.10	0.12	0.16	1.08	1.18	1.44	0.04	0.07	0.23	0.43	0.49	0.87			
	CR5	0.12	0.14	0.15	1.23	1.34	1.49	0.10	0.13	0.17	0.55	0.67	0.87			
Slope Variance Radians x 10 ⁶ at 20yr. Life	AC	0.44	0.55	1.10	47.66	53.59	89.17	0.07	0.18	6.19	12.95	17.86	73.87			
	CR1	0.30	0.38	0.72	32.84	38.78	57.82	0.06	0.17	1.83	5.44	6.95	22.83			
	CR5	0.44	0.55	0.68	40.0	48.27	59.27	0.34	0.60	1.00	8.80	13.40	22.0			
PSI at 20yr. Life	AC	3.56	3.50	3.23	---	---	---	3.83	3.74	2.04	1.13	0.65	---			
	CR1	3.65	3.60	3.41	---	---	---	3.83	3.75	2.98	2.12	1.87	0.19			
	CR5	3.57	3.50	3.43	---	---	---	3.63	3.48	3.29	1.62	1.08	0.27			

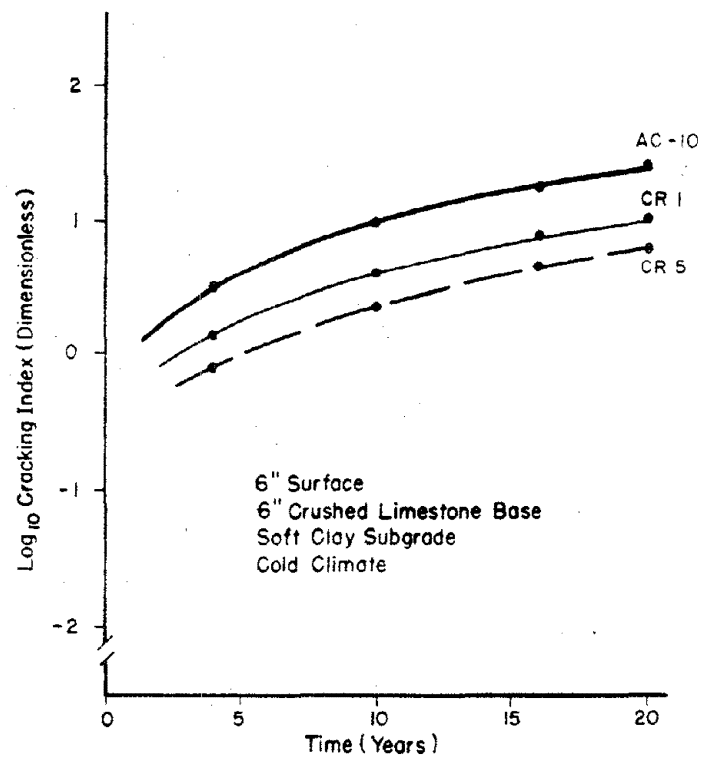


Figure 89. Cracking Index Versus Time (VESYS IIM Analysis).

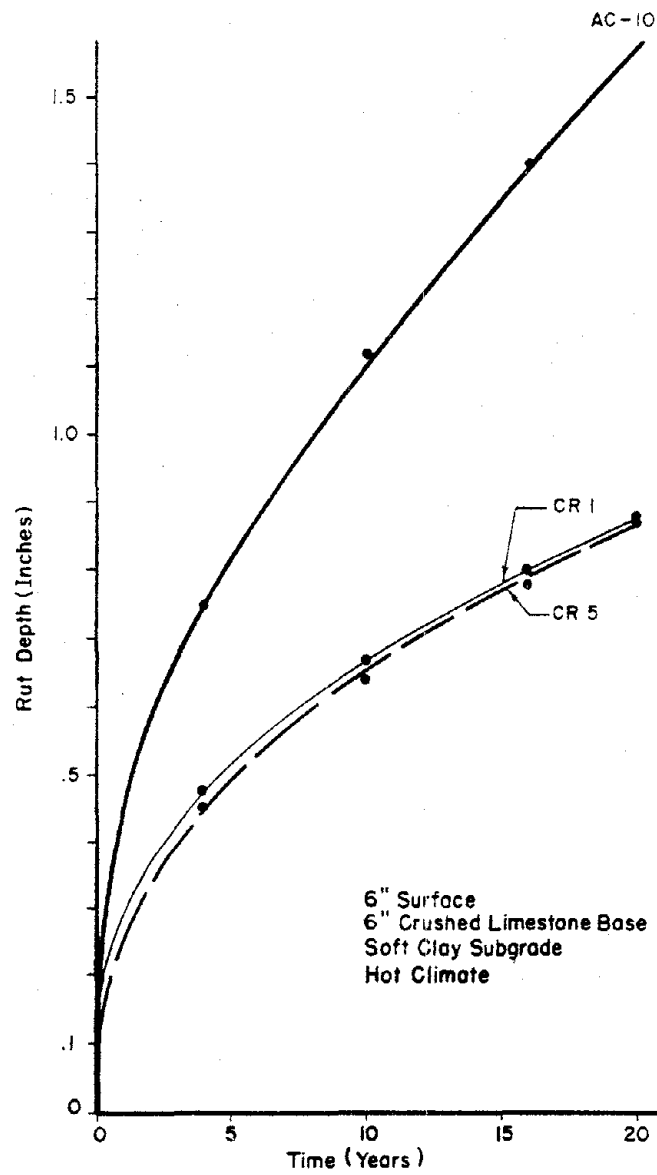


Figure 90. Rut Depth Versus Time (VESYS IIM Analysis).

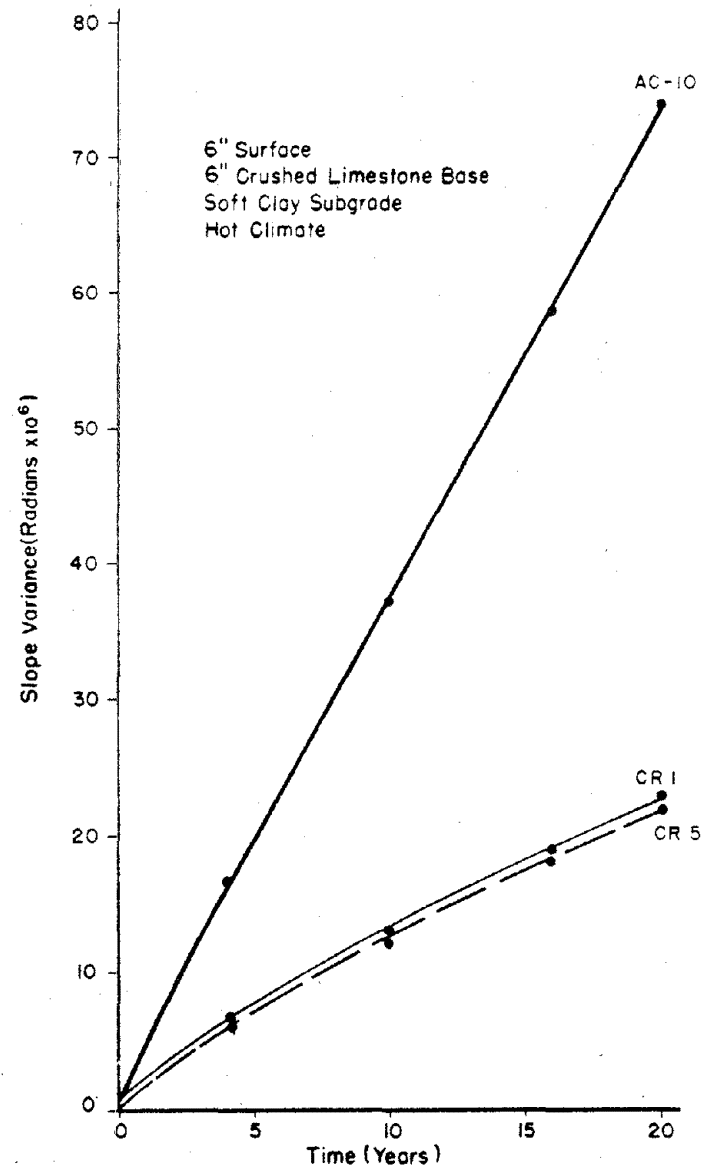


Figure 91. Slope Variance Versus Time (VESYS IIM Analysis).

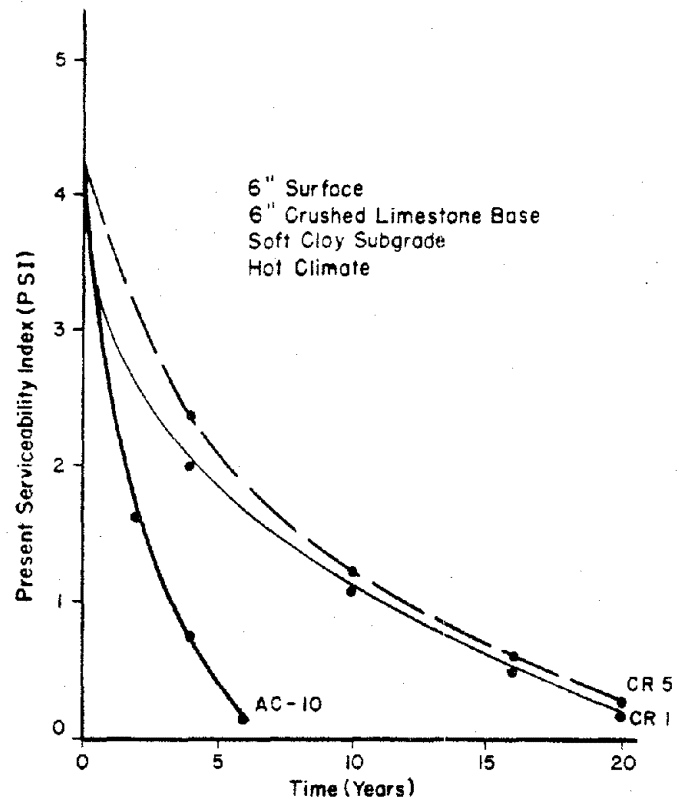


Figure 92. Serviceability Index Versus Time (VESYS IIM Analysis).

of rut depth and slope variance increased with warmer climates. All 20-year rut depths were greater than one inch and were accompanied by excessive slope variances thereby dropping the PSI of each pavement below the minimum level. Maximum rut depth and slope variance again occurred with the AC pavement in the hot climate.

Thick Surface Over Hard Subgrade

The cracking index for these pavements shows that the AC pavement cracked first, followed by CR1 and CR5. Rut depths were much lower than the corresponding thin pavements with all at cold and moderate climates less than or equal to 0.13 inches. The most pronounced rut depths were for the AC pavement in the hot climate. Slope variances were also much less than those of corresponding thin pavements since those at the cold and moderate climate were less than or equal to 0.60×10^{-6} radians. The maximum slope variance occurred in the hot climate with the AC pavement. All combinations, except the AC in the hot climate, met the minimum level of serviceability.

Thick Pavement Over Soft Subgrade

The worse case for each type of distress for the thick pavements was developed with a soft subgrade. The change of these distresses over time are shown in Figures 89 to 92. The similarity between CR5 and AC was more pronounced in this case than with the hard subgrade. Based on the cracking index (Figure 89) the order of cracking was the same as with the hard subgrade. Rut depths were significantly increased when compared to the hard subgrade section. The maximum always occurred in the AC section while the minimum rut depth was always developed in the CR1 section. Rut depths in the hot climate were almost the same for CR1 and CR5 and are shown in Figure 90. The AC section also developed the maximum slope variance for all climates while the CR1 section demonstrated the minimum amount. Due to the magnitude of rutting and roughness, all of the sections failed to meet the minimum PSI.

CHAPTER XI

CONCLUSIONS AND RECOMMENDATIONS

On the basis of the research accomplished in the study, the following conclusions are enumerated:

1. SULPHLEX is the trade name of a group of plasticized sulfur binders developed by Southwest Research Institute which are capable of producing mixtures with characteristics similar to asphalt concrete.

2. The thermal stability and engineering performance of SULPHLEX binders in bulk and/or in mixtures (thin films) are highly dependent not only on the chemical composition of the plasticizers and ratio of plasticizers to sulfur but also the process parameters of reaction time and temperature.

3. SULPHLEX mixtures with equal percentages of binder by weight, as compared to asphalt cement, provide acceptable stabilities but are highly susceptible to moisture deterioration.

4. The air void requirements normally specified for asphalt concrete mixtures, i.e., between 3 and 5 percent, are also necessary to insure acceptable durability in SULPHLEX mixtures. In other words, at least an equal volume percentage of SULPHLEX binder is required as compared to asphalt cement.

5. The preparation of SULPHLEX mixtures in the laboratory as compared to asphalt mixtures shows a similar sensitivity to fabrication variables such as mixing temperature, compactive effort, compaction temperature, method of compaction, etc. SULPHLEX mixtures may be prepared in accordance with the procedures and standards traditionally used for asphalt concrete.

6. On the basis of Marshall mixture design procedures, optimally designed SULPHLEX mixtures exhibited a unique property of very high stabilities (substantially greater than for the asphalt concrete control) and concomitant flows which were approximately twice as great as for the control asphalt concrete mixtures. This obvious difference in behavior between SULPHLEX and asphalt mixtures made it impossible to indiscriminately apply mixture design criteria empirically developed for asphalt concrete.

7. The design of optimum SULPHLEX mixtures based on the principles of maximum strain energy (toughness) and the failure envelope resulted in mixtures with optimum SULPHLEX binder contents slightly higher by volume than would be required for asphalt cement.

8. The failure envelope concept provides a unique mixture design method based on fundamental material properties which can be evaluated against mechanistically derived (non-empirical) failure criteria. The failure envelope shifts with changes in binder content as would be logically predicted.

9. The failure envelope mixture design procedure as outlined in Chapter IV is recommended for SULPHLEX mixtures.

10. SULPHLEX mixtures are generally more brittle and thus more susceptible to fatigue cracking than similar mixtures of asphalt concrete.

11. Fracture mechanics principles were successfully employed and reveal the relatively brittle nature of SULPHLEX but also the substantially large damage zone at the crack tip. Fracture mechanics is a sensitive enough approach to easily distinguish the difference between asphalt concrete and SULPHLEX as well as among various SULPHLEX binders.

12. SULPHLEX binder CR5 proved significantly different from other CR series SULPHLEX binders based on phenomenological flexural fatigue testing. Binder CR5 responded similarly to AC-10 in terms of fatigue cracking potential at 70°F and 104°F. However, at 40°F, the lowest temperature for flexural beam fatigue testing, the flexural fatigue response of CR5 was significantly poorer than that of AC-10. Fracture mechanics testing clearly illustrated the high level sensitivity of SULPHLEX CR5 to temperature variation. When compared to asphalt concrete controls, fracture toughness of SULPHLEX CR5 rapidly degraded as the test temperature dropped from 77°F.

13. Binder CR5 possesses the ability to "heal" across small fracture faces when sufficiently long rest periods are introduced between cyclic loads during fracture fatigue testing. The CR5 binder showed "healing" characteristics similar to AC-10 binders in the control mix. The healing phenomenon was shown to be the primary contributor to laboratory-to-field fatigue shift factors. Based on

these results, identical laboratory-to-field shift factors were used for both the control asphalt concrete mixtures and the SULPHLEX mixtures.

14. The J^* integral computed from the overlay test device was shown to be a material property following the evaluation of the effects of specimen size and rate of cyclic loading.

15. Although the flexural fatigue response and crack propagation rates of the CR5 SULPHLEX binder were similar to AC-10 at 70°F, the energy required to initiate crack growth at low temperatures was substantially lower for all SULPHLEX binders than for the asphalt concrete control. The parameter most sensitive to the low temperature fracture potential of the various binders was the critical J integral, J_{IC} , computed from three-point bend specimens (a variation of ASTM E 813). Although substantially lower than asphalts, the J_{IC} 's for CR5 mixtures were significantly larger than for other SULPHLEX CR series binders at similar low temperatures.

16. The combination of high glass transition temperatures, about 20°F higher than for comparable asphalt concrete mixtures, and low J_{IC} values make SULPHLEX binders very susceptible to low-temperature damage or to damage associated with rapid drops in temperature.

17. The traditional low-temperature fracture testing based on the indirect tensile test at low temperatures and slow-loading rates was a much less sensitive evaluator of low-temperature cracking potential among SULPHLEX binders. However, all SULPHLEX binders possessed ultimate strengths approximately 100 percent greater than those of comparable asphalt concrete. On the other hand, failure strains were an order of magnitude less for the SULPHLEX mixtures than for comparable asphalt concrete mixtures.

18. SULPHLEX mixtures are much less compliant or are much stiffer than comparable asphalt concrete mixtures except at very long (10^5 seconds or greater) load durations. At very long load durations or very high temperatures SULPHLEX binders and/or mixtures exhibit a degradation resulting in a very noticeable loss in stiffness or increase in compliance when compared with the control asphalt concretes.

19. Despite the much higher glass transition plateau for SULPHLEX mixtures, the substantially higher T_g , and the more apparent linear degradation at very long durations of loading, SULPHLEX mixtures exhibit a temperature sensitivity much like that of asphalt concrete. SULPHLEX paving materials must be engineered to consider the effects of temperature sensitivity.

20. The VESYS permanent deformation parameters of ALPHA and GNU for SULPHLEX indicate no potential premanent deformation problems under normal, moving traffic.

21. The analysis of deformation potential based on the Shell Method corroborates the predictions based on the ALPHA and GNU parameters. The $S_{mix} - S_{binder}$ plots for SULPHLEX and asphalt concrete also corroborate the significantly greater degradation of stiffness for SULPHLEX binders than for asphalt binders at extremely long load durations coupled with high temperatures.

22. An evaluation of the modulus properties of SULPHLEX (resilient, dynamic, flexural, and stiffness modulus) establishes that (1) SULPHLEX mixtures are substantially stiffer than asphalt concrete and (2) SULPHLEX mixtures possess a substantial temperature sensitivity.

23. SULPHLEX binders are generally more susceptible to moisture damage than asphalt cement binders. A tight mixture of low air void content is required to resist moisture degradation.

24. The aging of SULPHLEX at high temperatures (140°F) is quite different in nature than that of asphalt. The aging process in SULPHLEX is chiefly due to crystallization and loss of volatiles from the plasticizers. This results in a much more rapid aging process when compared to asphalt concrete.

25. SULPHLEX paving mixtures can be designed to provide highly acceptable pavement layers in a variety of climate and loading environments. However, the inherent properties of high stiffness, high T_g , low temperature cracking potential, moisture susceptibility, and temperature sensitivity must be considered.

Although a lengthy list of recommendations could be presented, it is clear that the immediate objectives of SULPHLEX research should be to:

1. Research the development of second generation SULPHLEX binders which possess a lower T_g and less susceptibility to low-temperature fracture or fracture due to rapid temperature drops.

2. Develop SULPHLEX formulations which will retain the structural advantages of SULPHLEX at mid-range temperatures while achieving reasonable low-temperature fracture resistance and resistance to stiffness degradation at combinations of high temperatures and very long durations of loading.

3. Improve the moisture and thermal aging durability of SULPHLEX through the investigation of alternate chemical formulations and variations in process parameters.

Present research at Texas A&M University is pursuing the three objectives listed above.

REFERENCES

1. Haxo, H. E., Busso, C. J., Gage, M., Miedema, J., Newey, H., and White, R. M. "Design and Characterization of Paving Mixtures Based on Plasticized Sulfur Binders - Chemical Characterization," FHWA Contract DTFH-61-80-C-0048, Matrecon Inc., Oakland, CA, 1984.
2. Little, D. N. and Richey, B. L. "Mixture Design of SULPHLEX Based on the Failure Envelope Concept," Draft Report Submitted to FHWA, under contract DTFH-61-80-C-0048, July 1984.
3. American Society of Testing and Materials - Standard Specifications, Parts 14, 10, and 15, 1982.
4. American Association of State Highway and Transportation Officials, Part II, Methods of Sampling and Testing, 1983.
5. Manual of Testing Procedures, State Department of Highways and Public Transportation, Volume 1, Austin, Texas, 1984.
6. Traxler, R. N., et al. "Loss of Durability in Bituminous Pavement Surfaces - Importance of Chemically Active Solar Radiation," Research Report 127-3, Texas Transportation Institute, Texas A&M University.
7. Personal Communication with Dennis James, Center for Trace Characterization, Texas A&M University, College Station, Texas, 1982.
8. Hveem, F. N. "Establishing the Oil Content for Dense - Graded Bituminous Mixtures," California Highways and Public Works, July-August 1942.
9. "Mix Design Methods for Asphalt Concrete," The Asphalt Institute, Manual Series No. 2 (MS-2), Fourth Edition, March, 1974.
10. Schmidt, R. J. "A Practical Method for Measuring the Resilient Modulus of Asphalt-Treated Mixes," Highway Research Record No. 404, Highway Research Board, 1972.
11. Pickett, et al. "Extension and Replacement of Asphalt Cement with Sulfur," Report No. FHWA-RD-78-95, March 1978.
12. Kenis, W. J. "Predictive Design Procedures, VESYS Users Manual," Report No. FHWA-RD-77-154, January 1978.
13. Anagnos, J. N. and Kennedy, T. W. "Practical Method of Contracting the Indirect Tensile Test," University of Texas at Austin, Research Report 98-10, August 1972.

REFERENCES (continued)

14. Hadley, W. D., Hudson, W. R., and Kennedy, T. W. "A Method of Estimating Tensile Properties of Materials Tested in Indirect Tension," Center for Highway Research, University of Texas at Austin, Research Report 98-7, July 1970.
15. Shell Pavement Design Manual, Shell International Petroleum Company Ltd., London, 1978.
16. Lottman, R. P. "Predicting Moisture - Induced Damage to Asphalt Concrete," NCHRP Report 192, Washington, D. C., 1978.
17. Lottman, R. P., "Predicting Moisture - Induced Damage to Asphalt Concrete - Field Evaluation," NCHRP Report 246, Washington, D. C., 1982.
18. Ludwig, A. C., Gerhardt and Dale, J. "Materials and Techniques for Improving the Engineering Properties of Sulfur," Interim Report, Report FHWA/RD-80/023, March 1980.
19. Haxo, H. E., Busso, C. J., Newey, H. A. and Little, D. N. "Design and Characterization of Paving Mixtures Based on Plasticized Sulfur Binders - Task A," Interim Report, FHWA Contract DTFH-61-80-C-0048, April 1981.
20. Monismith, C. L., Unpublished Class Notes on Mix Design, University of California, 1966.
21. Lentz, H. J. and Harrigan, E. T. "Laboratory Evaluating of SULPHLEX-233: Binder Properties and Mix Design," Report FHWA/RD-80/146, January 1981.
22. Harrigan, E. T. and Little, D. N. "Performance of SULPHLEX Pavements Constructed During 1980 and 1981," Presented to "Sulfur-84" Conference, Calgary, Alberta, June 1984.
23. Hudson, W. R. and Kennedy, T. W. "An Indirect Tension Test for Stabilized Materials," Center for Highway Research, University of Texas at Austin, Research Report 98-1, 1968.
24. Maupin, Jr., G. W. and Freeman, Jr., J. R., "Simple Procedure for Fatigue Characterization of Bituminous Concrete," Federal Highway Administration, Report FHWA-RD-76-102, June 1976.
25. Schoen, W. A., Epps, J. A., Gallaway, B. N. and Little, D. N. "Economics Bituminous Treated Bases Report No. TTI-2-6-74-2041, Texas A&M University, College Station, Texas, 1977.
26. Richey, B. L., "A Method of Evaluating SULPHLEX Mix Designs Based on the Indirect Tensile Test Masters Thesis, Texas A&M University, August 1982.
27. Smith, T. L., "Stress - Strain - Time - Temperature Relationships for Polymers," American Society for Testing Materials, Special Technical Publication No. 325, 1962.

REFERENCES (continued)

28. Chang, H. S., Lytton, R. L. and Carpenter, S. H. "Prediction of Thermal Reflection Cracking in West Texas," Texas Transportation Institute, Research Report 18-3, March 1976.
29. Bolk, H. J. N. A. "The Creep Test," SCN Record 5, Study Center for Road Construction, Arnhem, The Netherlands, February 1981.
30. Claessen, A. I. M., Edwards, J. M., Somner, P., and Ugé, P., "Asphalt Pavement Design: The Shell Method," Proceedings of the Fourth International Conference on the Structural Design of Asphalt Pavements, University of Michigan, 1977.
31. Santucci, L. E. "Thickness Design Procedure for Asphalt and Emulsified Asphalt Mixes," Proceedings of the Fourth International Conference on the Structural Design of Asphalt Pavements, University of Michigan, 1977.
32. Epps, J. A. and Monismith, C. L. "Fatigue of Asphalt Concrete Mixtures - Summary of Existing Information," Fatigue of Compacted Bituminous Aggregate Mixtures, American Society for Testing and Materials, Special Technical Publication No. 508, 1972.
33. Majidzadeh, K., Kauffman and Sarat, C. "Analysis of Fatigue of Paving Mixtures from a Fracture Mechanics Viewpoint," ASTM Special Technical Publication, No. 508, 1972.
34. Majidzadeh, K. and Ramsamooj, D. "Applications of Fracture Mechanics for Improved Design of Bituminous Concrete FHWA Report FHWA-RD-76-91, June 1976.
35. Ramsamooj, D. "Analysis and Design of Flexible Pavements," Ph.D. Dissertation, Ohio State University, 1970.
36. German, P. F. and Lytton, R. L. "Methodology for Predicting the Reflection Cracking Life of Asphalt Concrete Overlays," Report No. TT-2-8-75-207-5, Texas Transportation Institute, College Station, Texas, 1977.
37. Pickett, D. L. and Lytton, R. L. "Laboratory Evaluation of Selected Fabrics for Reinforcement of Asphalt Concrete Overlays," Report No. TTI-2-8-80-261-1, Texas Transportation Institute, College Station, Texas, 1983.
38. Lytton, R. L. and Shanmugham, Ulpala "Analysis and Design of Pavements to Resist Thermal Cracking Using Fracture Mechanics," Proceedings of Fifth International Conference - Structural Design of Asphalt Pavements, Delft, 1982.
39. Paris, P. C. and Erdogan, F. J. Journal of Basic Engineering, Series D of the Transaction of ASME, JBAEA, Vol. 85, 1963.
40. Irwin, G. R. "Analysis of Stresses and Strains Near the Tip of a Crack Transversing a Plate," Transaction of ASME, Journal of Applied Mechanics, Vol. 24, 1957.

REFERENCES (continued)

41. Orowan, E. "Fatigue and Fracture of Metals," MIT Press, Cambridge, Mass., 1950.
42. Paris, P. C. and Sih, G. C. "Stress Analysis of Cracks," ASTM Special Technical Publication 381, 1965.
43. Saxena, A. and Hjdak, S. J. "Review and Extension of Compliance Information for Common Crack Growth Specimens," Scientific Paper 77-9E7-AFCGR-P1, Westinghouse R&D Center, Pittsburgh, PA, 1977.
44. Hertzberg, R. W. Deformation and Fracture Mechanics of Engineering Materials, John Wiley and Sons, New York, 1976.
45. Rice, J. A. "A Path Independent Integral and the Approximate Analysis of Strain Concentration by Notches and Cracks," J. Applied Mechanics, 35, 1968.
46. Personal Communication with R. L. Lytton, Texas A&M University, 1984.
47. Rice, J. R. and Johnson, M. A. "The Role of Large Crack Tip Geometry Changes in Plane Strain Fracture," Inelastic Behavior of Solids, Kanninen Ed., McGraw Hill, 1970.
48. Wells, A. A. "Applications of Fracture Mechanics at and beyond General Yielding," British Welding Research Ass. Rep. M13, 1963.
49. Broek, D. Elementary Engineering Fracture Mechanics, Third Ed., Martinus Nijhoff Publishers, The Hague, 1983.
50. Monismith, C. L., Epps, J. A., Kasianchuk, D. A. and McLean, D. B. "Asphalt Mixture Behavior in Repeated Flexure," Soil Mechanics and Bituminous Materials Research Laboratory, Report No. TE70-5, Institute of Transportation and Traffic Engineering, Univ. of California, Berkeley, 1970.
51. Monismith, C. L., Hicks, R. G. and Salam, Y. M. "Basic Properties of Pavement Components," Report No. FHWA-RD-72-19, Federal Highway Administration, 1971.
52. Barksdale, R. D. "Development of Equipment and Techniques for Evaluating Fatigue and Rutting Characteristics of Asphalt Concrete Mixes," Georgia DOT Research Projects No. 7305, School of Civil Engineering, Georgia Institute of Technology, June 1977.
53. Chevron Asphalt Research Company, "Bitumals Mix Manual," Richmond California, 1975.
54. Sherwood, J. A. and Kenis, W. J. "SULPHLEX Pavement Performance Evaluation from Laboratory Tests," Transportation Research Record No. 852, Transportation Research Board, 1981.

REFERENCES (continued)

55. Rauhut, J. B., O'Quin, J. C. and Hudson, W. R. "Sensitivity Analysis of FHWA Structural Model VESYS II, Volume 1 Preparatory and Related Studies," Report FHWA-RD-76-23, March 1976.
56. Pickett, D. E. et al. "Extension and Replacement of Asphalt Cement by Sulfur," Report FHWA-RD-78-95, March 1978.
57. Rauhut, J. B. and Kennedy, T. W. "Characterizing Fatigue Life for Asphalt Concrete Pavements," Paper Presented to Transportation Research Board, Washington, D. C., 1983.
58. Rauhut, J. B., O'Quin, J. C. and Hudson, W. R., "Sensitivity Analysis of FHWA Structural Model VESYS II, Volume II, Sensitivity Analysis," Report FHWA-RD-76-24, March 1976.
59. Bucknall, C. B., "Fracture and Failure of Multiphase Polymers and Polymer Composition," Advances in Polymer Science, Volume 27, Failure in Polymers, 1978.
60. Wool, R. P. and O'Connor, K. M. "A Theory of Crack Healing in Polymers," Journal of Applied Physics, Vol. 52, No. 10, pp. 5953-5963, 1981.
61. Kim, Y. H. and Wool, R. P., "A Theory of Healing at a Polymer Interface," Macromolecules, Vol. 16, No. 7, pp. 1115-1120, 1983.
62. Jud, K., Kausch, H. H. and Williams, J. G. "Fracture Mechanics Studies of Crack Healing and Welding of Polymers," Journal of Materials Science, Vol. 16, No. 1, pp. 204-210, 1981.
63. Wool, R. P., and Rockhill, A. T., "Molecular Aspects of Healing and Fracture in Glassy-Polymers," Abstracts of the American Chemical Society, Vol. 180, August, p. 76, 1980.
64. Wool, R. P., "Crack Healing and Related Problems," Journal of Rheology, Vol. 26, No. 6, p. 575, 1982.
65. Wool, R. P., and O'Connor, K. M., "Time Dependence of Crack Healing," Journal of Polymer Science - Polymer Letters Edition, Vol. 20, No. 1, pp. 7-16, 1982.
66. Van Dijk, W., "Practical Fatigue Characterization of Bituminous Mixes," Proceedings Association of Asphalt Paving Technologists, Vol. 44, 1975.
67. Finn et al. "Development of Pavement Structural Subsystems," Final Report Project 1-10B, NCHRP, February 1977.
68. Santucci, L. E., "Thickness Design Procedure for Asphalt and Emulsified Asphalt Mixes," Proceedings Fourth International Conference Structural Design of Asphalt Pavements, University of Michigan, 1977, pp. 444-456.

REFERENCES (continued)

69. Sharma, J., et al. "Implementation and Verification of Flexible Pavement Design Methodology," Proceedings Fourth International Conference Structural Design of Asphalt Pavements, University of Michigan, 1977.
70. Unpublished communication with R. L. Lytton, Texas A&M University, College Station, Texas, 1984.
71. Rijkswaterstaat Directie Wegen Afdeling Gorinchen and Rijswegen boua laboratorium, Proefuakken rijksweg 15 - deel 1: Doel, opzet en Voorbereiding. Rijkswaterstaat Publicatie Nr. 8, March 1972.
72. Yandell, W. and Lytton, R. L. "Residual stresses Due to Traveling Loads and Reflection Cracking," Texas Transportation Institute Report No. 207-6, 1980.
73. Lytton, R. L. and Yandell, W. "The Effect of Residual Stress and Strain Built Up in a Flexible Pavement by Repeated Rolling of a Tire," Draft Report RF4087-1, Texas A&M University, 1980.
74. Finn, F. N. "Factors Involved in the Design of Asphaltic Pavement Surfaces," NCHRP Report 39, 1982.
75. McLeod, N. W. "Reduction in Transverse Pavement Cracking by Use of Sulfur Asphalt Cements," Highway Research Board Western Meeting, Denver, Colorado, 1968.
76. Saal, R. N. J. "III. Physical Properties of Asphaltic Bitumen Surface Phenomena, Thermal and Electrical Properties, Etc.," In the Properties of Asphaltic Bitumen, Elsevier, 1950.
77. Monismith, C. C., "Fatigue of Asphalt Paving Mixtures," Paper Presented at First Annual Street and Highway Conferences, University of Nevada, 1966.
78. Christison, J. T. and Anderson, K. C., "The Response of Asphalt Pavements to Low Temperature Climatic Environments," Proceedings Third International Conference on Structures Design of Asphalt Pavements, London, 1972.
79. Finn, F. et al. COLD Computer Model, Final Report Project 1-10B, NCHRP, pp. 47-73 and Appendix A, February 1977.
80. Rolfe, S. T. and Barsom, J. M., Fracture and Fatigue Control in Structures, Prentice-Hall, Inc., Englecliffs, N. J., 1977.
81. ASTM E 813-81, "Test for J_{IC} , a Measure of Fracture Toughness," Part 10, 1982.
82. ASTM E 399-81, "Test for Plane-Strain Fracture Toughness of Metallic Materials," Part 10, 1982.

REFERENCES (continued)

83. Paris, P.C. and Hayden, B.R. "A New System for Fatigue Crack Growth Measurement and Control," Presented at ASTM Symposium on Crack Growth, Pittsburgh, PA, October 1979.
84. Secor, K. E. and Monismith, C. L. "Analysis and Interrelation of Stress-Strain-Time Data for Asphalt Concrete." Trans. Soc. Rheology, Vol. 8, 1964.
85. Papazian, H. S. "The Response of Linear Viscoelastic Materials in the Frequency Domain with Emphasis on Asphaltic Concrete." Proc. Internat. Conf. on Structural Design of Asphalt Pavements, Univ. of Michigan, 1962.
86. Pagen, C. A. "Rheological Response of Bituminous Concrete." Hwy. Res. Record No. 67, 1965.
87. Deacon, J. A. "Fatigue of Asphalt Concrete." Thesis, D. Eng. (Transportation Eng.), Univ. of California, 1964.
88. Pagen, C. A. and Ku, B. "Effect of Asphalt Viscosity on Rheological Properties of Bituminous Concrete." Hwy. Res. Record No. 104, 1965.
89. Krokosky, E. M., Tons, E., and Andrews, R. D. "Rheological Properties of Asphalt-Aggregate Compositions." Proc. ASTM, Vol. 63, 1963.
90. Brodnyan, J. G. "Use of Rheological and Other Data in Asphalt Engineering Problems." HRB Bull. 192, 1963.
91. Davis, E. F., Krokosky, E. M. and Tons, E. "Stress Relaxation of Bituminous Concrete in Tension." Hwy. Res. Record No. 67, 1965.
92. Little, D. N., Holmgreen, R. J. and Epps, J. A. "Effects of Recycling Agents on the Structural Performance of Recycled Asphalt Concrete Materials," Proceedings, AAPT, Vol. 50, 1981.
93. Shell Pavement Design Manual, Shell International Petroleum Co. Ltd., London, 1978.
94. Van de Loo, P. J. "A Practical Approach to the Prediction of Rutting on Asphalt Pavements: The Shell Method," Transportation Research Board, Washington, D. C., 1976.
95. Claessen, A. I. M., Edwards, J. M., Sommer, P. and Uge, P. "Asphalt Pavement Design - The Shell Method," Proceedings Fourth International Conference Structural Design of Asphalt Pavements, Univ. of Michigan, 1977.
96. Hills, J. F., Brien, D. Van de Loo, P. J. "The Correlation of Rutting and Creep Tests on Asphalt Mixes," Journal of the Institute of Petroleum, Paper IP74-001, 1974.
97. Van de Poel, C. "A General System Describing the Viscoelastic Properties of Bitumens and the Relation to Routine Test Data," Shell Bitumen Reprint No. 9, Shell Laboratorium - Koninklijke, 1954.

REFERENCES (continued)

98. Lee, K. W. "Prediction and Evaluation of Moisture Effects on Asphalt Concrete Mixtures in Pavement Systems," Ph.D. Dissertation, Univ. of Texas, Austin, Texas, 1982.
99. Soles, J. A., Carette, G. C. and Malhotra, V. M. "Stability of Sulfur - Infiltrated Concrete in Various Environments," New Uses in Sulfur - II, 1977.
100. Personal Communication with E. T. Harrigan, FHWA, May 1984.
101. Ludwig, A. C., Gerhardt, B. B. and Dale, J. M., Unpublished Data Submitted to FHWA, 1979.
102. Scrivner, F. H., Moore, W. M., McFarland, W. F. and Carey, G. R. "A Systems Approach to the Flexible Pavement Design Problem," Research Report 32-11, Texas Transportation Institute, 1968.
103. DeJong, D. L., Pentz, M. G. F. and Korswagen, A. R., "Computer Program BISAR - Layered Elastic Systems Under Normal and Tangential Surface Loads," Kohin Klijkel Shell - Laboratorium, Amsterdam, External Report AMSR. 0006. 73, 1973.
104. AASHTO Interim Guide for Design of Pavement Structures - 1972, AASHTO, 1974.
105. Scrivner, F. H. and McFarland, W. F. "Texas Tries a Flexible Pavement Design System," Texas Transportation Research, Vol. 6, No. 3, July 1970.
106. Lu, D. Y., Shih, C. S. and Scrivner, F. H. "The Optimization of a Flexible Pavement System Using Linear Elasticity," Research Report 123-17, Texas Transportation Institute, 1973.
107. Duncan, J. M., Byrne, P., Wang, K. S. and Mabry, P., "Strength, Stress-Strain and Bulk Modulus Pavements for Finite Element Analyses of Stresses and Movements in Soil Masses," Report No. UCB/GT/80-01, University of California, Berkley, August 1980.
108. Barksdale, R. D., "Repeated Load Test Evaluation of Base Course Materials," GHD Research Project No. 7002, Georgia Institute of Technology, May 1972.
109. Lytton, R. L., Personal Communication, Texas A&M University, College Station, Texas, 1984.
110. Santucci, L. E. "Thickness Design Procedure for Asphalt and Emulsified Asphalt Mixes," Proceedings of Fourth International Conference Structural Design of Asphalt Pavements, Univeristy of Michigan, 1977, p. 434.

REFERENCES (continued)

111. Jung, F. W., Kher, R. and Phang, W. A. "Subsystem for Flexible Pavement Performance Prediction," Presented at Transportation Research Board Annual Meeting, Washington, D. C., 1975.
112. Lu, D., Lytton, R. L. and Moore, W. M., "Forecasting Serviceability Loss of Flexible Pavements," Research Report 57-1F, Texas Transportation Institute, 1974.

APPENDIX A

PREPARATION OF BINDERS

Five SULPHLEX binders were included in the mixture testing and characterization program. Four of the five mixtures were fabricated by Cal-Resin of Vallejo, California, under the supervision of Matrecon, Inc. The fifth binder was fabricated at Texas A&M University's research annex. This binder, SULPHLEX 233A, is similar to the SULPHLEX binders which were ultimately used in the SULPHLEX field test pavements throughout the United States.

The formulations and processing conditions of all five binders are shown in Table 9 of the text.

The four SULPHLEX binders produced by Cal-Resin under the direction and supervision of Matrecon, Inc. were prepared in a 13-gallon pilot plant, Figure 93.

The general format of the production process was to charge the reaction vessel with sulfur and heat to the appropriate temperature, add a SULPHLEX catalyst obtained from Southwest Research Institute and stir until dissolved (about 10 minutes). The plasticizers; dicyclopentadiene, dipentene, and vinyl toluene, were premixed. The mixed olefins were then added to the melted sulfur at an even rate over a 1/2-hour period maintaining the reactor temperature within $\pm 3^{\circ}\text{F}$ of the desired reaction temperature.

During the addition of the premixed olefin the reaction temperature was controlled by cooling. After completion of the olefin addition the reaction was continued for six hours in each case.

The batches were cooled to about 275°F , packaged in 1-gallon cans and shipped from Matrecon, Inc. to Texas A&M University for testing of the SULPHLEX in mixtures with crushed limestone, silicious river gravel, and basaltic aggregate.

From the chemical and bulk properties of the SULPHLEX binders studied by Matrecon, Inc., the following trends were expected:

1. Lower reaction temperatures, 302°F versus 338°F , favor a higher viscosity, lower free sulfur and greater plasticization

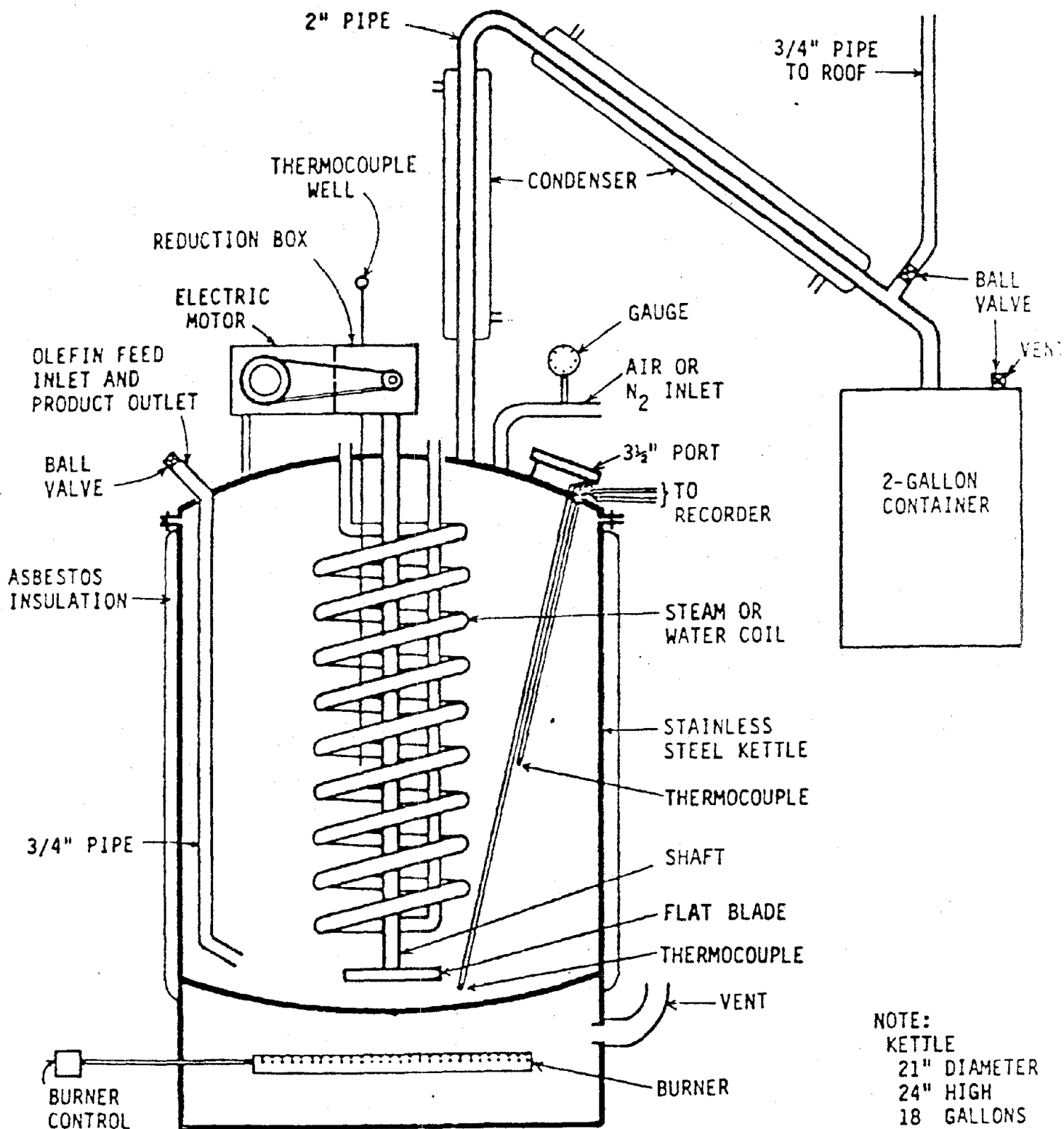


Figure 93. Schematic of Kettle Used to Prepare Pilot Quantities of SULPHLEX 233 at Different Temperatures.

efficiency (slower crystallization rate). This is attributed to the greater sulfur rank in the lower temperature reaction product, i.e., high x in the $R-S_x-R$ products.

2. All reaction products are thermally unstable. Aging at high temperatures, greater than 349°F, result in a continuing loss of volatile sulfur compounds and some hydrogen sulfide with a concomitant increase in viscosity, presence of volatile sulfur compounds and the continuing generation of reaction sites by the dehydrogenation activity of the free sulfur present.

Binder 233A was produced at Texas A&M research annex on March 11, 1982. The binder was produced in the reactor shown in Figure 94. The product temperature was maintained, during the addition of the olefin plasticizers to the sulfur, within $\pm 3^\circ\text{F}$ of the target processing temperature of 320°F. The isothermal condition was maintained by the ability to cool the product using the cooling case within the reactor and by controlling the rate of olefin addition during the processing of the SULPHLEX 233A. Prior to the olefin addition, the sulfur was melted and maintained at 270°F.

The olefin addition to the molten sulfur took place over a one hour and 45-minute period. The entire reaction time was six hours and 30 minutes.

Olefin plasticizers used were as follows:

Dicyclopentadiene (DCPD) (97 percent pure and manufactured by Exxon Chemical Company, Houston, Texas),

Vinyl Toluene (manufactured by DOW Chemical Company, Midland, Michigan) and

Solvenol #2 (a terpene solvent manufactured by Hercules, Inc., Wilmington, Delaware).

The DCPD was added first followed by the Solvenol #2 followed by vinyl toluene. Plasticizers were thoroughly mixed prior to addition to the sulfur.

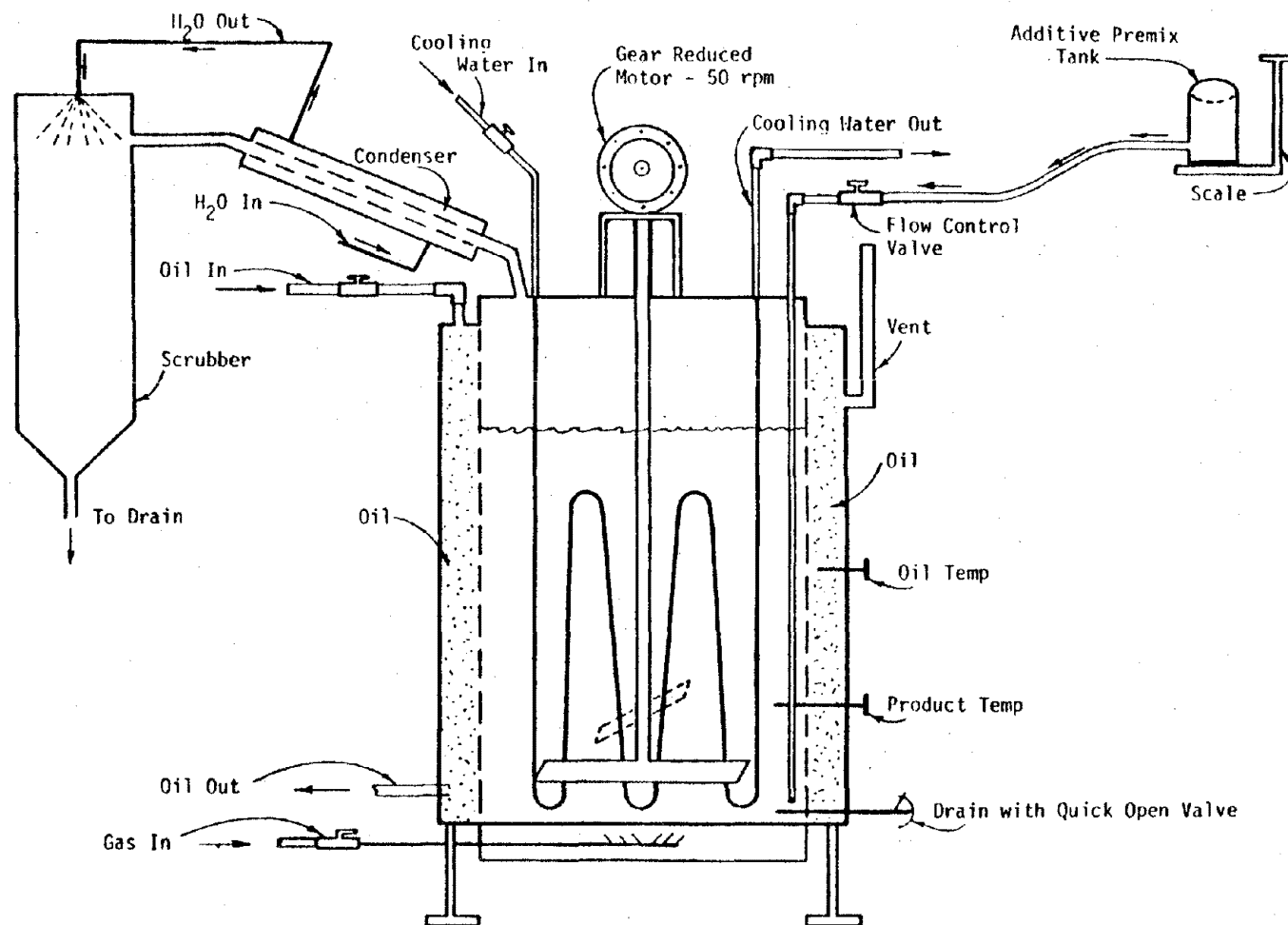


Figure 94. Schematic of 25-Gallon SULPHLEX Pilot Plant.

APPENDIX B

OVERLAY TESTER

The "overlay tester" Figure 27 of the text, developed at Texas A&M University, is essentially a displacement-controlled fatigue testing machine designed to initially produce a small crack (due to tension) in a test specimen and then continue to induce repetitive longitudinal displacements at the base of the crack which causes the crack to propagate upward through the specimen. This process is intended to simulate the cyclic stressing of a pavement due to periodic thermal variation. Results obtained with this apparatus should prove very useful in predicting pavement service life extension effected by systems purported to reduce reflection cracking.

After allowing the test specimens to age at room temperature for at least 2 weeks, each specimen was epoxied to two rigid plates; one fixed, the other regulated to oscillate at a constant displacement of either 0.020 or 0.070 inches and at a rate of 6 cycles per minute. The initial movement was outward which caused tensile stresses at the center of the specimen. All these tests were conducted at 77°F. Load was measured by a strain gage load transducer and displacement of the moving plate was monitored by a linear variable differential transformer (LVDT). Load as a function of displacement was recorded on an X-Y recorder. An example of recorded data is given in Figure 28 of the text. The length of the crack was periodically measured on each side of the specimen. The average of the two measurements was used as the crack length corresponding to the given number of cycles. The machine was allowed to oscillate until complete specimen failure, that is, until the crack propagated completely through the beam specimen. Ideally, complete failure would be defined as the cycle at which the load approached zero.

